Topical Report: DE-FC26-04NT15513

Phase II (Year 2) Summary of Research – Establishing the Relationship between Fracture-Related Dolomite and Primary Rock Fabric on the Distribution of Reservoirs in the Michigan Basin

DOE Award Number: DE-FC26-04NT15513

Reporting Period Start: October 1, 2005
Reporting Period End: September 30, 2006

Principal Author and Project Manager:
G. Michael Grammer, Ph.D.
Associate Professor
Department of Geosciences
Western Michigan University
1903 W. Michigan Ave.
Kalamazoo, MI 49008-5241

Topical Report Issued: November 3, 2006

DISCLAIMER

"This report was prepared as an account of work sponsored by an agency of the United States Government. Neither the United States Government nor any agency thereof, nor any of their employees, makes any warranty, express or implied, or assumes any legal liability or responsibility for the accuracy, completeness, or usefulness of any information, apparatus, product, or process disclosed, or represents that its use would not infringe privately owned rights. Reference herein to any specific commercial product, process, or service by trade name, trademark, manufacturer, or otherwise does not necessarily constitute or imply its endorsement, recommendation, or favoring by the United States Government or any agency thereof. The views and opinions of authors expressed herein do not necessarily state or reflect those of the United States Government or any agency thereof".

ABSTRACT

This topical report covers the year 2 of the subject 3-year grant, evaluating the relationship between fracture-related dolomite and dolomite constrained by primary rock fabric in the 3 most prolific reservoir intervals in the Michigan Basin (Ordovician Trenton-Black River Formations; Silurian Niagara Group; and the Devonian Dundee Formation).

The characterization of select dolomite reservoirs has been the major focus of our efforts in Phase II/Year 2. Fields have been prioritized based upon the availability of rock data for interpretation of depositional environments, fracture density and distribution as well as thin section, geochemical, and petrophysical analyses. Structural mapping and log analysis in the Dundee (Devonian) and Trenton/Black River (Ordovician) suggest a close spatial relationship among gross dolomite distribution and regional-scale, wrench fault-related NW-SE and NE-SW structural trends. A high temperature origin for much of the dolomite in the 3 studied intervals (based upon initial fluid inclusion homogenization temperatures and stable isotopic analyses,) coupled with persistent association of this dolomite in reservoirs coincident with wrench fault-related features, is strong evidence for these reservoirs being influenced by hydrothermal dolomitization.

For the Niagaran (Silurian), a comprehensive high resolution sequence stratigraphic framework has been developed for a pinnacle reef in the northern reef trend where we had 100% core coverage throughout the reef section. Major findings to date are that facies types, when analyzed at a detailed level, have direct links to reservoir porosity and permeability in these dolomites. This pattern is consistent with our original hypothesis of primary facies control on dolomitization and resulting reservoir quality at some level. The identification of distinct and predictable vertical stacking patterns within a hierarchical sequence and cycle framework provides a high degree of confidence at this point that results will be exportable throughout the basin.

Ten petrophysically significant facies have been described in the northern reef trend, providing significantly more resolution than the standard 4-6 that are used most often in the basin (e.g. Gill, 1977). Initial petrophysical characterization (sonic velocity analysis under confining pressures) shows a clear pattern that is dependent upon facies and resulting pore architecture. Primary facies is a key factor in the ultimate diagenetic modification of the rock and the resulting pore architecture. Facies with good porosity and permeability clearly show relatively slow velocity values as would be expected, and low porosity and permeability samples exhibit fast sonic velocity values, again as expected. What is significant is that some facies that have high porosity values, either measured directly or from wireline logs, also have very fast sonic velocity values. This is due to these facies having a pore architecture characterized by more localized pores (vugs, molds or fractures) that are not in communication.

TABLE OF CONTENTS

Abstract p. 3

Executive Summary p. 5

Project Approach and Discussion of Results by Task (Phase I and II) p. 7

Discussion:
- Phase I and II- Initial Results from Tasks 2 and 3 p. 45
  "Controls on Dolomitization in the Middle Devonian Dundee Formation - Oil Field Scale Structure and the Distribution of Log-Based Dolomite Lithofacies"

Initial Summary of Currently Available Geologic Data (Task 2) p. 69
- Ordovician Trenton/Black River Trend - Production Analysis Data and Graphs
- Silurian Niagaran Trend - Production Analysis Graphs
- Devonian Trend - Production Analysis Graphs

References Cited p. 81

Bibliography – part of Task 2 (Compilation of currently available geologic data and literature). p. 84

Appendix 1: Summary of Currently Available Geologic Data (Task 2) p. 119
1. Ordovician Trenton/Black River
2. Silurian Niagaran
3. Devonian Dundee

Appendix 2: Project presentations at professional meetings (Year 2/Phase II) p. 162

EXECUTIVE SUMMARY

This topical report covers Year 2 of the subject 3-year grant, evaluating the relationship between fracture-related dolomite and dolomite constrained by primary rock fabric in the 3 most prolific reservoir intervals in the Michigan Basin (Ordovician Trenton-Black River Formations; Silurian Niagara Group; and the Devonian Dundee Formation). Phase I tasks, including Developing a Reservoir Catalog for selected dolomite reservoirs in the Michigan Basin (Tasks 2.1, 2.2, and 2.3), Characterization of Dolomite Reservoirs in Representative Fields (Tasks 3.1, 3.2, 3.3, 3.4 and 3.5) and Technology Transfer (Task 5) have continued through Phase II and progress is consistent with our original scheduling.

The characterization of select dolomite reservoirs (Task 3) has been the major focus of our efforts in Phase II/Year 2. Fields have been prioritized (after being identified in Phase I/Task 2) based upon the availability of rock data for interpretation of depositional environments, fracture density and distribution as well as thin section, geochemical, and petrophysical analyses. The majority of our Task 3 efforts in the first half of the year were focused on the Devonian and Silurian sections, with the enhanced efforts in the Ordovician section ramping up in the 3rd and 4th quarters of 2006. Task 3 objectives are on time and target for Phase II as per our original proposal.

Structural mapping and log analysis in the Trenton/Black River (Ordovician) and Dundee (Devonian) suggest a close spatial relationship among gross dolomite distribution and regional-scale, wrench fault-related NW-SE and NE-SW structural trends. A high temperature origin for much of the dolomite in the 3 studied intervals (based upon fluid inclusion homogenization temperatures and stable isotopic analyses) coupled with persistent association of this dolomite in reservoirs coincident with wrench fault-related features, is strong evidence in support of these reservoirs being influenced by hydrothermal dolomitization. Ongoing efforts will be focused on determining whether the hydrothermal dolomite represents the only phase of dolomite in these fault-related fields, or whether there is evidence of low temperature dolomitization as well. In either case, our main concentration is whether the reservoir quality of the dolomite can be tied to primary facies type and/or an established sequence stratigraphic framework, either of which will enhance the predictability of such reservoirs.

For the Niagaran (Silurian), a comprehensive high resolution sequence stratigraphic framework has been developed for a pinnacle reef in the northern reef trend where we had 100% core coverage throughout the reef section. Our next step is to test this sequence framework within a larger reef complex in the southern reef trend (Ray Reef Field). We have started a detailed geological characterization of the field utilizing 18 cores for development of a 3-D rock-based reservoir model that is scheduled to be developed during Phase III. Major findings to date are that facies types, when analyzed at a detailed level, have direct links to reservoir porosity and permeability in these dolomites. This pattern is consistent with our original hypothesis of primary facies control on dolomitization and resulting reservoir quality at some level. The identification of distinct and predictable vertical stacking patterns

within a hierarchical sequence and cycle framework provides a high degree of confidence at this point that results will be exportable throughout the basin.

The initial stages of data evaluation and synthesis in Task 4 are well underway per our original proposal. Most of the effort on this task has necessarily had to follow results of Phase I results from Tasks 2 and Phase II results of Task 3. We have entered into an agreement with Dr. Matthew Pranter, University of Colorado, who will be collaborating with us on the 3-D modeling efforts during Phase III.

Technology transfer efforts (Task 5) continue with formal presentations on the state and national levels as well as ongoing advertisement of the project's scope, anticipated results and funding agency on the WMU Department of Geosciences web site. During Year 2, we presented two papers at the National AAPG Meeting in Houston, TX (see Appendix 2), 2 papers at the Midwest Regional PTTC workshop on carbonate reservoirs, and 7 papers (3 professional and 4 student presentations) at the Eastern Section of AAPG in Buffalo. We also received an award, the Vincent E. Nelson Memorial Award, for the Best Poster presented at the 2005 ES AAPG Meeting (Sandomierski, Grammer and Harrison).

PROJECT APPROACH AND DISCUSSION OF RESULTS BY TASK (PHASE I AND II)

Task 2.0 – Development of a Reservoir Catalog for selected dolomite reservoirs in the Michigan Basin

Wireline Log Scanning – to date we have scanned about 14,000 wireline logs and are well underway digitizing selected logs for further data manipulation. The scans are digital raster images captured by using a Neuralog Scanner. Each image is a TIFF type image, scanned at 200 dpi resolution. These images can be used directly in Petra software for creating cross-sections and for stratigraphic correlation. They can also be pasted into text files as illustrations or used in PowerPoint presentations or on posters. These images can also be digitized into LAS files using the Neuralog software. Numerous logs for the Devonian section, the Ray Reef Field (Silurian) and the Albion-Scipio fields have been digitized and are currently being used for analysis within the Petra software.

Digital Conventional Porosity and Permeability Core Analyses – students have been key punching core analysis data from paper copies into Excel spreadsheets to supplement our current digital data bases. To date they have completed an additional 250 wells from 5 northern Michigan and 2 southern Michigan counties across the Niagaran Reef trend. This data includes the depth of the analyzed core sample, conventional air permeability and helium porisimetry, oil and water saturations, descriptive lithology and (when available) gas chromatographic analyses of C-1 through C-5 on selected footages.

Brine Chemistry Data – Students have key punched a paper data set from Dow Chemical containing brine analyses from the Michigan Basin. This data contains 218 analyses from numerous formations throughout the state and supplements our current digital data base. These have been entered into an Excel spreadsheet and added to a previous data set of 165 wells. To give a reasonably comprehensive data set of 383 wells. Data includes well location information, depth of sample, total dissolved solids (salinity), major elements, some trace elements and some temperature data.

Dolomitized intervals in wells of Albion/Scipio Field – An Excel spreadsheet has been created for all wells in the Albion/Scipio and Stoney Point fields, and wells have been ranked based on available data for further study. Albion/Scipio is the largest field in Michigan and the largest Trenton-Black River Field in our study. The field contains 746 wells. The data set includes well location information and footage intervals in the Trenton and Black River formations that are dolomitized. This data will be used in concert with other databases to define the distribution of the Albion Scipio reservoir and construct a three-dimensional model of the reservoir. It will also be useful in selecting wells to analyze that might have core or cuttings. The dolomitized intervals were identified from drilling records for each well.

Organizing and compiling other large digital datasets – Numerous digital datasets for Michigan oil and gas wells are being combined into a single complete dataset (we currently have >25 million cells of data) for use in this project. An example of the parameters included are as follows:

- Cored wells – this is a listing of all known cored wells from Michigan. This list is compiled from private and public sources. It includes well location information, cored interval, cored formations, storage location of the core (if known), any analyses performed on the core (e.g. P&P).

- Thin sections – well name, footage interval, formation and repository location of thin sections.

- Core Analyses – conventional or special core analyses with footage analyzed and core properties (usually P&P) as reported in item #2 above.

- Drill cutting samples – well name and location along with depths and sample increment. There is also a database with numerous chromatographic analyses of bulk cuttings. Data includes abundance of C-5 though C-26 derived from solvent extraction on cuttings samples.

- Engineering parameters – lists of selected parameters and data including: bottomhole pressure, gas chemistry, and oil/gas ratio.

- Mudlogs – contains lithologic descriptions, gas log and drilling comments.

- Wireline logs – catalog of all logs run in Michigan wells, list of those in WMU collection, list of scanned images, and list of LAS digital logs.

Compiling exhaustive bibliography and reference reprint collection – Using Endnotes software and extensive database of geologic and engineering references has been compiled and entered into the Endnotes software system.

- Subtask 2.1 We currently have >1200 references compiled and entered into an Endnote data base on reservoirs aspects of dolomite. Of these, 372 are specifically on the Michigan Basin reservoirs in the zones of interest, with the remaining references covering various aspects of dolomitization and dolomite reservoirs that may have application to our project goals. The references will be added to a digital collection for distribution through WMU to Michigan Basin operators and others with interest.

  We are on schedule per our original proposal whereby the majority of Subtask 2.1 was completed during Phase I with additional work continuing through Phase II and finalizing in Phase III.

- Subtask 2.2 Individual producing unit data bases have been constructed in Microsoft Access and Excel that include fields, numbers of wells, oil and gas production, brine production, active and abandoned wells. Currently we have over 25 million data points in various categories including well location coordinates and ID, TD, IP, Salinity and Water Chemistry, Production History, Core and Perforation locations, Formation tops, and results of various core analyses. Additional engineering parameters including porosity, permeability, derived water saturations and type/style of dolomite are still being added, and will continue to be added during Phase III to the 3 data bases.

Production summaries and curves have been created for 44 fields in the Trenton/Black River, 1151 fields in the Niagaran, and 141 fields in the Devonian. These data are currently being analyzed in relationship to the distribution of mapped fracture areas in the basin, with our initial focus on the Devonian as mentioned previously. These results are being correlated to fields with core data and petrophysical analyses to facilitate selection of samples for further petrographic and geochemical analysis for dolomite genesis and reservoir quality.

We are on schedule per our original proposal whereby the majority of Subtask 2.2 was completed during Phase I with continuing work through Phase II and finalizing in Phase III.

- Subtask 2.3
    1. Devonian Dundee well penetration Petra projects (i.e. data bases) for 39 central Michigan Basin counties have been created with detailed structure contour maps for a 24 county region (using error checked tops data). Data base includes digital logs for ~450 wells with numerous cross sections showing log-based (litho-density) variations in lithofacies. Dundee Formation, member scale mapping and member tops/log character analysis is ongoing, with our intention being to test the feasibility of identifying primary facies (and therefore porosity/permeability distribution) from combined gamma ray and litho-density log analysis.

    2. Silurian Niagaran well penetration Petra projects (data bases) for Macomb County (northern trend) and Ray Reef Field (southern trend) have been developed along with preliminary structure maps. Included to date are spatial data for ~700 wells and digitized logs for ~30 wells from Ray Reef.

3. Ordovician Trenton/Black River Group well penetration Petra project (data base) currently includes spatial data for 2080 wells and digital logs for 169 wells. An extensive library of maps and cross sections have been made from the Albion-Scipio and Stoney Point fields with an emphasis on lithofacies identification based upon litho-density log signatures.

We are on schedule per our original proposal whereby the majority of Subtask 2.3 was completed during Phase I with continuing work through Phase II and finalizing in Phase III.

Task 3.0 – Characterization of Dolomite Reservoirs in Representative Fields

The characterization of select dolomite reservoirs (Task 3) has been the major focus of our efforts in Phase II/Year 2. Fields have been prioritized (after being identified in Task 2, Phase I) based upon the availability of rock data for interpretation of depositional environments, fracture density and distribution as well as thin section, geochemical, and petrophysical analyses. The majority of our Task 3 efforts to date have been in the Devonian and Silurian sections, and we have presented results at the regional and national AAPG meetings (see Appendix 2). Our major push on the Ordovician part of the section ramped up in Quarter 3 and significant progress has been made. As an example, at the ES AAPG in October 2006, we presented one oral paper as well as a poster with core workshop on the Ordovician Trenton/Black River. Task 3 objectives are on time and target for Phase II as per our original proposal.

Approach and Methodology

In order to investigate the geological origins and controls on the occurrence of dolostone reservoirs in the three formations of interest we have been compiling available digital subsurface geological data (mostly from the Michigan Department of Environmental Quality, Geological Survey Division {MDEQ-GSD}) including formation tops, wire-line logs, and driller's reports. Where appropriate we compiled these data into tabular spatial databases as discussed above. These spatial databases were used to construct Geographic Information Systems files (utilizing both ArcGIS and Petra software), maps and cross sections of important geological properties including the spatial distribution of dolomite versus limestone relative to structural features and oil field occurrences in the Michigan Basin. For the Devonian, quality controlled Dundee Formation tops from a well database with more than 25,000 wells (originating from J. R. Wood, MTU Subsurface Visualization Lab) were used in the structural mapping.

Results to Date – Devonian and Ordovician (Figures 1-6, and 26-28 respectively)

Structural mapping and log analysis in the Dundee (Devonian) and Trenton/Black River (Ordovician) suggest a close spatial relationship among gross dolomite distribution and regional-scale, wrench fault-related NW-SE and NE-SW structural trends. A high temperature origin for much of the dolomite in the 3 studied intervals (based upon initial fluid inclusion homogenization temperatures and stable isotopic analyses, see Table 1) coupled with persistent association of this dolomite in reservoirs coincident with wrench fault-related features, is strong evidence for these reservoirs being influenced by hydrothermal dolomitization. Ongoing efforts will be focused on determining whether the hydrothermal dolomite represents the only phase of dolomite in these fault-related fields, or whether there is evidence of low temperature dolomitization as well. In either case, our main concentration is whether the reservoir quality of the dolomite can be tied to primary facies type and/or an established sequence stratigraphic framework, either of which will enhance the predictability of such reservoirs beyond that of just regional structural control.

Devonian Dundee Formation

The Middle Devonian Dundee Formation consists of two subsurface units, the Reed City and the Rogers City (Gardner, 1974). The Reed City Member initially transgressed the Michigan basin following restricted marine conditions that existed throughout lower Middle Devonian Detroit River Group time. The Reed City member is interpreted as a generally shoal water assemblage including grainy carbonates, stromatoporoid reefs, and supratidal/evaporitic facies in a overall regressive pattern stratigraphically. More open marine facies (Reed City "equivalent") predominate in the eastern basin, while more restricted evaporite-bearing facies (Reed City Member) occur to the west (Gardner, 1974). The Reed City comprises a complex primary facies package in the basin that is not well known. The Rogers City Member overlies various facies of the Reed City at a generally sharp, probable marine flooding surface marking rapid marine transgression. Primary depositional facies in the Rogers City are incompletely known but, in general, were apparently lithologically homogeneous basin wide and consisted mostly of open marine lime wackestone to mudstone.

Our analyses to date have important implications for both new exploration plays and improved enhanced recovery methods, especially in the Dundee Formation "play" in Michigan – i.e. on the basis of interpreted (first order) fracture-related dolomitization control on the distribution of hydrocarbon reservoirs. In an exploration context high-resolution structure mapping using quality controlled well data should provide leads to convergence zones of fault/fracture trends not necessarily related to structural elevation. Acquisition of high-resolution seismic data in areas with prospective structural grain may provide decreased risk for fractured Dundee exploration drilling.

Field scale structural mapping of top Dundee with high quality well data indicates a spatial correlation between subtle structure and reservoir facies variations in the Rogers City Member. In fields with suitable well log control, mapped structure suggests faults with limited throw (generally less than tens of feet). These faults and related fractures may have provided geometrically-complex fracture conduits for dolomitizing fluids permeating through otherwise tight lime wackestone of the Rogers City.

Preliminary fluid inclusion homogenization temperatures and stable isotopic (C/O) analyses from Devonian Dundee/Rogers City dolostone samples suggest pervasive hydrothermal dolomitization in core samples from 2 wells studied to date.

Both the saddle dolomite which occurs as vein and vug fill, as well as much of the matrix dolomite is apparently of hydrothermal origin in these samples.

Application of fracture models to reservoir characterization in secondary and tertiary recovery projects in existing fractured Dundee fields, especially when tied to detailed facies mapping, may result in substantial additional recovery from fields that typically had low (<30%) primary recovery factors. Careful consideration of fracture orientations and water coning problems should decrease risk in enhanced recovery activities.

Undoubtedly more complex, hybrid reservoir types exist in dolomitized lower Dundee/Reed City Member lithofacies in the central basin as a result of complex, early fluid flow through primary limestone porosity conduits in a reflux system(?) in addition to fracture generated pathways in fault/fracture convergence zones. Continuing work in Phase 3/Year 3 is necessary to understand Reed City Member dolomitization processes in Michigan with respect to the relationship between primary facies and/or sequence stratigraphic framework.

<u>Trenton/Black River Formations</u>

Fields in the Ordovician Trenton/Black River Formations in Michigan, most notably the Albion-Scipio Field, are classic examples of geometrically complex dolomite reservoirs modeled by the hydrothermal dolomite reservoir facies (HTDRF) concept. Application of models for reservoirs of this generic type are controversial but of great current interest for both exploration and enhanced recovery in the petroleum industry. Structural analysis of Michigan Trenton/Black River (e.g. Hurley and Budros, 1990) suggests a relationship between probable reactivated basement wrench faults, anticlines with steep margins, and fractured, hydrothermal dolomite reservoirs. Riedel shear deformation mechanisms, including complex flower structure fracture patterns, are suggested as important components in the development of these dolomitized fields. The transport of dolomitizing hydrothermal fluids delivered to various reservoir units is thought to result from flow through fractures, associated with periodically reactivated wrench faults, as well as primary permeability conduits.

The presence of a regional hydrothermal fluid "aquifer" unit may be a critical component of these complex hydrothermal fluid flow systems.

Trenton-Black River Pools are characterized by stratigraphic traps in dolomitized limestone within the Upper and Middle Ordovician Trenton and Black River groups. The Albion-Pulaski-Scipio-Stoney Point trend, which was discovered in 1957 (Figure 5), makes up the largest field in the Michigan Basin (~120 MMBO). The Trenton/Black River rocks are present in the subsurface throughout the Lower Peninsula and in parts of the Upper Peninsula and Wisconsin, but, to date, almost all discoveries have been from the southern part of the Lower Peninsula of Michigan and the adjoining parts of Indiana and Ohio. Oil and gas pools occur mainly as stratigraphic traps resulting from porosity and permeability variations between porous dolostone and tight regional limestone. In a definitive study by Hurley and Budros (1990) Trenton/Black River production in the Albion-Scipio field was shown to be from classic fracture-controlled dolostone reservoirs related to northwest-southeast fault and fold trends related to a regional structural grain. In the Albion-Pulaski-Scipio-Stoney Point trend, generally low porosity limestone is altered to a relatively "narrow fairway of vuggy, fractured, and cavernous dolomite" (Hurley and Budros, 1990).

An increased percentage of activity in Quarters 3 and 4 was focused upon the Trenton/Black River formations. Based upon production data analysis completed during quarters 1 & 2, and a review of available core materials, it was decided to concentrate upon developing a new, updated analysis and interpretation of the Trenton – Black River cores from the Albion Scipio Field. This field is the only giant field (>120 MMBO) found to-date in Michigan. Discovered in 1957, this field has never been subjected to more recently developed geological analytical techniques and interpretation. In particular, there has never been a sequence stratigraphic framework developed for the producing Ordovician Trenton – Black River reservoirs in the field area. Work this past quarter has shown that it is possible to develop just such a stratigraphic framework, and that this framework will in turn allow for the development of new exploration models and concepts. Specific accomplishments include:

(1.) The exploration, discovery and early drilling history of the Albion-Pulaski-Scipio Trend were complied and analyzed for field-wide similarities and differences. These data were assembled into poster format and presented along with portions of three Trenton – Black River, Albion-Scipio Field cores at the "Core Blast" presentation at the "American Association of Petroleum Geologist (AAPG) Eastern Section Meeting" in Buffalo, New York during October 10-16, 2006.

(2.) The Hergert #2, Skinner #1 and Mann #6 cores from the Albion-Scipio field were examined in detail, fully described, and calibrated to other available data types such as electric logs, driller reports, porosity and permeability analyses, etc. These data were all assembled into poster format and presented at the "Core Blast" for the "American Association of Petroleum Geologist (AAPG) Eastern Section Meeting" in Buffalo, New York during October 10-16, 2006.

(3.) Preliminary results from the examination of the Hergert, Skinner and Mann wells were compiled and organized into a presentation entitled "Albion-Scipio Field - What Does a Detailed Look at Cores Tells Us about the Reservoir?" (Gillespie, Robb; Barnes, David; Grammer, G. Michael; and Harrison, William, III). This was presented by Robb Gillespie at the "American Association of Petroleum Geologist (AAPG) Eastern Section Meeting" in Buffalo, New York during October 10-16, 2006.

(4.) Samples were selectively collected from the Hergert, Skinner and Mann cores for isotopic (C/O) analysis. Preliminary examination of the data indicates no difference between fracture fill dolomites and dolomite recrystallized within the host rock (matrix). It appears that: (1) all the dolomites resulted from the same emplacement episode, or (2) the matrix dolomites have been “reset” by high hydrothermal temperatures of subsequent episodes.

Results to Date – Silurian (Figures 7-25)

For the Niagaran (Silurian), a comprehensive high resolution sequence stratigraphic framework has been developed for a pinnacle reef in the northern reef trend (Fig. 7) where we had 100% core coverage throughout the reef section. Our next step is to test this sequence framework within a larger reef complex in the southern reef trend (Ray Reef Field). We have started a detailed geological characterization of the field utilizing 18 cores for development of a 3-D rock-based reservoir model that is scheduled to be developed during Phase III. Major findings to date are that facies types, when analyzed at a detailed level, have direct links to reservoir porosity and permeability in these dolomites (Figures 8-25). This pattern is consistent with our original hypothesis of primary facies control on dolomitization and resulting reservoir quality at some level. The identification of distinct and predictable vertical stacking patterns within a hierarchical sequence and cycle framework provides a high degree of confidence at this point that results will be exportable throughout the basin.

Ten petrophysically significant facies have been described in the northern reef trend, providing significantly more resolution than the standard 4-6 that are used most often in the basin (e.g. Gill, 1977). Figures 24 & 25 illustrate how the higher resolution facies analysis can be crucial for establishing porosity and permeability relationships in these reservoirs. Porosity and permeability values tend to increase towards the top in both the large and smaller (higher frequency) cycles (see Figure 15).

Initial petrophysical characterization (sonic velocity analysis under confining pressures) show a clear pattern that is dependent upon facies and resulting pore architecture (see Figures 16-21). Primary facies is a key factor in the ultimate diagenetic modification of the rock and the resulting pore architecture. Facies with good porosity and permeability clearly show relatively slow velocity values as would be expected, and low porosity and permeability samples exhibit fast sonic velocity values, again as expected. What is significant is that some facies that have high porosity values, either measured directly or from wireline logs, also have very fast sonic velocity values. This is due to these facies having a pore architecture characterized by more localized pores (vugs, molds or fractures) that are not in communication, resulting in facies with good porosity but poor permeability (Figures 19-21).

Stable isotopic analyses (C/O) show that most of the reefs evaluated to date have matrix values near Silurian seawater values, suggesting that the dolomite is early (and therefore formed as a result of either multiple episodes of isotopically similar waters, or one episode that dolomitized the entire reef – considered unlikely). Minor excursions of carbon (+) and oxygen (-) occur at a number of cycle boundaries (Figure 15). In general there is about a 1 per mil enrichment in C for dolomite relative to calcite. Under normal circumstances, diagenetic products resulting from the influence of meteoric fluids results in highly negative del-C values. Voice's (2005) summary of Earlier Silurian isotopes show carbon values ranging from -1 to +2.5 per mil, so these are about the same. The slight enrichment of del-C, at the same time that del-O is depleted, was reported by Karen Cercone (1985) as possibly being due to anaerobic fermentation of organics related to organic rich layers deposited during the ensuing transgression.

Subtask 3 is on schedule to be mostly completed by the end of Phase II or early in Phase III.

<u>Task 4.0 – Development of Geological Models and Assessment of Application Potential</u>

The initial stages of data evaluation and synthesis in Task 4 are well underway per our original proposal. Most of the effort on this task has necessarily had to follow results of Phase I (Task 2) and Phase II results of Task 3. We have entered into an agreement with Dr. Matthew Pranter, University of Colorado, who will be collaborating with us on the 3-D modeling efforts during Phase III.

Task 5.0 – Technology Transfer

Technology transfer efforts (Task 5) continue with formal presentations on the state and national levels as well as ongoing advertisement of the project's scope, anticipated results and funding agency on the WMU Department of Geosciences web site. During Year 2, we presented two papers at the National AAPG Meeting in Houston, TX (see Appendix 2), 2 papers at the Midwest Regional PTTC workshop on carbonate reservoirs, and 7 papers (3 professional and 4 student presentations) at the Eastern Section of AAPG in Buffalo. We also received an award, the Vincent E. Nelson Memorial Award for Best Poster presented at the 2005 ES AAPG Meeting (Sandomierski, Grammer and Harrison).

Equipment purchased during Phase II:

No capital equipment has been purchased in Phase II.

Summary Financial Records

Financial reports covering the period were mailed to NETL AAD Document Control, Pittsburgh, from Carole Nelson and Nick Griffith at WMU, most recently dated Oct. 30, 2006.

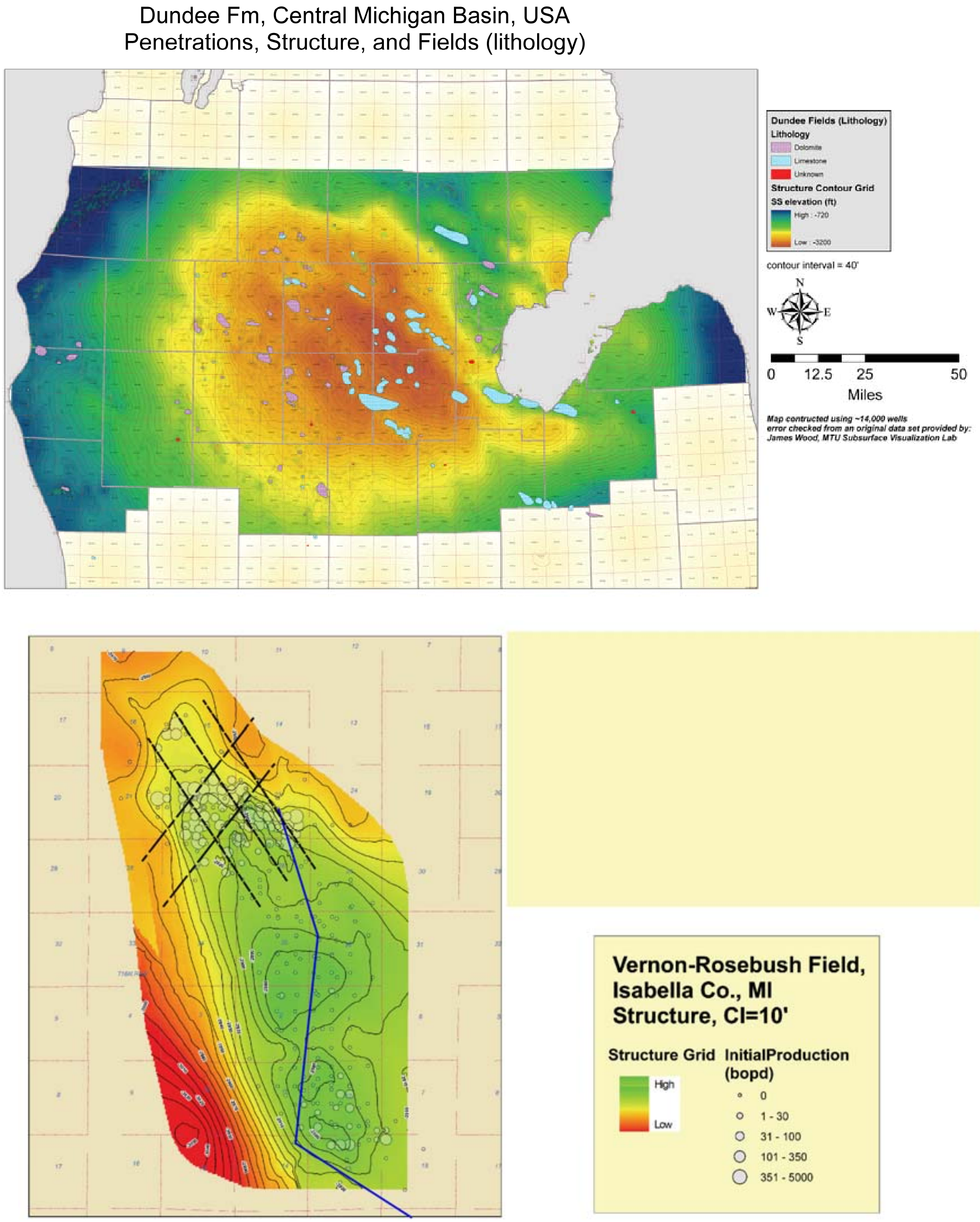

Figure 1. Structure contour map of the Devonian Dundee Formation (top) and details of one of the fields of interest.

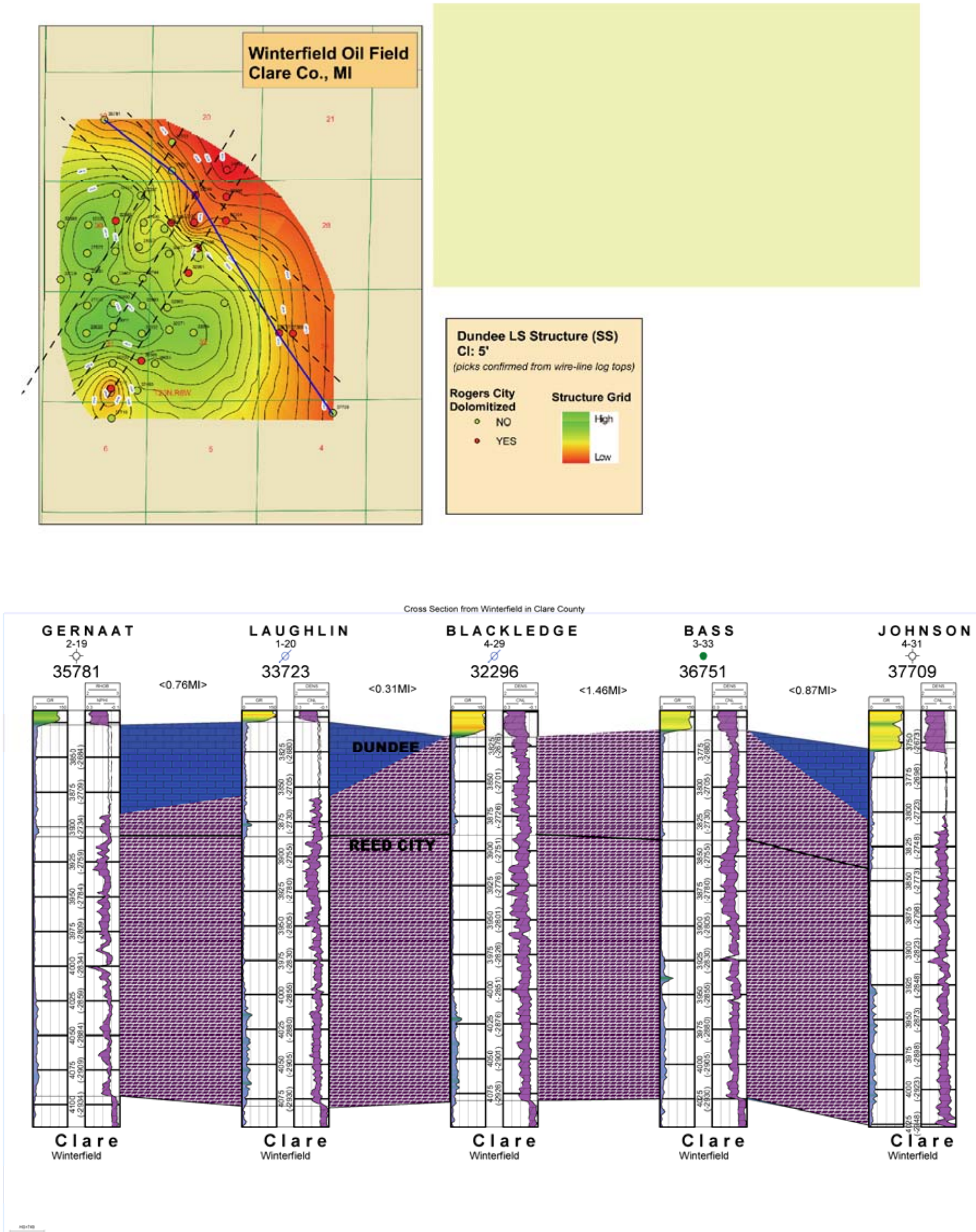

Figure 2-3. Structure contour map of the Devonian in Winterfield Oil Field with cross section showing pervasive regional scale dolomitization of the Reed City member of the Devonian Dundee.

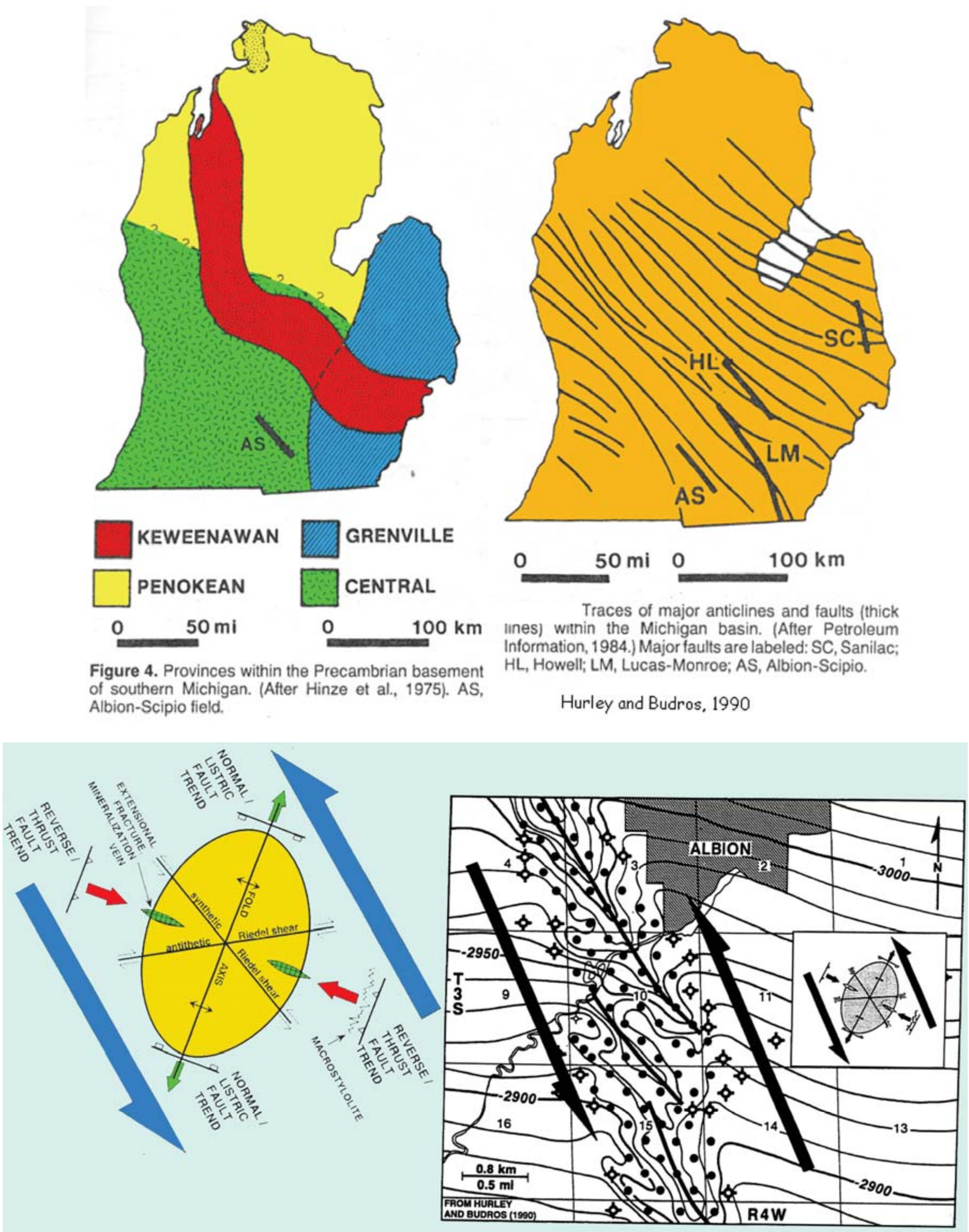

Figure 5. Riedel shear model for major fracture control at the Albion-Scipio fields in south-central Michigan (Trenton/Black River reservoirs).

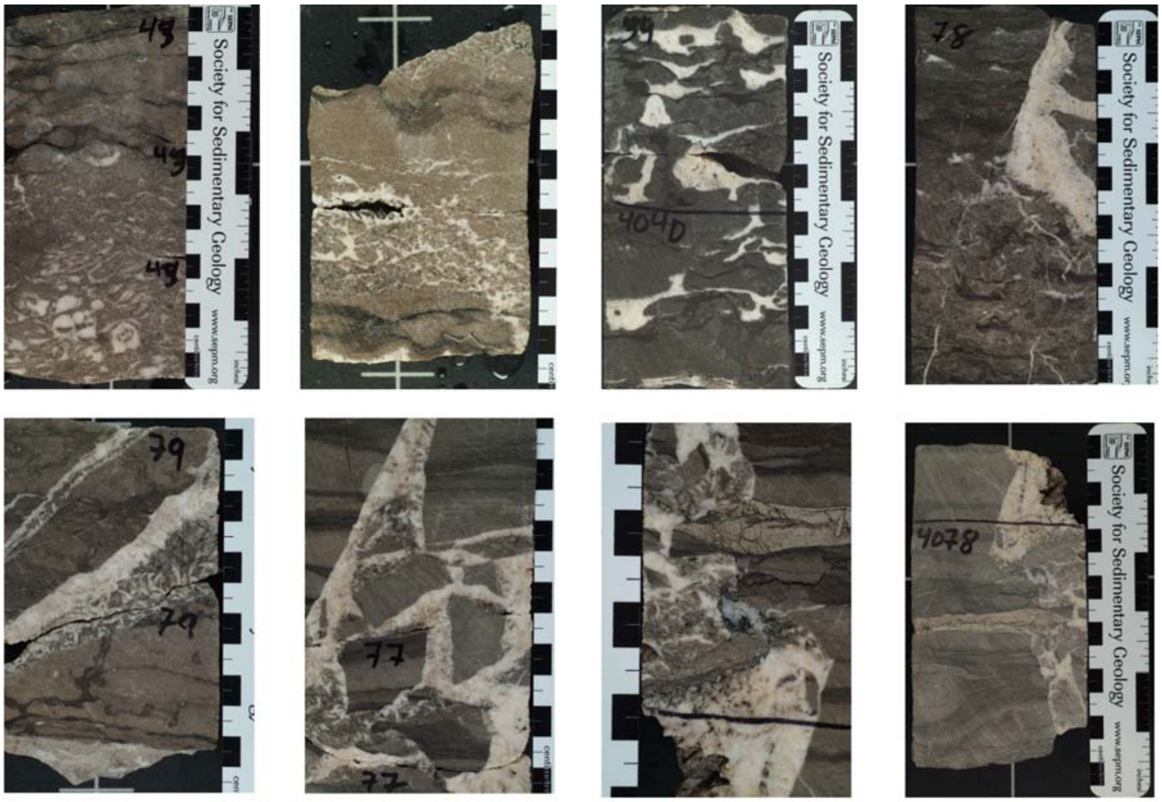

Figure 6. Hydrothermal dolomite filling fractures and primary porosity in Devonian Dundee and Trenton/Black River Formations.

Carbon and Oxygen Isotopic Composition of Saddle Dolomite: Selected Devonian Examples

Source	$\delta^{18}O$ ‰ PDB	$\delta^{13}C$ ‰ PDB	Reference
M. Dev., Manatoe, NWT	-17.33 to -6.25	-5.5 to -1.45	Morrow et al, 1990
M. Dev., Elk Point, N. Alb.	-12 to -14	-1.0 to +2.0	Dravis & Muir, 1992
M. Dev., Pine Point, NWT	-16.0 to -7.0	-3.8 to +1.7	Qing & Mountjoy, 1994
Dev., Sidang-Burdan, China	-9.58 to -6.78	-3.08 to -0.78	Schneider et al, 1991
U. Dev., Wabaman, Alb.	-8.99 to -5.71	-0.69 to +0.12	Mountjoy & Dihardja, 1991
U. Dev., Wabaman, Alb.	-6.7 +/- 0.7	0.55 +/- 0.5	Packard et al, 1989
Devonian, Michigan Basin	**-8.2 to -10**	**-0.6 to +1.34**	**This Study**

Table 1. Stable isotopic values for Devonian hydrothermal dolomites in Canada and China. Note values from Devonian fit well within published range. Fluid inclusion data from the same Devonian samples show homogenization temperatures of 105-140^{0}C, with an average of 122^{0}C (N=38).

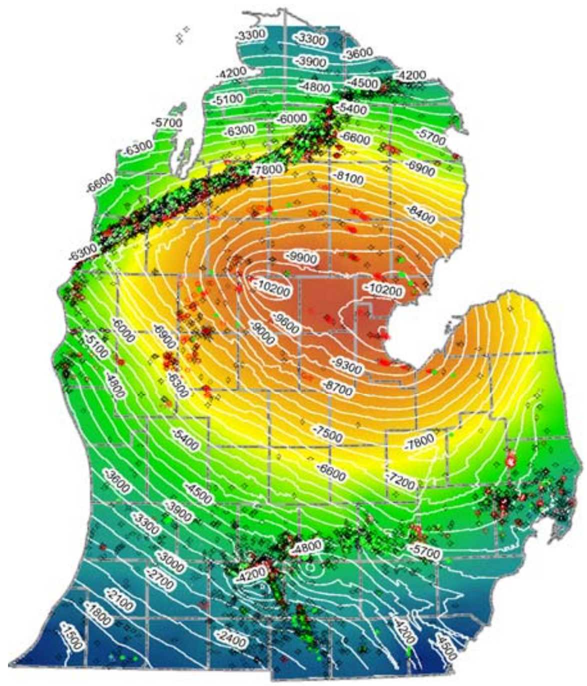

Brown Niagaran ("Niagaran Reefs", Middle Silurian) in the Lower Peninsula, MI. Structure depth (ss) interpolated from 9156 well penetrations.

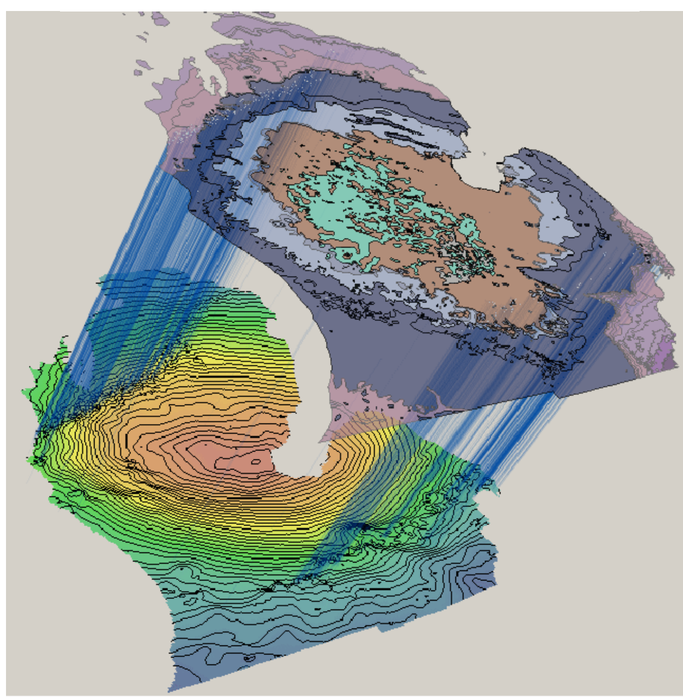

Brown Niagaran surface structure model with Michigan subcrop map and fields

Figure 7. Maps showing structure contour of Brown Niagaran with well penetrations.

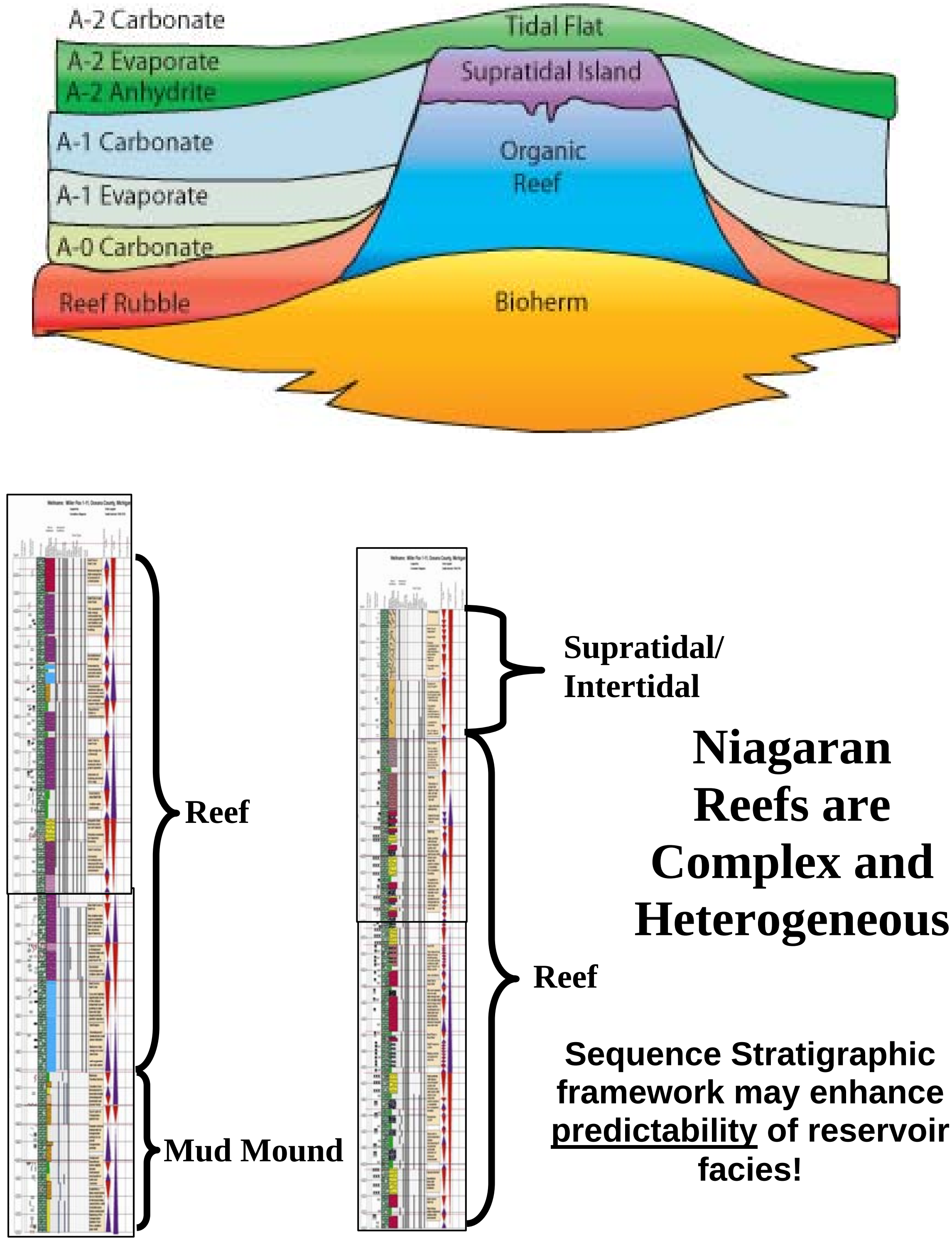

Figure 8. Schematic model for Niagaran reefs currently in use within the Michigan Basin (top) and detailed, high resolution facies analysis and sequence stratigraphic hierarchy established for the northern reef trend in work done to date.

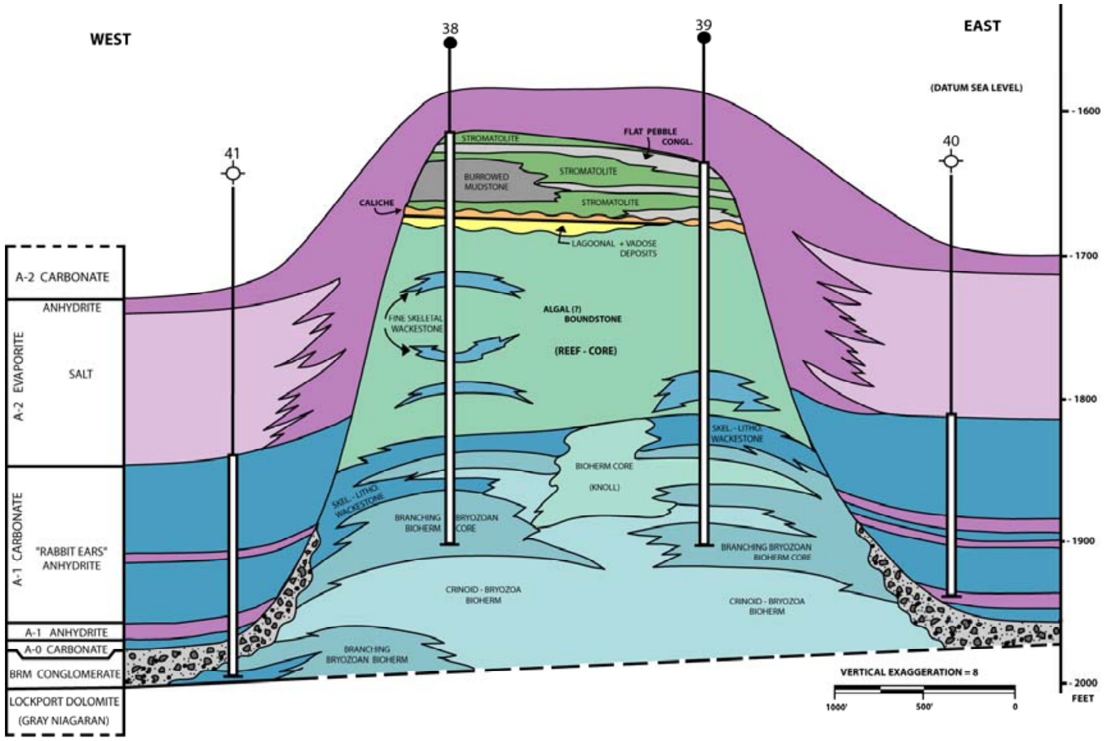

Figure 9. Schematic facies model of Belle River Mills reef showing evidence of lateral and vertical variability in facies (Gill, 1977). Detailed rock-based characterization of Niagaran reefs in this study illustrate that reservoir heterogeneity is much more complex, but that predictable patterns are revealed after constructing a sequence stratigraphic framework.

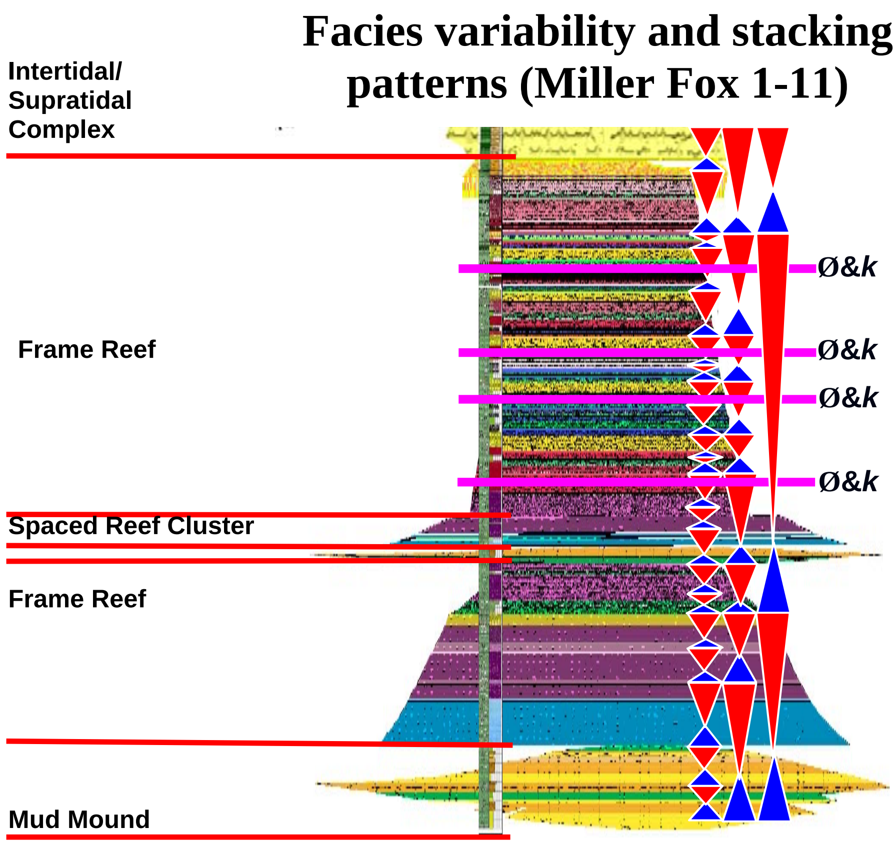

Figure 10. Schematic diagram for the 480 ft. Miller Fox 1-11 Niagaran reef showing the complex, but predictable facies succession and the sequence stratigraphic hierarchy established in this reef.

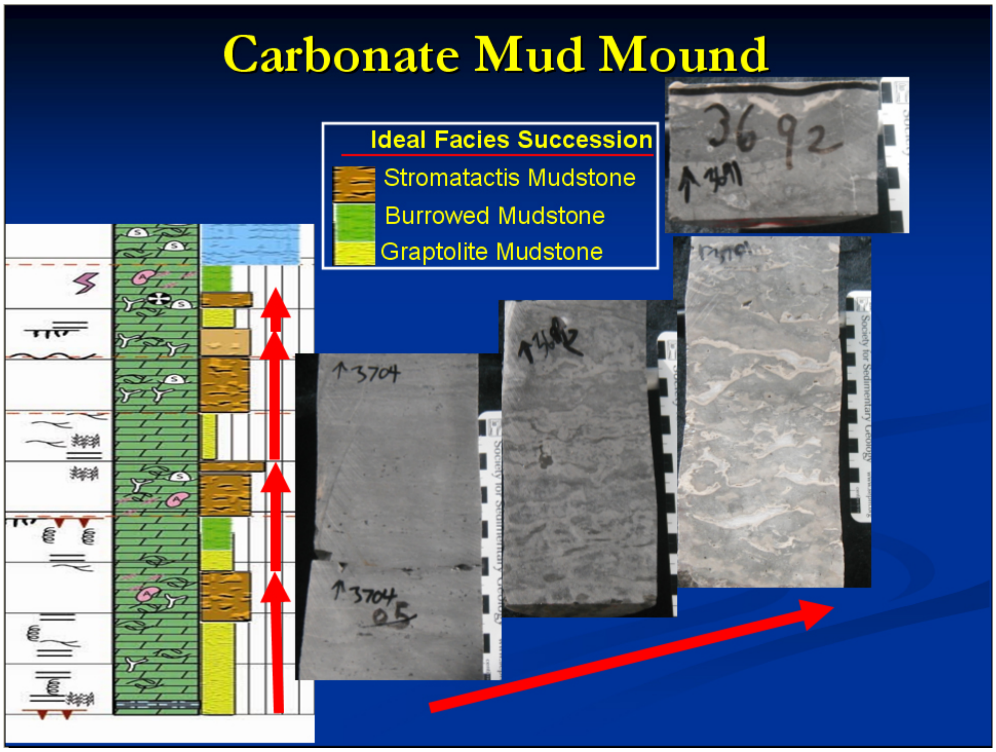

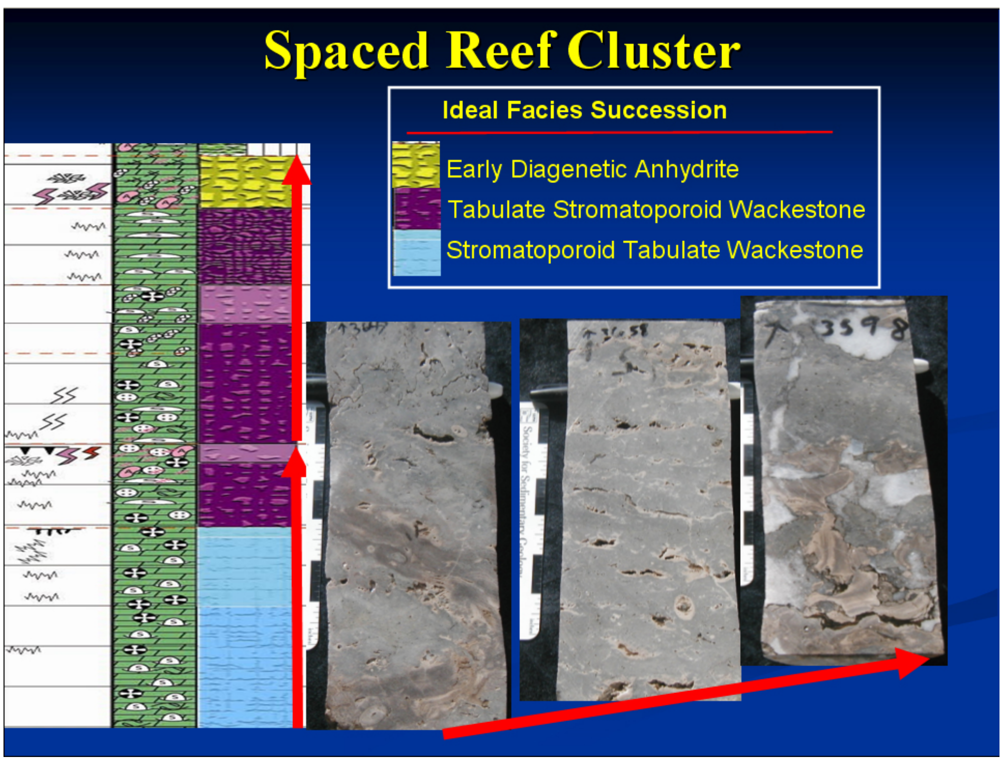

Figures 11 and 12. Examples of shallowing upward high frequency cycles that make up Niagaran reefs in this study.

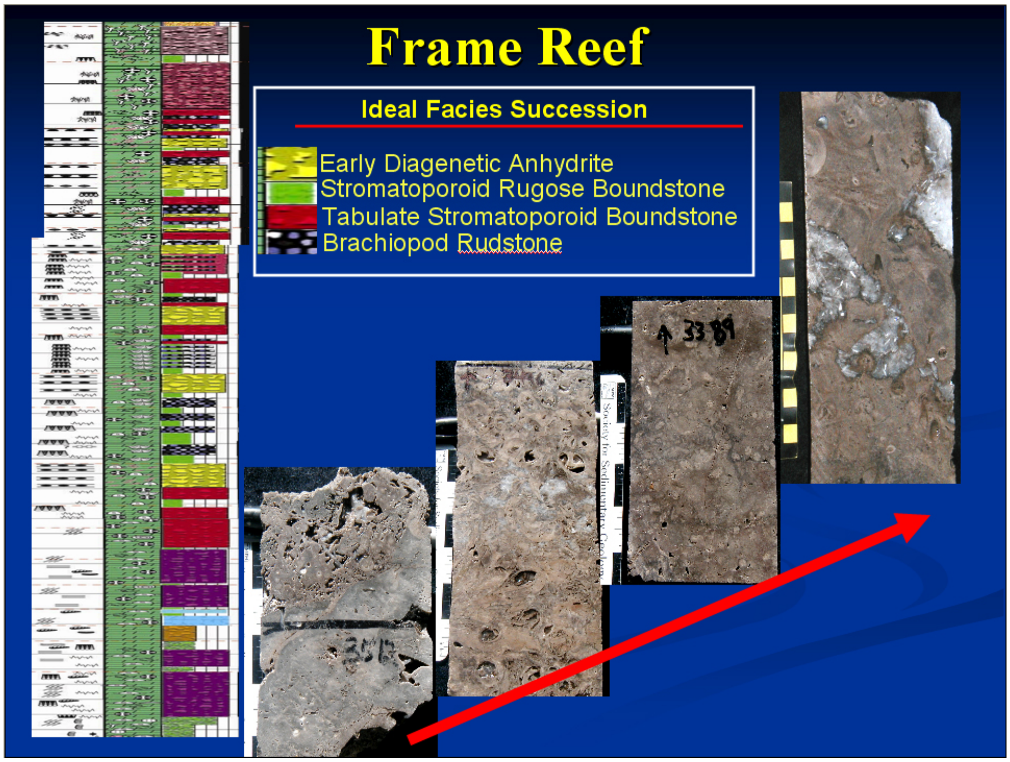

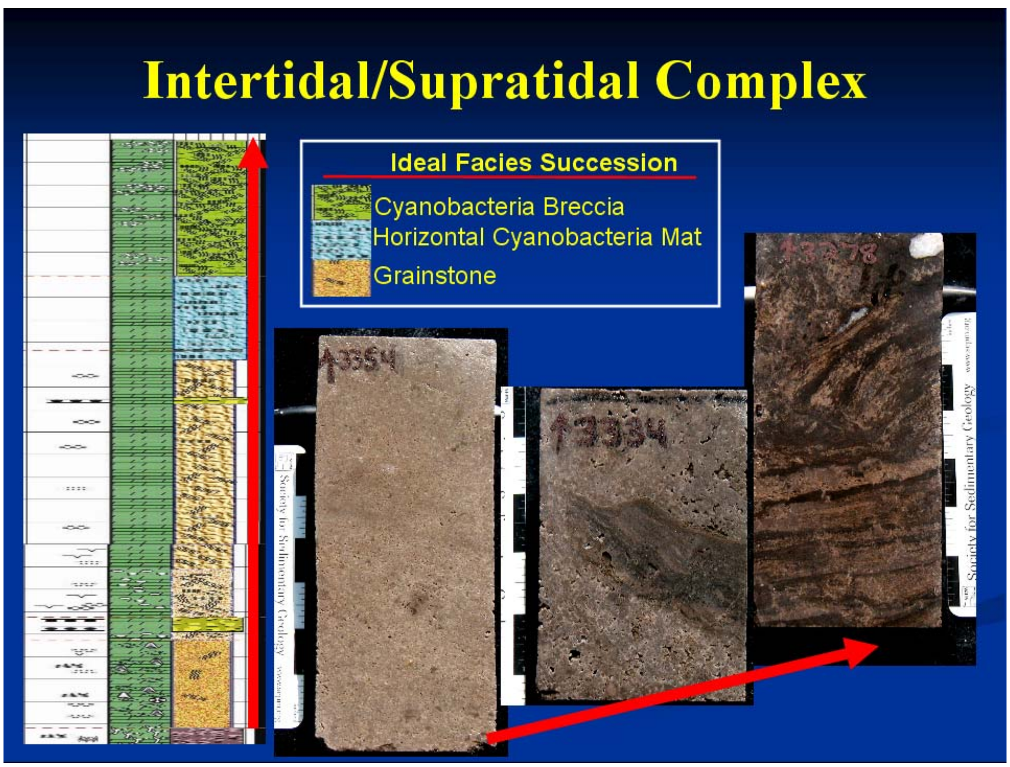

Figures 13 and 14. Examples of shallowing upward high frequency cycles that make up Niagaran reefs in this study.

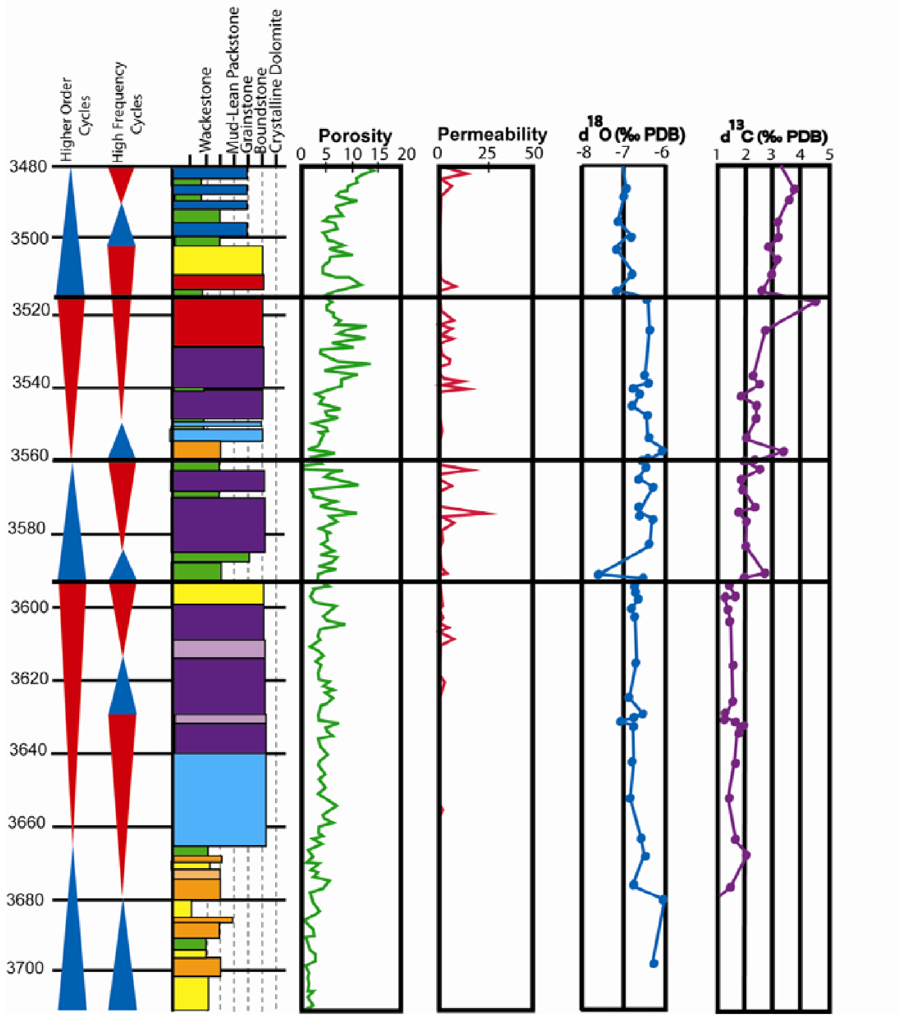

Figure 15. Details of portion of Miller Fox 1-11 reef illustrating the complex variability in facies vertically, and the correlation between porosity and permeability spikes near the top (regressive portion) of many of the high frequency cycles.

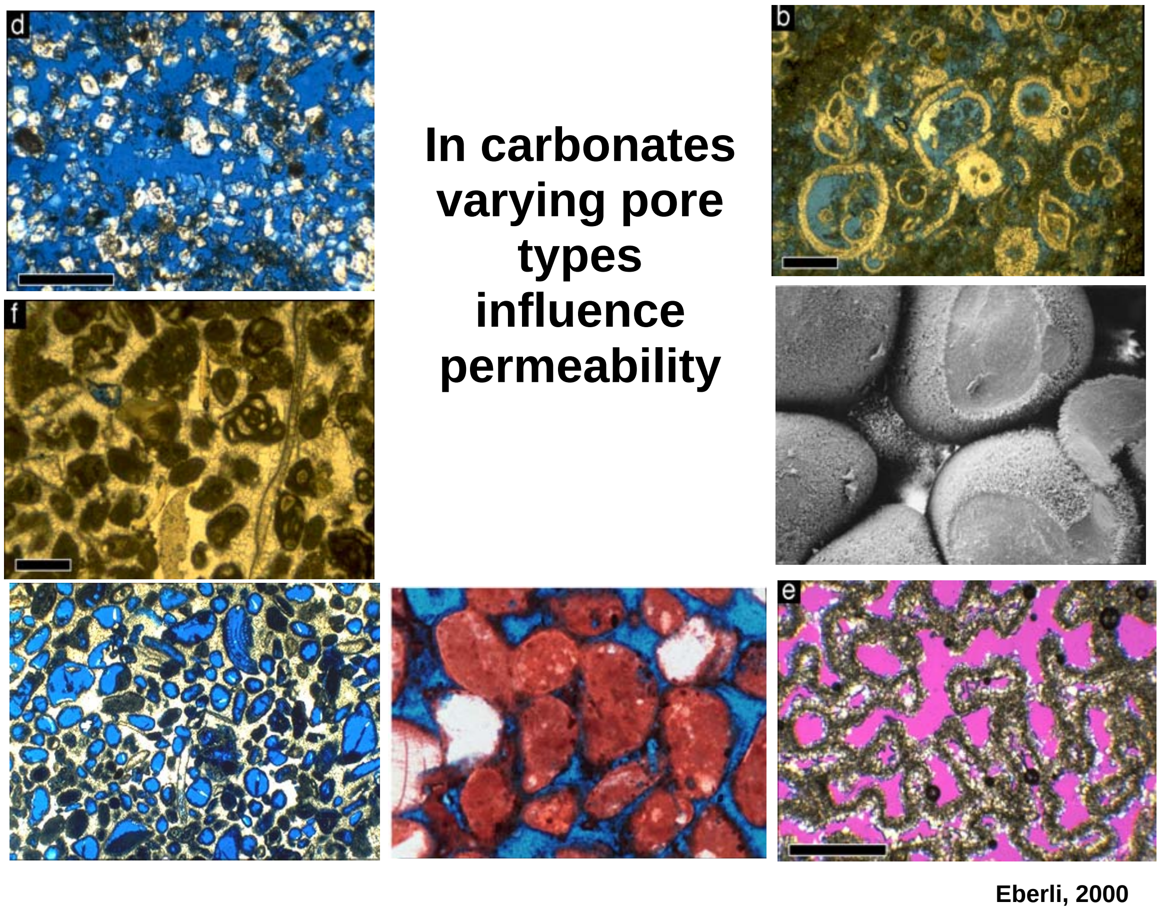

Figure 16. Examples of varying types of pore architectures common in carbonate rocks. Depending on the connectivity (i.e. permeability) of the pore network, carbonate rocks exhibit significant variability in sonic velocities.

Velocity versus Porosity in Carbonates

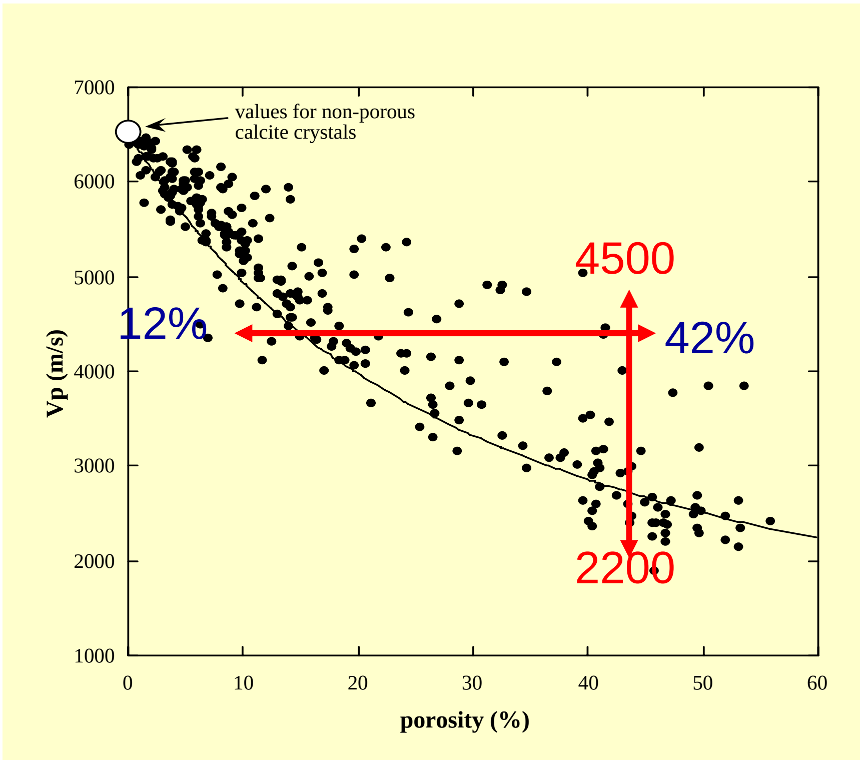

Figure 17. Plot illustrating variability in porosity, permeability and sonic velocity in carbonate rocks as a function of pore architecture (Eberli, 2004). Examples show how rocks with 42% porosity can have sonic velocities ranging from 2200 to 4500 m/s, or how rocks with an equivalent sonic velocity (in this case around 4500 m/s) may have porosities that range from 12-42%. This variability is a function of pore architecture which can be correlated back to primary depositional facies and positioning within a sequence stratigraphic framework.

Miller Fox 1-11

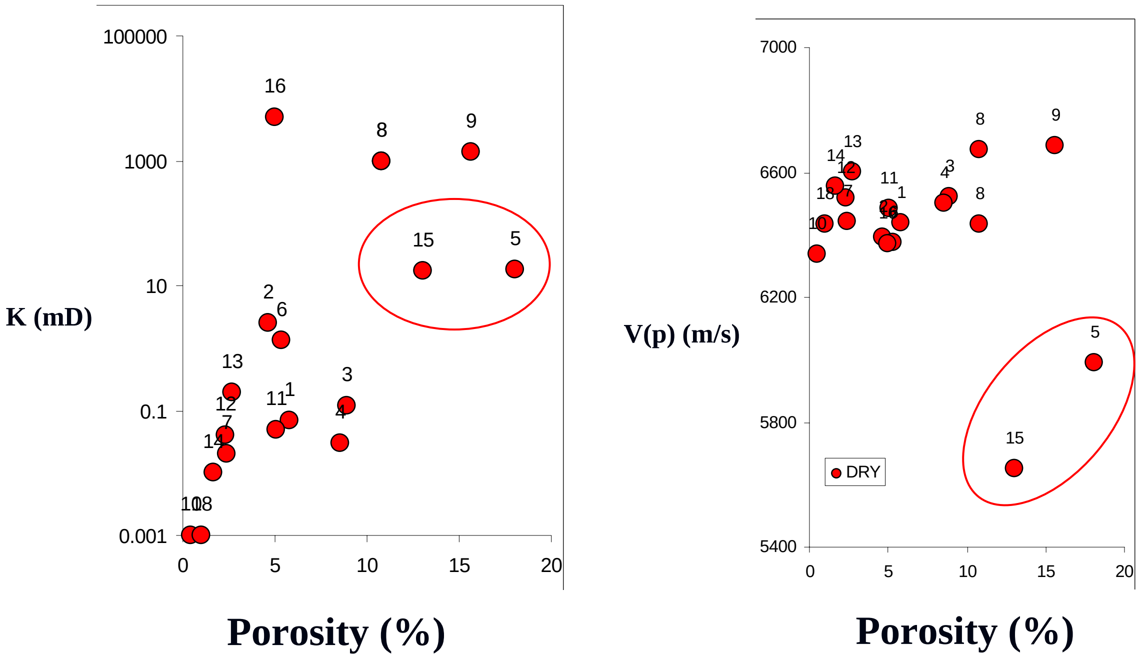

Figure 18. Porosity vs. P-wave velocity values for Niagaran reef facies. Cluster in upper left exhibits normal behavior (i.e. low porosity and high velocities) as does samples 5 and 15 (higher porosities with slower velocities). Velocity values were measured under confining pressures of 20-30 MPa, where 20 MPa equals about 1km of burial depth. Therefore, 30 MPa would equal approximately 1500m or 4920 feet which is consistent with the average burial depths for most Niagaran reefs in the Michigan Basin.

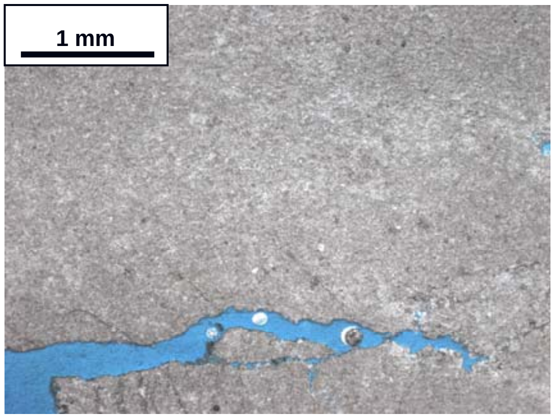

Isolated vugs and local fractures with no matrix

3572 ft.
ϕ = 5.0%
K = .05 mD
Vp = 6480m/s

Small (pin-point) vugs with minor matrix

3430 ft.
ϕ = 8.9%
K = .12 mD
Vp = 6400m/s

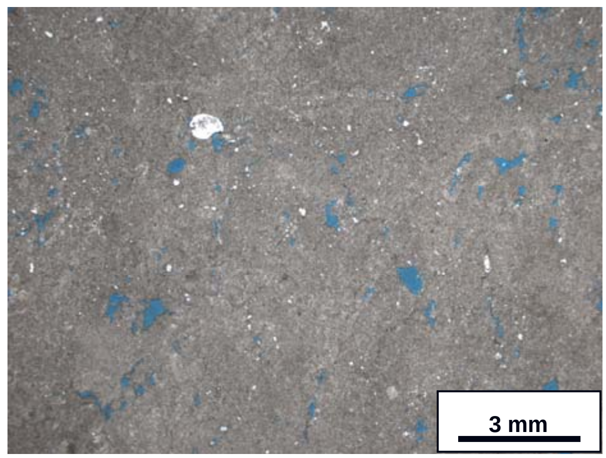

Figure 19. Thin section photomicrographs illustrating variability in porosity, permeability and sonic velocity dependent upon pore type and pore architecture.

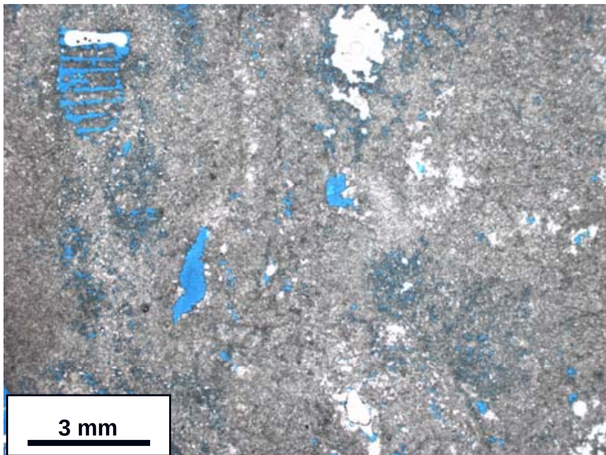

Large vugs + IX matrix

3480 ft.
ϕ = 18%
K = 17.8 mD
Vp = 5900m/s

Large vugs + IX matrix

3631 ft.
ϕ = 13%
K = 17.3 mD
Vp = 5630m/s

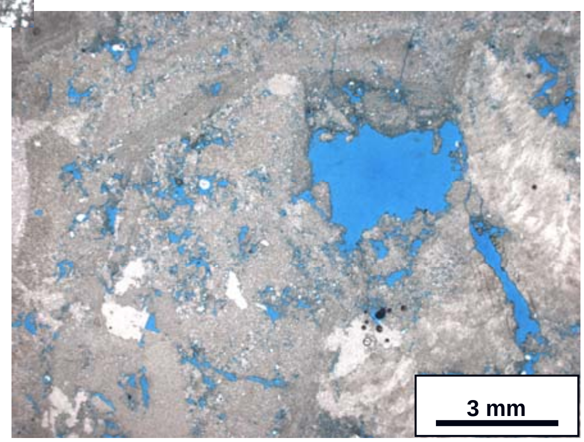

Figure 20. Thin section photomicrographs illustrating variability in porosity, permeability and sonic velocity dependent upon pore type and pore architecture.

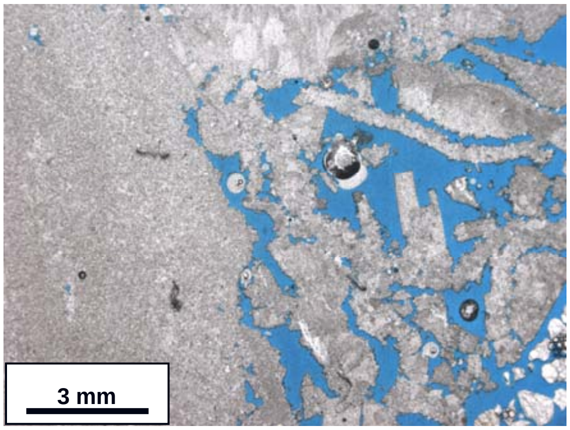

Large isolated vugs and fractures
Low matrix porosity

3524 ft.
ϕ = 10.8%
K = 990 mD
Vp = 6240m/s

Large isolated vugs and fractures
Low matrix porosity

3540 ft.
ϕ = 15.6%
K = 1368 mD
Vp = 6660m/s

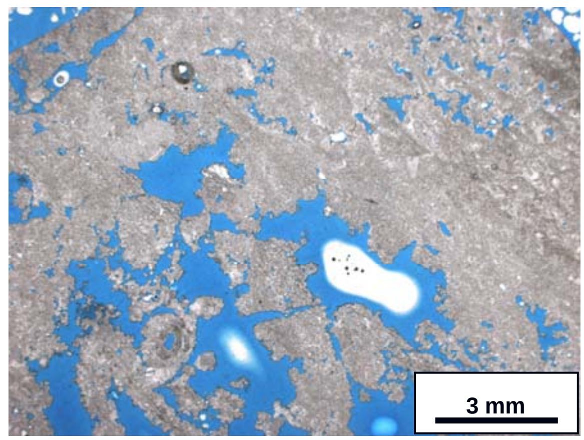

Figure 21. Thin section photomicrographs illustrating variability in porosity, permeability and sonic velocity dependent upon pore type and pore architecture.

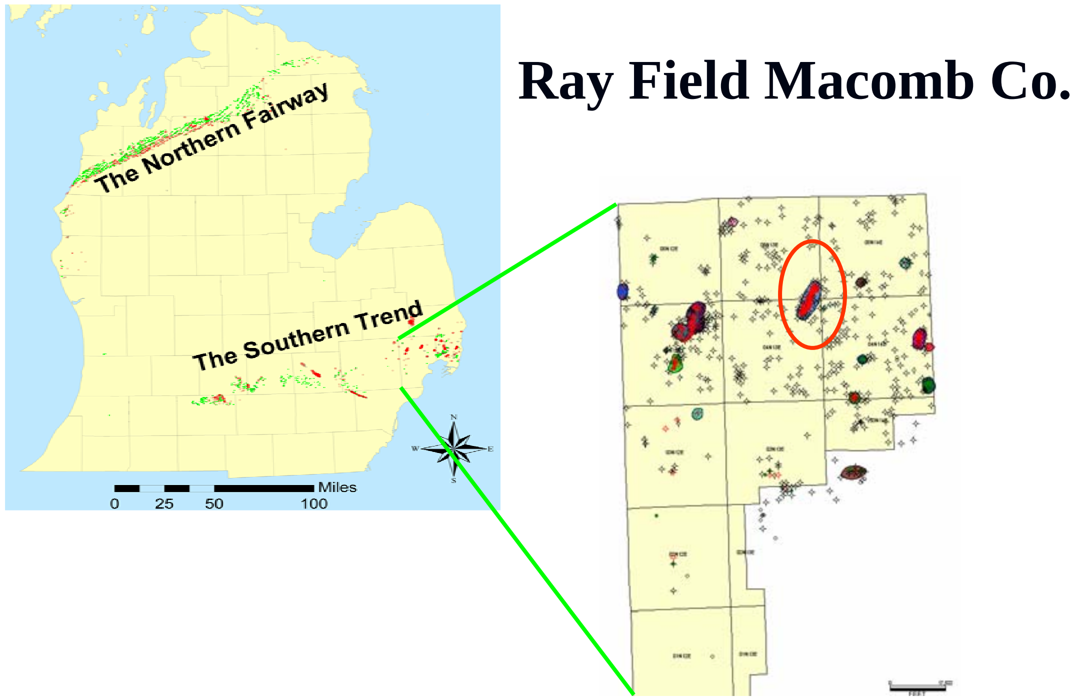

Figure 22. Location of Ray Reef field in the southern reef trend. Three graduate students are currently working on various aspects of reservoir characterization within this field, utilizing 18 cores for rock-based reservoir characterization and modeling.

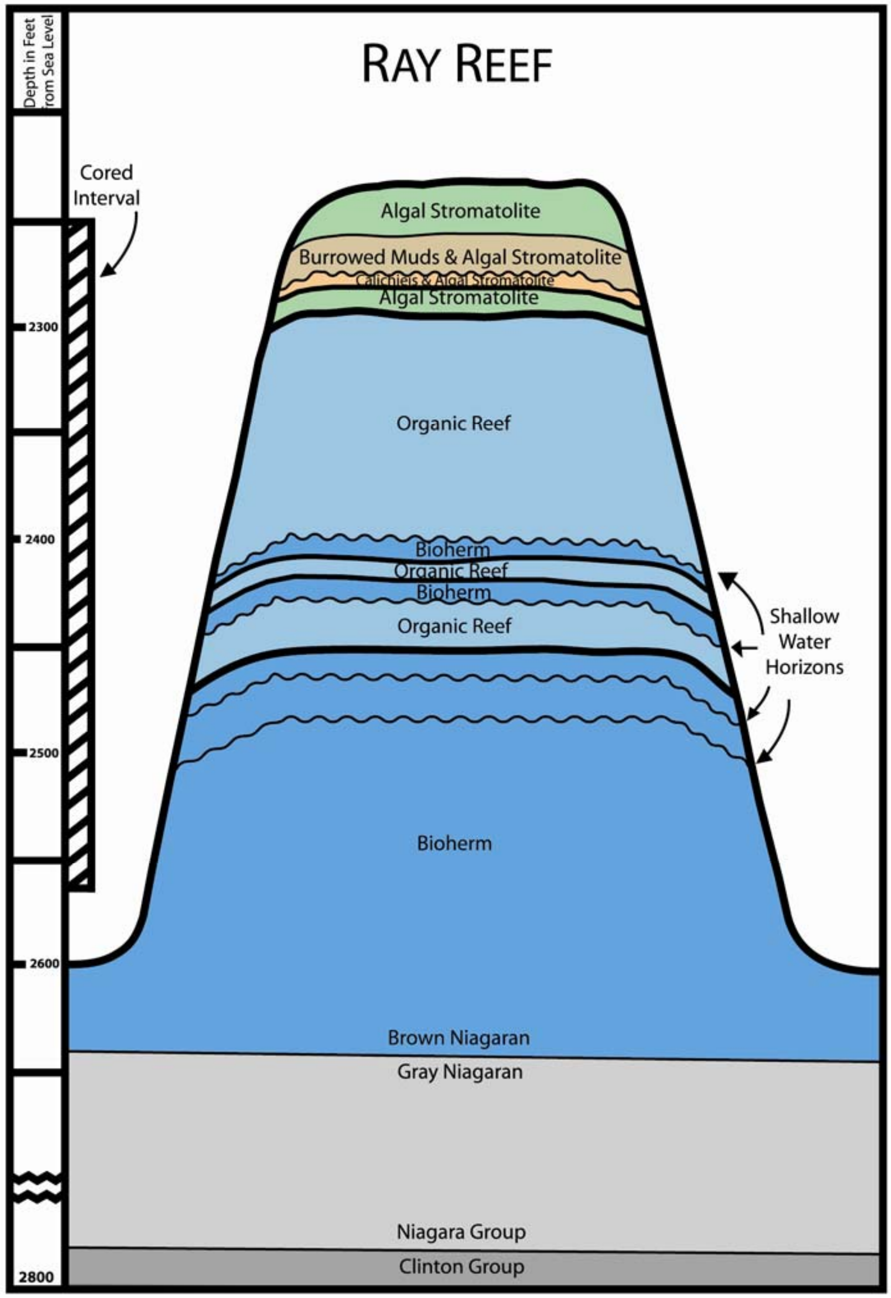

Modified from Balogh (1981)

Figure 23. Schematic diagram showing general vertical variability in Ray Reef identified by Balogh (1981).

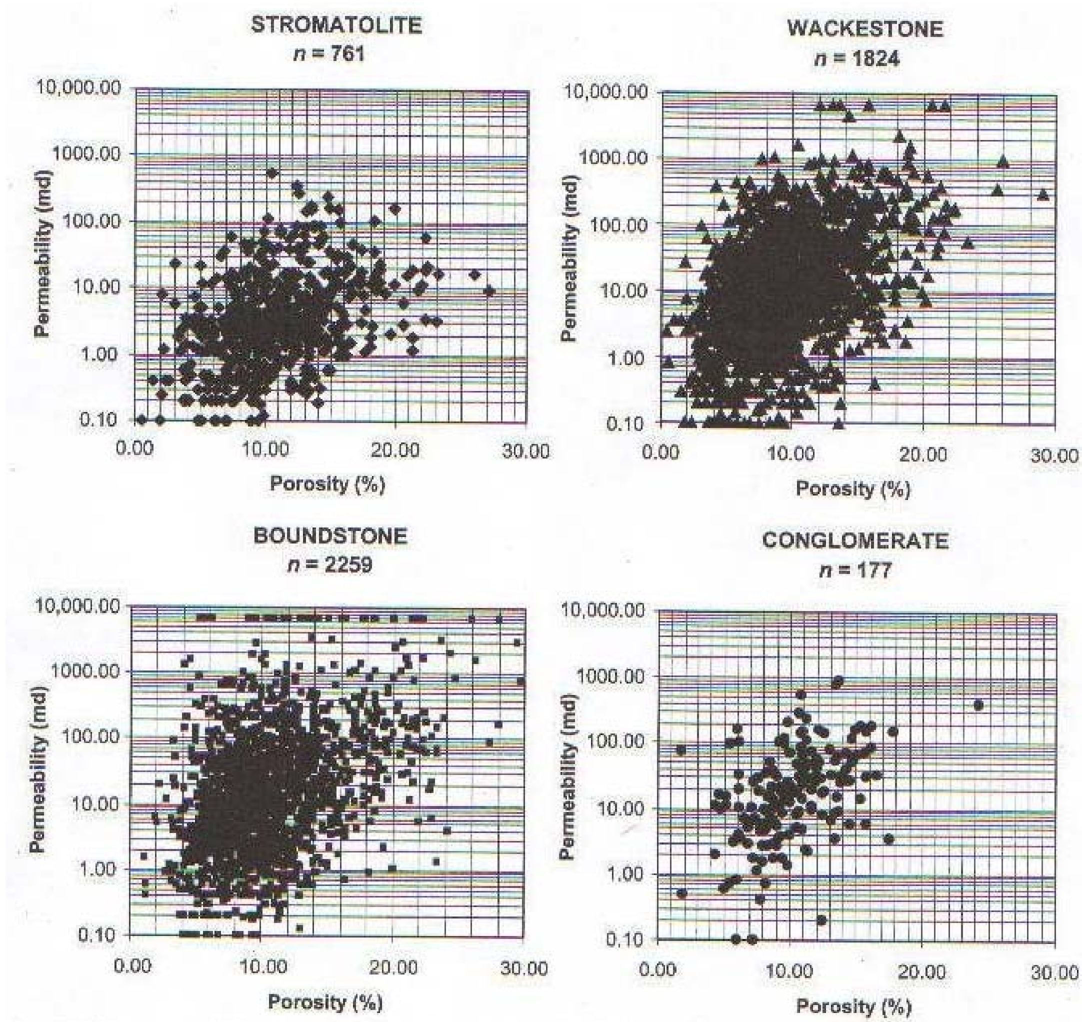

Figure 24. Core porosity and permeability from the Belle River Mills (southern reef trend) from Wylie and Wood, 2005, AAPG Bulletin, v. 89. The authors conclude that "**no apparent trend exists between the core permeability and core porosity by rock type", p. 420.**

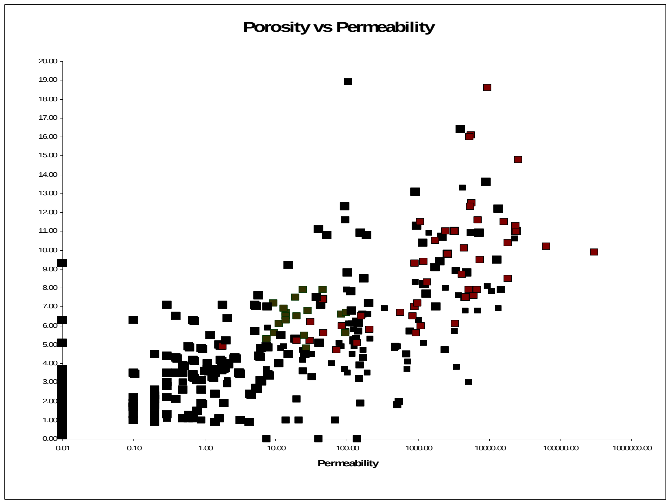

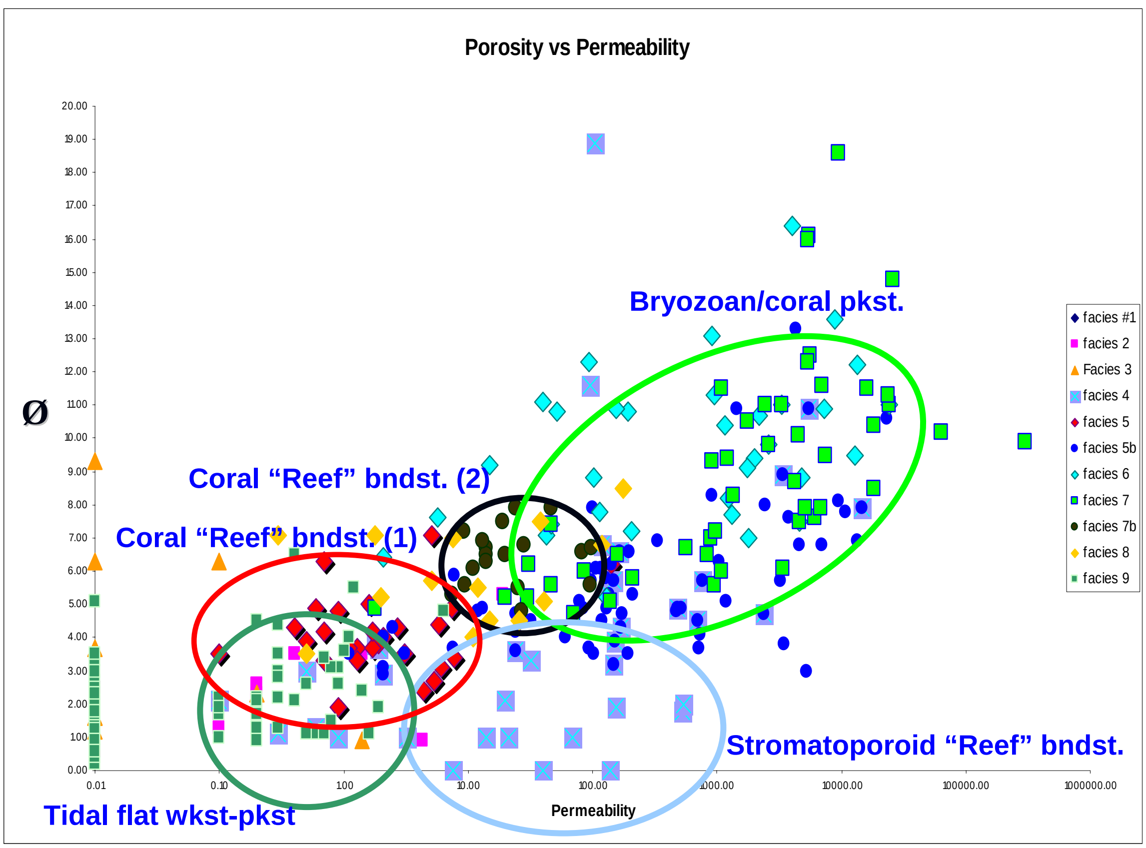

Figure 25. Top figure show similar distribution of core porosity and permeability for the Miller Fox 1-11 as observed in the Belle River Mills field data published by Wylie and Wood (2005). Lower figure illustrates how when the facies are broken up into more detailed geological-based units, there is a distinct correlation between facies type and reservoir quality (porosity and permeability).

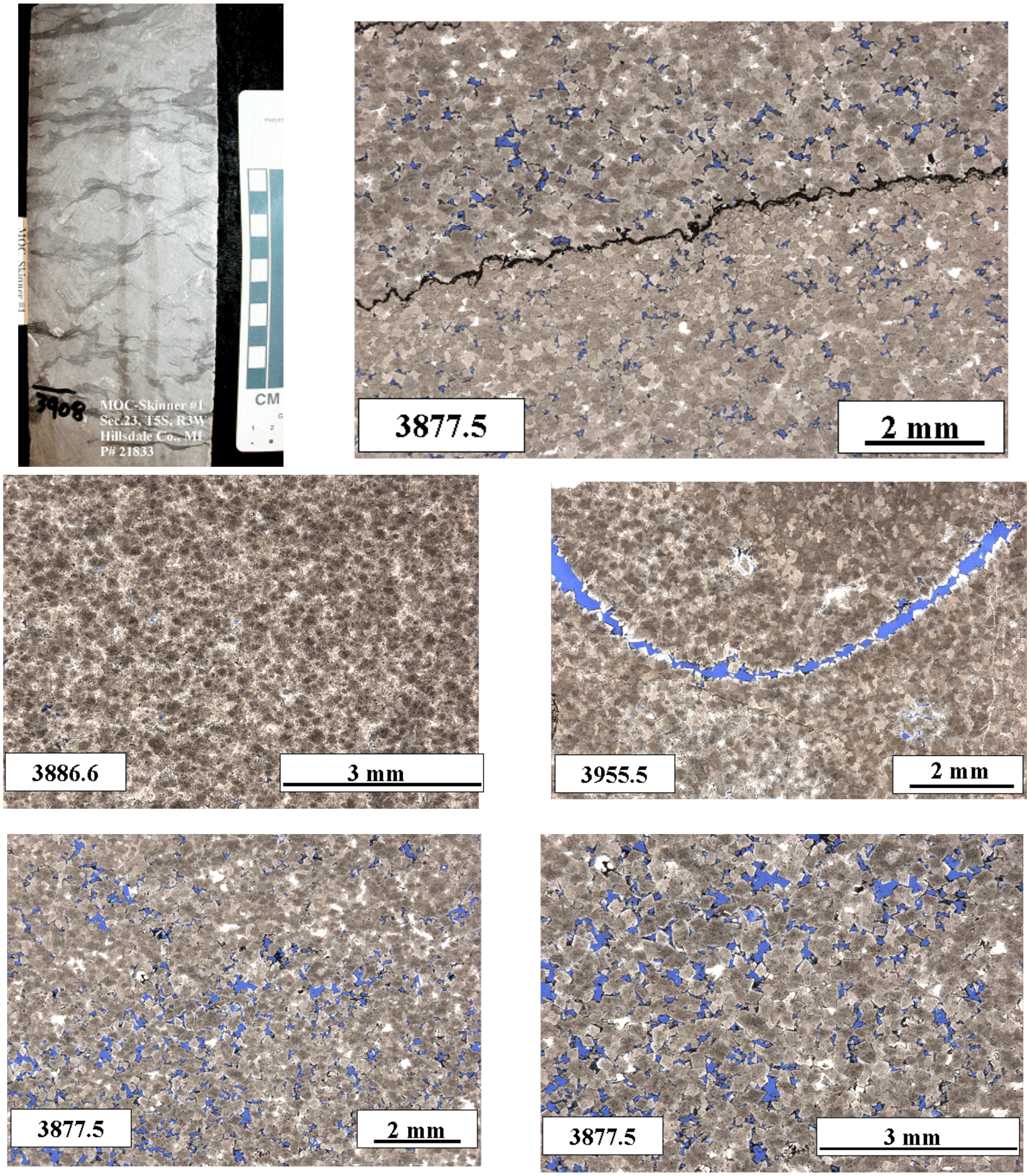

Figure 26. Core photo and thin section photomicrographs illustrating the variability in facies and pore systems in the Trenton/Black River formations.

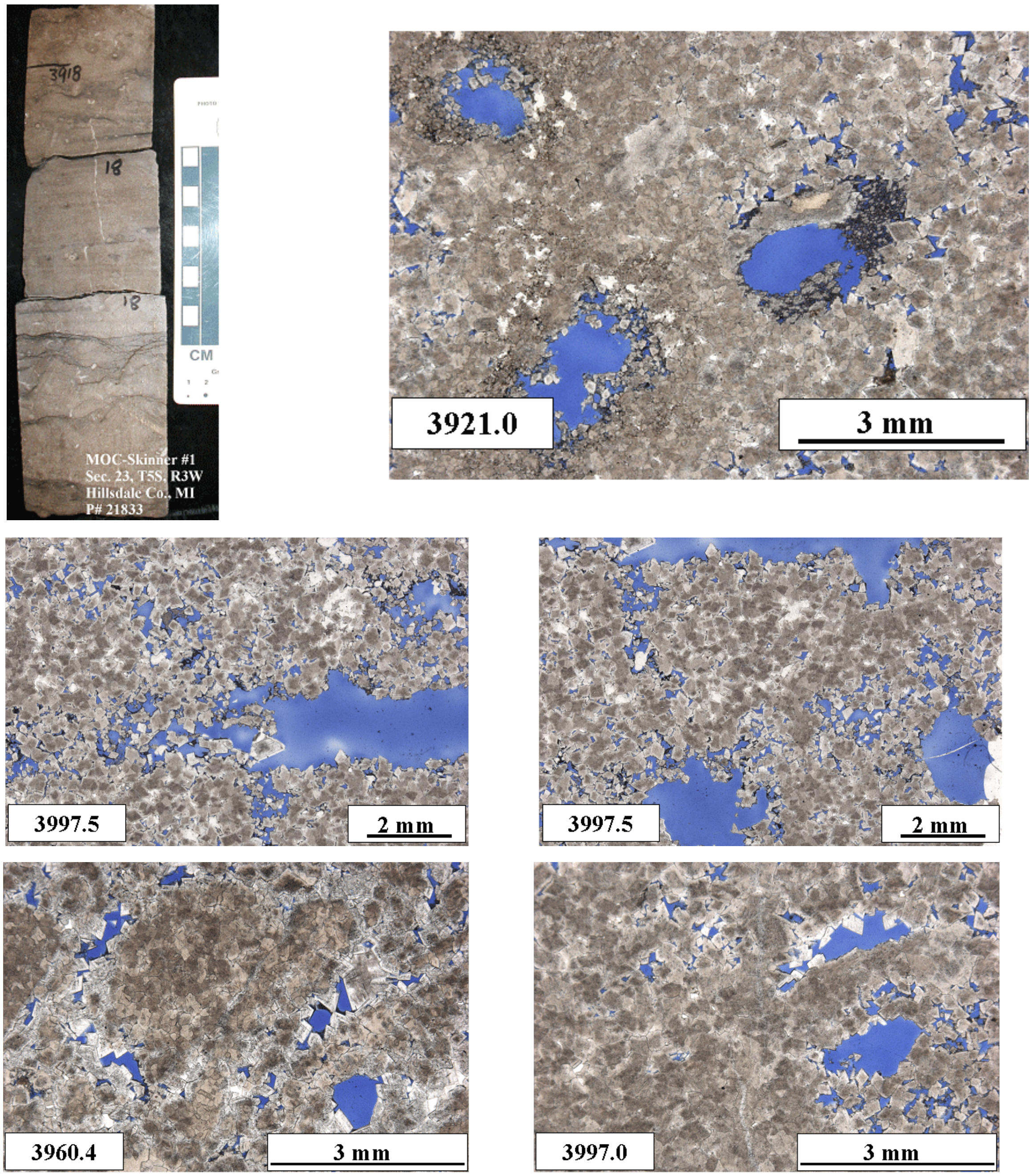

Figure 27. Core photo and thin section photomicrographs illustrating the variability in facies and pore systems in the Trenton/Black River formations.

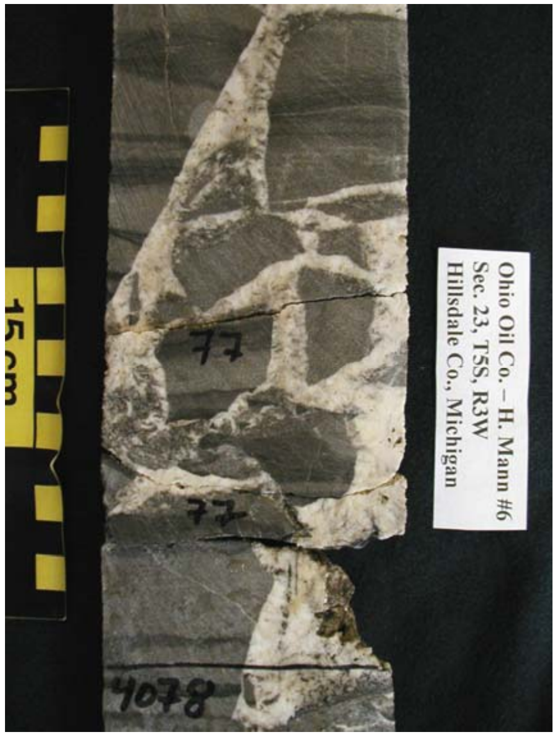

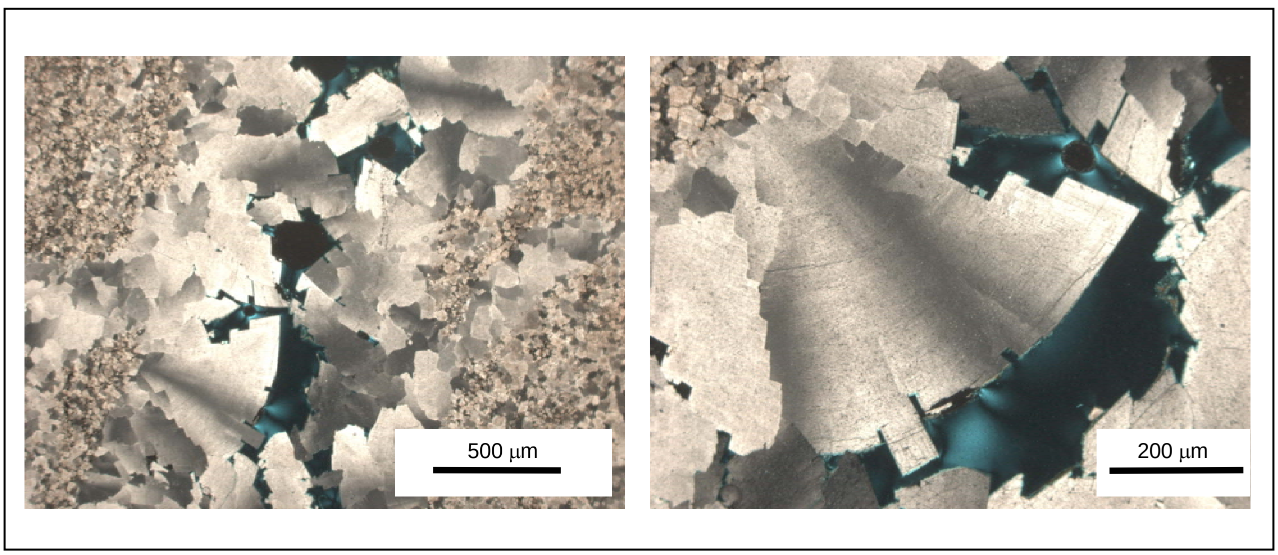

Figure 28. Slab photograph and thin section photomicrographs illustrating hydrothermal dolomite in the Trenton/Black River of Albion-Scipio Field. Note well-developed, classic baroque (saddle) dolomite crystals identified by their curved crystal lattice.

DISCUSSION: PHASE I AND II - INITIAL RESULTS FROM TASKS 2 AND 3

Controls on Dolomitization in the Middle Devonian Dundee Formation - Oil Field Scale Structure and the Distribution of Log-Based Dolomite Lithofacies:

Introduction

The Middle Devonian Dundee Formation (Figure 29) is a prolific oil and gas producer, initially discovered in 1927, with cumulative oil production to date in excess of 350 MMBOE from over 130 fields in the Michigan Basin (Figure 30). Exploration and production drilling in the Dundee in the 1920’s through the 1940’s was conducted prior to the advent of modern drilling technology or acquisition of quantitative reservoir characterization data. Furthermore, many Dundee wells were “top set”; that is, drilled to within a few feet of the top of the producing horizon and completed for production with little or no sampling or logging of reservoir rock types. Oil and gas production is known from both primary limestone and secondary dolomite reservoirs in the Dundee.

Limited modern logs and rare core from more recent drilling activity in the Dundee provide an incomplete picture of important reservoir lithofacies, their distribution, and geological origin in Michigan. Geological models for the origin of prolific oil producing dolomite reservoir facies, most common in the central Michigan basin, are of particular interest. A better understanding of the origin, regional distribution, and reservoir scale characteristics of this dolomite reservoir facies should have significant impact on continued exploration for novel and untested exploration targets, and increase the effectiveness of secondary and tertiary recovery operations in the Basin in the Dundee Formation.

On the basis of unpublished work by numerous petroleum geologists in Michigan during the Dundee boom years of the 1930' and 1940's and more recent work, petroleum production is thought to occur from at least three different reservoir lithofacies types (Knapp, pers. comm., Fig. 31a and b):

1) Sedimentary Facies-controlled ("early diagenetic") dolomite reservoirs, dominantly in the western third of the central basin such as in the Reed City Member (e.g. Reed City Field).

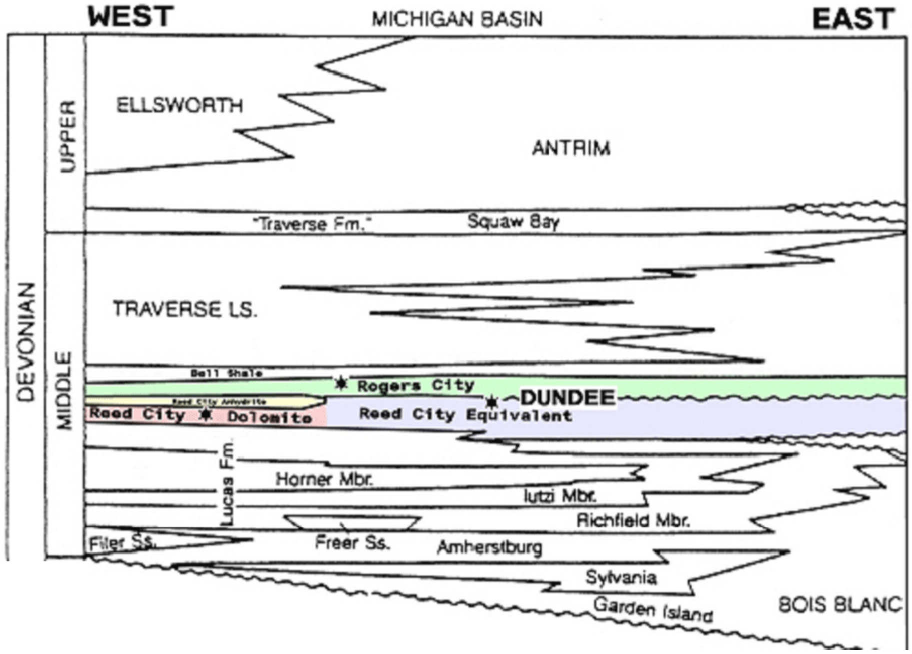

Figure 29. Devonian stratigraphy in the Michigan basin, from Gardener, 1971 (Drafted by Eric Taylor)

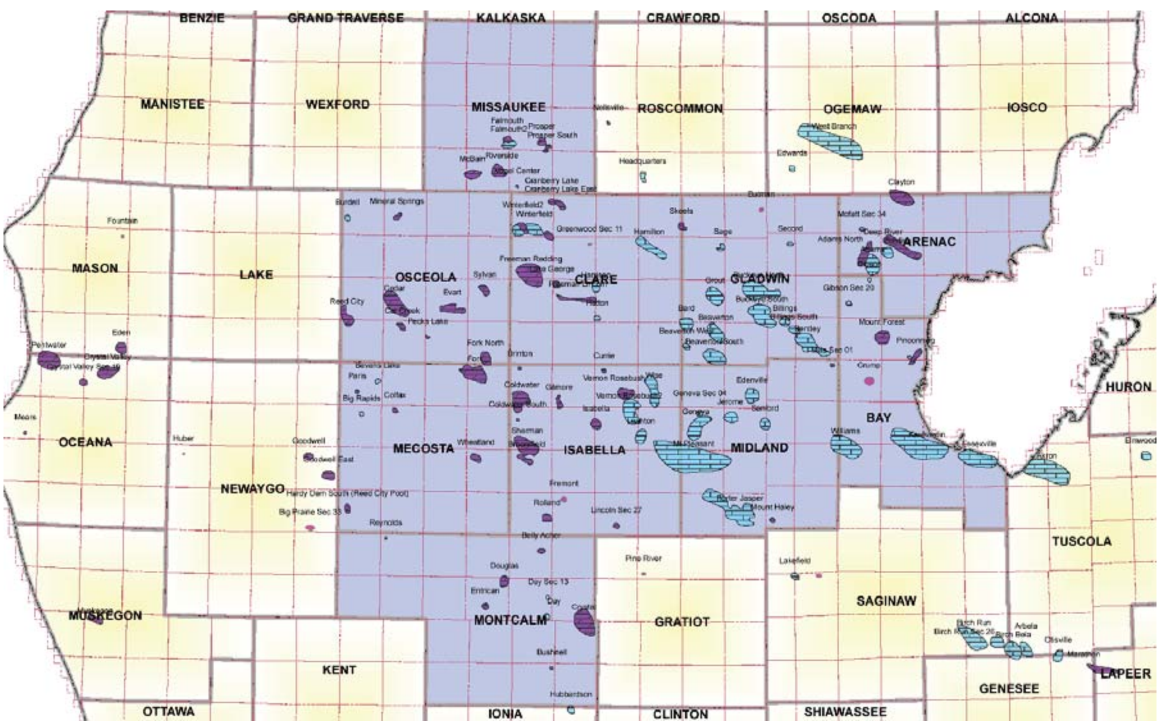

Figure 30. Dundee Formation fields in Michigan. Probable producing lithology indicated by dolomite and limestone symbols

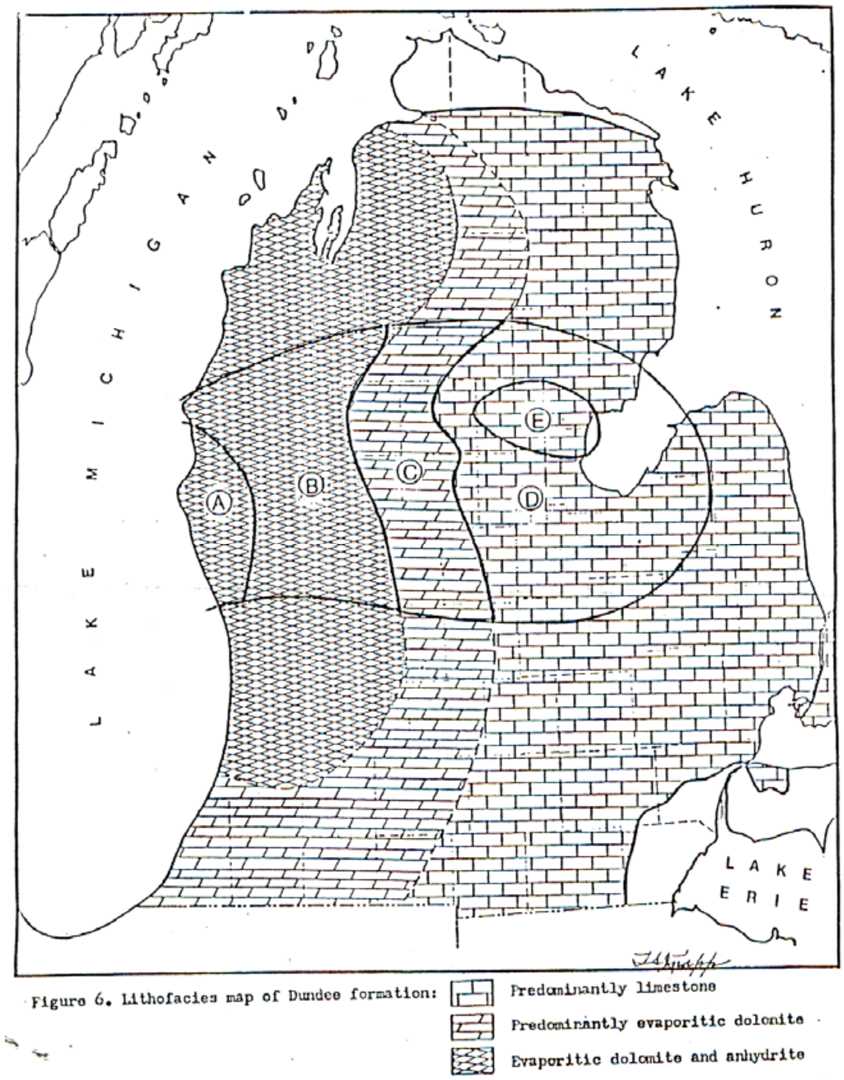

Figure 31a. Generalized lithofacies and spatial distribution of reservoir types in the Dundee Formation, from Tom Knapp, personal communication

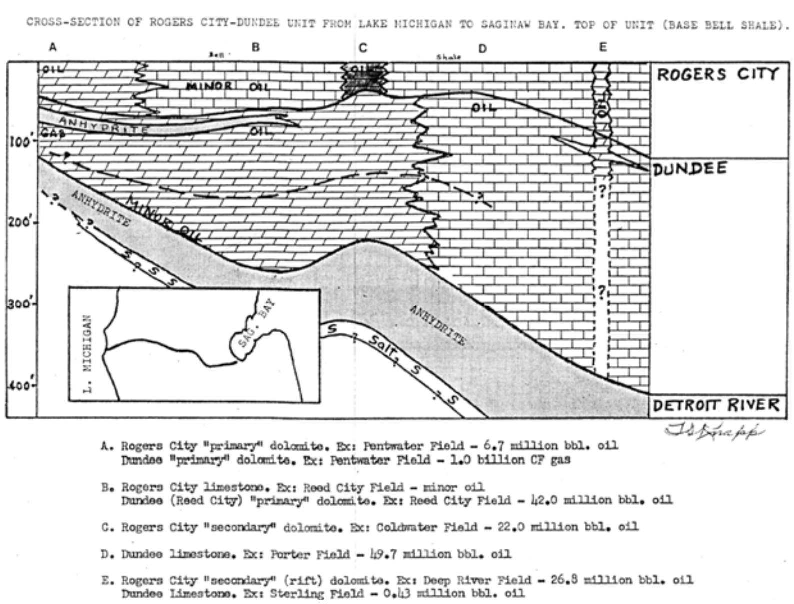

Figure 31b. Generalized lithofacies and spatial distribution of reservoir types from Tom Knapp, personal communication. “Dundee” unit refers to Reed City Member of this report.

2) Sedimentary Facies-controlled limestone reservoirs, mainly in the eastern third of the central basin in the Reed City "equivalent" Member (e.g. South Buckeye, Mt. Pleasant, and West Branch fields).

3) Dolomite reservoirs of controversial origin in the upper Dundee/Rogers City Member predominantly in the central basin (e.g. Vernon Field), but also noteworthy both to the far west (e.g. Pentwater field) and east (e.g. Deep River Field). Some fields of this type have been referred to as "dolomite chimneys" due to linear, fracture-related field geometry.

Geological Background - Dundee Formation

The Dundee Formation in the Michigan Basin consists of two subsurface members, the Reed City and overlying Rogers City members (Gardner, 1974, see Figure 29). A diverse lithologic assemblage of predominantly fossiliferous and grainy carbonate rocks of the Reed City member overlies dolomicrite, anhydrite and salt of the Lucas formation, deposited in sabkha, peritidal, and restricted lagoon environments (Gardner, 1974, Figure 29). The Reed City Member is most distinct in the western parts of the basin where it consists of restricted marine, peritidal facies, including a prominent anhydrite unit informally called the Reed City anhydrite near the top of the member. The primary depositional facies in the Reed City member basin-wide consists of a shallow marine shelf carbonate assemblage including, grainy carbonate, stromatoporoid reef, and peritidal to supratidal/evaporitic facies that generally shoal upwards to the Rogers City contact (Gardner, 1974; Montgomery, 1986; Curren and Hurley, 1992, Montgomery, and others, 1998). More open marine limestone facies (Reed City “equivalent”) are predominant in the eastern basin, while more restricted, dolomitized and evaporite-bearing facies (Reed City Member) occur to the west (Gardner, 1974, Figure 32) suggesting that the Reed City was deposited on a carbonate ramp that transgressed the basin from east to west. Pervasive alteration of grainy and fossiliferous primary limestone facies to dolomite occurs in the Reed City member throughout most of the western parts of the Michigan Basin. The Reed City member comprises a complex primary facies mosaic that is not well known due to the lack of outcrop and subsurface core material in the basin.

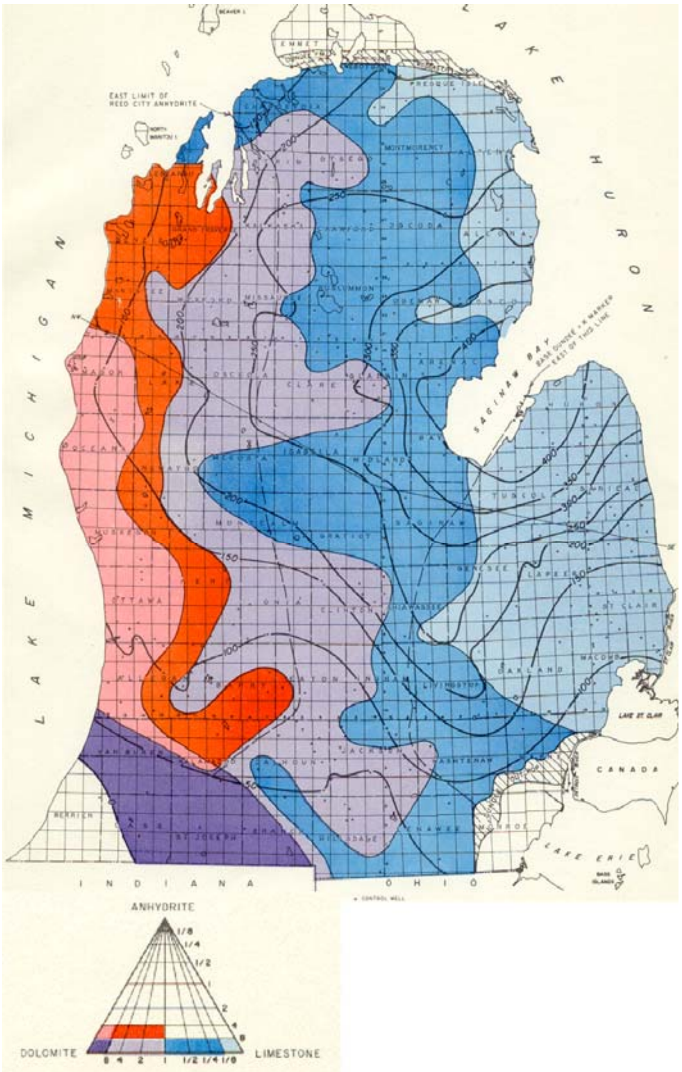

Figure 32. Dundee Formation (Reed City Member) lithofacies and isopach map from Gardner, 1974.

The Rogers City Member overlies various rock types of the Reed City Member at a generally sharp, probable marine flooding surface (as determined in core, Curran and Hurley, 1992) that marks an apparent rapid marine transgression. This contact is not easily recognized in logs, especially in the east, and its origin may vary throughout the basin. Primary depositional facies in the Rogers City, although incompletely known due to limited core, are generally lithologically homogeneous and consist of mostly open marine nodular lime wackestone to mudstone. Biostromal buildups and spatially-related fossiliferous grainstone-packstone deposits in the upper Reed City-Rogers City interval found in several oil fields in the eastern basin, suggest possible syn-depositional structural relief on the sea floor and resulting shoal water facies in some parts of the Michigan Basin during the transition from the upper Reed City equivalent to the Rogers City member (Montgomery, 1986).

Dolomite Reservoirs in the Dundee Formation

Some of the most productive (initial production {IP} of 2000-9000 BOPD) reservoirs in the Dundee are found in dolomite facies in the central and western parts of the basin. Some of the largest fields include the Reed City Field (42.9 MMBO); Deep River Field (27.2 MMBO); Coldwater Field (22.3 MMBO); Freeman-Redding Field (17 MMBO); and North Adams Field (9.5 MMBO). Dolomite reservoirs in the Reed City Member are thought by some basin geologists to originate as "early diagenetic" or "facies related" dolomite that is spatially related to the stratigraphic distribution of the Reed City Anhydrite (see Figure 31b and 32) and formed through seepage reflux mechanisms (Jones and Xiao, 2005, Figure 33). This is likely the case in several fields in the western basin (Reed City, most notably). Application of a seepage reflux model to the distribution of dolomite reservoirs in the central basin, however, is strongly dependant on an inferred pinch-out of the Rogers City Member over a proposed “shell bank” or shoal water bathymetric feature that existed in the central basin during the transition between Reed City and Rogers City time (Figure 34). A pinch out of the Rogers City member is interpreted to exist over this “shell bank”, and magnesium-rich saline fluids are thought to have migrated basin-ward and up-section, dolomitizing porous primary limestone facies in the Reed City Member that extended to the top of Dundee Formation at the base of the Bell Shale.

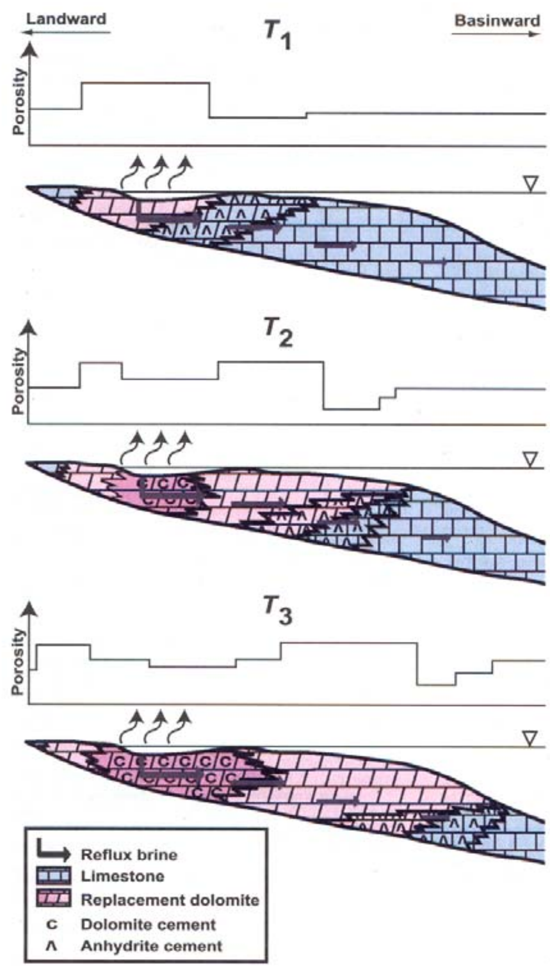

Figure 33. Model for lithofacies distribution in a reflux system, from Jones and Xiao, 2005.

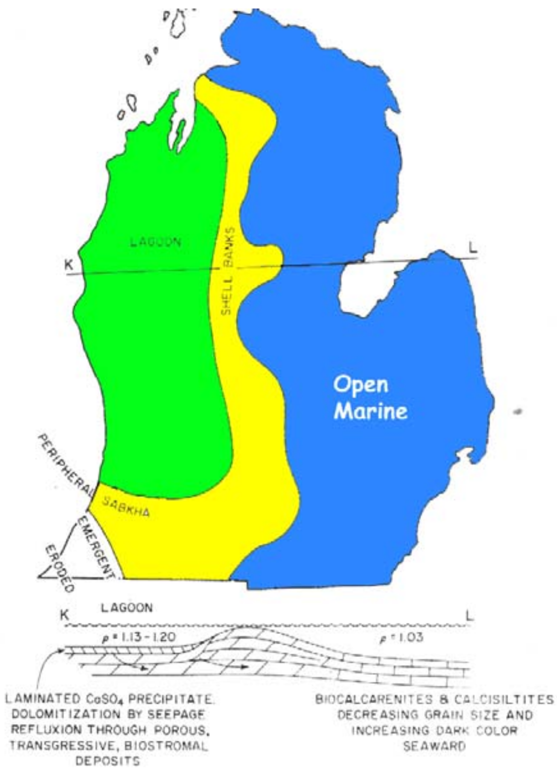

Figure 34. Paleogeographic map and cross section during regressive, Reed City member time, from Gardner, 1974. Note the inferred paleo-bathymetric high in the central basin that is interpreted by many basin geologists to be responsible for pinch-out of the overlying Reed City Member in this area. It is important to note, however, that this "interpretation" has not been substantiated in the literature but is more of a general impression in the basin.

An alternative model for dolomitization of the upper Dundee, Rogers City member in the central basin has been suggested as resulting from fracture-related mechanisms and hydrothermal alteration (see model by Strecker and others, 2005 after Boreen and Davis, 2001, Figure 35). This is a much more feasible hydrodynamic model for dolomitization in the central basin if the upper Dundee originally comprised Rogers City member limestone because primary porosity in this predominantly lime mudstone to wackestone unit would preclude flow of significant dolomitizing fluids through primary permeability conduits. It is a widespread industry perception that such fracture mechanisms are the probable origin of linear “dolomite chimney” fields in the eastern Michigan Basin (e.g. Deep River, Pinconning, and North Adams fields in Arenac and Bay counties, Wood and Harrison, 1999), although this inference is based primarily on anecdotal drillers reports, mud logs and the distinctive linear geometry of the developed fields.

The importance of distinguishing mechanisms for dolomitization in Dundee Formation reservoirs is fundamental to maximizing production of hydrocarbons from this interval. Regional flow systems that delivered dolomitizing fluids to the Dundee, eastward of the probable source of these fluids in the western basin, would result in dolomitized reservoirs that may have significant lateral continuity dependant mainly on the lateral continuity of facies controlled, primary fluid flow conduits. In sharp contrast is the abrupt lateral discontinuity that should exist between primary limestone and dolomite as a result of fracture-controlled delivery of hydrothermal dolomitizing fluids. These distinct mechanisms for dolomitization would result in fundamentally different timing of reservoir and trap development, oil migration pathways, and reservoir geometry relative to structural features.

Study Methodology and Objectives

In order to investigate the geological origins and controls on the occurrence of dolomite reservoirs in the Dundee Formation in Michigan, we compiled available digital subsurface geological data (mostly from the Michigan Department of Environmental Quality, Geological Survey Division, MDEQ-GSD) including formation tops, wire-line logs, and driller’s reports. Where appropriate we compiled these data into tabular spatial databases. These spatial databases were used to construct Geographic Information Systems files (both ArcGIS and Petra software),

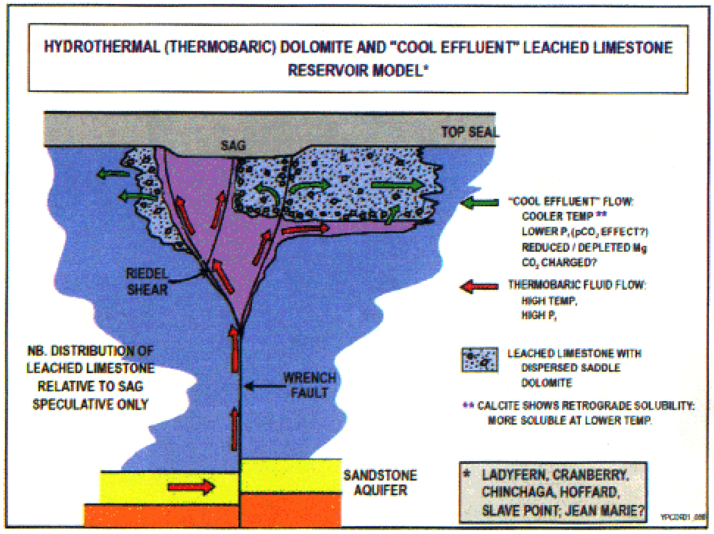

Figure 35. Generalized geometry and lithofacies model for fracture related hydrothermal dolomite reservoirs, from Strecker and others, 2005

as well as maps and cross sections of important geological properties in the Dundee - including the spatial distribution of dolomite versus limestone in the Dundee Formation relative to structural features and oil field occurrences in the Michigan Basin. Modern wireline logs in digital format were analyzed from over 400 wells. Quality controlled Dundee Formation tops from a data base with more than 25,000 wells (data base originated from J. R. Wood, MTU Subsurface Visualization Lab) were used in the structural mapping. The current availability of large institutional digital subsurface databases, modern digital well logs, readily accessible computational power, and appropriate software provides the opportunity to evaluate correlations amongst general structural and lithologic trends in the Dundee from a wide range of data sources. A limited number of modern litho-density well logs from across the basin provide an important source of information available for investigation of lithology in the Dundee Formation relative to spatial location and structural features in the Michigan Basin subsurface.

Dundee Field Water Production Characteristics

Field production characteristics in Dundee Formation fields (Figure 36a and b) define at least two distinct drive mechanisms basin-wide on the basis of water production and pressure decline: 1) bottom water and 2) gas expansion. Figure 36a shows per well water production from representative fields with two distinct trends of 1) relatively high water production per well from inferred bottom water drive dolomite fields (Fork, Vernon, Crystal; central basin dolomite fields, and Deep River; an eastern basin dolomite chimney field) versus 2) relatively low water production from probable gas expansion drive limestone fields (West Branch and South Buckeye; eastern basin limestone fields). Pressure decline is substantially greater in the gas expansion fields and initial bottom hole pressures are generally preserved in the inferred bottom water drive, dolomite fields. A similar breakout of field drive mechanisms is suggested by percent water cut plot (Figure 36b). The increase in water cut later in the production history of the eastern limestone fields is, in part, influenced by secondary recovery water flood projects. Facies related fields (both limestone and dolomite) in the Reed City member typically possess gas expansion type drive while upper Dundee/Rogers City dolomite fields possess bottom water

A.

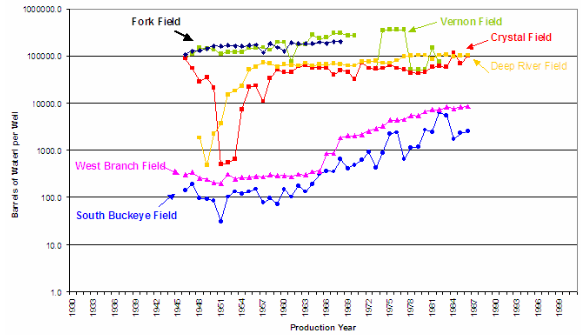

B.

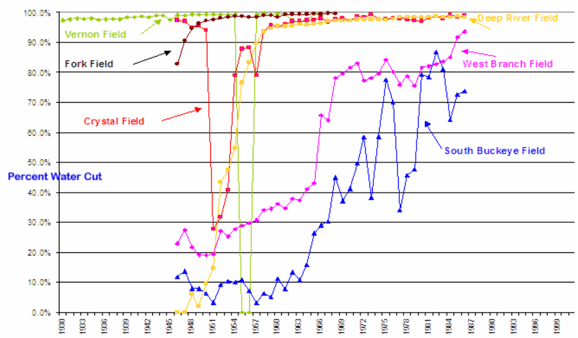

Figure 36a and b. Water production characteristics of Dundee field types.

drives that apparently tap a regional aquifer of substantially greater volume than any individual field.

Fracture Related Hydrothermal Reservoirs in Michigan

The significance of fracture-related mechanisms in the origin of important hydrocarbon reservoirs in Michigan is virtually undisputed. Fields in the Ordovician Trenton/Black River formation in Michigan, most notably the Albion-Scipio Field, are classic examples of geometrically complex dolomite reservoirs effectively modeled by the hydrothermal dolomite reservoir (HTDR) concept (Figure 37). Application of models for reservoirs of this generic type in other Michigan formations is controversial but of great current interest for both exploration and enhanced recovery in the petroleum industry.

Structural analysis of Michigan Trenton Black River (Hurley and Budros, 1990) and (more recently) Dundee Formation Fields (Prouty, 1988; Wood, 2003; and Budros, 2004; and others) suggests a relationship between probable reactivated basement wrench faults, anticlines with steep margins, and oil field occurrences. Riedel shear deformation mechanisms including complex flower structure fracture patterns are suggested as important components in the development of these dolomitized fields. The transport of dolomitizing hydrothermal fluids delivered to generally low permeability, primary limestone facies in the Rogers City Member in particular, is thought to result from flow through fractures associated with periodically reactivated wrench faults. Recent petrologic study of central basin, fractured upper Dundee/Rogers City lithofacies (Luczaj, 2001), suggests temperatures of saddle dolomite formation in excess of 120^{o}C in several central basin wells, which is well above ambient burial temperatures.

Distribution of Wire-line Log Based Lithofacies in the Dundee Formation

Lithofacies in the Dundee Formation were investigated using an industry standard "quick-look" overlay methodology and digital litho-density wire-line logs. When Neutron porosity and Bulk Density logs are overlain on a common, limestone equivalent porosity scale, changes in lithology can be inferred with depth (Figure 38). Shale, tight and porous

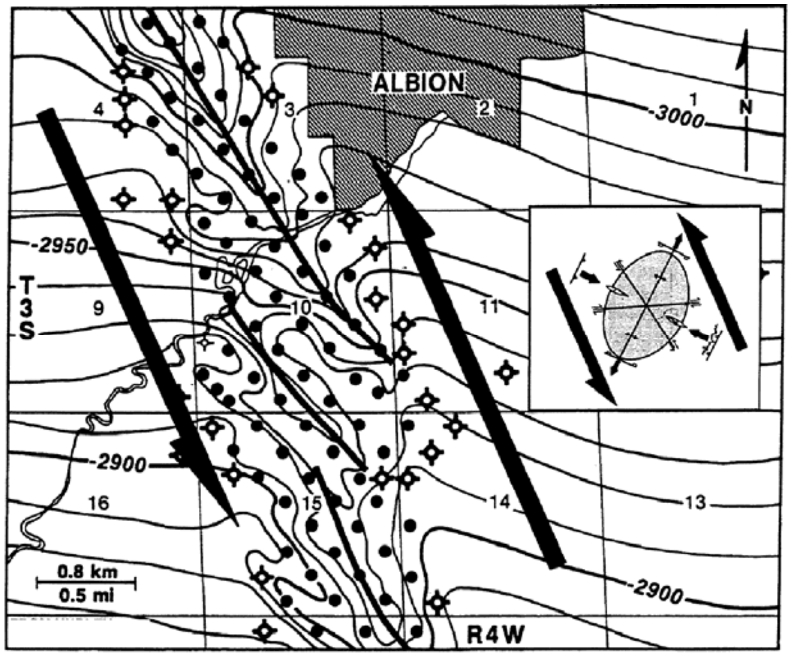

Figure 37. Model for Riedel shear control on the Albion-Scipio fractured dolomite field, Michigan basin, from Hurley and Budros, 1990.

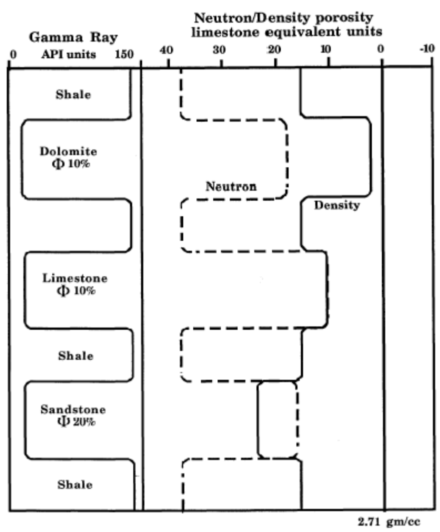

Figure 38. Hypothetical neutron-density overlay patterns for simple log-based lithofacies. The overlay uses a common calibration to an equivalent limestone porosity scale. (From Doveton, 1986).

limestone, dolomite, and anhydrite are relatively confidently identified using this "quick look" overlay method and log-based lithofacies in the Dundee Formation can be interpreted. Since log-based lithofacies are dependant on bulk density properties it is not possible to distinguish dolomite facies with different textural properties or geological origins including overprinted dolomitization.

A wide range of dolomite versus limestone successions are observed throughout the basin (figures 39a-f; in both producing and dry holes) including six distinctive assemblages:

1. No dolomite in the Dundee in the eastern basin (Gladwin Co., Figure 39a; lithofacies assemblage 1)
2. Complete dolomitization of Reed City Member (and associated Reed City “Anhydrite”) with no dolomite in the Rogers City member; western-most central basin, (Mason Co., Figure 39b; lithofacies assemblage 2)
3. Complete dolomitization of both Dundee members in the central basin (Isabella Co., Figure 39c; lithofacies assemblage 3)
4. Partial/minor dolomitization of the Reed City (and associated Reed City Anhydrite) and no dolomite in the Rogers City west-central basin (Mecosta Co. Figure 39d; lithofacies assemblage 4)
5. Partial dolomitization (bottom up) of the Reed City and no dolomite in the Rogers City in the central basin (Isabella Co., Figure 39e; lithofacies assemblage 5)
6. Partial dolomitization in the Reed City/Rogers City undivided (top down) and minor associated Reed City Anhydrite in the northwestern central basin (Missaukee Co., Figure 39f; lithofacies assemblage 6).

Regional Dundee Structure Mapping and Log-based Lithofacies Distribution

Top Dundee structure was mapped using an extensive tops data base compiled from data made available by James Wood, Michigan Tech, Subsurface Visualization Lab. Ten central Michigan Basin counties were each individually analyzed using geostatistical methodology and industry standard ArcGIS software. Structure contour and grid maps were created for each county through a quality control procedure involving iterative error analysis. Apparently spurious data points were eliminated from the tops data set by county until root mean square error (RMSE) of measured versus predicted tops in that county was less than 20 ft (the displayed contour interval). Some analyses produced RMSE well below 20' (Figure 40). A ten county composite Dundee top structure prediction map was then produced (Figure 41) that shows a strong preferred northwest-southeast grain and a less pronounced, essentially conjugate, northeast-southwest grain.

The distribution of productive, Dundee dolomite fields in the central basin is typically associated with structural trends with a predominant 310^{o} - 130^{o} and a conjugate 40^{o} - 220^{o} orientation. Areas marked by a convergence of these structural grains typically coincide with dolomitized Dundee fields. Small-scale spatial variation and complex geometric patterns of dolomitization in several counties supports local rather than regional dolomitization in the upper Dundee due to fracture-related fluid migration pathways (e.g. Figure 42). Dolomitization patterns in the lower Dundee, Reed City Member have wider spatial distribution but may represent a complex interplay between primary facies controlled dolomitizing fluid conduits and fracture related conduits. If the geometrically complex dolomitization in the upper parts of the Dundee occurs in what was regional tight primary limestone of the Rogers City, this relationship is almost certainly the result of fracture related hydrothermal dolomitization associated with geometrically complex matrix fracturing.

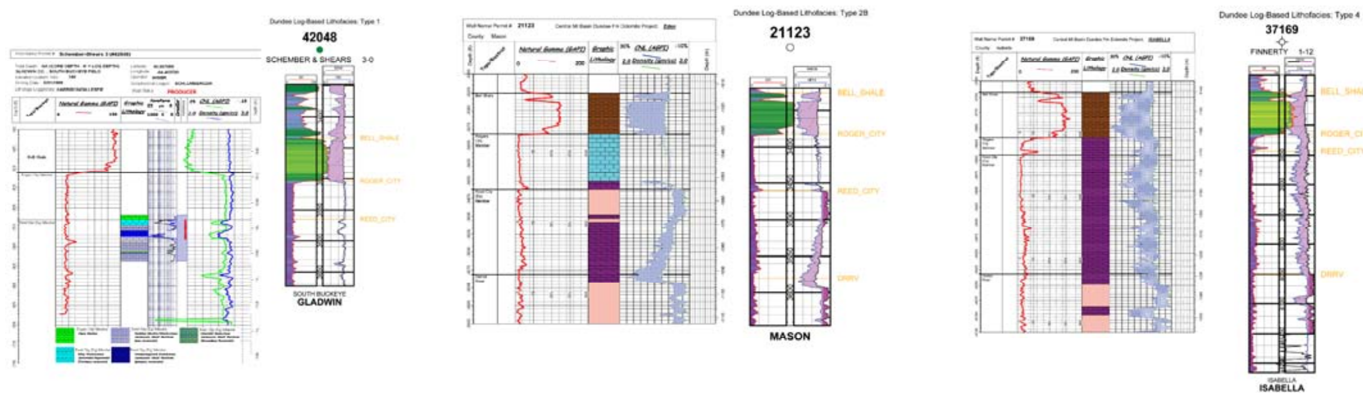

39a 39b 39c

Figure 39a,b, and c. Litho/density log-based Dundee Formation lithofacies assemblages 1, 2, and 3 respectively. See text for discussion.

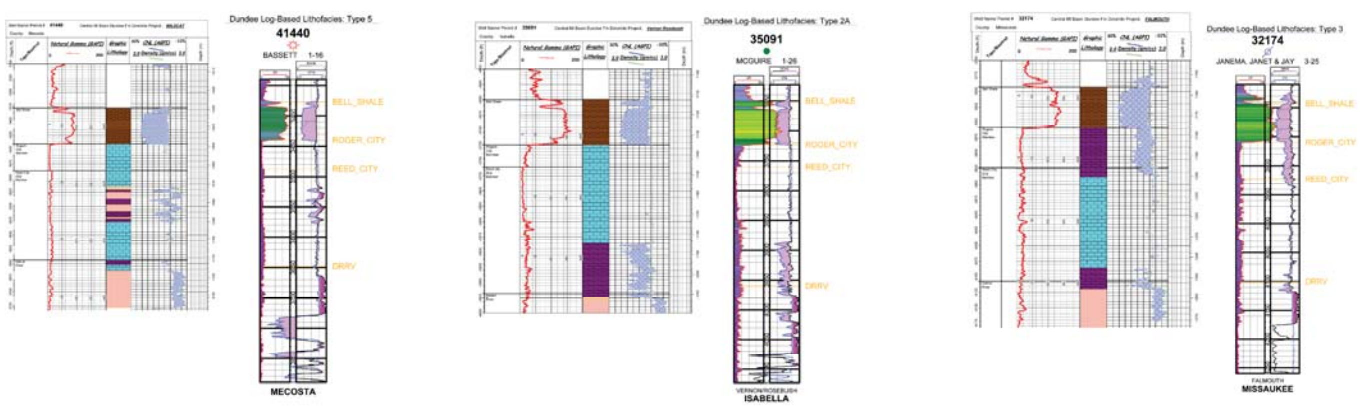

39d 39e 39f

Figure 39d,e, and f. Litho/density log-based Dundee Formation lithofacies assemblages 4, 5, and 6 respectively. See text for discussion.

Field Scale Structure Mapping and Log-based Lithofacies

Field scale structural mapping of top Dundee with high quality, wire-line log controlled well data indicates a geometrically complex spatial correlation between subtle structure and reservoir facies variations in the Upper Dundee/Rogers City Member. High resolution structure contour mapping (5'-10' contour interval) based on high quality top and lithofacies picks, suggests top Dundee surface irregularities that are best interpreted as faults with small throw of generally less than tens of feet in two Dundee fields, Winterfield (Clare Co., Figure 43a) and Vernon-Rosebush (Isabella Co, Figure 43a). In the Winterfield field a transition from dolomitized upper Dundee/Rogers City to undolomitized upper Dundee occurs within less than 0.3 mi. The alignment of wells with dolomitized upper Dundee/Rogers City is in accordance with a 40°- 220° orientation superimposed on an overall 310° - 130° trend for the field. A nearby extension of the Winterfield field (not shown) with a linear, 310° - 130° field orientation and probable fracture-related Dundee production (Chittick, 1996).

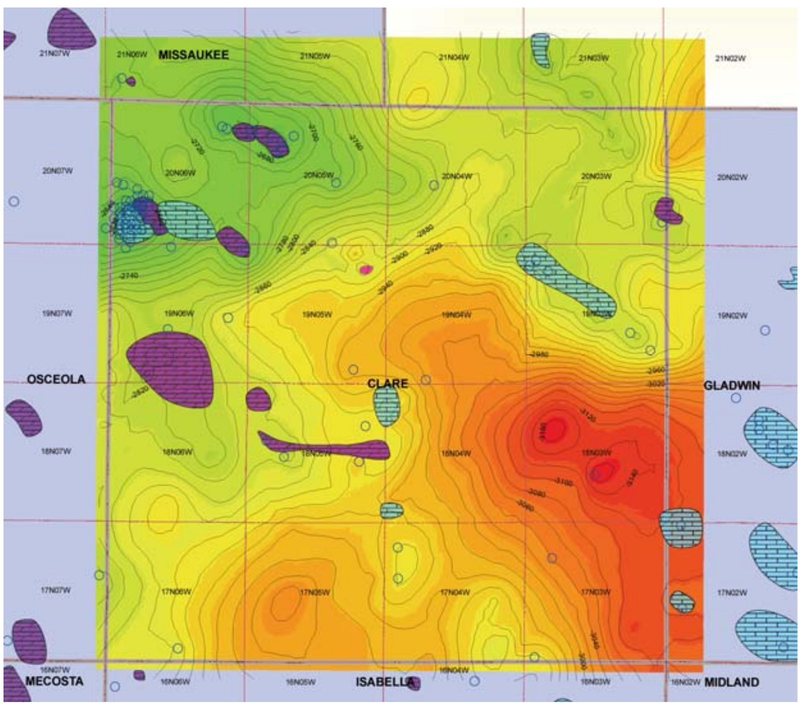

Figure 40. Example of central Michigan basin county structure map on top Dundee Formation with superimposed Dundee fields and inferred reservoir lithofacies.

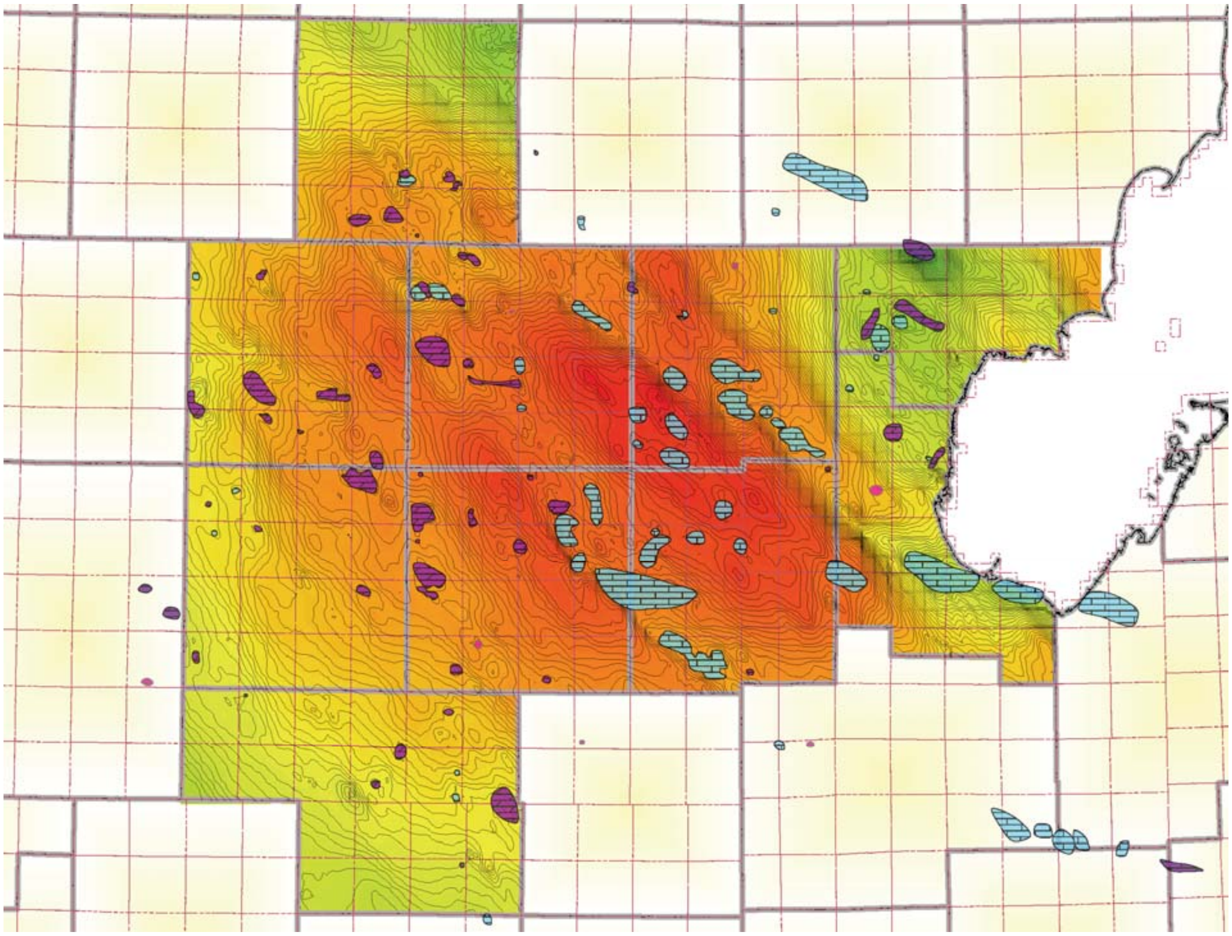

Figure 41. Michigan central basin 10 counties structure map on top Dundee Formation with superimposed Dundee fields.

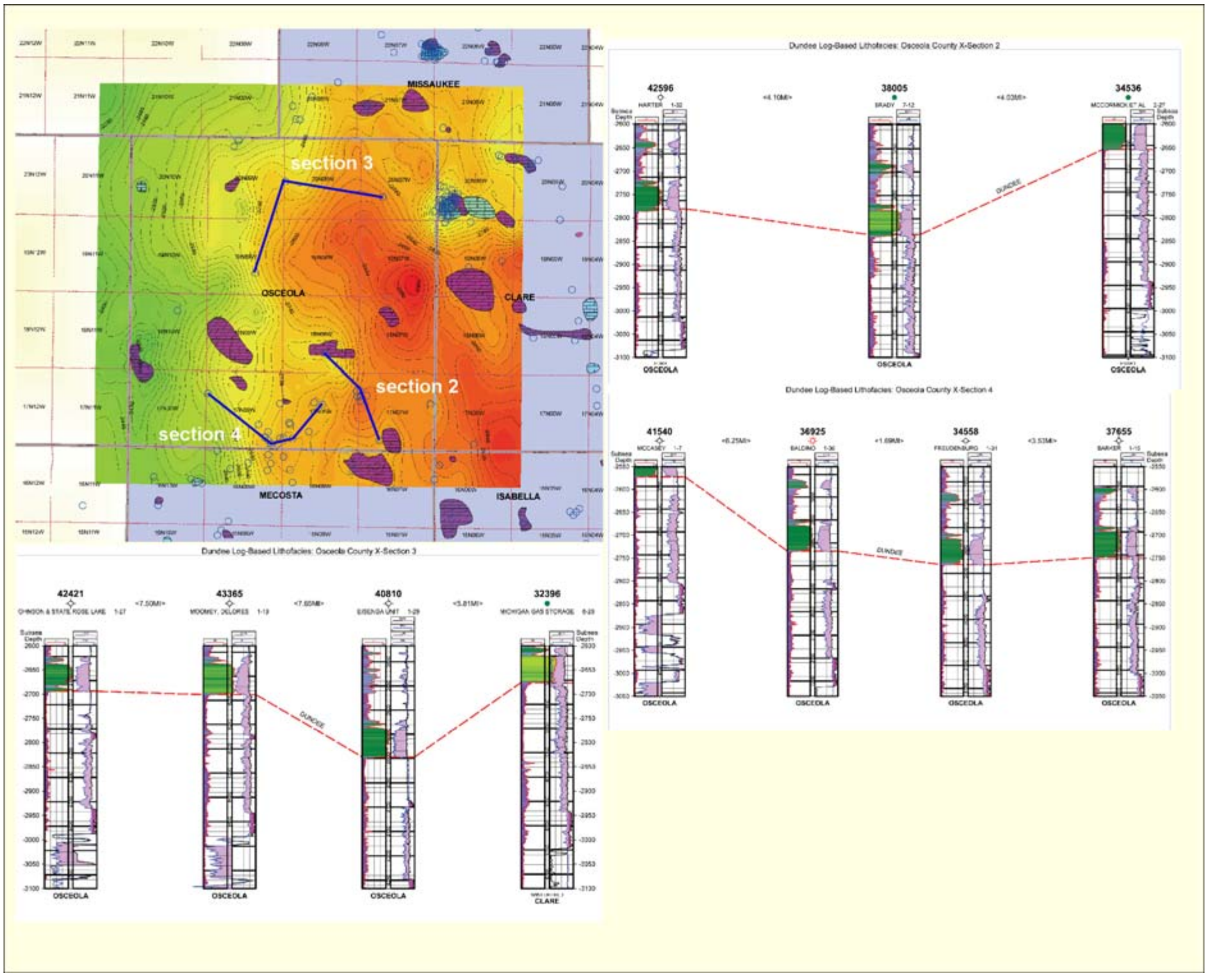

Figure 42. Osceola County structure map on top Dundee and litho-density "quick look" lithofacies assemblage cross-section. Small-scale spatial variation and complex geometric patterns of dolomitization supports local rather than regional dolomitization in the upper Dundee/Rogers City due to fracture related fluid migration pathways.

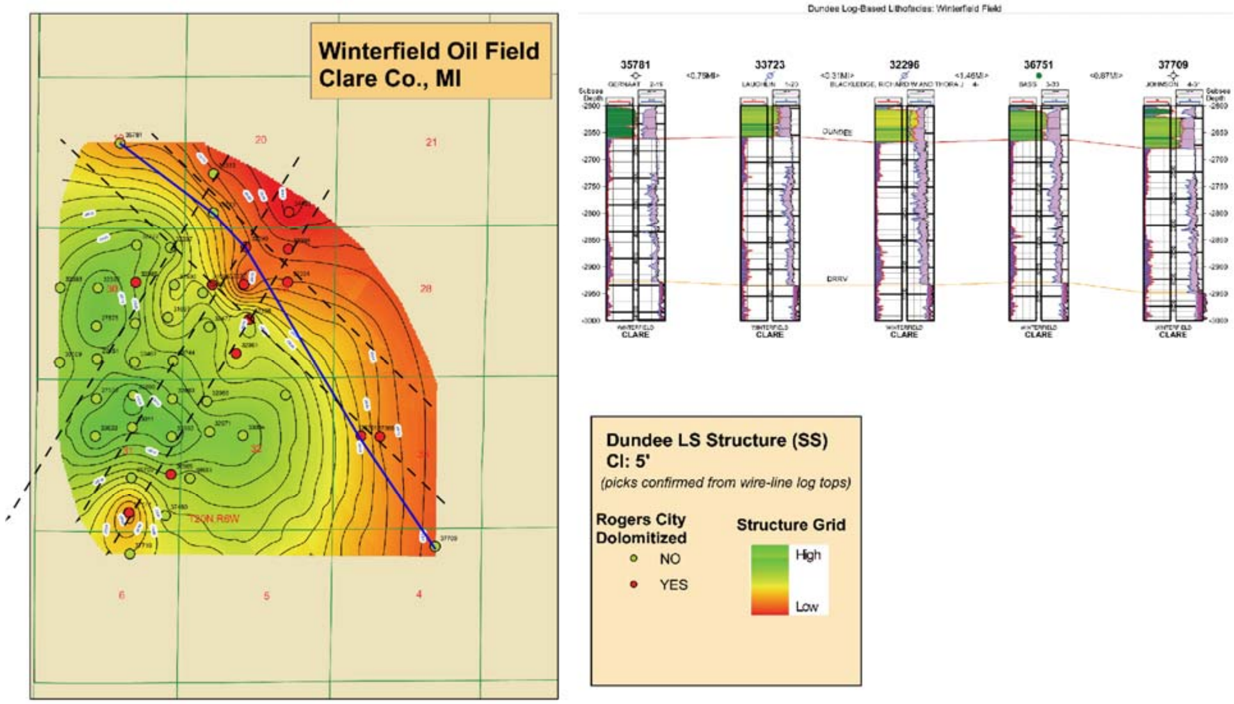

Figure 43a. High resolution (5’ contour interval) structure contour map of the Winterfield field, Clare Co. Note small spatial scale variation in upper Dundee dolomite distribution associated with interpreted small throw displacement faults (dashed lines) with ~310 ^{o}-130^{o} and 40^{o} -220^{o} orientation.

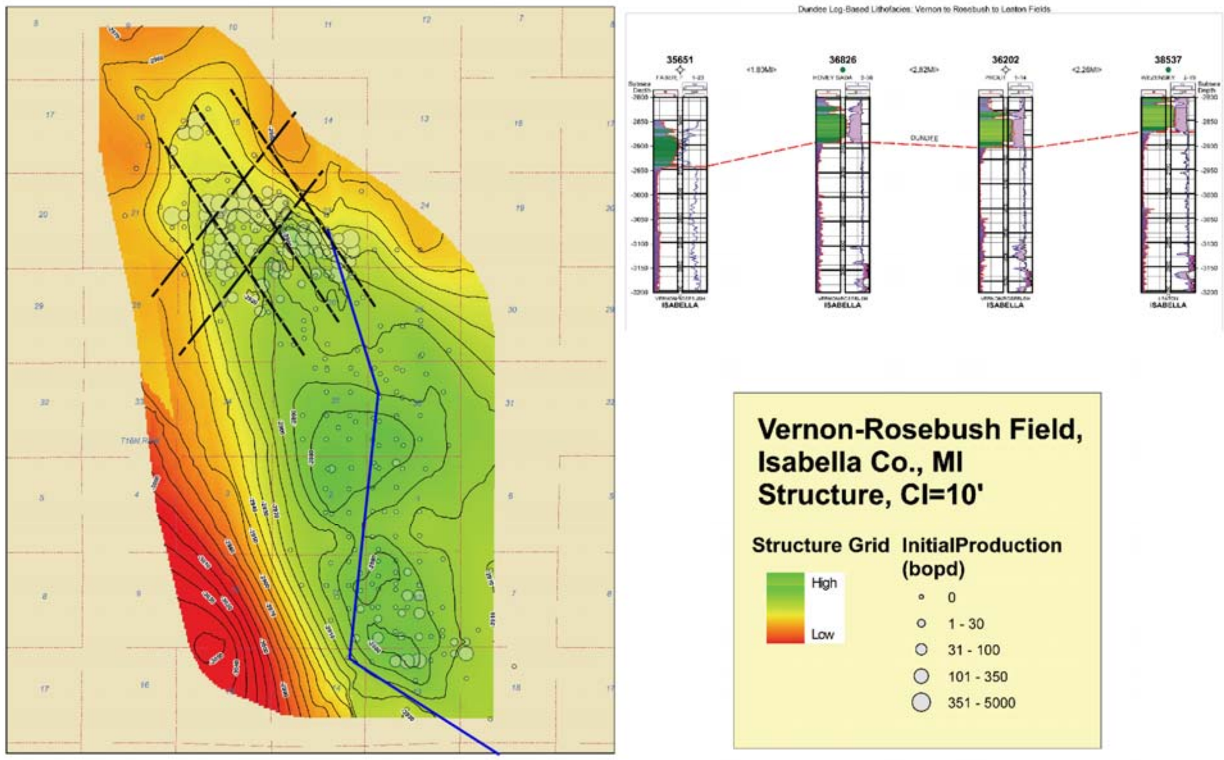

Figure 43b. High resolution (10’ contour interval) structure contour map of the Vernon-Rosebush field, Isabella Co. High initial production in wells in the Vernon (northwest, down structure) portion of the field coincide with interpreted small throw displacement faults (dashed lines) with ~310 ^{o}-130^{o} and 40 ^{o} -220^{o} orientation. One litho/density well log in the Vernon area (Faber well) suggests complete dolomitization of the entire Dundee section while wells to the southeast (Rosebush area) are mostly limestone coincident with relatively simple, open structural style.

A similar, relationship between small scale structure and the inferred distribution of Dundee dolomite reservoirs is interpreted in the Vernon-Rosebush field of Isabella Co. Small scale structural deformation of the top Dundee surface is mapped in the north-northwest extension of the Vernon-Rosebush structure (Figure 43b). In the down dip north and west portion of the Vernon-Rosebush field, sparse log control can be interpreted to indicate complete dolomitization of the Dundee associated with high initial oil production rates. The IP’s (to several thousand BOPD) are comparable to many central basin Dundee fields that are probably fracture-related. Less than 2 miles to the south and east, which is up structure, the Dundee contains limestone from bottom to top.

Interpreted faults and related fractures apparently propagated to the Dundee-Bell Shale contact in places throughout the central basin (and apparently elsewhere in the basin) and may have provided geometrically complex secondary conduits locally for dolomitizing fluids that permeated upwards through the otherwise regional tight limestone of the upper Dundee/Rogers City.

Implications for Petroleum Geology in Michigan and other U.S. Hydrocarbon Basins

Our mapping efforts to date, have important implications for both new exploration plays and improved enhanced recovery methods in the Dundee and Ordovician Trenton/Black River "plays" in Michigan – i.e. the interpreted fracture-related dolomitization control on the distribution of hydrocarbon reservoirs. In an exploration context, high-resolution structure mapping using quality-controlled well data should provide leads to convergence zones of fault/fracture trends that are not necessarily related to structural elevation. Acquisition of high-resolution seismic data in areas with prospective structural grain may provide decreased risk for fractured Dundee or Trenton/Black River exploration drilling.

Application of fracture models to reservoir characterization in secondary and tertiary recovery projects in existing fractured Dundee or Trenton/Black River fields, may result in substantial additional recovery from fields that typically had low (<30%) primary recovery factors. Careful consideration of fracture orientations and water coning problems should decrease risk in enhanced recovery activities.

Undoubtedly more complex, hybrid reservoir types exist in dolomitized lower Dundee/Reed City Member lithofacies in the central basin. This is anticipated as a result of complex, early fluid flow through primary limestone pore conduits within a reflux system, in addition to fracture generated pathways in fault/fracture convergence zones. Much additional work is necessary to understand Reed City Member dolomitization processes in Michigan and implications for petroleum geology and is a primary goal of continuing efforts.

INITIAL SUMMARY OF CURRENTLY AVAILABLE GEOLOGIC DATA (TASK 2)

Ordovician Trenton/Black River Production

The Ordovician Trenton-Black River Formation is a fractured, dolomitized reservoir that has produced 140 MMBO and 260 BCFG in the State of Michigan. However, theories concerning the nature of fracturing, the controls exerted by the original depositional rock type and pattern, the extent of dolomitization, the types of fluids involved, and the various stages of diagenesis are still evolving. All previous studies deal only with data from specific field areas. There has never been a basin-wide synthesis and analysis of these data despite the fact that the Trenton-Black River Formation is one of the largest hydrocarbon producing reservoirs in the state. It is doubtful that the current Trenton-Black River exploration model, developed from independent field studies, adequately encompasses all the exploration and exploitation opportunities that exist for this reservoir in the Michigan Basin. Increasing the current total recovery for this unit by only 1% would add 1,380,000 BO and 2.6 BCF to the already recovered reserves. It is reasonable to expect that a comprehensive, basin-wide examination of the Trenton-Black River Formation, resulting in the development of additional exploration models and methods could ultimately produce a 5% increase in recoverable reserves (6.90 MMBO and 13 BCF).

Trenton-Black River Discovery and Development

Drilling began in 1884 along the Findlay-Kankakee Arch in Indiana and Ohio (Davies, 1996, 2000) resulting in the first Trenton-Black River discoveries. This led to the drilling of over 100,000 wells and the production of 500 MBO along the Bowling Green Fault Zone.

The first commercial Trenton-Black River discovery in the State of Michigan occurred in 1936 in Monroe County. This resulted in the Deerfield Field located along the Lucas-Monroe monocline, an extension of Bowling Green Fault zone in Ohio. Reservoir quality dolomite lenses in the upper 125’ of the Trenton Group produced more than 608 MBO by 1959 from 40 wells drilled on 360 acres.

The Albion-Scipio Field, a giant (>120 MMBO) Trenton-Black River field located in Calhoun & Hillsdale Counties, Michigan was discovered in 1955 – 1958 (Davies, 1996, 2000). The Scipio Field discovery well was the Houseknecht No. 1 (Sec 10, T5S-R3W – Hillsdale Co.) which was originally drilled for Devonian gas but proved dry. It was then deepened based upon the advice of a psychic family friend, encountered oil at 3900', and was completed at 140 BOPD with "considerable" gas. The Albion Field was discovered by the Rosenau No. 1 (Sec 23, T3S-R4W, Calhoun Co.) and completed for 200 BOPD. Subsequent drilling discovered the Pulaski, Barry, Sponseller, Van Wert, and Cal-Lee Fields; all to become part of the Albion-Scipio Trend. Over 961 wells were drilled by 1986, of which 573 are still producing.

Stoney Point Field (5 miles east and sub-parallel to Albion-Scipio) was not discovered until 27 years later in 1982 when the JEM Casler No. 1-30 (Sec 30, T4S-R2W, Jackson Co.) encountered dolomite reservoir 115' into the Trenton at 3910'. This well hit lost circulation at 4248'. Casing was set and the well was tested at 2000 BOPD from perforations at 4161' - 4179'. The bottom hole pressure drop never exceeded 3 psi and the well was put on production at 220 BOPD. Two hundred and ten wells were drilled around the Stoney Point Trend between 1983 and 1987. Seventy five wells were oil and gas producers.

Estimated oil-in-place figures are difficult to accurately calculate due to difficulties in establishing a reliable porosity number; however, Scipio Field is estimated to have 170 MMB OOIP, Albion Field is estimated to have 120 MMB OOIP. No figures are available for Stoney Point Field. There are 18 Trenton-Black River fields that have produced in Michigan.

Stratigraphy and Structure

The Trenton-Black River Formation was originally deposited during the Ordovician in open marine conditions. Wackestone - mudstones were deposited on a basin-wide scale. Trenton-Black River carbonates in the Stoney Point Field area (south-central Michigan) are open marine, subtidal carbonates, typically crinoidal packstones/wackestones and mudstones with pervasive burrowing. Trenton rocks in the

Deerfield Field area (SE Michigan) prograde from open marine to intertidal carbonates while Black River rocks remain subtidal (Davies, 1996, 2000). The Trenton is overlain by the Utica Shale that forms a regional seal. This is in turn overlain by reef and inter-reef carbonates of the Niagara Formation and Salina Formation evaporates.

Repeated reactivation of a Precambrian left-lateral wrench fault system (en echelon faults with a total of 2.5 miles of offset) occurred throughout the early to mid Paleozoic. These faults (dominant set oriented N30W, conjugate set oriented east-west) are thought to have provided conduits through which dense Salina residual evaporite brines were able to flow downward into the Trenton-Black River formation. Dissolution and dolomitization of the Trenton-Black River occurred immediately adjacent to faults resulting in long, linear, porous dolomite reservoirs associated with downward collapse of overlying units. The collapsed interval extends into the Devonian section where it dies out. Fractures in the Utica Shale must have healed at the cessation of faulting to provide a seal for the Trenton-Black River reservoir. Tight un-dolomitized limestones act as lateral stratigraphic seals (Allen and Wiggens, 1993). DeHaas and Jones (1984, 1989) proposed cave development related to karsting responsible for lost-circulation zones; however, this theory has been largely discounted by recent workers.

Budros (APPG Annual Meeting, 2004) proposes that “sags” or “grabens” overlying dolomitized reservoirs (thereby defining Trenton-Black River fields) are in fact negative flower structures due to Reidel shear faulting with trans-tension and are not the result of previously considered collapse due to dissolution. He also proposes that some fields are characterized by positive flower structures produced by Reidel shear faulting with compression.

Faulting has compartmentalized the Albion-Scipio Trend. These compartments are probably due to a combination of Reidel shear negative and positive flower structures along the same fault trend; however, this hypothesis demands further investigation. These discontinuities do account for dry holes drilled apparently “directly on trend” (Davies, 1996, 2000).

Fields such as Deerfield Field exhibit a more circular pattern rather than a long, linear NW - SE pattern typically considered indicative in the current Trenton-Black River exploration model. It is thought that secondary east-west oriented faults may have played a more significant role in the development of dolomitized reservoir facies in the Deerfield Field. Fractures and faults with minor displacement play an important roll controlling dolomitization and porosity development (Davies, 1996, 2000).

<u>Trenton-Black River Reservoir Characteristics</u>

Reservoir dolomites are composed of coarse crystalline dolomitized limestone host rocks that are vuggy and cavernous. Fractures and vugs are often solution enlarged and contain white saddle dolomite with minor anhydrite. Porosity normally ranges from 2-5%, but 8-12% porosity is present, though uncommon. Permeability is extremely variable (0.01 – 800 md) but is generally low (85% of samples < 10 md). Porosity and permeability plots do not show any uniform relationships. Isotopic, fluid inclusion and water chemistry analyses all indicate a hydrothermal genesis for reservoir dolomites with a dual source of fluids from the Salina and Trenton - Precambrian Formations (Allen and Wiggens, 1993).

<u>Origin of Dolomite</u>

Shortly after discovery of the Albion-Scipio Trend, Burgess (1960) determined that reservoir dolomite was a secondary mineral formed as Cambrian and Lower Ordovician waters moved up along fracture zones (analogs - Dover and Colchester Fields in Ontario).

Ells (1962) observed that Albion-Scipio Field dolomites were similar to Mississippi Valley-Type (MVT) lead-zinc mineral deposits. He proposed that magnesium-bearing waters ascending through fractures were responsible for dolomitization.

Beghini and Conroy (1966) stated that Trenton-Black River reservoirs were formed by pre-Black-River Group waters that moved through faults and fractures to produce secondary dolomite.

Buehner and Davis (1968) concluded that the Trenton-Black River reservoir facies was epigenetic dolomite related to a fault system.

Shaw (1975) described a mineral assemblage (including sphalerite) in Albion-Scipio cores similar to MVT mineral deposits. He noted 2-phase fluid inclusions in Albion-Scipio dolomites and pore filling saddle dolomites that he believed were precipitated from fluids at a minimum of 80 degree C. He also identified a liquid-hydrocarbon phase in some fluid inclusions indicating hydrocarbons were present at time of cementation. These observations allowed him to propose a model of replacement dolomitization and development of intercrystalline porosity during the Middle to Late Silurian by waters percolating through fractures. Magnesium was sourced from underlying Prairie du Chien dolomite or Trempealeau Formations. Then, a second phase of dolomitization occurred during Lower to Middle Devonian as hot fluids from the basin center created cavernous porosity, subsequent collapse, and precipitation of a MVT assemblage.

Ardrey (1978), DeHaas and Jones (1984, 1989) proposed that diagenesis of the Trenton-Black River in Albion-Scipio area was due to exposure as indicated by the top-of-Trenton unconformity. They also stated that dolomitization must have resulted from a mixing model based on the observation that Trenton Formation water is less saline than water in shallower horizons; therefore, it could not be of hydrothermal origin.

Taylor and Sibley (1986) identified 3 major types of dolomite (1) regional dolomite not associated with the field area, (2) cap dolomite that occurs in the top 40 feet (related to interaction of the Trenton with Fe-rich fluids formed during the de-watering of the overlying Utica Shale) (3) fracture-related dolomite (formed during deeper burial at approximately 80 degrees C based on geochemical results).

Budai and Wilson (1986) identified various MVT accessory minerals, including pyrite, calcite, anhydrite, barite, celestite, sphalerite, and fluorite in association with saddle dolomite cements. They proposed a hydrothermal model with Paleozoic and Precambrian basement rock as sources of iron, sulfur, and other trace metals.

Hurley and Cumella (1987) proposed a model based on (1) carbon, oxygen, and strontium isotopes, (2) fluid-inclusion geothermometry, (3) brine geochemistry, and (4) regional hydrologic constraints. Dolomitizing fluids were thought to be Silurian-Devonian hypersaline sea-waters that moved down fracture zones to meet with hot limestone-dissolving fluids moving up from the basement. These fluids mixed in a pattern consistent with the known distribution of dolomite reservoirs and lost-circulation zones. This model is supported by Coniglio et al (1994) for Ordovician rocks in Ontario (Davies, 1996, 2000).

Exploration

Originally, the Albion-Scipio Field was discovered by the advice of a psychic. "Trendology" quickly become the exploration method of choice as the linear field pattern began to emerge. Indications of a northwest-southeast linear fracture zone associated with a top-of-Trenton synclinal sag (up to 60' recognized in early producing wells) has been the long held exploration model for the Trenton-Black River Formation.

Gravity was used through the 1960's and early 70's to define basement faults along the Albion-Scipio Trend. This met with limited drilling success because dolomite porosity mutes the density contrast between the regional limestones and dolomite reservoir rocks.

Magnetics was used in the 1970's to detect basement discontinuities and faults; however, this also proved to have limited use. The giant Albion-Scipio does not appear as an individual feature on magnetic maps. Recently, micromagnetic surveys and resistivity profiles have been employed, but their significance is not yet proven.

Reflection-seismic is currently the primary exploration method; however, there are problems associated with this technique: (1) variable till overburden thicknesses produce noise and statics problems, (2) secondary porosity, the dominant reservoir characteristic, is not detected by P-waves, (3) reservoir dolomites (2-5% porosity) have an acoustic impedance similar to the regional limestones, and (4) reservoir geometries are difficult to image. To date, reflection-seismic Trenton-Black River discoveries have been based on: (1) disruptions (sags) at the Trenton event, (2) internal waveform changes, (3) disruption of lower events, and (4) recognition of faults from offsetting events and/or diffractions.

Soil gas geochemistry studies above Scipio field showed no correlation between soil gas and producing parts of the field; however, soil gas geochemistry reportedly played an important role in the Stoney Point Field discovery.

Exploitation

Secondary Recovery has been minimal. Results were discouraging from a pilot waterflood of the Haskell Unit (near south end Scipio Field). Marathon Oil has drilled a number of Trenton-Black River horizontal wells that show considerable promise for future exploitation.

Summary

This is the first comprehensive, systematic study to determine the basin-wide relationships of: (1) original carbonate depositional patterns, (2) formation of early stage diagenetic dolomites vs. later stage burial and hydrothermal dolomites, (3) types and patterns of faulting, (4) types and patterns of dolomitization resulting from this faulting, (5) resulting reservoir rock quality, (6) oil accumulations (field delineation and orientation), and (7) hydrocarbon production. The current Trenton-Black River exploration model of looking for a seismic sag associated with basement faults in long linear patterns appears to be only partially correct. It is possible, in light of evolving geological concepts concerning the Michigan Basin, that other styles of Trenton-Black River fields exist. However, no exploration models covering these variations have yet been developed. This work will provide numerous opportunities to expand our understanding of Trenton-Black River hydrocarbon accumulations and significantly add to known reserves.

Silurian Niagaran Production

General Observations

1. Production data for the Niagaran Trend is generally good. The play began in the early 1950's and hit its peak during the 1970's-1980's. Digital data bases

developed by the state beginning in 1981 include a large portion of the data for this play.

2. The log plot of the data displays a curve typical of that for a mature play. Nearly all field sizes are represented and no “gaps” in field size occur. The slope of the curve is shallow indicating full representation of each field size. Future potential is probably resource limited for this particular exploration model; however, new technology, combined with a new/expanded exploration model could potentially re-set the curve to a higher level.

3. There are 1,162 fields in this play. There are 1,063 fields producing oil. This volume of data makes it difficult to plot trends including individual field names. Rather, data can best be examined as categories based upon field size. “Cumulative Oil Production” can be broken down into 5 basic categories: 1) Fields 1-10 million barrels cumulative oil production, 2) Fields 100,000 – 1 million barrels cumulative oil production, 3) fields 10,000 – 100,000 barrels cumulative oil production, 4) fields 1,000 – 10,000 barrels oil cumulative production and 5) fields less than 1,000 barrels cumulative oil production.

4. Fields making less than 1,000 barrels oil cumulative production are probably not economic based upon oil production alone. The sharp drop-off in fields of this size is probably due to the fact that no one purposely looks for this sized field. However, a few disappointing fields of this size do occur and are produced to recover at least some of the cost of exploration and development. These fields, in most cases, are associated with gas production that makes the venture economic.

5. Gas is produced in 991 fields compared to oil being produced in 1,063 fields. Gas production volumes remain somewhat level in relationship to oil production volume (1 million BOE).

6. Brine is produced in 664 fields. Production of brine is roughly related to oil production. The larger oil fields all produce brine whereas the smaller the oil field, the less likely it is to produce brine. Only 8 fields produce only gas and brine. Brine volumes are roughly related to oil volumes. Only 28 fields produce more brine than oil. (refer to Cumulative Oil-Gas-Brine Production by field Graph)

7. The State of Michigan imposes a 200 barrel-per-day maximum allowable on production which often distorts the true capabilities/performance of the affected wells.

8. The graph of "Discovery Size (Cumulative Oil) by Year of Discovery" displays a wide variety of field performance for each year. Although originally kicked-off in 1950, Niagaran fields did not hit peak oil productivity until 1971 when drilling boomed with the discovery of 32 new fields that year. The 1970's represent the "best times" for Niagaran discoveries, with a sharp decline after 1981. This data set does not include the onset of horizontal drilling during the 1990's.

9. There are 1,162 fields in the Niagaran Trend. The oldest field in the trend was discovered in 1950. Only 9 fields in the Niagaran Trend have produced more than 35 years. Nearly one half of the fields have produced for 15 – 30 years (531 fields). Only 181 fields have produced for 5 years or less. Seventy-three fields were either produced for less than one year or not produced at all.

10. "Cumulative Oil Production" varies substantially when plotted against "Years of Production." However, the best producers in each age bracket show impressive results. Nearly 10,000,000 barrels of cumulative oil have been produced by fields in the 30 to 50 year age bracket. Fields in production from 22 years to 30 years have top producers in the 1-5 million barrel range. Top producing fields in the 5 –

22 year bracket still hit the 1 million barrel mark other than for year 9. Even fields in production for only 1 year have obtained the 100,000 barrel mark.

Current Activity

1. Fields from each of the 5 basic categories defined above will be correlated to the newly developed index covering data quantity, quality and availability for each field. Fields in each category ranking high in data coverage will be selected for detailed study.

Devonian Dundee Trend Production

General Observations

1. Production data for the Dundee Trend is generally good. Dundee production statistics go back to 1934 although commercial Dundee production began in 1928 and has remained a stalwart of the Michigan Basin ever since. Its production ranks second only to that of the Niagaran Trend; however, the Niagaran Trend contains 1,162 fields vs. only 178 fields in the Dundee Trend.

2. The log plot of the data displays a curve typical of that for a mature play. Nearly all fields sizes are represented and no "gaps" in field size occur. The slope of the curve is shallow indicating full representation of each field size. Future potential is probably resource limited for this particular exploration model; however, new technology, combined with a new/expanded exploration model could potentially re-set the curve to a higher level.

3. There are 178 fields in this play. There are 155 fields producing oil. This volume of data makes it difficult to plot trends including individual field names; therefore, data has been examined as categories based upon field size. "Cumulative Oil Production" can be broken down into 7 basic categories: 1.) 8 Fields making 10-50 million barrels cumulative oil production, 2.) 30 fields 1 – 10 million barrels

cumulative oil production, 3.) 50 fields making 100,000 – 1 million barrels cumulative oil production, 4.) 39 fields making 10,000 – 100,000 barrels oil cumulative production and 5.) 20 fields making 1,000 – 10,000 barrels cumulative oil production, 6.) 8 fields making 0 – 1,000 barrels cumulative oil production, and 7.) 14 fields making 0 oil production.

4. Fields making less than 1,000 barrels oil cumulative production (9 fields) are probably not economic based upon oil production alone. The sharp drop-off in fields of this size is probably due to the fact that no one purposely looks for this sized field. However, a few disappointing fields of this size do occur and are produced to recover at least some of the cost of exploration and development.

5. Gas is produced in 41 fields compared to oil being produced in 155 fields (although many fields may have initially had gas, production was limited due to infrastructure and much of the gas production was flared).

6. Brine is produced in 141 fields. Only 13 oil fields do not produce brine. Only 4 gas fields do not produce brine.

7. The State of Michigan imposes a 200 barrel-per-day maximum allowable on production which often distorts the true capabilities/performance of the affected wells.

Current Activity

1. Work is currently underway to further develop data covering Reed City vs. overall Dundee Formations.

2. Dundee Cumulative production vs. Year Discovered data is currently being edited for analysis.

3. Fields from each of the 7 basic categories defined above will be correlated to the newly developed index covering data quantity, quality and availability for each field. Fields in each category ranking high in data coverage will be selected for detailed study.

REFERENCES CITED

Ardrey, R.H., 1978, Diagenesis of Middle Ordovician Trenton Formation in southern Michigan (M.S. thesis): Ann Arbor, Michigan, University of Michigan, 52 p.

Beghini, V.G., and Conroy, T.R., 1960, A history of the Trenton Albion-Scipio trend of Michigan: 5th Annual Ontario Petroleum Institute Conference Proceedings, London, Ontario, p. 1-21.

Budai, J.M., and Wilson, J.L., 1986, Depositional Patterns and diagenetic history of Trenton-Black River Formations in Michigan Basin (abs.): American Association of Petroleum Geologists Bulletin, v. 70, p. 1063.

Budros, Ron 2004, *Structural Styles of Hydrothermal Dolomite Reservoirs in the Michigan Basin*, abst., AAPG National Meeting, 2004 AAPG Bulletin Vol. 88, No. 13

Buehner, J.H., and Davis, Jr., S.H., 1968, Albion-Pulaski-Scipio Trend field: Michigan Basin Geological Society Oil and Gas Field Symposium, Lansing, Michigan, p. 37-48.

Burgess, R.J., 1960, Eastern Canada has a new exploratory target… oil in Trenton synclines: Oil and Gas Journal, v. 58, n. 33, p. 124-131.

Chittick, Steven, 1996, Unpublished M.S. Thesis, MTU, Houghton, MI.

Curran, B.C., and Hurley, N.F, 1992, *Geology of the Devonian Dundee Reservoir, West Branch Field, Michigan*. American Association of Petroleum Geologists Bulletin, V. 76, No. 9, pp. 1363-1383.

DeHaas, R.J. and Jones, M.W., 1984, Cave levels of Trenton-Black River in south-central Michigan (abs.): American Association of Petroleum Geologists Bulletin, v. 68, p. 1918.

DeHaas, R.J. and Jones, M.W., 1989, Cave levels of Trenton-Black River in central southern Michigan, *in* B.D. Keith, ed., the Trenton Group (Upper Ordovician Series) of eastern North American: American Association of Petroleum Geologists Studies in Geology, No. 29, p. 237-266.

Ells, G.D., 1962, Structures associated with the Albion-Scipio oil field trend: Michigan Geological Survey, East Lansing, Michigan, 86 p.

Gardner, W.C., 1974, *Middle Devonian Stratigraphy and Depositional Environments in the Michigan Basin.* Mich. Basin Geol. Soc., Spec. Papers no.1, 138p.

Gray, J., 1983, Prospects for deep drilling in Ohio: Ohio Oil and Gas Association, Winter Meeting, Columbus, Ohio, 27 p.

Hurley, N.F. and Budros, R., 1990, Albion-Scipio and Stoney Point fields – U.S.A., Michigan Basin, *in* Beaumont, E.A., and N.H. Foster, eds., Stratigraphic Traps I, Treatise of Petroleum Geology, Atlas of Oil and Gas Fields: Tulsa, Oklahoma, American Association of Petroleum Geologists, p. 1-37.

Hurley, N.F., and Cumella, S.P., 1987, Dolomitization and reservoir development, Albion-Scipio field, Michigan (abs.): SEPM Annual Midyear Meeting, Program with Abstracts, v. 4, p. 37.

Jones G.D. and Xiao Y., 2005*: Dolomitization, anhydrite cementation, and porosity evolution in a reflux system: Insights from reactive transport models.* American Association of Petroleum Geologists Bulletin 89, no.5, p. 577-601

Keith, B.D., 1985, Facies, diagenesis, and the upper contact of the Trenton Limestone of northern Indiana, *in* Cercone, K.R. and Budai, J.M., eds., Ordovician and Silurian rocks of the Michigan Basin and its margins: Michigan Basin Geological Society, Lansing Michigan, Special Paper 4, p. 15-32.

Luczak, John A., 2001, *Preliminary Results Of A Fluid-Inclusion Study On Fractured Carbonate Reservoirs Of The Dundee Formation, Central Michigan Basin, U.S.A*: GSA Annual Meeting, November 5-8, 2001.

Montgomery, Eric, 1986, *Facies development and porosity relationships in the Dundee Limestone of Gladwin County, Michigan*. Master's Thesis, Western Michigan University, 89 p.

Montgomery S.L.; Wood J.R.; Harrison W.B. III, 1998**:** *Devonian Dundee Formation, Crystal Field, Michigan Basin: recovery of bypassed oil through horizontal drilling.* American Association of Petroleum Geologists Bulletin 82, no.8, p. 1445-1462

Prouty, C.E., 1988, *Trenton Exploration and Wrenching Tectonics – Michigan Basin and Environs*, *in* B.D. Keith, ed. The Trenton Group, (Upper Ordovician Series) of Eastern North America: AAPG Studies in Geology, pp. 207-236.

Rooney, L.F., 1966, Evidence of unconformity at top of Trenton Limestone in Indiana and adjacent states: American Association of Petroleum Geologists Bulletin, v. 50, p. 533-546.

Shaw, B. 1975, Geology of the Albion-Scipio trend, southern Michigan (M.S. thesis): Ann Arbor, Michigan, University of Michigan, 69 p.

Strecker, U., Carr, M., Knapp, S., Smith, M., Uden, R., and Taylor, G., 2005: *Matching to Mode and Cut Risk,* AAPG Explorer, V. 26, no.7, p. 26.

Taylor, T.R. and Sibley, D.F., 1986, Petrographic and geochemical characteristics of dolomite types and the origin of ferron dolomite in the Trenton Formation, Ordovician, Michigan Basin, U.S.A.: Sedimentology, v. 33, p. 61-86.

Wood, J.R. and Harrison, W.B., 1999, *Mapping and Visualization of Dolomite "Chimneys" in the Michigan Basin*: DOE-PTTC Joint 1999 Oil and Gas Conference, Exploration Methods and Basin Analysis, (www version).

Wood, J.R., 2003, *Mapping Large-Scale Faults in the Michigan Basin using Tops Data:* AAPG National Meeting, 2003 AAPG Bulletin Vol. 87, No. 13

BIBLIOGRAPHY (TASK 2.1)

Abbott, P. L., 1974, Calcitization of Edwards Group dolomites in the Balcones Fault Zone aquifer, south-central Texas, v. 2, p. 359-362.

Abdel-Gawad, A. M., and P. F. Kerr, 1963, Alteration of Chinle siltstone and uranium emplacement, Arizona and Utah: Geological Society of America Bulletin, v. 74, p. 23-46.

Adams, J. E., and M. L. Rhodes, 1960, Dolomitization by seepage refluxion, v. 44, p. 1912-1920.

Ahsan, N., 1998, Tithonian to Danian sedimentation in Hazara Basin, northern Pakistan: AAPG Foundation grants-in-aid recipients for 1998; abstracts AAPG Bulletin, v. 82, p. 2158.

Aitken, J. D., 1967, Classification and environmental significance of cryptalgal limestones and dolomites, with illustrations from the Cambrian and Ordovician of SW Alberta, v. 37, p. 1163-1178, 22 Figs.

Aitken, J. D., 1977, Classification and environmental significance of cryptalagal limestones and dolomites. With illustrations from the Cambrian and Ordovician of southwest Alberta, v. 14, p. 405-441.

Al-Aasm, I. S., and J. J. Packard, 2000, Stabilization of early-formed dolomite: a tale of divergence from two Mississippian dolomites, v. 131, p. 97-108, 7 Figs., 1 Tab.

Allan, J. R., and W. D. Wiggins, 1993, Dolomite reservoirs, geochemical techniques for evaluating origin and distribution, v. 36, p. 167pp.

Al-Shaieb, Z., and J. W. Shelton, 1978, Secondary ferroan dolomite rhombs in oil reservoirs, Chadra sands, Gialo Field, Libya: AAPG Bulletin, v. 62, p. 463-468.

Amiri-Garroussi, K., 1988, Eocene spheroidal dolomite from the western Sirte Basin, Libya, v. 35, p. 577-585, 4 Figs.

Amthor, J. E., E. W. Mountjoy, and H. G. Machel, 1993, Subsurface dolomites in Upper Devonian Leduc Formation buildups central part of Rimbey-Meadowbrook reef trend, Alberta, Canada, v. 41, p. 164-185, 15 Figs., 5 Tabs.

Amthor, J. E., and J. Okkerman, 1998, Influence of early diagenesis on reservoir quality of Rotliegende sandstones, northern Netherlands: AAPG Bulletin, v. 82, p. 2246-2265.

Antonellini, M., and P. L. Mollema, 2000, A Natural Analog for a Fractures and Faulted Reservoir in Dolomite: Triassic Sella Group, Northern Italy: The American Association of Petroleum Geologists Bulletin, v. 84, p. 314-344.

Antonellini, M., and P. N. Mollema, 2000, A natural analog for a fractured and faulted reservoir in dolomite; Triassic Sella Group, northern Italy: AAPG Bulletin, v. 84, p. 314-344.

Aref, M. A. M., 1998, Biogenic carbonates; are they a criterion for underlying hydrocarbon accumulations? An example from the Gulf of Suez region, Egypt: AAPG Bulletin, v. 82, p. 336-352.

Arvidson, R. S., and F. T. Mackenzie, 1997, Tentative kinetic model for dolomite precipitation rate and its application to dolomite distribution: Aquatic Geochemistry, v. 2, p. 273-298.

Arvidson, R. S., and F. T. Mackenzie, 1999, The dolomite problem: control of precipitation eunetics by temperature and saturation state, v. 299.

Arvidson, R. S., F. T. Mackenzie, and M. Guidry, 2002, Ocean/atmosphere history and carbonate precipitation rates: a solution to the 'dolomite problem'?, v. 66, p. 1-5, 4 Figs.
Assereto, R., and R. L. Folk, 1980, Diagenetic fabrics of aragonite, calcite, and dolomite in an ancient peritidal-spelean environment; Triassic Calcare rosso, Lombardia, Italy: Journal of Sedimentary Petrology, v. 50, p. 371-394.
Assereto, R., and R. L. Folk, 1980, Diagenetic fabrics of aragonite, calcite and dolomite in ancient peritidal-spelean environment: Triassic Calcare Rosso, Lombardia, Italy, v. 50/2, p. 371-394, 17 Figs.
Assereto, R. L., and A. Rizzini, 1975, Reworked ferroan dolomite grains in the Triassic 'oolite a gasteropodi' of Camoniche Alps (Italy) as indicators of early diagenesis, v. 148/2, p. 215-232, 13 Figs.
Atchley, S. C., M. G. Kozar, and L. A. Yose, 1999, A predictive model for reservoir distribution in the Permian (Leonardian) Clear Fork and Glorieta formations, Robertson Field area, West Texas: AAPG Bulletin, v. 83, p. 1031-1056.
Ayyildiz, T., E. Tekin, and M. Satir, 2004, Water circulation near the mixed-water and microbiologic activity of the Mesozoic dolomite sequence, an example from the central Taurus, Turkey: Carbonates and Evaporites, v. 19, p. 107-117.
Babic, L., 1969, Sphaerocodium or onkoids from the Upper Triassic Dolomite of Western Yougoslavia, v. 23, p. 11-19, 1 Fig., 1 Pl.
Baker, P. A., and S. J. Burns, 1985, Occurrence and formation of dolomite in organic-rich continental margin sediments: AAPG Bulletin, v. 69, p. 1917-1930.
Baker, P. A., and M. Kastner, 1981, Constraints on the formation of sedimentary dolomites, v. 213, p. 214-216.
Balog, A., J. F. Read, and J. Haas, 1999, Climate-controlled early dolomite, Late Triassic cyclic platform carbonates, Hungary, v. A69, p. 267-282, 17 Figs., 3 Tabs.
Banner, J. L., G. N. Hanson, and W. J. Meyers, 1988, Rare earth element and Nd isotopic variations in regionally extensive dolomites from the Burlington-Keokuk Formation (Mississippian); implications for REE mobility during carbonate diagenesis: Journal of Sedimentary Petrology, v. 58, p. 415-432.
Banner, J. L., G. N. Hansson, and W. J. Meyers, 1988, Rare earth elements and Nd isotopeic variations in regionally extensive dolomites from the Burlington-Keoku Formation (Mississippian): implications for the Ree Mobility during carbonate diagenesis, v. 58/3, p. 415-432, 15 Figs.
Banner, J. L., G. N. Hansson, and W. J. Meyers, eds., 1988, Water-rock interaction history of regionally extensive dolomites of the Burlington-Keokuk Formation (Mississippian): Isotope evidence, v. 43: Tulsa, 97-111, 12 Figs. p.
Barber, D. J., R. J. Reeder, and D. J. Smith, 1985, A TEM microstructural study of dolomite with curved facies (saddle dolomite), v. 91, p. 82-92.
Barclay, S. A., R. H. Worden, J. Parnell, D. L. Hall, and S. M. Sterner, 2000, Assessment of fluid contacts and compartmentalization in sandstone reservoirs using fluid inclusions; an example from the Magnus oil field, North Sea: AAPG Bulletin, v. 84, p. 489-504.
Barnaby, R. J., and J. F. Read, 1992, Dolomitization of a carbonate platform during late burial: Lower to Middle Cambrian Shady dolomite, Virginia Appalachians, v.

62/6, p. 1023-1043, 16 Figs., 1 Tab.

Bassias, Y., and P. Cros, 1992, Dolomite and chert diagenesis in Upper Cretaceous pelagic sediments. Southern Kerguelen Plateau Md48: Naska dredges, v. 184, p. 359-388, 4 Pls., 5 Figs., 4 Tabs.

Baum, G. R., W. B. Harris, and P. E. Drez, 1985, Origin of dolomite in the Eocene Castle Hayne Limestone, North Carolina: Journal of Sedimentary Petrology, v. 55, p. 506-517.

Baum, G. R., W. B. Harris, and P. E. Drez, 1985, Origin of dolomite in the Eocene Castle Hyne Limestone, North Carolina, v. 55/4, p. 506-517, 10 Figs.

Bausch, W. M., and J. Hoefs, 1972, Die Isotopenzusammensetzung von Dolomiten und Kalken aus dem süddeutschen Malm, v. 37, p. 121-130, 5 Figs., 2 Tabs.

Beales, F. W., and J. L. Hardie, 1980, Criteria for the recognition of diverse dolomite types with an emphasis on studies of host rocks for Mississippian Valles-type ore deposits, v. 28, p. 197-213, 4 Figs.

Bein, A., and L. S. Land, 1983, Carbonate sedimentation and diagenesis associated with Mg-Ca-chloride brines; the Permian San Andres Formation in the Texas Panhandle: Journal of Sedimentary Petrology, v. 53, p. 243-260.

Bernasconi, S. M., 1994, Geochemical and microbial controls on dolomite formation in anoxic envrionments: a case study from the Middle Triassic (Ticino, Switzerland), v. 19, p. 1-109, 7 Pls., 20 Figs., 6 Tabs.

Bernoulli, D., L. Gasperini, E. Bonatti, and P. Stille, 2004, Dolomite formation in pelagic limestone and diatomite, Romanche fracture zone, Equatorial Atlantic: Journal of Sedimentary Research, v. 74, p. 924-932.

Bertrand-Sarfati, J., and A. Moussine-Pouchkine, 1983, Platform-to-basin facies evolution; the carbonates of late Proterozoic (Vendian) Gourma (West Africa): Journal of Sedimentary Petrology, v. 53, p. 275-293.

Biddle, K. T., 1983, Girvanella oncoids from Middle to Upper Triassic allochthonous boulders of the Dolomite Alps, Northern Italy: Berlin, Springer, p. 390-397,6 Figs.

Biddle, K. T., W. Schlager, K. W. Rudolph, and T. L. Bush, 1991, Seismic model of a progradational carbonate platform, Picco di Vallandro, the Dolomites, Northern Italy, v. 76/1, p. 14-50, 11 Figs.

Biddle, K. T., W. Schlager, K. W. Rudolph, and T. L. Bush, 1992, Seismic model of a progadational carbonate platform, Picco di Vallandro, the dolomites, Italy, v. 76, p. 14-30.

Biddle, K. T., W. Schlager, K. W. Rudolph, and T. L. Bush, 1992, Seismic model of a progradational carbonate platform, Picco di Vallandro, the Dolomites, Northern Italy: American Association of Petroleum Geologists Bulletin, v. 76, p. 14-30.

Blake, D. F., D. R. Peacor, and B. H. Wilkinson, 1982, The sequence and mechanism of low-temperature dolomite formation: Calcian dolomites in a Pennsylvanian echinoderm, v. 52/1, p. 59-70, 4 Figs.

Blau, J., 1987, Neue Foraminiferen aus dem Lias der Lienzer Dolomiten Teil I: Die Foraminiferenfauna einer roten Spaltenfüllung in Oberrhätkalken, v. 129, p. 495-523, 2 Figs., 7 Pls.

Blau, J., 1987, Neue Foraminiferen aus dem Lias der Lienzer Dolomiten Teil II:

Foraminiferen (Involutinen, Spirillinen) aus der Lavanter Breccie (Lienzer Dolomiten) und den Nördlichen Kalkalpen, v. 130, p. 5-23, 1 Fig., 5 Pls.
Blau, J., and B. Grün, 1992, Calpionelen der tiefen Unterkreide im Apt/Alb der Lienzer Dolomiten: Ein Beispiel für umgelagerte Faunen, v. 48, p. 9-28, 2 Pls., 3 Figs.
Blau, J., B. Grün, and M. Senff, 1993, Crustaceen-Koprolithen aus der Trias der westlichen Tethys (Lienzer Dolomiten, Österreich; Pragser Dolomiten, Italien) und vom Gondwana-Westrand (oberes Magdalenatal, Kolumbien, Südamerika), v. 67, p. 193-214, 12 Figs.
Blendinger, W., 1985, Radiolarian limestones interfingering with Loferites (Triassic, Dolomites, Italy), v. 1985, p. 193-202, 7 Figs.
Blendinger, W., 1986, Isolated stationary carbonate platforms: the Middle Triassic (Ladinian) of the Marmolada area, Dolomites, Italy, v. 33, p. 159-183, 21 Figs.
Blendinger, W., 1994, The carbonate factory of Middle Triassic buildups in the Dolomites, Italy: a quantitative analysis: Sedimentology, v. 41, p. 1147-1159.
Blendinger, W., 1997, Dolomitization of the Dolomites (Triassic, Italy): pilot study, v. 204, p. 83-110.
Blendinger, W., 2001, Triassic carbonate buildup flanks in the dolomites, northern Italy: breccias, boulder fabric and the importance of early diagenesis, v. 48, p. 919-933, 11 Figs.
Blendinger, W., and E. Blendinger, 1989, Windward-leeward effect on Triassic carbonate bank margin facies of the Dolomites, northern Italy, v. 64, p. 143-166, 18 Figs.
Bleninger, W., 1994, The carbonate factory of Middle Triassic buildups in the Dolomites, Italy: a quantitative analysis: Sedimentology, p. 1147-1159.
Bliefnick, D. M., and W. C. Belfield, 1991, The Ordovician Arbuckle Group of Oklahoma - a karsted dolomite reservoir: Ortisei, p. 17-18.
Boles, J. R., C. A. Landis, and P. Dale, 1985, The Moeraki Boulders; anatomy of some septarian concretions: Journal of Sedimentary Petrology, v. 55, p. 398-406.
Bone, Y., N. P. James, and T. K. Kyser, 1992, Synsedimentary detrital dolomite in Quaternary cool-water carbonate sediments, Lacopede shelf, South Australia, v. 20, p. 109-112, 4 Figs., 1 Tab.
Bone, Y., N. P. James, and T. K. Kyser, 1992, Syndsedimentary detrital dolomite in Quaternary cool-water carbonate sediments, Lacepee shelf, South Australia: Geology, v. 20, p. 109-112.
Boni, M., G. Parente, T. Bechstadt, B. De Vivo, and A. Iannace, 2000, Hydrothermal dolomites in SW Sardinia (Italy): evidence for a widespread late-Variscan fluid flow event: Sedimentary Geology, v. 131, p. 181-200.
Boni, M., G. Parente, T. Bechstädt, B. De Vivo, and A. Iannace, 2000, Hydrothermal dolomites in SW Sardinia (Italy): evidence for a widespread late-Variscan fluid flow event, v. 131, p. 181-200, 12 Figs., 2 Tabs.
Boone, P. A., and D. B. Moore, 1975, Chunchula Field; giant in the making?: AAPG Bulletin, v. 59, p. 1723-1724.
Bornemann, E., and J. H. Doveton, 1983, Lithofacies mapping of Viola Limestone in south-central Kansas, based on wireline logs: AAPG Bulletin, v. 67, p. 609-623.
Bosellini, A., 1966, Protointraclasts: texture of some Werfenian (Lower Triassic) limestones of the Dolomites (Northeastern Italy), v. 6, p. 333-337, 2 Figs.

Bosellini, A., 1984, Progradation geometries of carbonate platforms: examples from the Triassic of the Dolomites, northern Italy: Sedimentology, v. 31, p. 1-24.
Bosellini, A., and D. Rossi, 1974, Triassic carbonate buildups of the dolomites, northern Italy: Referin TIme and Space, p. 209-233.
Brachert, T. C., and W. C. Dullo, 1994, Micrite crusts on ladinian foreslpoes of the dolomites seen in the light of a modern scenario from the Red Sea: Abh. Geol. B.-A., v. 50, p. 57-68.
Brachert, T. C., and W. C. Dullo, 1994, Micrite crusts on Ladinian foreslopes of the Dolomites seen in the light of a modern scenario from the Red Sea, v. 50, p. 57-68, 3 Pls., 3 Figs.
Brady, P. V., Krumhansl, J.L., adn Papenguth, H.W., 1996, Surface complexation clues to dolomite growth: Geochimica et Cosmochimica acta, v. 60, p. 727-731.
Braithwaite, C. J. R., 1986, Mechanical induced stylolites and loss of porosity in dolomites, v. 9, p. 343-348.
Brandner, R., E. Flügel, and B. Senowbari-Daryan, 1991, Microfacies of carbonate slope boulders: indicator of the source area (Middle Triassic: Mahlknecht Cliff, Western Dolomites), v. 25, p. 279-296, Pl. 69-74, 3 Figs., 1 Tab.
Bruckschen, P., S. Nöth, and D. K. Richter, 1990, Tempered microdolomites in crinoids: a new criterion for high diagenesis, v. 5, p. 197-207.
Bruckshen, P., S. Noeth, and D. K. Richter, 1990, Tempered microdolomites in crinoids: a new criterion for high-grade diagenesis, v. 5, p. 197-207, 9 Figs., 1 Tab.
Budai, J. M., K. C. Lohmann, and R. M. Owen, 1984, Burial dedolomite in the Mississippian Madison Limestone, Wyoming and Utah Thrust Belt: Journal of Sedimentary Petrology, v. 54, p. 276-288.
Budd, D. A., 1997, Cenozoic dolomites of carbonate islands: their attributes and origin, v. 42, p. 1-47.
Budros, R., and L. I. Briggs, 1975, Depositional environment of Ruff Formation in Southeast Michigan: AAPG Bulletin, v. 59, p. 1734-1735.
Buelter, D. P., and R. N. Guillemette, eds., 1988, Geochemistry of epigenetic dolomite associated with lead-zinc mineralization of the Viburnum Trend, Southeast Missouri: A reconnaissance study, v. 43: Tulsa, 85-93, 8 Figs. p.
Bullen, S. B., and D. F. Sibley, 1984, Dolomite selectivity and mimic replacement, v. 12, p. 655-658.
Burger, D., ed., 1989, Dolomite weathering and micromorphology of palaeosoils in the Franconian Jura, v. 15: Cremlingen, 261-267, 13 Figs. p.
Burns, S. J., and P. A. Baker, 1987, A geochemical study of dolomite in the Monterey Formation, California, v. 57/1, p. 128-139, 9 Figs.
Burns, S. J., P. A. Baker, and W. J. Showers, eds., 1988, The factors controlling the formation and chemistry of dolomite in organic-rich sediments.: Miocene Drakes Bay Formation, California, v. 43: Tulsa, 41-52, 10 Figs. p.
Burns, S. J., J. A. McKenzie, and G. Vasconcelos, 2000, Dolomite formation and biogeochemicla cycles in the Phanerozoic, v. 47, p. 49-61, 4 Figs.
Butler, P. E., 1961, Morphologic classification of sponge spicules, with descriptions of siliceous spicules from the Lower Ordovician Bellefonte dolomite in Central Pennsylvania, v. 35, p. 191-200, Pl. 39, 7 Figs.

Calver, C. R., and P. W. Baillie, 1990, Early diagenetic concretions associated with intrastratal shrinkage cracks in an upper Proterozoic dolomite, Tasmania, Australia: Journal of Sedimentary Petrology, v. 60, p. 293-305.
Calver, C. R., and P. W. Baillie, 1990, Early diagenetic concretions associated with interstratal shrinkage cracks in an Upper Proterozoic dolomite, Tasmania, Australia, v. 60/2, p. 293-305, 7 Figs.
Canaveras, J. C., S. Sanchez-Moral, J. P. Calvo, M. Hojos, and S. Ordonez, 1996, Dedolomites associated with karstification, an example of early dedolomitization in lacustrine sequences from the Tertiary Madrid Basin, Central Spain, v. 11, p. 85-103, 13 Figs.
Cander, H. S., 1994, An example of mixing-zone dolomite, Middle Eocene Avon Park Formation, Floridan aquifer system, v. A64, p. 615-629, 13 Figs.
Capo, R. C., C. E. Whipkey, J. R. Blachère, and O. A. Chadwick, 2000, Pedogenic origin of dolomite in a basaltic weathering profile, Kohala peninsula, Hawai, v. 28, p. 271-274, 3 Figs., 2 Tab.
Carpenter, A. B., 1980, The chemistry of dolomite formation I: the stability of dolomite, v. 28, p. 111-121, 7 Figs., 5 Tabs.
Catalov, A. G., 1999, Calcitization of dolomite in Spathian and Anisian carbonate rocks from the Western Balkanides, Bulgaria, v. 1999, p. 614-640, 8 Figs.
Cayeux, L., 1970, Les roches sédimentaires de France. Roches carbonatées (calcium et dolomies) - Sedimentary rocks of France. Carbonate rocks (limestones and dolomites): Darien, Hafner, 506 pp., 26 Figs. p.
Chafetz, H. S., and P. F. Rush, 1994, Diagenetically altered sabkha-type Pleistocene dolomite from the Arabian Gulf, v. 41, p. 409-421, 6 Figs., 3 Tabs.
Chafetz, H. S., and J. Zhang, 1998, Authigene euhedral megaquartz crystals in Quaternary dolomite, v. A68, p. 994-1000, 5 Figs.
Chahi, A., P. Duringer, M. Ais, M. Bouabdelli, F. Gauthier-Lafaye, and B. Fritz, 1999, Diagenetic transformation of dolomite into stevensite in lacustrine sediments from Jbel Rhassoul, Morocco, v. A69, p. 1123-1135, 14 Figs., 4 Tabs.
Chave, K. E., 1952, A solid solution between calcite and dolomite: Journal of Geology, v. 60, p. 190-192.
Chooquette, P. W., and R. P. Steinen, 1980, Mississippian non-supratidal dolomite: Ste. Genevieve Limestone, Illinois Basin: evidence for mixed-water dolomitization, v. 28, p. 163-1961.
Choquette, P. W., and R. P. Steinen, 1985, Mississippian oolite and non-supratidal dolomite reservoirs in the Ste. Genevieve Formation, North Bridgeport Field, Illinois Basin: New York, Springer, p. 207-225, 14 Figs.
Chow, N., and F. J. Longstaffe, 1995, Dolomites of the Middle Devonian Elm Point Formation, southern Manitoba; intrinsic controls on early dolomitization, v. 43, p. 214-255.
Cioppa, M. T., I. S. Al-Aasm, D. T. A. Symons, and K. P. Gillen, 2003, Dating penecontemporaneous dolomitization in carbonate reservoirs; paleomagnetic, petrographic, and geochemical constraints: AAPG Bulletin, v. 87, p. 71-88.
Clari, P., S. Cavagna, L. Martire, and J. Hunziker, 2004, A Miocene mud volcano and its plumbing system; a chaotic complex revisited (Monferrato, NW Italy): Journal of

Sedimentary Research, v. 74, p. 662-676.
Clasen, S., R. Jantschik, and D. Meischner, 1991, Authigenic dolomite in the North Atlantic deep sea: Ortisei, p. p. 53.
Compton, J. S., ed., 1988, Sediment composition and precipitation of dolomite and pyrite in the Neogene Monterey and Sisquoc Formations, Santa Maria Basin area, California, v. 43: Tulsa, 53-64, 7 Figs. p.
Compton, J. S., 1988, Degree of supersaturation and precipitation of organogenic dolomite, v. 16, p. 318-321.
Compton, J. S., D. L. Hall, D. J. Mallinson, and D. A. Hodell, 1994, Origin of dolomite in the phosphatic Miocene Hawthorn Group of Florida, v. A64, p. 638-649, 9 Figs., 5 Tabs.
Cooper, M., 1999, Exploring for hydrocarbons in the Cambro-Ordovician of Newfoundland and Quebec: 1999-2000 APPG distinguished lecturers AAPG Bulletin, v. 83, p. 1879.
Cooper, M., J. Weissenberger, I. Knight, D. Hostad, D. Gillespie, H. Williams, E. Burden, J. Porter-Chaudhry, D. Rae, and E. Clark, 2001, Basin evolution in western Newfoundland; new insights from hydrocarbon exploration: AAPG Bulletin, v. 85, p. 393-418.
Craig, D. H., 1988, Caves and other features of Permian karst in San Andres Dolomite, Yates Field Reservoir, West Texas: Berlin, Springer, p. 342-363, 18 Figs., 1 Tab.
Cros, P., 1977, Données nouvelles sur la dolomitisation des carbonates triasiques des Dolomites Italiennes, v. 21/4, p. 307-355, 4 Pls., 10 Figs.
Curtis, C. D., and M. L. Coleman, 1986, Controls on the precipitation of early diagenetic calcite, dolomite and siderite concretions in complex depositional sequences, v. 38, p. 23-33, 7 Figs.
Curtis, R., G. Evans, D. J. J. Kinsmann, and D. J. Shearman, 1963, Association of dolomite and anhydrite in the Rezent sedimentes of the Persian-Gulf, v. 197, p. 697-680.
Czurda, K., and L. Nicklas, 1970, Zur Mikrofazies und Mikrostratigraphie des Hauptdolomites und Plattenkalk-Niveaus der Klostertaler Alpen und des Rhätikon (Nördliche Kalkalpen, Vorarlberg), p. 165-253.
Danin, A., R. Gerson, K. Marton, and J. Garty, 1982, Patterns of limestone and dolomite weathering by lichens and blue-green algae and their palaeoclimatic significance, v. 37, p. 221-233, 10 Figs.
Dapples, E. C., 1962, Stages of diagenesis in the development of sandstones: Geological Society of America Bulletin, v. 73, p. 913-933.
Daughtry, A. C., D. Perry, and M. Williams, 1962, Magnesium isotopic distribution in dolomite, v. 26, p. 857-866, 3 Figs.
Davidson, P. M., 1994, Ternary iron, magnesium, calcium carbonates - a therodynamic model for dolomite as an ordered derivate of calcite-structure solutions, v. 79, p. 332-229.
Davies, G. R., 1979, Dolomite reservoir rocks: processes, controls, porosity development, v. 11, p. C1-C17.
Davies, G. R., 2000, Hydrpthermal Dolomite Reservoir Facies: Global and Western Canadian Perspectives: Calgary.

Davis, R. A., Jr., 1966, Willow River Dolomite: Ordoviician analogue of modern algal stromatolite environments: Journal of Geology, v. 74, p. 908-923.
Dawans, J. M., and P. K. Swart, 1988, Textural and geochemical alternations in Late Cenozoic Bahamian dolomites, v. 35, p. 385-403, 15 Figs.
Dawans, J. M., and P. K. Swart, 1988, Textural and geochemical alterations in Late Cenozoic Bahamian dolomites: Sedimentology, v. 35, p. 385-403.
De Deckker, P., and W. M. Last, 1989, Modern, non-marine dolomite in evaporitic playas of western Victoria, Australia, v. 64/4, p. 223-238, 6 Figs.
De Leeuw, N. H., 2002, Surface structures, stabilities, and growth of magnesian calcites_ a computational investigation from the perspective of dolomite formation, v. 87, p. 679-689.
de Souza, R. S., L. F. de Ros, and S. Morad, 1995, Dolomite diagenesis and porosity preservation in lithic reservoirs; Carmopolis Member, Sergipe-Alagoas Basin, northeastern Brazil: AAPG Bulletin, v. 79, p. 725-748.
DeCelles, P. G., and R. C. Gutschick, 1983, Mississippian wood-grained chert and its significance in the Western Interior United States: Journal of Sedimentary Petrology, v. 53, p. 1175-1191.
Deckker, P., and W. M. Last, 1988, Modern dolomite deposition in continental, saline lakes, western Victoria, Australia, v. 16, p. 29-32.
Deelman, J. C., L. S. Land, and R. L. Folk, 1975, Mg/Ca ratio and salinity; two controls over crystallization of dolomite: AAPG Bulletin, v. 59, p. 2056-2057.
Degens, E. T., and S. A. Epstein, 1964, Oxygen and carbon isotope ratios in coexisting calcites and dolomites from recent and ancient sediments, v. 28, p. 23-44.
Dehler, C. M., M. Elrick, J. D. Bloch, L. J. Crossey, K. E. Karlstrom, and D. J. Des Marais, 2005, High-resolution delta (super 13) C stratigraphy of the Chuar Group (ca. 770-742 Ma), Grand Canyon; implications for mid-Neoproterozoic climate change: Geological Society of America Bulletin, v. 117, p. 32-45.
Deike, R. G., 1990, Dolomite dissolution rates and possible Holocene dedolomitization of water-bearing units in the Edwards Aquifer, south-central Texas, v. 112, p. 335-373.
Demicco, R. V., 1983, Wavy and lenticular-bedded carbonate ribbon rocks of the Upper Cambrian Conococheague Limestone, central Appalachians: Journal of Sedimentary Petrology, v. 53, p. 1121-1132.
DeMis, W. D., and D. Petty, 1990, Depositional facies, textural characteristics, and reservoir properties of dolomites in Frobisher-Alida interval in Southwest North Dakota; discussion and reply: AAPG Bulletin, v. 74, p. 564-566.
Depowski, S., and T. M. Peryt, 1985, Carbonate Petroleum Reservoirs in the Permian Dolomites of the Zechstein, Fore-Sudetic Area, Western Poland: New York, Springer, p. 251-264, 11 Figs.
Derby, J. R., and J. T. Kilpatrick, 1985, Ordovician Red River Dolomite Reservoirs, Killdeer Field, North Dakota: New York, Springer, p. 59-69, 9 Figs.
Dickson, J. A. D., 2004, Echinoderm skeletal preservation; calcite-aragonite seas and the Mg/Ca ratio of Phanerozoic oceans: Journal of Sedimentary Research, v. 74, p. 355-365.
Dockal, J. A., 1988, Thermodynamic and kinetic description of dolomitization of calcite

and calcitization of dolomite (dedolomitization), v. 3/2, p. 125-141, 8 Figs.
Doglioni, C., A. Bosellini, and P. R. Vail, 1990, Stratal patterns: a proposal of classification and examples from the Dolomites, v. 2, p. 83-95, 18 Figs.
Doherty, P. D., G. S. Soreghan, and J. P. Castagna, 2002, Outcrop-based reservoir characterization; a composite phylloid-algal mound, western Orogrande Basin (New Mexico): AAPG Bulletin, v. 86, p. 779-795.
Donaldson, A. C., M. T. Heald, J. J. Renton, and S. M. Warshauer, 1975, Depositional environment of Rome Trough rocks, Mingo County Well, West Virginia: AAPG Bulletin, v. 59, p. 1735.
Dorobek, S. L., and R. H. Filby, 1988, Origin of dolomites in a downslope biostrome, Jefferson Formation (Devonian), Central Idaho: Evidence from ree patterns, stable isotopes, and petrography, v. 36, p. 202-215, 9 Figs.
Dorobek, S. L., T. M. Smith, and P. M. Whitsitt, 1990, Microfabrics and geochemical trends associated with meteoric alteration of early, near-surface dolomite, p. p. 33.
Dorobek, S. L., T. M. Smith, and P. M. Whitsitt, eds., 1993, Microfabrics and geochemistry ofmeteorically altered dolomite in Devonian and Mississippian carbonates, Montana and Idaho: New York, Springer, 205-225, 13 Figs. p.
dos Anjos, S. M. C., L. F. De Ros, R. Schiffer de Souza, C. M. de Assis Silva, and C. L. Sombra, 2000, Depositional and diagenetic controls on the reservoir quality of Lower Cretaceous Pendencia sandstones, Potiguar rift basin, Brazil: AAPG Bulletin, v. 84, p. 1719-1742.
Dozet, S., 1990, The Lofer cyclothem in the main dolomite (Hauptdolomit) of the Kocevje area, v. 37, p. 507-528.
Dozet, S., 1990, The Lofer cyclothems in the Main Dolomite (Hauptdolomit) ofthe Kocevje area, v. 37, p. 507-528, 4 Pls., 3 Figs.
Dozet, S., 1991, Norian oncoids in the Main Dolomite of the Kocevje area, v. 38, p. 79-95, 2 Pls., 1 Fig.
Dravis, J. J., and I. D. Muir, 1991, Controls on widespread dissolution of burial dolomites, Middle Devonian Upper Elk Point Group, western Canada: Ortisei, p. p. 64.
Durocher, S., and I. S. Al-Aasm, 1997, Dolomitization and neomorphism of Mississippian (Visean) upper Debolt Formation, Blueberry Field, northeastern British Columbia; geologic, petrologic, and chemical evidence: AAPG Bulletin, v. 81, p. 954-977.
Dworkin, S. I., and L. S. Land, 1991, Depositional and pore fluid controls on the formation of dolomite cements, Smackover Sandstones, Gulf of Mexico: Ortisei, p. p. 66.
Ehrenberg, S. N., and T. A. Svana, 2001, Use of spectral gamma-ray signature to interpret stratigraphic surfaces in carbonate strata; an example from the Finnmark carbonate platform (Carboniferous-Permian), Barents Sea: AAPG Bulletin, v. 85, p. 295-308.
Eichenseer, H. T., F. R. Walgenwitz, and P. J. Biondi, 1999, Stratigraphic control on facies and diagenesis of dolomitized oolitic siliciclastic ramp sequences (Pinda Group, Albian, offshore Angola): AAPG Bulletin, v. 83, p. 1729-1758.
El-Sayed, M. I., 2001, The nature and possible origin of dolomite in ArRub'Al Khali, The

UAE, v. 16, p. 210-223, 9 Figs., 1 Tab.
Epstein, S. A., D. L. Graf, and E. T. Degens, 1963, Oxygen isotope studies on the origin of dolomites: Amsterdam, North Holland Publ., p. 169-180.
Ernst, W. G., and E. D. Paylor, II, 1996, Study of the Reed Dolomite aided by remotely sensed imagery, central White-Inyo Range, easternmost California: AAPG Bulletin, v. 80, p. 1008-1026.
Eschard, R., P. Lemouzy, C. Bacchiana, G. Desaubliaux, J. Parpant, and B. Smart, 1998, Combining sequence stratigraphy, geostatistical simulations, and production data for modeling a fluvial reservoir in the Chaunoy Field (Triassic, France): AAPG Bulletin, v. 82, p. 545-568.
Fairchild, I. J., 1983, Chemical controls of cathodoluminescence of natural dolomites and calcites: new data and review: Sedimentology, v. 30, p. 579-583.
Farinacci, A., 1965, Breccias and laminated dolomites of the Gavignano exposure, v. 4, p. 129-144, 12 Figs.
Farr, M. R., 1989, Compositional zoning characteristics of late dolomite cement in the Cambrian Bonneterre Formation, Missouri: Implications for parent fluid migration pathways, v. 4/2, p. 177-194, 15 Figs.
Farr, M. R., 1992, Geochemical variation of dolomite cement within the Cambrian Bonneterre Formation, Missouri: evidence for fluid mixing, v. 62/4, p. 636-651, 13 Figs., 3 Tabs.
Fei, Q., and X.-P. Wang, 1984, Significant role of structural fractures in Renqiu buried-hill oil field in eastern China: AAPG Bulletin, v. 68, p. 971-982.
Fischer, H. J., ed., 1988, Dolomite diagenesis in the Metaline Formation, northeastern Washington State, v. 43: Tulsa, 209-219, 10 Figs. p.
Flood, P. G., J. A. Fagerstrom, and F. Rougerie, 1996, Interpretation of the origin of massive replacive dolomite within atolls and submerged carbonate platforms: strontium isotopic signature ODP Hole 866a, Resolution Guyot, Mid-Pacific Mountains, v. 101, p. 9-13, 2 Figs.
Flügel, E., and S. Kraus, 1988, The Lower Permian Sexten breccia (Sexten Dolomites) and the Tarvis breccia (Carnic Alps): microfacies, depositional environment and paleotectonic implications, v. 34, p. 67-90.
Foellmer, K. E. H., and F. A. Stoakes, 1987, Fault-controlled dolomite reservoirs in the Wabamun Group of the Peace River Arch, West Central Alberta, p. 1p.
Folk, R. L., and R. Assereto, 1974, Giant aragonite rays and baroque white dolomite in tepee-filling, Triassic of Lombardy, Italy (abs.), v. 164, p. 34-35.
Folk, R. L., and L. S. Land, 1975, Mg/Ca Ratio and Salinity; Two Controls over Crystallization of Dolomite: AAPG Bulletin, v. 59, p. 60-68.
Folkman, Y., 1969, Diagenetic dedolomitization in the Albian-Cenomanian Yagur Dolomite on Mount Carmel (Northern Israel), v. 37, p. 1204-1215.
Freeman, T., D. Rothbard, and A. Obrador, 1983, Terrigenous dolomite in the Miocene of Menorca (Spain): Provenance and diagenesis, v. 53/2, p. 543-548, 5 Figs.
Friedman, G. M., 1966, Occurrence and origin of Quaternary dolomite of Salt flat, West Texas, v. 36, p. 263-267, 2 Figs.
Friedman, G. M., 1972, Petrographic data and comments on the depositional environment of the Miocnen sulfates and dolomites at sites 124, 132 and 134 Western

Mediterranean Sea, v. 13, p. 695-707, 20 Figs.
Friedman, G. M., 1980, Dolomite is an evaporite mineral: evidence from the rock record and from sea-marginal ponds of the Red Sea, v. 28, p. 69-80, 9 Figs.
Friedman, G. M., 1989, Characteristics of deep-marine dolomite - discussion, v. 59/5, p. 879-880, 1 Fig.
Friedman, G. M., 1995, Diverse origin of modern dolomite in the Levant, v. 10, p. 65-78, 9 Figs., 5 Tabs.
Friedman, G. M., 1996, Strontium-isotopic signatures reflect an origin of dolomite by fresh-water efluent: The Pine Plains Formation (Wappinger Group, Cambrian) of southeastern New York, v. 11, p. 134-140, 4 Figs., 1 Tab.
Fritz, P., 1971, Geochemical characterizations of dolomite and the 18O content of Devonian oceans, v. 11, p. 277-282.
Fritz, P., and D. G. W. Smith, 1970, The isotopic concentration of secondary dolomites, v. 34, p. 1161-1163.
Füchtbauer, H., and H. Goldschmidt, 1965, Beziehungen zwischen Calciumgehalt und Bildungsbedingungen der Dolomite, v. 55, p. 29-40, 8 Figs., 2 Tabs.
Galli, G., 1989, Depositional mechanisms of storm sedimentation in the Triassic Dürrenstein Formation, Dolomites, Italy, v. 61, p. 81-93, 7 Figs.
Gao, G., 1991, Early Ordovician Cool Creek Dolomite, Middle Arbuckle group, Slick Hills, SW Oklahoma, U.S.A.; origin and modification, v. 61/2, p. 161-173, 8 Figs., 3 Tabs.
Gao, G., S. D. Hovorka, and H. H. Posey, 1990, Limpid dolomite in Permian San Andres Halite Rocks, Palo Duro Basin, Texas Panhandle: Characteristics, possible origin, and implications for brine evolution: Journal of Sedimentary Petrology, v. 60, p. 118-124.
Gao, G., L. S. Land, and R. L. Folk, 1992, Meteoric modification of early dolomite and late dolomitization by basinal fluids, upper Arbuckle Group, Slick Hills, southwestern Oklahoma: AAPG Bulletin, v. 76, p. 1649-1664.
Garrison, R. E., M. Kastner, and D. H. Zenger, 1984, Dolomites of the Monterey Formation and other organic-rich units: Los Angeles, 215 pp. p.
Gasiewicz, A., and T. M. Peryt, 1994, Biolaminites at the Zechstein (Upper Permian) Platy Dolomite (Ca3)-Main Anhydrite (A3) boundary: implications for evolution of an evaporite basin, v. 19, p. 91-101, 3 Pls., 1 Fig.
Gensmer, R. P., and M. P. Weiss, 1980, Accuracy of calcite/dolomite ratios by X-ray diffraction and comparison with results from staining techniques, v. 50/2, p. 626-629, 2 Figs.
Gerhard, L. C., 1974, Redescription and New Nomenclature of Manitou Formation, Colorado: AAPG Bulletin, v. 58, p. 1397-1402.
Germann, K., 1969, Reworked dolomite crusts in the Wettersteinkalk (Ladinian, Alpine Triassic) as indicators of early supratidal dolomitization and lithification, v. 12, p. 257-277, 13 Figs.
Gerthofferova, H., and M. Misik, 1971, Electron microscope study of some limestones and dolomites of the Carpathian Mountains, v. 21, p. 163-186, Pl. 26-40, 3 Figs.
Gianolla, P., C. Siorpaes, and P. Vail, 1991, Carnian stratigraphic record in the Dolomites. An example of outcrop sequence stratigraphy: Ortisei, p. 82-83.

Gilhaus, A., J. Meijer, D. K. Richter, and A. Stephan, 2000, Quantitative Kathodolumineszenz-Spektroskopie Mn2-aktivierter diagenetischer und hydrothermaler Dolomite, v. 43, p. 49-50.
Gillen, K. P., R. Van der Voo, and J. H. Thiessen, 1999, Late Cretaceous-early Tertiary remagnetization of the Devonian Swan Hills Formation recorded in carbonate cores from the Caroline gas field, Alberta, Canada: AAPG Bulletin, v. 83, p. 1223-1235.
Gillhaus, A., 2000, Petrographisch/geochemische Untersuchungen zur Genese und Diagenese der Dolomite von Hydra (Griechenland) unter besonderer Berücksichtigung der Kathodolumineszenz-Mikroskopie, v. 54, p. 1-123, 4 Pls., 31 Figs.
Gillhaus, A., D. K. Richter, J. Meijer, R. D. Neuser, and A. Stephan, 2001, Quantitative high resolution cathodoluminescenece spectroscopy of diagenetic and hydrothermal dolomites, v. 140, p. 191-199.
Gillott, J. E., 1963, Petrology of dolomitic limestones, Kingston, Ontario, Canada: Geological Society of America Bulletin, v. 74, p. 759-778.
Gindy, A. R., A. J. Al-Shakiry, and N. A. Sa'ad, 1985, Spheroidal weathering in marls and chalks of Gebel Gurnah near Luxor, southern Egypt: Journal of Sedimentary Petrology, v. 55, p. 762-768.
Given, R. K., and B. H. Wilkinson, 1987, Dolomite abundance and stratigraphic age: constraints on rates and mechanisms of Phanerozoic dolostone formation, v. 57/6, p. 1068-10787, 4 Figs., 2 Tabs.
Goldhammer, R. K., P. A. Dunn, and L. A. Hardie, 1991, Sequence stratigraphy and systems tract development of the Latemar platform, Middle Triassic of the Dolomites: outcrop calibration keyed by cycle stacking patterns: Ortisei, p. p. 90.
Goldhammer, R. K., and M. T. Harris, eds., 1989, Eustatic controls on the stratigraphy and geometry of the Latemar buildup (Middle Triassic), the Dolomites of Northern Italy, v. 44: Tulsa, 323-338, 18 Figs. p.
Goldhammer, R. K., M. T. Harris, P. A. Dunn, and L. A. Hardie, eds., 1993, Sequence stratigraphy and systems tract development of the Latemar platform, Middle Triassic of the Dolomites (Northern Italy): outcrop calibration keyed by cycle stacking patterns, v. 57: Tulsa, 353-387, 25 Figs. p.
Goldsmith, J. R., and D. L. Graf, 1958, Structural and compositional variations in some natural dolomites: Journal of Geology, v. 66, p. 678-692.
Goldsmith, J. R., D. L. Graf, J. Witters, and D. A. Northrop, 1962, Studies in the system CaCO3 - MgCO3 - FeCO3: 1. Phase relations; 2. A method for major-element spectrochemical analysis; 3. Compositions of some ferroan dolomites, v. 70/6, p. 659-668, 11 Figs., 10 Tabs.
Gotthardt, R., H. J. Hoppe, and E. Schiele, 1967, Das Sinterverhalten von Dolomiten unterschiedlicher Petrographie, v. 91, p. 121-125.
Gournay, J., B. L. Kirkland, R. L. Folk, and F. L. Lynch, 1999, Evidence for nannobacterially precipitated dolomite in Pennsylvanian rocks, Utah, v. 126, p. 243-252.
Gournay, J. P., 1998, Diagenesis and porosity/permeability prediction in Pennsylvanian phylloid algal bioherms of the Paradox Basin, southeastern Utah: AAPG

Foundation grants-in-aid recipients for 1998; abstracts AAPG Bulletin, v. 82, p. 2162-2163.
Gournay, J. P., B. L. Kirkland, R. L. Folk, and F. L. Lynch, 1999, Nanometer-scale features in dolomite from Pennsylvanian rocks, Paradox Basin, Utah, v. 126, p. 245-254.
Gregg, J. M., 1983, On the formation and occurrence of saddle dolomite; discussion: Journal of Sedimentary Petrology, v. 53, p. 1025-1026.
Gregg, J. M., 1985, Regional epigenetic dolomitization in the Bonneterre Dolomite (Cambrian), southeastern Missouri, v. 13, p. 503-506.
Gregg, J. M., ed., 1988, Origins of dolomite in the offshore facies of the Bonneterre Formation (Cambrian), Southeast Missouri, v. 43: Tulsa, 67-83, 13 Figs., 1 Tab. p.
Gregg, J. M., S. A. Howard, and S. J. Mazzullo, 1992, Early diagenetic recrystallization of Holocene (<3000 years old) peritidal dolomites, Ambergris Cay, Belize, v. 39, p. 143-160, 11 Figs., 2 Tabs.
Gregg, J. M., P. R. Laudon, R. E. Woody, and K. L. Shelton, 1993, Porosity evolution of the Cambrian Bonneterre Dolomite, south-eastern Missouri, USA, v. 40, p. 1153-1169, 9 Figs., 2 Tabs.
Gregg, J. M., and K. L. Shelton, 1990, Dolomitization and dolomite neomorphism in the back reef facies of the Bonneterre and Davis Formations (Cambrian), southeastern Missouri, v. 60/4, p. 549-562, 10 Figs.
Gregg, J. M., and D. F. Sibley, 1984, Epigenetic dolomitization and the origin of xenotopic dolomite texture, v. 54/3, p. 908-931, 19 Figs.
Grobe, M., and H. G. Machel, 1997, Petrographic and geochemical evidence for fault-controlled hydrothermal mineralization of the Brilon reef complex, Germany: AAPG Foundation grants-in-aid abstracts AAPG Bulletin, v. 81, p. 1775.
Gümbel, C. W., 1873, Mikroskopische Untersuchungen alpiner Triaskalke und Dolomite, v. 7/8, p. 141-144.
Gunatilaka, A., 1989, Spheroidal dolomites - arigin by hydrocarbon seepage?, v. 36, p. 701-710, 4 Figs.
Gunatilaka, A., 1991, Dolomite formation in coastal Al-Khiran, Kuwait Arabian Gulf - a re-examination of the sabkha model, v. 72, p. 35-53, 3 Figs., 2 Tabs.
Gunatilaka, A., A. Saleh, A. Al-Temeemi, and N. Nassar, 1984, Occurrence of Subtidal Dolomite in a Hypersaline Lagoon, Kuwait: Nature, v. 311, p. 450-452.
Guo, B., J. E. Sanders, and G. M. Friedman, 1996, Timing and origin of dedolomite in the Lower Ordovician (Wappinger Group) strata, southeastern New York, v. 11, p. 113-133, 14 Figs., 2 Tabs.
Guoqiu, G., L. S. Land, and R. L. Folk, 1992, Meteoric modification of early dolomite and late dolomitization by basinal fluids, Upper Arbuckle Group, slick Hill, Southwestern Oklahoma, v. 76, p. 1649-1664, 10 Figs., 3 Tabs.
Guthrie, J. M., and L. M. Pratt, 1995, Geochemical character and origin of oils in Ordovician reservoir rock, Illinois and Indiana, USA: AAPG Bulletin, v. 79, p. 1631-1649.
Habermann, D., R. D. Neuser, and D. K. Richter, 1996, REE-activated cathodoluminescence of calcite and dolomite: high-resolution spectrometric

analysis of CL emission (HRS-CL), v. 101, p. 1-7, 7 Figs.
Hanor, J. S., 2004, A model for the origin of large carbonate- and evaporite-hosted celestine (SrSO (sub 4)) deposits: Journal of Sedimentary Research, v. 74, p. 168-175.
Hardie, L. A., E. N. Wilson, and R. K. Goldhammer, 1991, Cyclostratigraphy and dolomitization of the Middle Triassic Latemar buildup, te Dolomites, northern Italy, p. 56 pp.
Harris, M. T., 1994, The Foreslope and toe-of-facies of the middle triassic latemar buildup (Dolomites, Northern Italy): Sedimentary Research, v. 64, p. 132-145.
Haynes, F. M., and S. E. Kesler, 1989, Pre-Alleghenian (Pennsylvanian-Permian) hydrocarbon emplacement along Ordovician Knox unconformity, eastern Tennessee: AAPG Bulletin, v. 73, p. 289-297.
Hendry, J. P., M. Wilkinson, A. E. Fallick, and N. H. Trewins, 2000, Dissepimented'jigsaw piece' dolomite in Upper Jurassic shelf sandstones, Central North Sea: an example of cement growth during bioturbation?, v. 47, p. 631-644, 7 Figs., 1 Tab.
Henessy, J., and L. P. Knauth, 1985, Isotopic variations in dolomite concretions from the Monterey Formation, California, v. 55/1, p. 120-130, 10 Figs.
Hennessy, J., and L. P. Knauth, 1985, Isotopic variations in dolomite concretions from the Monterey Formation, California: Journal of Sedimentary Petrology, v. 55, p. 120-130.
Hennings, P. H., 2002, Present and future of building, sharing, and exploiting 3-D models for characterization of strongly deformed reservoirs: 2001-2002 AAPG distinguished lecturers; North America distinguished lecture abstracts AAPG Bulletin, v. 86, p. 197-198.
Henrich, R., and J. Mirsal, 1982, A comparative study of the Supratidal and Basin Dolomites in the Anisian and Ladinian Carbonates of the Hohenstaufen Massiv (Northern limestone Alps), v. 28, p. 95-108, 2 Pls., 3 Tabs.
Henton, J., 1991, Geochemical constraints on uplift-related calcitization of Triassic dolomites in the Catalan Basin, Northeast Spain: Ortisei, p. p. 109.
Heydari, E., 2003, Meteoric versus burial control on porosity evolution of the Smackover Formation: AAPG Bulletin, v. 87, p. 1779-1797.
Hoholick, J. D., T. Metarko, and P. E. Potter, 1984, Regional variations of porosity and cement; St. Peter and Mount Simon sandstones in Illinois Basin: AAPG Bulletin, v. 68, p. 753-764.
Holail, H., 1994, Carbon and oxygen rations of Middle Eocene dolomite, Gebel Ataqu, Egypt, v. 191, p. 111-124, 4 Figs., 1 Tab.
Holser, W. T., and M. Magaritz, 1985, The Late Permian carbon isotope anomaly in the Bellerophon Basin, Carnic and Dolomite Alps, v. 128, p. 75-82, 3 Figs.
Hood, S. D., C. S. Nelson, and P. J. J. Kamp, 2003, Modification of fracture porosity by multiphase vein mineralization in an Oligocene nontropical carbonate reservoir, Taranaki Basin, New Zealand: AAPG Bulletin, v. 87, p. 1575-1597.
Hsü, J., 1966, Origin of dolomite in sedimentary sequences: a critical analysis, v. 2, p. 133-138, 2 Figs.
Hsü, K. J., 1967, Chemistry of dolomite formation: Amsterdam, p. 169-191.

Hsü, K. J., and C. Siegenthaler, 1969, Preliminary experiments and hydrodynamic movement induced by evaporation and their bearing on the dolomite problem, v. 12, p. 11-25.
Hubert, J. F., and A. A. Reed, 1978, Red-bed diagenesis in the East Berlin Formation, Newark Group, Connecticut Valley: Journal of Sedimentary Petrology, v. 48, p. 175-184.
Hulen, J. B., S. R. Bereskin, and L. C. Bortz, 1990, High-temperature hydrothermal origin for fractured carbonate reservoirs in the Blackburn oil field, Nevada: AAPG Bulletin, v. 74, p. 1262-1272.
Humphrey, J. D., and T. M. Quinn, 1989, Coastal Mixing Zone Dolomite, Forward Modeling, and Massive Dolomitization of Platform-Margin Carbonates: Journal of Sedimentary Petrology, v. 59, p. 438-545.
Huntoon, J. E., P. L. Hansley, and N. D. Naeser, 1999, The search for a source rock for the giant Tar Sand Triangle accumulation, southeastern Utah: AAPG Bulletin, v. 83, p. 467-495.
Hurst, R. W., 1986, Chemical and Sr isotopic variations during diagenesis of Miocene siliceous sediments of the Monterey Formation, California; discussion of the Sr isotopic data and its relevance to the timing of Monterey Formation fracturing: Journal of Sedimentary Petrology, v. 56, p. 569-573.
Hyde, M. K., 1979, A Study of the Dolomite/Calcite Ratios Relative to the Structures and Producing Zones of the Kawkawlin Oil Field, Bay County, Michigan: MS thesis, Michigan State University, Lansing, 92 p.
Ifechukwu, O. P., 1997, Sequence stratigraphy and reservoir geology of the Glauconitic Sandstone Member and adjacent strata, Mannville Group, central Alberta: AAPG Foundation grants-in-aid abstracts AAPG Bulletin, v. 81, p. 1780.
Ilich, M., 1974, Hydrothermal-Sedimentary Dolomite: the Missing Link?: AAPG Bulletin, v. 58, p. 1331-1347.
Illing, L. V., A. J. Wells, and J. C. Taylor, eds., 1965, Penecontemporary dolomite in the Persian Gulf, v. 13: Tulsa, 89-111, 10 Figs., 1 Tab. p.
Jacka, A. D., 1976, Factors controlling porosity relations in Pennsylvanian and Permian carbonate reservoirs of Permian Basin: AAPG Bulletin, v. 60, p. 325-326.
Jahn, B., J. Bertrand-Sarfati, N. Morin, and J. Mace, 1990, Direct dating of stromatolitic carbonates from the Schmidtsdrif Formation (Travsvaal Dolomite), South Africa, with implications on the age of the Ventersdorp Supergroup: Geology, v. 18, p. 1211-1214.
Jarosewich, E., and I. G. MacIntyre, 1983, Carbonate reference samples for electron microprobe and scanning electron microscope analyses: Journal of Sedimentary Petrology, v. 53, p. 677-678.
Jingquan, Z., 1998, Characteristics and origin of polycrystalline dolomite needles in the Triassic Jialingjiang Formation, Upper Yangtze Platform, southwest China, v. 118, p. 119-126, 4 Figs.
Jingquan, Z., 1998, Characteristics and origin of polycrsystalline dolomite needles in the Triassic Jialingijang Formation, Upper Yangtze Platform, southwest China, v. 118, p. 119-126, 4 Figs.
Joergensen, N. O., 1983, Dolomitization in chalk from the North Sea central graben:

Journal of Sedimentary Petrology, v. 53, p. 557-564.
Johnson, C. L., and S. A. Graham, 2004, Cycles in perilacustrine facies of late Mesozoic rift basins, southeastern Mongolia: Journal of Sedimentary Research, v. 74, p. 786-804.
Johnson, J. G., 1974, Great Basin Silurian to Lower Lower Devonian; a Biostratigraphic Case History: AAPG Bulletin, v. 58, p. 139-141.
Jones, B., 1989, Syntaxial overgrowth on dolomite crystals in the Bluff Formation, Grand Cayman, British West Indies, v. 59/5, p. 839-847, 6 Figs.
Jones, B., 2004, Petrography and significance of zoned dolomite cements from the Cayman formation (Miocene) of Cayman Brac, British West Indies, v. 74, p. 95-109, 12 Figs.
Jones, B., 2005, Dolomite Crystal Architecture: Genetic Implications for the Origin of the Tertiary Dolostones of the Cayman Islands: Journal of Sedimentary Research, v. 75, p. 177-189.
Jones, B., and R. W. Luth, 2003, Petrography of finely crystalline Cenozoic dolostones as revealed by backscatter electron imaging; case study of the Cayman Formation (Miocene), Grand Cayman, British West Indies: Journal of Sedimentary Research, v. 73, p. 1022-1035.
Jones, B., S. M. Pleydell, N. Kwok-Choi, and F. J. Longstaffe, 1989, Formation of poikilotopic calcite-dolomite fabrics in the Oligocene-Miocene Bluff Formation of Great Cayman, British West Indies, v. 37/3, p. 255-265, 5 Figs.
Jones, G. D., and Y. Xiao, 2005, Dolomitization, anhydrite cementation, and porosity evolution in a reflux system: Insights from reactive transport models: The American Association of Petroleum Geologists Bulletin, v. 89, p. 577-601.
Jorgenson, N. O., 1988, Dolomite and dedolomitization in Danian bryozoan limestone from Fakse, Denmark, v. 37, p. 63-74, 15 Figs.
Jorgenson, N. O., 1991, Oxygen isotope fraction between dolomite and calcite - evidence from a natural system in a recent marine environment: Ortisei, p. 128-129, 1 Fig.
Kahle, C. F., and C. J. Livchack, 1996, Peritidal carbonates and evaporative drawdown: A case study from the Silurian Tymochtee Dolomite, Ohio, *in* B. A. Van der Pluijm, and P. A. Catacosinos, eds., Basement and Basins of Eastern North America, v. Special Paper 308: Boulder, Colorado, Geological Society of America, p. 157-168.
Kaldi, J., and J. Gidman, 1982, Early diagenetic dolomite cements: examples from the Permian Lower Magnesian Limestone of England and the Pleistocene carbonates of the Bahamas, v. 52/4, p. 1073-1085, 10 Figs.,.
Kantor, J., and M. Misik, 1992, Isotopic composition of oxygen and carbon in selected Mesozoic and Tertiary limestones and dolomites in Slovakia, v. 15, p. 7-27.
Kargel, J. S., J. F. Schreiber, and C. P. Sonett, 1996, Mud cracks and dedolomitization in the Wittenoom Dolomite, Hamersley Group, Western Australia, v. 14, p. 73-96, 5 Figs.
Kastner, M., 1983, Origin of dolomite and its spatial and chronological distribution; a new insight: AAPG Bulletin, v. 67, p. 2156.
Kastner, M., 1983, Origin of dolomite and its spatial and chronological distribution - a new insight, v. 67, p. 21-56.

Kastner, M., 1984, Control of dolomite formation, v. 311, p. 410-411.
Katz, A., 1968, Calcian dolomites and dedolomitization, v. 217, p. 439-440.
Katz, A., 1971, Zoned dolomite crystals, v. 79, p. 38-51, 3 Pls., 4 Figs.
Keim, L., and W. Schlager, 1999, Automicrite facies on steep slopes (Triassic, Dolomites, Italy), v. 41, p. 15-26, Pl. 5-7, 4 Figs., 1 Tab.
Kendall, A. C., M. W. Longman, T. G. Fertal, and J. S. Glennie, 1984, Origin and geometry of Red River Dolomite reservoirs, western Williston Basin; discussion and reply: AAPG Bulletin, v. 68, p. 776-784.
Kendall, G. W., J. G. Johnson, J. O. Brown, and G. Klapper, 1983, Stratigraphy and facies across Lower Devonian-Middle Devonian boundary, central Nevada: AAPG Bulletin, v. 67, p. 2199-2207.
Kenig, F., R. Baltzer, J. C. Fontes, and B. H. Purser, 1991, Possible relationship between organic matter and dolomite in the sabkha of Abu dhabi (U.A.E.): Ortisei, p. 132-133, 3 Figs.
Kenny, R., 1992, Origin of disconformity dedolomite in the Martin Formation (Late Devonian, northern Ariozona), v. 78, p. 137-146, 7 Figs., 1 Tab.
Kessels, L. A., D. F. Sibley, and S. H. Nordeng, 2000, Nanotopography of synthetic and natural dolomite crystals, v. 47, p. 173-186, 11 Figs.
Klupsch, N., A. T. S. Ramsay, and P. Rothe, 1988, Intertidal- und Supratidal-Phasen im Kalktertiär-Profil (Oberoligozän-Untermiozän) Mainz-Weisenau - Caliche und frühdiagenetische Dolomite, v. 110, p. 165-172, 3 Figs.
Klusman, R. W., 2003, A geochemical perspective and assessment of leakage potential for a mature carbon dioxide-enhanced oil recovery project and as a prototype for carbon dioxide sequestration; Rangely Field, Colorado: AAPG Bulletin, v. 87, p. 1485-1507.
Kolkas, M. M., and G. M. Friedman, 1998, Diagenetic history and geochemistry of the Beekmantown-Group dolomites (Sauk Sequence) of New York, USA, v. 13, p. 69-85, 17 Figs.
Kretz, R., 1992, Caroused model for the crystallization of saddle dolomite, v. 62/2, p. 190-195, 9 Figs., 1 Tab.
Kupecz, J. A., 1990, Recrystallization of dolomite with time, p. p. 37.
Kupecz, J. A., and L. S. Land, 1991, Status of 'burial dolomite' and an alternative interpretation for post-lithification dolomite: Ortisei, p. p. 141.
Kupecz, J. A., I. P. Montanez, and G. Gao, eds., 1993, Recrystallization of dolomite with time: New York, Springer, 187-194 p.
Kuslansky, G. H., and G. M. Friedman, 1981, Chertification of crinoids may yield a product resembling "dedolomite": Journal of Sedimentary Petrology, v. 51, p. 795-798.
Kuznetsov, V. G., 1999, Petrography and origin of dolomite in carbonate deposits in various paleoclimates, v. 14, p. 125-137, 8 Figs.
Laghi, G. F., G. Martinelli, and F. Russo, 1984, Localization of minor elements by Eds microanalysis in aragonic sponges from the St. Cassian Beds, Italian Dolomites, p. 133-138, 3 Tabs.
Land, L. S., 1980, The isotopic and trace element geochemistry of dolomite: the state of the art, v. 28, p. 87-110.

Land, L. S., 1985, The Origin of Massive Dolomite: Journal of Geological Eductaion, v. 33, p. 112-125.
Land, L. S., 1986, Environments of limestone and dolomite diagenesis: some geochemical considerations, v. 81, p. 26-41.
Land, L. S., M. R. I. Salem, and D. W. Morrow, 1975, Paleohydrology of ancient dolomites; geochemical evidence: AAPG Bulletin, v. 59, p. 1602-1625.
Lane, A. C., C. S. Prosser, W. H. Sherzer, and A. W. Grabau, 1909, Nomenclature and subdivision of the Upper Siluric strata of Michigan, Ohio, and Western New York: GSA Bulletin, v. 19, p. 553-556.
Langbein, R., and S. Röhling, 1991, Appearance and distribution of ferroan calcite and low-concentration dolomite in Lower Palaeozoic deep-water carbonates of the Thuringikum, v. 51, p. 241-249, 10 Figs.
Lasemi, Z., M. R. Boardman, and P. A. Sandberg, 1989, Cement origin of supratidal dolomite, Andros Island, Bahamas, v. 59/2, p. 249-257, 5 Figs.
Laskaridis, K., 1987, Beurteilung griechischer weißer Kalke und Dolomite für den industriellen Einsatz (z.B. in der Papierindustrie), p. 241 pp., 121 Figs., 30 Tabs., 1 Pl.
Last, W. M., 1990, Lacustrine dolomite - an overview of Modern, Holocene, and Pleistocene occurrences, v. 27, p. 221-263.
Laubach, S., R. Marrett, and J. Olson, 2000, New directions in fracture characterization: The Leading Edge, p. 704-711.
Laughrey, C. D., and F. J. Baldassare, 1998, Geochemistry and origin of some natural gases in the Plateau Province, central Appalachian Basin, Pennsylvania and Ohio: AAPG Bulletin, v. 82, p. 317-335.
Lawrence, M. J. F., 1994, Concepual model for early diagenetic chert and dolomite, Amuri Limestone Group, north-eastern South Island, New Zealand, v. 41, p. 479-498, 9 Figs., 4 Tabs.
Leach, D. L., G. S. Plumlee, A. H. Hofstra, G. P. Landis, E. L. Rowan, and J. G. Viets, 1991, Origin of late dolomite cement by CO_2-saturated deep basin brines: Evidence from the Ozark region, Central United States: Geology, v. 19, p. 348-351.
Lee, M.-K., and C. M. Bethke, 1994, Groundwater flow, late cementation, and petroleum accumulation in the Permian Lyons Sandstone, Denver Basin: AAPG Bulletin, v. 78, p. 217-237.
Leutloff, A. H., and W. J. Meyers, 1984, Regional distribution of microdolomite inclusions in Mississippian echinoderms from southwestern New Mexico, v. 54/2, p. 432-446, 9 Figs.
Lilling, L. V., A. J. Wells, and J. C. Taylor, eds., 1965, Penecontemporaneous dolomite in the Persian Gulf, v. 13: Tulsa, 89-111 p.
Lock, B. E., L. J. Williams, and D. P. Cheney, 1991, Dolomite cements in modern supratidal sands, western Sonora, Mexico: Ortisei, p. p. 150.
Lohmann, K. C., and W. J. Meyers, 1977, Microdolomite inclusions in cloudy prismatic calcites: a proposed criterion for former high-magnesium calcites, v. 47/3, p. 1078-1088, 6 Figs.
Longacre, S. A., 1980, Dolomite reservoirs from Permian biomicrites, v. 1, p. 105-117.

Longman, M. W., T. G. Fertal, and J. S. Glennie, 1983, Origin and geometry of Red River dolomite reservoirs, western Williston Basin: AAPG Bulletin, v. 67, p. 744-771.

Lopez-Gomez, J., and B. Mamet, 1990, Sedimentology and Petrology of the Canete Dolomite and Limestone Formation (Muschelkalk Facies, Middle to Upper Triassic) Southern Iberian Ranges, Eastern Spain, v. 23, p. 1-16, 9 Figs., Pls. 1-2.

Loucks, R. G., and J. H. Anderson, 1980, Depositional facies and porosity development in Lower Ordovician Ellenburger Dolomite, Puckett Field, Pecos County, Texas, v. 1, p. 1-31, 17 Figs., 2 Tabs.

Loucks, R. G., and J. H. Anderson, 1985, Depositional Facies, Diagenetic Terranes, and Porosity Development in Lower Ordovician Ellenburger Dolomite, Puckett Field, West Texas: New York, Springer, p. 19-37, 14 Figs.

Lucia, F. J., 2000, Origin and petrophysics of carbonate rock fabrics: 2000-2001 AAPG distinguished lecturers; abstracts AAPG Bulletin, v. 84, p. 1879.

Lucia, F. J., 2000, Dolomitization; a porosity-destructive process: 2000-2001 AAPG distinguished lecturers; abstracts AAPG Bulletin, v. 84, p. 1879.

Luebking, G. A., M. W. Longman, and W. J. Carlisle, 2001, Unconformity-related chert/dolomite production in the Pennsylvanian Amsden Formation, Wolf Springs fields, Bull Mountains Basin of central Montana: Chert reservoirs of North America AAPG Bulletin, v. 85, p. 131-148.

Lumsden, D. N., 1979, Discrepancy between thin-section and x-ray estimates of dolomite in limestone, v. 49/2, p. 429-436, 5 Figs.

Lumsden, D. N., 1985, Secular variations in dolomite abundance in deep marine sediments: Geology, v. 13, p. 766-769.

Lumsden, D. N., 1988, Characteristics of deep-marine dolomite, v. 58/6, p. 1023-1031, 6 Figs.

Lumsden, D. N., and J. S. Chimahuskey, eds., 1980, Relationship between dolomite nonstoichiometry and carbonate facies parameters, v. 28, 123-127 p.

Lumsden, D. N., and R. V. Lloyd, eds., 1988, An update of ESR spectroscopy studies of dolomite origin., v. 43: Tulsa, 3-10, 4 Figs. p.

Lyday, J. R., 1985, Atokan (Pennsylvanian) Berlin Field; genesis of recycled detrital dolomite reservoir, deep Anadarko Basin, Oklahoma: AAPG Bulletin, v. 69, p. 1931-1949.

Macaulay, C. I., A. J. Boyce, A. E. Fallick, and R. S. Haszeldine, 1997, Quartz veins record vertical flow at a graben edge; Fulmar oil field, central North Sea: AAPG Bulletin, v. 81, p. 2024-2033.

Machel, H. G., 1985, Cathodoluminescence in calcite and dolomite and its chemical interpretation, v. 12, p. 139-142, 8 Figs.

Machel, H. G., 1987, Saddle dolomite as a by-product of chemical compaction and thermochemical sulfate reduction, v. 15, p. 936-940, 7 Figs.

Machel, H. G., ed., 1988, Fluid flow direction during dolomite formation as deduced from trace-element trends, v. 43: Tulsa, 115-125, 5 Figs. p.

Machel, H. G., 1997, Recrystalization versus neomorphism, the concept of "significant recrystalization" in dolomite research: Sedimentary Geology, v. 113, p. 161-168.

Machel, H. G., 2000, Dolomite formation in Caribbean islands - driven by plate

tectonics?, v. A70, p. 977-984, 7 Figs.
Machel, H. G., and E. A. Burton, eds., 1991, Factors governing cathodoluminscence in calcite and dolomite, and their implications for studies of carbonate diagenesis, v. 25: Tulsa, 37-57, 16 Figs. p.
Machel, H. G., and E. A. Burton, 1991, Barbados dolomite: origin from seawater with variable temperature and/or modified by evaporation, bacterial metabolism, or oxidized methane: Ortisei, p. 137-138.
Machel, H. G., and E. A. Burton, 1994, Golden Grove dolomite, Barbados: origin from modified seawater, v. A64, p. 741-751, 13 Figs., 1 Tab.
Machel, H. G., R. A. Mason, A. N. Mariano, and A. Mucci, 1991, Causes and Emission of Luminescence in Calcite and Dolomite, *in* C. E. Barker, and O. C. Kopp, eds., Luminescence Microscopy: Quantitative and Qualitative Aspects: Tulsa, SEPM, p. 9-25.
Machent, P. G., 2000, Spatial distribution and style of carbonate cements in distal, sandstone sequences; Upper Cretaceous Panther Tongue Member and Kenilworth Member, Book Cliffs, east-central Utah, USA: AAPG Foundation grants-in-aid recipients for 2000 AAPG Bulletin, v. 84, p. 1867.
MacNeil, A. J., 1999, Diagenesis and dolomitization of the Pliocene Pedro Castle Formation, Cayman Brac, British West Indies: AAPG Foundation grants-in-aid abstracts AAPG Bulletin, v. 83, p. 1890.
Madsen, B. M., 1984, Micromarker beds in the Upper Permian Castile Formation, Delaware Basin, West Texas and southeastern New Mexico: Journal of Sedimentary Petrology, v. 54, p. 1169-1174.
Major, R. P., M. R. Lloyd, and F. J. Lucia, 1992, Oxygen isotope compostion of Holocene dolomite formed in a humid hypersaline setting: Geology, v. 20, p. 586-588.
Maliva, R. G., G. P. Kennedy, W. K. Martin, T. M. Missimer, E. S. Owosina, and J. A. D. Dickson, 2002, Dolomitization-induced aquifer heterogeneity; evidence from the upper Floridan Aquifer, Southwest Florida: Geological Society of America Bulletin, v. 114, p. 419-427.
Maliva, R. G., and R. Siever, 1990, Influences of dolomite precipitation on quartz surface textures, v. 60/6, p. 820-826, 2 Figs.
Malone, M. J., P. A. Baker, and S. J. Burns, 1994, Recrystallization of dolomite: evidence from the Monterey Formation (Miocene), California, v. 41, p. 1223-1239, 12 Figs., 1 Tab.
Malpas, J. A., 2000, Integrated sedimentology and palaeontological analysis of marine flooding surfaces; a case study of the Miocene, Nukhul Formation, Gulf of Suez: AAPG Foundation grants-in-aid recipients for 2000 AAPG Bulletin, v. 84, p. 1867-1868.
Mancini, E. A., T. A. Blasingame, R. Archer, B. J. Panetta, J. C. Llinas, C. D. Haynes, and D. J. Benson, 2004, Improving recovery from mature oil fields producing from carbonate reservoirs; Upper Jurassic Smackover Formation, Womack Hill Field (eastern Gulf Coast, U.S.A.): AAPG Bulletin, v. 88, p. 1629-1651.
Marcantel, J., 1975, Late Pennsylvanian and early Permian sedimentation in northeast Nevada: AAPG Bulletin, v. 59, p. 2079-2098.

Maresch, O., 1970, Elektronenmikroskopische Untersuchungen von Kalken und Dolomiten, v. 1970/4, p. 648-672, 8 Pls., 2 Figs., 1 Tab.
Marss, T., 1999, A new Late Silurian or Early Devonian thelodont from the Boothia Peninsula, Arctic Canada: Palaeontology, v. 42, p. 1079-1099.
Martin, A. J., S. T. Solomon, and D. J. Hartmann, 1997, Characterization of petrophysical flow units in carbonate reservoirs: AAPG Bulletin, v. 81, p. 734-759.
Martin, J. B., and R. A. Rymerson, 2002, A coupled fluid-inclusion and stable isotope record of paleofluids in the Monterey Formation, California: Geological Society of America Bulletin, v. 114, p. 269-280.
Masetti, D., C. Neri, and A. Bosellini, 1991, Deep-Water asummetric cycles and progradation of carbonate platforms governed by hig0frequency eustatic oscellations (Triassic of the Dolomites, Italy): Geology, v. 19, p. 336-339.
Mastandrea, A., and F. Russo, 1995, Microstructure and diagenesis of calcified demosponges from the Upper Triassic of the northeastern Dolomites (Italy), v. 69, p. 416-431, 10 Figs., 4 Tabs.
Mattavelli, L., 1966, Osservazioni petrografiche sull sostituzione della dolomite con la calcite (dedolomitizzazione) in alcune facies carbonate italiane, v. 105/3, p. 294-316, 16 Figs.
Maurer, F., 2000, Growth mode of Middle Triassic carbonate platforms in the Western Dolomites (Southern Alps, Italy), v. 134, p. 275-286.
Maurer, F., J. J. G. Reijmer, and W. Schlager, 2003, Quantification of input and compositional variations of calciitrubidites in a Middle Triassic basinal succession (Seceda, Dolomites, southern Alps), v. 92, p. 593-609, 14 Figs., 3 Tabs.
Mazzullo, S. J., 1986, Mississippi valley-type sulfides in Lower Permian dolomites, Delaware Basin, Texas; implications for basin evolution: AAPG Bulletin, v. 70, p. 943-952.
Mazzullo, S. J., 1992, Geochemical and neomorphic alteration of dolomite: a review, v. 7, p. 21-37, 10 Figs.
Mazzullo, S. J., and A. M. Reid, 1988, Sedimentary textures of recent Belizean peritidal dolomite, v. 58/3, p. 479-488, 6 Figs.
McCunn, H. J., 1976, Origin of dolomite; model based on cyclic interaction of continental soda-rich waters with concentrated sea water: AAPG Bulletin, v. 60, p. 696.
McHargue, T. R., and R. C. Price, 1982, Dolomite from clay in argillaceous or shale-associated marine carbonates, v. 52/3, p. 873-886, 9 Figs.
McKenzie, J. A., 2001, Deep-sea dolomite formation and the microbial factor.
McKenzie, J. A., K. J. Hsü, and J. F. Schneider, 1980, Movement of subsurface waters under the sabkha, Abu Dhabi, Uae and its relation to evaporative dolomite genesis, v. 28, p. 11-30.
McNeill, D. F., and M. Aissaoui, 1991, Magnetostratigraphy in shallow-water limestone and dolomite: the legacy of magnetization through early recrystallization: Ortisei, p. p. 166.
Meischner, D., and R. Vollbrecht, 1991, Dolomite-free carbonate environment: the Bermuda carbonate platform: Ortisei, p. p. 167.

Melim, L. A., P. K. Swart, and G. P. Eberli, 2004, Mixing-zone diagenesis in the subsurface of Florida and the Bahamas: Journal of Sedimentary Research, v. 74, p. 904-913.

Mercurio, R. N., and L. E. Monley, 1976, Block 16 Field, Ward County, Texas: AAPG Bulletin, v. 60, p. 327.

Merino, E., 1975, Diagenesis in Tertiary sandstones from Kettleman North Dome, California; I, Diagenetic mineralogy: Journal of Sedimentary Petrology, v. 45, p. 320-336.

Metwalli, M. H., and Y. E. Abd El-Hady, 1975, Petrographic characteristics of oil-bearing rocks in Alamein Oil Field; significance in source-reservoir relations in northern Western Desert, Egypt: AAPG Bulletin, v. 59, p. 510-523.

Meyers, W. J., and K. C. Lohman, 1978, Microdolomite-rich syntaxial cements: Proposed meteoric-marine mixing zone phreatic cements from Mississippian Limestones, New Mexico: Journal of Sedimentary Petrology, v. 48, p. 475-488.

Meyers, W. J., and K. C. Lohmann, 1978, Micro-dolomite rich syntaxial cements: proposed meteoric-marine mixing zone phreatic cements from Mississippian limestones, New Mexico, v. 48, p. 475-488.

Meyers, W. J., and K. C. Lohmann, 1978, Microdolomite-rich syntaxial cements: Proposed meteoric-marine mixing zone phreatic cements from Mississippian Limestones, New Mexico: Journal of Sedimentary Petrology, v. 48, p. 475-488.

Middelburg, J. J., G. J. de Lange, and R. Kreulen, 1990, Dolomite fromation in anoxic sediments of Kau Bay, Indonesia: Geology, v. 18, p. 399-402.

Middleburg, J. J., G. J. d. Lange, and R. Kreulen, 1990, Dolomite formation in anoxic sediments of Kau Bay, Indonesia, v. 18, p. 399-402, 2 Figs.

Mitchell, J. T., L. S. Land, and D. E. Miser, 1987, Modern marine dolomite cement in a north Jamaica fringing reef, v. 15, p. 557-560.

Molnar, B., 1980, Hypersaline lacustrine dolomite formation in the Danube - Tisza interfluve, v. 110, p. 45-64, 2 Pls., 9 Figs., 2 Tabs.

Molnar, B., M. I. Murvai, and J. Hegyi-Pako, 1976, Recent lacustrine dolomite formation in the Great Hungarian Plain, v. 20, p. 179-198, 9 Figs., 2 Tabs.

Molnar, B., M. Szonoky, and S. Kovacs, 1980, Diagenetic and lithification processes of recent hypersaline dolomites on the Danube-Tisza interfluve, v. 24, p. 315-337, 5 Pls., 6 Figs.

Molnar, B., M. Szonoky, and S. Kovacs, 1981, Modern hypersaline dolomites in the Danube - Tisza interfluve: diagenetic and lithification processes, v. 111, p. 119-144, 5 Pls., 6 Figs.

Montanaze, I. P., and J. F. Read, 1992, Fluid-rock interaction history during stabilization of early dolomites, Upper Knox Group (Lower Ordovician), U.S. Appalachians, v. 62/5, p. 753-778, 17 Figs., 2 Tabs.

Montanez, I. P., 1994, Late diagenetic dolomitization of Lower Ordovician, upper Knox carbonates; a record of the hydrodynamic evolution of the southern Appalachian Basin: AAPG Bulletin, v. 78, p. 1210-1239.

Montgomery, S. L., S. Goolsby, and D. Pierini, 1998, Permian (Wolfcampian) Admire "C"; new exploratory potential in the northern Denver Basin: AAPG Bulletin, v. 82, p. 2173-2191.

Moore, R. E., and J. M. Gregg, 1991, Geochemistry and sedimentology of dolomite used in refractories in metallurgical furnace construction: Ortisei, p. 172-173, 1 Tab.
Moraes, M. A. S., 1991, Diagenesis and microscopic heterogeneity of lacustrine deltaic and turbiditic sandstone reservoirs (Lower Cretaceous), Potiguar Basin, Brazil: AAPG Bulletin, v. 75, p. 1758-1771.
Moraes, M. A. S., and R. C. Surdam, 1993, Diagenetic heterogeneity and reservoir quality; fluvial, deltaic, and turbiditic sandstone reservoirs, Potiguar and Reconcavo rift basins, Brazil: AAPG Bulletin, v. 77, p. 1142-1158.
Morrow, D., 1982, Diagenesis 2. Dolomite-Part 2 Dolomitization Models and Ancient Dolostones: Geoscience Canada, v. 9, p. 95-107.
Morrow, D. W., Diagenesis 1. Dolomite-part 1: The Chemistry of Dolomitization and Dolomite Precipitation: Geoscience Canada, v. 9, p. 5-13.
Morrow, D. W., 1978, Dolomitization of lower Paleozoic burrow-fillings: Journal of Sedimentary Petrology, v. 48, p. 295-305.
Morrow, D. W., 1982, Diagenesis 1; Part 1: The Chemistry of Dolomitization and Dolomite Precipitation: Geoscience Canada, v. 9, p. 5-13.
Morrow, D. W., 1982, Dolomite - part 2: dolomitization models and ancient dolostones, v. 9, p. 95-107.
Morrow, D. W., ed., 1990, Dolomite - part 1: the chemistry of dolomitization and dolomite precipitation, v. 4: St. John's, Geol. Assoc. Canada, 113-123, 8 Figs., 1 Tab. p.
Morrow, D. W., ed., 1990, Dolomite - part 2: dolomitization models and ancient dolostones, v. 4: St. John's, Geol. Assoc. Canada, 125-139, 9 Figs. p.
Morrow, D. W., 2001, Distribution of porosity and permeability in platform dolomites: insight from the Permian of west Texas: discusssion, v. 85, p. 525-529, 2 Figs.
Morrow, D. W., G. L. Cumming, and R. B. Koepnick, 1986, Manetoe facies; a gas-bearing, megacrystalline, Devonian dolomite, Yukon and Northwest Territories, Canada: AAPG Bulletin, v. 70, p. 702-720.
Morrow, D. W., and B. D. Ricketts, 1986, Chemical controls on the precipitation of mineral anlogues of dolomite: The sulfate enigma, v. 14, p. 408-410, 2 Figs.
Morrow, D. W., and B. D. Ricketts, eds., 1988, Experimental investigation of sulfate inhibition of dolomite and its mineral analogues, v. 43: Tulsa, 25-38, 7 Figs. p.
Morrow, D. W., A. H. Saller, and N. Henderson, 2001, Distribution of porosity and permeability in platform dolomites; insight from the Permian of West Texas; discussion and reply: AAPG Bulletin, v. 85, p. 525-532.
Morrow, D. W., M. Zhao, and L. D. Stasiuk, 2002, The gas-bearing Devonian Presqu´ile Dolomite of the cordova embayment region of British columbia; Canada: dolomitization and the stratigraphic template, v. 86, p. 1609-1638, 13 Figs.
Mountjoy, E. W., H. G. Machel, D. Green, J. Duggan, and A. E. Williams-Jones, 1999, Devonian matrix dolomites and deep burial carbonate cements: a comparison between the Rimbey-Meadowbrook reef trend and the deep basin of west-central Alberta, v. 47, p. 487-509.
M'Rabet, A., 1981, Differentiation of environments of dolomite formation, Lower Cretaceous of central Tunisia: Sedimentlolgy, v. 28, p. 331-352.
Muir, M., D. Lock, and C. Von der Borch, 1980, The Coorong model for

penecontemporaneous dolomite formation in the Middle Proterozoic McArthur Group, Northern Territories, Australia, v. 28, p. 51-67, 10 Figs.
Mukhopadhyay, J., S. K. Chanda, M. Fukuoka, and A. K. Chaudhuri, 1996, Deep-water dolomites from the Proterozoic Penganga Group in the Pranhita-Godavari Valley, Andhra Pradesh, India, v. A66, p. 223-230, 15 Figs., 1 Tab.
Müller, G., 1970, High-magnesian calcite and protodolomite in Lake Balaton (Hungary) sediments, v. 226, p. 749-750.
Muller, G., and M. Ilic, 1975, Hydrothermal-sedimentary dolomite; the missing link?: AAPG Bulletin, v. 59, p. 1690-1692.
Müller-Wille, S., and J. Reitner, 1993, Palaeobiological reconstructions of selected sphinctozoan sponges from the Cassian Beds (Lower Carnian) of the Dolomites (Northern Italy), v. E9, p. 253-281, 4 Pls., 8 Figs.
Mullins, H. T., G. R. Dix, A. F. Garduliski, and L. S. Land, eds., 1988, Neogene deep-water dolomite from the Florida-Bahamas platform, v. 43: Tulsa, 235-243, 7 Figs. p.
Murray, R. C., 1964, Preservation of primary structures and fabrics in dolomite: New York, Wiley, p. 388-403.
Murray, R. C., and F. J. Lucia, 1967, Cause and control of dolomite distribution by rock selectivity, v. 78, p. 21-36, 5 Pls., 7 Figs.
Myszkowska, J., 1992, Lithofacies and sedimentation of Diplopora dolomite (Middle Muschelkalk) in the east part of the Cracovian-Silesian Region, v. 62, p. 19-62, 9 Figs.
Nahnsen, M., 1913, Über die Gesteine des norddeutschen Korallenooliths, insbesondere die Bildungsweise der oolithe und Dolomite, v. 35, p. 277-.
Naiman, E. R., A. Bein, and R. L. Folk, 1983, Complex polyhedral crystals of limpid dolomite associated with halite, Permian upper Clear Fork and Glorieta formations, Texas: Journal of Sedimentary Petrology, v. 53, p. 549-555.
Naiman, E. R., A. Bein, and R. L. Folk, 1983, Complex polyhedral crystals of limpid dolomite associated witrh hallite, Permian Upper Clear Fork and Glorietta Formations, Texas, v. 53/2, p. 549-555, 6 Figs., 3 Tabs.
Narkiewicz, M., 1979, Telo- and mesogenetic dolomites in subsurface Upper Devonian to Lower Carboniferous sequences of southern Poland, v. 158, p. 180-208, 19 Figs., 1 Tab.
Narkiewicz, M., 1983, Dolomite from clay in argillaceous or shale-associated marine carbonates - discussion, v. 52/4, p. 1353-1359.
Narkiewicz, M., R. C. Price, and T. R. McHargue, 1983, Dolomite from clay in argillaceous or shale-associated marine carbonates; discussion and reply: Journal of Sedimentary Petrology, v. 53, p. 1353-1355.
Nash, A. J., and E. D. Pittman, 1975, Ferro-magnesian calcite cement in sandstones: Journal of Sedimentary Petrology, v. 45, p. 258-265.
Neri, C., 1991, Sequence stratigraphy of the early Triassic Werfen Formation (Dolomites, Northern Italy): Ortisei, p. 194-195.
Neumann, E. R., 1978, Experimental recrystallization of dolomite and comparison of preferred orientations of calcite and dolomite in deformed rocks, v. 77, p. 426-438.

Neuweiler, F., and J. Reitner, 1995, Epifluorescence microscopy of selected automicrites from lower Carnian Cipit-boulders of the San Cassian Formation (Seeland Alpe, Dolomites), v. 32, p. 26-28, Pl. 6.
Newman, J., and G. Mitra, 1994, Fluid-induced deformation and recrystallization of dolomite at low temperatures along a natrual fault zone, Mountain City Window, Tennesssee, v. 106, p. p. 1642.
Nielsen, P., and R. Swennen, 1991, Influence of recrystallization phenomena on the isotopic signature within massive ancient dolomite units: an example from the Lower Visean of E-Belgium: Ortisei, p. p. 198.
Nielsen, P., R. Swennen, and E. Keppens, 1994, Multiple-step recrystallization within massive ancient dolomite units: an example from the Dinantian of Belgium, v. 41, p. 567-584, 7 Figs., 4 Tabs.
Nordeng, S. H., and D. F. Sibley, 1996, A crystal growth rate equation for ancient dolomites: evidence for millimeter-scale flux-limited growth, v. A66, p. 477-481, 3 Figs., 1 Tab.
Nöth, S., P. Bruckschen, and D. K. Richter, 1991, Conodont color alteration and microdolomite composition - implications to the Muschelkalk limestones (Upper Triassic) overlying the Upper Cretaceous intrusive body of the Vlotho Massif (Weserbergland, Northwest Germany), v. 70, p. 265-273, 8 Figs.
Oglesby, T. W., W. J. Meyers, and K. C. Lohmann, 1979, Microdolomite-rich syntaxial cements; proposed meteoric-marine mixing zone phreatic cements from Mississippian limestones, New Mexico: Journal of Sedimentary Petrology, v. 49, p. 670-676.
Orpin, A. R., 1997, Dolomite chimneys as possible evidence of coastal fluid expulsion, uppermost Otago continental slope, southern New Zealand, v. 138, p. 51-67.
Packard, J. J., I. Al-Aasm, I. Samson, Z. Berger, and J. Davies, 2001, A Devonian hydrothermal chert reservoir; the 225 bcf Parkland Field, British Columbia, Canada: Chert reservoirs of North America AAPG Bulletin, v. 85, p. 51-84.
Patterson, R. J., and D. J. J. Kinsman, 1982, Formation of diagenetic dolomite in coastal sabkhas along the Arabian (Persian) Gulf, v. 66, p. 28-43.
Patterson, R. J., and J. J. Kinsman, 1982, Formation of diagenetic dolomite in coastal sabkha along Arabian (Persian) Gulf: AAPG Bulletin, v. 66, p. 28-43.
Pedone, V. A., and J. A. D. Dickson, 2000, Replacement of aragonite by quasi-rhombohedral dolomite in a Late Pleistocene tufa mound, Great Salt Lake, Utah, U.S.A., v. A70, p. 1152-1159, 4 Figs., 3 Tabs.
Peryt, T., 1991, Dolomitization model of evaporite-associated dolomites: lesson from the Zechstein (Upper Permian) of Poland: Ortisei, p. p. 208.
Peryt, T. M., 1985, Permian beach in the Zechstein dolomites of western Poland: influence on reservoirs, v. 8, p. 463-474, 4 Figs.
Peryt, T. M., 1986, The Zechstein (Upper Permian) Main Dolomite deposits of the Leba Elevation, Northern Poland: Facies and depositional history, v. 14, p. 151-200, Pls. 24-37, 10 Figs.
Peryt, T. M., 1992, Debris-flow deposits in the Zechstein (Upper Permian) Main dolomite of Poland: significance for the evolution of the basin, v. 185, p. 1-19, 8 Figs.

Petty, D. M., 1988, Depositional facies, textural characteristics, and reservoir properties of dolomites in Frobisher-Alida interval in Southwest North Dakota: AAPG Bulletin, v. 72, p. 1229-1253.
Pfeil, R. W., and J. F. Read, 1980, Cambrian Carbonate Platform Margin Facies, Shady Dolomite, Southwestern Virginia, U.S.A.: Journal of Sedimentary Petrology, v. 50 ,No.1, p. 91-116.
Pichler, T., and J. D. Humphrey, 2001, Formation od dolomite in recent island-arc sediments due to gas-seawater.sediment interaction, v. A71, p. 394-399, 5 Figs.
Pierre, C., L. Ortlieb, and A. Person, 1984, Supratidal evaporitic dolomite at Ojo de Liebre Lagoon: mineralogical and isotopic arguments for primary crystallization, v. 54/4, p. 1049-1061, 8 Figs.
Pierson, B. J., 1981, The control of cathodoluminescence in dolomite by iron and manganese, v. 28, p. 601-610.
Pitman, J. K., T. D. Fouch, and M. B. Goldhaber, 1982, Depositional setting and diagenetic evolution of some Tertiary unconventional reservoir rocks, Uinta Basin, Utah: AAPG Bulletin, v. 66, p. 1581-1596.
Pokrovsky, O. S., J. Schott, and F. Thomas, 1999, Dolomite surface speciation and reactivity in aquatic systems, v. 63, p. 3133-3143.
Pomar, L., and W. C. Ward, 1999, Reservoir-scale heterogeneity in depositional packages and diagenetic patterns on a reef-rimmed platform, upper Miocene, Mallorca, Spain: AAPG Bulletin, v. 83, p. 1759-1773.
Pope, M. C., and J. F. Read, 1997, High-resolution surface and subsurface sequence stratigraphy of late Middle to Late Ordovician (late Mohawkian-Cincinnatian) foreland basin rocks, Kentucky and Virginia: AAPG Bulletin, v. 81, p. 1866-1893.
Pranter, M. J., 1998, Use of petrophysical-based reservoir zonation and time-lapse, multicomponent (4D, 3C) seismic attributes for improved geologic modeling: AAPG Foundation grants-in-aid recipients for 1998; abstracts AAPG Bulletin, v. 82, p. 2167.
Purser, B. H., 1985, Dedolomite porosity and reservoir properties of Middle Jurassic carbonates in the Paris Basin, France: Berlin, p. 343-355, 12 Figs.
Purser, B. H., 1991, Origins and distribution of porosity in the dolomites of Mururoa Atoll French Polynesia: Ortisei, p. p. 219.
Purser, B. H., M. E. Tucker, and D. H. e. Zanger, 1994, Dolomites, v. 21, p. 464 pp., 279 Figs.
Purser, B. H., M. E. Tucker, and D. H. e. Zenger, 1994, Dolomites. A volume in honor of Dolomieu, v. 21, p. 464 pp., 279 Figs.
Purser, N. H., A. Brown, and D. M. Aissaoui, 1994, Nature, origins and evolution of porosity in dolomites: Spec. Pub. Inter, Assoc. of Sedimentologists, v. 21, p. 283-308, 15 Figs.
Purser, N. H., A. Brown, and D. M. Aissaoui, eds., 1994, Nature, origins and evolution of porosity in dolomites, v. 21: Oxford, 283-308, 15 Figs. p.
Qing, H., 1998, Petrography and geochemistry of early-stage, fine- and medium-crystalline dolomites in the Middle Devonian Presqu'ile Barrier at Pine Point, Canada, v. 45, p. p. 433-.

Qing, H., and E. W. Mountjoy, 1994, Formation of coarsely crystalline, hydrothermal dolomite reservoirs in the Presqu'ile barrier, Western Canada sedimentary basin: AAPG Bulletin, v. 78, p. 55-77.

Qing, H., and E. W. Mountjoy, 1994, Rare earth element geochemistry of dolomites in the Middle Devonian Presqu'ile barrier, Western Canada Sedimentary Basin: implications for fluid-rock ratios during dolomitization, v. 41, p. 787-804, 14 Figs., 3 Tabs.

Quing, H., and E. Mountjoy, 1991, Presqu'ile Dolomite at Pine Point and adjacent subsurface: evidence for hydrothermal dissolution and a Late Cretaceous maximum burial origin for saddle dolomites and mineralization: Ortisei, p. 220-221.

Radke, B. M., and R. L. Mathis, 1980, On the formation and occurrence of saddle dolomite, v. 50/4, p. 1149-1168, 12 Figs.

Rao, C. G., 1969, Dolomitization, dedolomitization and the dolomite question in carbonate rocks, v. 1, p. 209-216.

Read, J. F., and R. W. Pfeil, 1983, Fabrics of allochthonpus reefal blocks, Shady dolomite (Lower to Middle Cambrian), Virginia Appalachians, v. 52/3, p. 761-778, 9 Figs.

Reeder, R. J., and J. L. Prosky, 1986, Compositional sector zoning in dolomite, v. 56/2, p. 237-247, 10 Figs.

Reid, S. A., and J. L. McIntyre, 2001, Monterey Formation porcelanite reservoirs of the Elk Hills Field, Kern County, California: Chert reservoirs of North America AAPG Bulletin, v. 85, p. 169-189.

Reijmer, J. J. G., 1998, Compositional variations during phases of progradation and retrogradation of a Triassic carbonate platform (Picco di Vallandro/Dürrenstein Dolomites, Italy), v. 87, p. 436-448, 5 Figs., 4 Tab.

Reinhold, C., 1998, Multiple episodes of dolomitization and dolomite recrystallization during shallow burial in Upper Jurassic shelf carbonates: eastern Swabian Alb, southern Germany, v. 121, p. 71-95, 14 Figs.

Richter, D. K., 1972, Eine subrezente spätdiagenetische Dolomitisierung mit prätertiären Dolomiten als Keime (Bucht von Volos, Griechenland), v. 1972/8, p. 490-506, 10 Figs., 1 Tab.

Richter, D. K., 1974, Entstehung und Diagenese der devonischen und permotriassischen Dolomite in der Eifel, v. 2, p. 1-101.

Richter, D. K., 1985, Mikrodolomite om Crionoiden des Trochitenkalks (mo1) und die Wärmeanomalie von Vlotho, v. 1985, p. 681-690.

Ricketts, B. D., 1982, Comment on Precambrian dolomites: petrographic and isotopic evidence that they differ from Phanerozoic dolomites, v. 10, p. p. 663.

Riley, R. A., J. Wicks, and J. Thomas, 2002, Cambrian-Ordovician Knox production in Ohio; three case studies of structural-stratigraphic traps: AAPG Bulletin, v. 86, p. 539-555.

Rock, L., 1998, Differences between limestone and dolomite reservoir properties of Swan Hills Ante Creek pools and Leduc Simonette Pool, west central Alberta: AAPG Foundation grants-in-aid recipients for 1998; abstracts AAPG Bulletin, v. 82, p. 2167.

Rosen, M. R., and L. Coshell, 1992, A new location of Holocene dolomite formation , Lake Hayward, Western Australia, v. 39, p. 161-166, 2 Figs.
Rosen, M. R., and G. R. Holdren, 1986, Origin of Dolomite Cement in Chesapeake Group (Miocene) Siliciclastic Sediments: An Alternaative Model To Burial Dolomitazation: Journal of Sedimentary Petrology, v. 56, p. 788-798.
Rosen, M. R., and G. R. Holdren, Jr., 1986, Origin of dolomite cement in Chesapeake Group (Miocene) soliciclastic sediments: an alternative model to burial dolomitization, v. 56/6, p. 788-798, 8 Figs.
Rosen, M. R., D. E. Miser, M. A. Starcher, and W. J.K., 1989, Formation of dolomite in the Coorong region, South Australia, v. 53, p. 661-669, 6 Figs.
Ross, R. J., Jr., 1975, Ordovician sedimentation in western United States: Rocky Mountain sections, AAPG and SEPM annual meeting; Rocky Mountain energy resources, discovery and development AAPG Bulletin, v. 59, p. 921.
Rudolph, K. W., W. Schlager, and K. T. Biddle, 1989, Seismic models of a carbonate foreslope-to-basin transition, Picco di Vallandro, Dolomite Alps, nothern Italy: Geology, v. 17, p. 453-456.
Rudolph, K. W., W. Schlager, and K. T. Biddle, 1989, Seismic models of a carbonate foreslope-to-basin transition, Picco di Vallandro, Dolomite Alps, northern Italy, v. 17, p. 453-456.
Russo, F., A. Mastandrea, M. Stefani, and C. Neri, 2000, Carbonate facies dominated by syndepositional cements: a key component of MIddle Triassic platforms. The Marmolada case history (Dolomites, Italy), v. 42, p. 211-226, Pl. 38-43, 4 Figs.
Russo, F., C. Neri, A. Mastandrea, and A. Baracca, 1997, The mud mound nature of the Cassian platform margins of the Dolomites. A case history: the Cipit boulders from Punta Grohmann (Sasso Piatto Massif, Northern Italy), v. 36, p. 25-36, Pl. 8-10, 4 Figs., 1 Tab.
Ruzyla, K., and G. M. Friedman, 1985, Factors controlling porosity in dolomite reservoirs of the Ordovician Red River Formation, Cabin Creek Field, Montana: Berlin, Springer, p. 41-58, 12 Figs.
Sabins, F. F. J., 1962, Grains of detrital, secondary, and primary dolomite from Cretaceous strata of the Western Interior, v. 73, p. 1183-1196, 5 Figs.
Saller, A., B. Ball, S. Robertson, B. McPherson, C. Wene, R. Nims, and J. Gogas, 2001, Reservoir characteristics of Devonian cherts and their control on oil recovery; Dollarhide Field, West Texas: Chert reservoirs of North America AAPG Bulletin, v. 85, p. 35-50.
Saller, A. H., 1984, Petrologic and geochemical constraints on the origin of subsurface dolomite, Enewetak Atoll: an example of dolomitization by normal seawater, v. 12, p. 217-220.
Saller, A. H., and N. Henderson, 1998, Distribution of porosity and permeability in platform dolomites; insight from the Permian of West Texas: AAPG Bulletin, v. 82, p. 1528-1550.
Saller, A. H., and N. Henderson, 2001, Distribution of porosity and permeability in platform dolomites: insight from the Permian of west Texas: reply, v. 85, p. 530-532, 2 Figs.
Sander, B., 1936, Beiträge zur Kenntnis der Anlagerungsgefüge (Rhythmische Kalke und

Dolomite aus der Trias), v. 48, p. 27-139, 36 Figs., 7 Pls.
Sano, H., 1983/1984, Displaced dolomites in radiolarian cherts of the Chichibu belt on Shikoku Island, southwest Japan, v. 37, p. 203-223, 9 Figs.
Sargent, K. A., 1976, Chemical and isotopic investigation of stratigraphic and tectonic dolomites in Arbuckle Group, Arbuckle Mountains, South-central Oklahoma: AAPG Bulletin, v. 60, p. 719.
Sarin, D. D., 1962, Cyclic sedimentation of primary dolomite and limestone, v. 32/3, p. 451-471, 16 Figs., 1 Tab.
Sass, E., 1965, Dolomite-calcite relationships in seawater: theoretical considerations and preliminary experimental results, v. 35, p. 339-347, 4 Figs.
Sass, E., and A. Bein, eds., 1988, Dolomites and salinity: a comparative geochemical study, v. 43: Tulsa, 223-233, 7 Figs. p.
Sass, E., and A. Katz, 1982, The origin of platform dolomites: new evidence, v. 282, p. 1184-1213.
Schaefer, K. W., and E. Usdowski, 1992, Application of stable carbon and sulfur isotope models to the development of ground water in a limestone-dolomite-anhydrite-gypsum area: Berlin, Springer, p. 157-163, 3 Figs., 3 Tabs.
Schauer, M., and T. Aigner, 1997, Cycle stacking pattern, diagenesis and reservoir geology of peritidal dolostones, Trigonodus-Dolomite, Upper Muschelkalk (Middle Triassic, SW-Germany, v. 37, p. 99-114, Pl. 23-25, 8 Figs., 2 Tabs.
Schindler, J. L., 1999, Quantification of vuggy porosity using electrical borehole images, nuclear magnetic resonance images, and core in the Upper Pennsylvanian of the Indian Basin Field, New Mexico: AAPG Foundation grants-in-aid abstracts AAPG Bulletin, v. 83, p. 1896.
Schlanger, S. O., 1957, Dolomite growth in coralline algae, v. 57, p. 181-186.
Schmoker, J. W., K. B. Krystinik, and R. B. Halley, 1985, Selected characteristics of limestone and dolomite reservoirs in the United States: AAPG Bulletin, v. 69, p. 733-741.
Scudeler Baccelle, L., and L. Secco, 1991, Relation between crystal chemistry and genetic processes in sedimentary dolomites: Ortisei, p. p. 242.
Searl, A., 1991, Discontinuous solid solution in calcium-rich dolomites: Ortisei, p. 243-244, 3 Figs.
Searl, A., 1992, Dolomite-carbonate replacement textures in veins cutting Carboniferous rocks in East Fife, v. 77, p. 1-14, 9 Figs.
Senowbari-Daryan, B., R. Zühlke, T. Bechstädt, and E. Flügel, 1993, Anisian (Middle Triassic) buildups of the Northern Dolomites (Italy): the recovery of reef communities after the Permian/Triassic crisis, v. 28, p. 181-256, Pl. 40-65, 17 Figs.
Shearman, D. J., J. Khouri, and S. Taha, 1961, On replacement of dolomite by calcite in some Mesozoic limestones from the French Jura, v. 72/1, p. 1-12, Pl. 1.
Sheehan, P. M., 1980, The Late Ordovician and Silurian of the Eastern Great Basin, Part 3: Brachiopods of the Tony Grove Lake Member of the Laketown Dolomite: Contributions in Biology and Geology of the Milwaukee Public Museum, v. 30, p. 1-23.
Shimmield, G. B., and N. B. Price, eds., 1984, Recent dolomite formation in hemipelagic

sediments of Baja California, Mexico: Los Angeles, 5-18 p.
Shinn, E. A., and R. N. Ginsburg, 1964, Formation of recent dolomite in Florida and the Bahamas (abs.), v. 48, p. p. 547-.
Shinn, E. A., R. N. Ginsburg, and R. M. Lloyd, 1965, Recent supratidal dolomite from Andros Island, Bahamas: Society of Economic Paeontologists and Mineralogists Special Publication, p. 112-123.
Shinn, E. A., R. N. Ginsburg, and R. M. Lloyd, eds., 1965, Recent supratidal dolomite from Andros Island, Bahamas, v. 13: Tulsa, 112-123, 8 Figs. p.
Shiyun, T., and J. M. Gregg, 1991, Application of multivariate statistical analysis to geochemical differentiation of dolomite, v. 6, p. 75-81, 3 Figs., 2 Tabs.
Shukla, V., 1986, Epigenetic dolomitization and the origin of xenotopic dolomite texture - discussion, v. 56/5, p. 733-734, 1 Fig.
Shukla, V., ed., 1988, Sedimentology and geochemistry of regional dolostones: Correlation of trace elements with dolomite fabrics, v. 43: Tulsa, 145-157, 14 Figs. p.
Sibley, D. F., 1982, The origin of common dolomite fabrics: clues from the Pliocene, v. 52/4, p. 1087-1100, 8 Figs., 1 Tab.
Sibley, D. F., 1991, Secular changes in the amount and texture of dolomite: Geology, v. 19, p. 151-154.
Sibley, D. F., 1991, Dolomite mineralogy and texture in time and space: Ortisei, p. p. 255.
Sibley, D. F., and J. M. Gregg, 1987, Classification of dolomite rock textures, v. 57/5, p. 967-975, 11 Figs.
Sibley, D. F., J. M. Gregg, R. G. Brown, and P. R. Laudon, 1990, Dolomite crystal size distribution in the burial environment, p. p. 36.
Sibley, D. F., J. M. Gregg, R. G. Brown, and P. R. Laudon, 1993, Dolomite crystal size distribution, p. 195-204, 12 Figs.
Siegmund, H., and B.-D. Erdtmann, 1994, Facies and diagenesis of some Upper Proterozoic dolomites of South China, v. 31, p. 255-264, Pl. 29-30, 2 Figs., 1 Tab.
Simonson, B. M., and D. G. Jarvis, eds., 1993, Microfabrics of oolites and pisolites in the Early Precambrian Carawine dolomite of Western Australia: New York, Springer, 227-237, 13 Figs. p.
Skilliter, C. C., 1998, Stratigraphic and geochemical investigation of Middle to Upper Devonian "aquitards" in west-central Alberta, Canada: AAPG Foundation grants-in-aid recipients for 1998; abstracts AAPG Bulletin, v. 82, p. 2168.
Smith, T. M., and S. L. Dorobek, 1993, Alteration of early-formed dolomite during shallow to deep burial: Mississippian Mission Canyon Formation, central to southwestern Montana: GSA Bulletin, v. 105, p. 1389-1399.
Sonnenfeld, P., 1963, Dolomites and dolomitization: a review, v. 12, p. 101-132.
Soreghan, G. S., M. H. Engel, R. A. Furley, and K. A. Giles, 2000, Glacioeustatic Transgressive Reflux: Stratiform Dolomite in Pennsylvanian Bioherms of the Western Orogrande Basin, New Mexico: Journal of Sedimentary Research, v. 70, p. 1315-1332.
Spence, B. R., 1997, Sedimentology and diagenesis of the Lower Cretaceous Basal Quartz Formation, Crossfield/Delacour Field, Calgary area: AAPG Foundation

grants-in-aid abstracts AAPG Bulletin, v. 81, p. 1782.
Spencer-Cervato, C., and J. Mullis, 1991, Fluid inclusions in dolomite: determination of the composition of the dolomitizing paleo-fluid: Ortisei, p. p. 261.
Sperber, C. M., B. H. Wilkinson, and D. R. Peacor, 1984, Rock composition, dolomite stoichiometry, and rock/water reactions in dolomitic carbonate rocks: Journal of Geology, v. 92, p. 609-622.
Stauffer, C. R., 1937, A diminutive fauna from the Shakopee Dolomite (Ordovician) at Cannon Falls, Minnesota: Journal of Paleontolgy, v. 11, p. 55-60.
Stauffer, C. R., 1937, Mollusca from the Shakopee Dolomite (Ordovician) at Stillwater, Minnesota: Journal of Paleontolgy, v. 11, p. 61-68.
Sternbach, C. A., and G. M. Friedman, 1986, Dolomites formed under conditions of deep burial: Hunton Group carbonate rocks (upper Ordovician to Lower Devonian) in the deep Anadarko Basin of Oklahoma and Texas., v. 1/1, p. 69-73, 19 Figs.
Sternbach, C. A., and G. M. Friedman, 1986, Dolomites formed under conditions of deep burial: Hunton Group carbonate rocks (Upper Ordovician to Lower Devonian) in the deep Anaarko Basin of Oklahoma and Texas, v. 1, p. 69-73, 19 Figs.
Stock, H. W., 1994, Spurenfossilien als Faziesindikatoren im Campan der NE' Dolomiten (Italien), v. 51, p. 277-289.
Stock, H. W., 1994, Stratigraphie, Sedimentologie und Paläogeographie der Oberkreide in den nordöstlichen Dolomiten (Italien)x, v. 137, p. 393-406, 3 Pls., 11 Figs.
Stoessell, R. K., and C. H. Moore, 1983, Chemical constraints and origins of four groups of Gulf Coast reservoir fluids: AAPG Bulletin, v. 67, p. 896-906.
Strahan, R. K., 1975, Geology of Chatom Field, Washington County, Alabama: AAPG Bulletin, v. 59, p. 1731.
Suhm, R. W., 1974, Stratigraphy of Everton Formation (Early Medial Ordovician), Northern Arkansas: AAPG Bulletin, v. 58, p. 685-707.
Sun, S. Q., 1994, A reappraisal of dolomite abundance and occurrence in the Phanerozoic, v. A64, p. 396-404, 4 Figs., 3 Tabs.
Sun, S. Q., 1995, Dolomite reservoirs; porosity evolution and reservoir characteristics: AAPG Bulletin, v. 79, p. 186-204.
Swart, P. K., D. L. Cantrell, H. Westphal, C. R. Handford, and C. G. Kendall, 2005, Origin of dolomite in the Arab-D reservoir from the Ghawar Field, Saudi Arabia: Evidence from petrographic and geochemical constraints: Journal of Sedimentary Research, v. 75, p. 476-491.
Swart, P. K., and L. A. Melim, 2000, The Origin of dolomites in Tertiary sediments from the margin of Great Bahama Bank: Journal of Sedimentary Petrology Research, v. 70, p. 738-748.
Swart, P. K., E. A. Shinn, J. A. McKenzie, C. G. S. C. Kendall, and S. E. Hajari, 1987, Spontaneous precipitation of dolomite in brines from Umm Sid sabkha (qatar (abstr.), v. 39, p. 1202-1228.
Tagai, H., 1957, On the texture of salking-proof dolomite clinker observed by electronmicroscope, v. 65, p. 175-179, 11 Figs.
Tan, F. C., and J. D. Hudson, 1971, Carbon and oxygen isotopic relationships of dolomite and co-existing calcites, Great Estuarine Series (Jurassic), Scotland, v. 35, p. 755-767.

Tanguay, L. H., and G. M. Friedman, 2001, Petrophysical characteristics and facies of carbonate reservoirs; the Red River Formation (Ordovician), Williston Basin: AAPG Bulletin, v. 85, p. 491-523.
Tatarskyi, V. B., 1949, Distribution of rocks in which dolomite is replaced by calcite, v. 69, p. 849-851.
Taylor, T. R., and D. F. Sibley, 1986, Petrographic and geochemical characteristics of dolomite tpes and the origin of ferroan dolomite in the Trenton Formation, Ordovician, Michigan Basin, U.S.A., v. 33, p. 61-86, 17 Figs.
Taylor, T. R., and C. H. Soule, 1993, Reservoir characterization and diagenesis of the Oligocene 64-Zone sandstone, North Belridge Field, Kern County, California: AAPG Bulletin, v. 77, p. 1549-1566.
Tlig, S., and A. M'Rabet, 1985, A comparative study of the Rare Earth Element (Ree) distributions within the Lower Cretaceous dolomites and limestones of Central Tunisia, v. 32, p. 897-907, 8 Figs.
Torok, A., 2000, Formation of dolomite mottling in Middle Triassic ramp carbonates (Southern Hungary): Sedimentary Geology, v. 131, p. 131-145.
Török, A., 2000, Formation of dolomite mottling in the Middle Triassic ramp carbonates (Southern Hungary), v. 131, p. 131-145, 16 Figs., 1 Tab.
Tucker, K. E., P. M. Harris, and R. C. Nolen-Hoeksema, 1998, Geologic investigation of cross-well seismic response in a carbonate reservoir, McElroy Field, West Texas: AAPG Bulletin, v. 82, p. 1463-1503.
Tucker, M. E., 1982, Precambrian dolomites: petrographic and isotopic evidence that they differ from Phanerozoic dolomites, v. 10, p. 7-12.
Tucker, M. E., 1983, Diagenesis, geochemistry, and origin of a Precambrian dolomite: The Beck Spring Dolomite of eastern California, v. 53/4, p. 1097-1119, 15 Figs.
Underwood, C. A., M. L. Cooke, J. A. Simo, and M. A. Muldoon, 2003, Stratigraphical controls on vertical fracture patterns in Silurian dolomite, northeastern Wisconsin, v. 87, p. 121-142, 15 Figs.
Usdowski, E., 1994, Synthesis of dolomite and geochemical implications, v. 21, p. 345-360, 8 Figs., 5 Tabs.
Usdowski, H. E., 1989:, Synthesis of dolomite and magnesite at 60°C in the system Ca2+-Mg2+-Cl22--H2O, v. 76, p. 374-375, 1 Tab.
Usdowski, H. E., 1991, Synthesis of dolomite and magnesite at 60° C and geochemical implications: Ortisei, p. p. 277.
Üsenmez, S., G. M. Friedman, and D. C. Kopaska-Merkel, 1988, Fabric and composition of dolostones and dedolomites from near Karapinar (Adana, southern Turkey), v. 2/2, p. 101-108, 16 Figs., 2 Tabs.
Vahrenkamp, V. C., and P. K. Swart, 1990, New distribution coefficient for the incorporatoin of strontium into dolomite and its implications for the formation of ancient dolomites: Geology, v. 18, p. 387-391.
Vahrenkamp, V. C., and P. K. Swart, 1990, New distribution coefficient for the incorporation of strontium into dolomite and its implications for the formation of ancient dolomites, v. 18, p. 387-391, 5 Figs.
Vahrenkamp, V. C., and P. K. Swart, 1990, New districution coefficient for the incorporatoin of strontium into dolomite and its implications for the formation of

ancient dolomites: Geology, v. 18, p. 387-391.
Vahrenkamp, V. C., and P. K. Swart, 1991, Late Cenozoic sea water generated dolomites of the Bahamas: metastable analogues for the genesis of ancient platform dolomites: Ortisei, p. 279-280, 5 Figs.
Vasconcelos, C., and J. A. McKenzie, 1997, Microbial mediation of modern dolomite precipitation and diagenesis under anoxic conditions (Lagoa Vernelha, rio de janeiro, Brazil, v. 67, p. 378-390.
Vegh-Neubrandt, E., 1963, Die durch Gispauslösung entstandene Porosität in den ungarischen Trias-Dolomiten, v. 6, p. 203-211, 4 Pls., 3 Figs.
Von der Borch, C. C., and D. Lock, 1979, Geological significance of Coorong dolomites, v. 23, p. 587-591.
Voss, R. L., R. D. Hagni, and J. M. Gregg, 1989, Sequential deposition o zoned dolomite and its relationship to sulfide mineral paragenetic sequence in the Viburnum Trend, southeast Missouri, v. 4/2, p. 195-209, 11 Figs.
Wacey, D., and D. T. Wright, 2001, Microbial mediation of dolomite precipitation in the Coorong region, South Australia.
Wan, M., 1998, Dolomitization of an Eocene lacustrine carbonate oil reservoir, Eagle Springs Field, east-central Nevada: AAPG Foundation grants-in-aid recipients for 1998; abstracts AAPG Bulletin, v. 82, p. 2169-2170.
Wanas, H. A., 2002, Petrography, geochemistry and primary origin of spheroidal dolomite from the Upper Cretaceous/Lower Tertiary Maghra El-Bahari Formation at Gabal Ataqa, Northwest Gulf of Suez, Egypt, v. 151, p. 211-224.
Wardlaw, N. C., 1976, Pore geometry of carbonate rocks as revealed by pore casts and capillary pressure: AAPG Bulletin, v. 60, p. 245-257.
Warren, J., 2000, Dolomite: occurrence, evolution and economically important associations, v. 52, p. 1-81.
Warren, J. K., 1988, Sedimentology of Coorong dolomite in the Salt Creek region, South Australia., v. 3/2, p. 175-199, 13 Figs.
Warren, J. K., 1990, Sedimentology and mineralogy of dolomite Coorong Lakes, South Australia, v. 60/6, p. 843-858,10 Figs.
Warthmann, R., Y. van Lith, C. Vasconcelos, J. A. MacKenzie, and A. M. Karpoff, 2000, Bacterially induced dolomite precipitation in anoxic culture experiments: Geology, v. 28, no.12, p. 1091-1094.
Watney, W. L., W. J. Guy, and A. P. Byrnes, 2001, Characterization of the Mississippian chat in south-central Kansas: Chert reservoirs of North America AAPG Bulletin, v. 85, p. 85-113.
Welch, C. L., 2000, Petrography and geochemistry of dolomites in the Lower Cretaceous Edwards Formation in Taylor County, Texas: AAPG Foundation grants-in-aid recipients for 2000 AAPG Bulletin, v. 84, p. 1875.
Wheeler, C. W., P. Aharon, and R. E. Ferrell, 1999, Successions of Late Cenozoic platform dolomites distinguished by texture, geochemistry, and crystal chemistry: Niue, south Pacific, v. A69, p. 239-255, 8 Figs., 2 Tabs.
Willems, H., and M. Wuttke, 1987, Lithogenese lakustriner Dolomite und mikrobiell induzierte "Weichteil-Erhaltung" bei Tetrapoden des Unter-Rotliegenden (Perm, Saar-Nahe-Becken, SW-Deutschland). v. 174, p. 213-238, 5 Figs.

Wilson, E. N., L. A. Hardie, and O. M. Phillips, 1990, Dolomitization front geometry, fluid flow patterns, and the origin of massive dolomite: the Triassic Latemar buildup, Northern Italy, v. 290, p. 741-796, 23 Figs., 3 Tabs.

Winston, G. O., 1978, Rebecca Shoal reef complex (Upper Cretaceous and Paleocene) in South Florida: AAPG Bulletin, v. 62, p. 121-127.

Winter, B. L., J. W. Valley, J. A. Simo, G. C. Nadon, and C. M. Johnson, 1995, Hydraulic seals and their origin; evidence from the stable isotope geochemistry of dolomites in the Middle Ordovician St. Peter Sandstone, Michigan Basin: AAPG Bulletin, v. 79, p. 30-48.

Wright, D. T., 1999, The role of sulphate-reducing bacteria and cyanobacteria in dolomite formation in distal ephemeral lakes of the Coorong region, South Australia, v. 126, p. 147-157.

Wright, D. T., 2002, Benthic microbial communities and dolomite formation in marine and lacustrine environments - a new dolomite model, v. 66, p. 7-20, 10 Figs.

Wright, P., S. Vanstone, and J. Marshall, 1991, Contrasting drowning histories of Mississippian platforms: 'marine' alteration of paleosols and dolomite formation: Ortisei, p. 292-293, 1 Fig.

Yoo, C. M., and Y. I. Lee, 1998, Origin and modification of early dolomites in cyclic shallow platform carbonates, Yeongheung Formation (middle Ordovician), Korea, v. 118, p. 141-157, 10 Figs., 1 Tab.

Yoo, C. M., and Y. I. Lee, 1998, Orogin and modification of early dolomites in cyclic shallow water platform carbonates, Yeongheung Formation (middle Ordovician), Korea, v. 118, p. 141-158, 10 Figs.

Zankl, H., and M. U. E. Merz, 1994, The possible contribution fo fresh water cyanobacteria to Northern Alpine Hauptdolomite sedimentation, v. 19, p. 261-264.

Zeeh, S., T. Bechstädt, M. Fröhler, C. Klebahn, and U. Walter, 1991, Dedolomitization of Cambrian dolomites of southwestern Sardinia: Ortisei, p. 295-296.

Zempolich, W. G., 2002, Dolomite reservoirs created through fault-related burial dolomitization; analogs from the Italian Alps: 2001-2002 AAPG distinguished lecturers; North America distinguished lecture abstracts AAPG Bulletin, v. 86, p. 200.

Zempolich, W. G., and L. A. Hardie, 1997, Geometry of Dolomite Bodies WIthin Deep-Water Resedimented Oolite of teh Middle Jurassic Vajont Limestone, Venetian Alps, Italy: Analogs for Hydrocarbon Reservoirs Created Through Fault-Related Burial Dolomitization: AAPG Memoir, p. 127-162.

Zempolich, W. G., B. H. Wilkinson, and K. C. Lohmann, 1988, Diagenesis of late Proterozoic carbonates: the Beck Spring Dolomite of eastern California, v. 58, p. 656-672, 18 Figs.

Zenger, D. H., 1973, Syntaxial calcite borders on dolomite crystals, Little Falls Formation (Upper Cambrian), New York, v. 43, p. 118-124.

Zenger, D. H., 1981, On the formation and occurrence of saddle dolomite - discussion, v. 51/4, p. 1350-1352.

Zenger, D. H., 1982, Comment on Precambrian dolomites: petrographic and isotopic evidence that they differ from Phanerozoic dolomites, v. 10, p. 662.

Zenger, D. H., 1992, Burrowing and dolomitization patterns in the Steamboat Point Member, Bighorn Dolomite (Upper Ordovician), northwest Wyoming, v. 29/2, p. 133-142, 6 Figs., 1 Tab.

APPENDIX 1
INITIAL SUMMARY OF CURRENTLY AVAILABLE GEOLOGIC DATA (TASK 2)

Ordovician - Trenton-Black River Production Analysis Data and Graphs
(Prairie du Chien, Trempealeau generally not productive)

DISCOVERY

1884 – Drilling begins on Findlay-Kankakee Arch in Indiana and Ohio
    Indiana-Lima trend
        100,000 wells
        500 MBO Bowling Green Fault Zone (Albion-Scipio analog)
1917 – SW Ontario – Dover Field
        narrow, elongate, east-west trending dolomitized reservoir with synclinal expression
        highly variable dolomitization
        4 separate pools
        production from 2800-3200'
        249 KBO and 12.8 BCF CUM
1920 – Dundee Township, Monroe County, Michigan
        First Trenton oil in Michigan
        Noncommercial
1936 – Deerfield Field, Monroe County Michigan
        First Commercial Trenton oil in Michigan
        Along the Lucas-Monroe monocline
            Extension of Bowling Green Fault zone in Ohio
        Dolomite lenses in upper 125' of Trenton Group
        1959 – 40 wells drilled on 360 acre field
        1959 – 608 KBO CUM
1954 – Northville Field, Washtenaw, Oakland and Wayne Counties, Michigan
        drilled as gravity prospect
        faulted anticline
        production from
            Dundee (Devonian)
            Salina-Niagaran (Silurian)
            Trenton-Black River (Ordivican)
                Fractured and dolomitized limestones
                East flank of structure
                Production is fault associated
1955-58 – Albion-Scipio, Calhoun & Hillsdale Counties Michigan
        1955 - Scipio Discovery Well – Houseknecht No. 1 (Sec 10, T5S-R3W – Hillsdale Co.)
            Originally drilled for Devonian gas - Dry
            Deepened on advice of family psychic friend

1/57 - Encountered oil @ 3900'
Comp @ 140 BOPD and "considerable" gas
9/57 – Confirmation well – Stephens No. 1 (Sec 10, T5S-R3W – Hillsdale Co.)
Spetacular blowout – hit lost circulation @ 3769' (235' into Trenton)
Shut-in – craters began to form around location
Flowed for 25 houras @ 15 MMCFGPD
11/58 – Albion Discovery well Rosenau No. 1 (Sec 23, T3S-R4W, Calhoun Co.)
Comp @ 200 BOPD
Subsequent drilling discovered Pulaski (1959), Barry, Sponseller, Van Wert, Cal-Lee Fields – All part of the Albion-Scipio Trend
1986 - 961 wells drilled, 573 still producing
1989 – 330 Trenton penetrations in Albion Field
631 Trenton penetrations in Scipio Field

12/82 – Stoney Point Field Discovery (sub-parallel to Albion-Scipio 5 miles east)
JEM Casler No. 1-30 (Sec 30, T4S-R2W, Jackson Co.)
Encountered dolomite reservoir 115' into Trenton @ 3910'
Hit lost circulation @ 4248', casing set
Tested @ 2000 BOPD from perfs 4161'-4179'
BHP drop never exceeded 3 psi
Put on production @ 220 BOPD (1/83)
1983 –1987 – 210 wells drilled around Stoney Point Trend
1987 – 75 wells oil and gas producers in Stoney Point Trend

STRATIGRAPHY

Trenton – Limestone, brown-gray, fossiliferous with carbonaceous partings
Top-of-Trenton Unconformity:
Rooney (1966) – southward thinning of Trenton toward Findlay arch in Ohio
DeHaas and Jones (1984,1989) – Exposure and karsting to produce caverns
Keith (1985) and Gray (1983) – dismissed any top-of-Trenton unconformity, considered this surface to be a marine hardground

Black River – Limestone, tan-gray, lithographic; altered to porous dolomite

TRENTON-BLACK RIVER TRAP

<u>Deerfield Field</u>

Lucas-Monroe monocline (extension of Bowling Green Fault Zone)

<u>Northville Field</u>

Faulted anticline

<u>Albion-Scipio Trend and Stoney Point Trend</u>

Stratigraphic traps, limited development of porous, fractured dolomite reservoirs within the tight regional Trenton-Black River limestone northwest-southeast, left-lateral strike slip faulting (en echelon faults) offset 2.5 miles

Reactivated basement faults, primarily Precambrian, w/ additional reactivation during Late Ordovician-Early Silurian?, Late-Silurian-Early Devonian?, Mississippian?

Synclinal sag-like compartments related to down-dropping over partly extensional, en echelon breaks in the underlying section

Diagenetic porosity development (dolomitization) near faults

Sharp contacts between dolomite and regional limestone

Albion-Scipio, Stoney Point Fields– no anticlinal closure

TRENTON-BLACK RIVER SEAL

(1) Overlying Utica Shale

(2) Non-porous, finely crystalline, ferron "cap dolomite" at the top of the Trenton Group

(3) Non-dolomitized regional Trenton-Black River limestone

(4) Trace fluorite, sphalerite, barite mineralization observed as late-stage pore fillings

TRENTON-BLACK RIVER CHARACTERISTICS

<u>Porosity</u>

Vuggy, cavernous

Intercrystalline

Open fractures, often solution enlarged

2-5% normal

8-12% present but uncommon

<u>Permeability</u>

Extremely variable (0.01 – 8000 md)

Generally low (85% of samples < 10 md)

Porosity/Permeability plots show no uniform relationship

<u>Capillary Pressure</u>

High entry pressures in cap dolomite (confirms seal)

High entry pressures in Trenton-Black River = moderate to poor reservoir rocks

Log Signatures

Lost circulation – most wells cased and then logged
Gamma ray – neutron log typical
Neutron porosities range 2-10% (4-6% most common)
Modern gamma-ray logs, porosity of 26% observed at Utica Shale
  baseline
Many wells show < 0% neutron porosity = no cement behind casing
  Base of zone usually at gas/oil contact
Thin shale layers acted as flow barriers during dolomitization, so most
  Reservoirs located below persistent shale layers - particularly true for "E" Shale (Best developed in northern portion of Albion Field) and Black River Shale (Best developed in southern portion of Albion Field)
Typical log – Figure 18 in Hurley and Budros

Fractures

Dominant trend N30W
Secondary trend east-west (Finnigan's Finger north of Haskell Unit)
Open, partially filled, and filled
  Filling = saddle dolomite w/ calcite and anhydrite locally present, trace amounts of MVT minerals

Lost Circulation Zones/Caves

Some zones encountered in cap dolomite (seal)
30% of wells in Albion-Scipio encountered lost circulation
54% of wells in Stoney Point encountered lost circulation
Bit drops up to 62' reported in Albion-Scipio - rare
Bit drops up to 8' reported in Stoney Point – rare
  DeHaas and Jones (1984, 1989) propose cave development related to karsting responsible for lost-circulation zones; however, few others agree with this relationship due to:

1.) bit drops rare, most zones solution-enlarged fractures or vuggy rock
2.) Trenton-Black River arbitrarily divided into 4 levels w/ no true geological relationship to caves and lost-circulation zones
3.) Synclinal depression across field persists through Early Devonian - Cave formation would collapse under 1500' of overburden
4.) Geochemical data shows reservoir dolomites precipitated from hot solutions, some dissolution porosity is a late-stage event

5.) No cave features such as flowstone, cave sediments, cave pearls observed
6.) Core shows no karst features at Trenton/Utica contact – rather phosphatic and pyritic mineralization suggest a hardground (same as top-of-Trenton contact in Indiana)
7.) If caves formed during Ordovician – then Utica Shale should have filtered down into subsurface and this is not observed.

It appears that Mammoth Cave analog is not correct, rather, lost-circulation zones were probably developed by fracturing and dolomitization in a hydrothermal setting in a burial environment (Hurley and Budros)

RESERVOIR COMPARTMENTS

Determined by:
- Structure Maps
- Fluid Contacts
- Oil and Gas Ratios
- Bottom-hole Pressures
- Lateral Well Drilling Data

Inter-well Scale shows en echelon synclinal compartments

Field Scale shows free gas cap with 150’-200’ oil column

Pulaski Break – Major non-dolomitized discontinuity of fluid levels between Albion and Scipio Field

Stoney Point Field – 4 major compartments based on BHP’s and decline rates

Albion Field – 3 major compartments based on BHP’s and decline rates

Albio, Scipio and Stoney Point Fields – subtle east-west permeability barriers due to fracture zones that have undergone mylonitization and/or pervasive cementation

Finnigan’s Finger – east-west production due to incomplete late-stage crystallization

Compartment Boundaries vs. Lost Circulation Zones
- Most lost circulation zones on up-dip (south) side of barriers between Group 2 and 4, and Groups 1 and 2 (Figure 27, Hurley and Budros)
- Lost circulation zone decrease southward in Group 2 Suggesting that dolomitizing fluids move upward along east-west fracture zones
- Dolomites also formed on undersides of shales suggesting upward fluid flow
- Stoney Point - Dolomites/lost circulation zones concentrated in lower part

ORIGIN OF DOLOMITE

1) Burgess (1960) – Reservoir dolomite was a secondary mineral formed as Cambrian and Lower Ordovician water moved up along the fracture zone (analogs- Dover and Colchester Fields in Ontario)

2) Ells (1962) – Magnesium-bearing waters ascending through fractures responsible to dolomitization (Albion-Scipio Field similar to Mississippi Valley-type [MVT] lead-zinc mineral deposits)

3) Beghini and Conroy (1966) – Reservoir formed by pre-Black-River Group water that moved through faults and fractures to produce secondary dolomite

4) Buehner and Davis (1968) – Reservoir is epigenetic dolomite related to a fault system

5) Shaw (1975) – Described a mineral assemblage (including sphalerite) in Albion-Scipio cores similar to MVT mineral deposits. He noted 2-phase fluid inclusions in Albion-Scipio dolomites. Pore filling saddle dolomites precipitated from fluids at minimum of 80 degree C temperature. He identified a liquid-hydrocarbon phase in some fluid inclusions indicating hydrocarbons were present at time of cementation. Proposed a model of replacement dolomitization and development of intercrystalline porosity during Middle to Late Silurian by waters percolating through fractures. Magnesium is sourced from underlying Prairie du Chien dolomite or Trempealeau formations. Second phase - during Lower to Middle Devonian as hot fluids from basin center created cavernous porosity, subsequent collapse, and precipitation of MVT assemblage.

6) Ardrey (1978), DeHaas and Jones (1984, 1989) Diagenesis of Trenton-Black River in Albion-Scipio area due to exposure (top of Trenton Unconformity). Dolomitization is the result of mixing models based on the observation that Trenton formation water is less saline than water in shallower horizons; therefore, it could not be of hydrothermal origin.

7) Taylor and Sibley (1986) – They identified 3 major types of dolomite (1) regional dolomite not associated with Field, (2) Cap dolomite that occurs in the top 40 feet (related to interaction of the Trenton with Fe-rich fluids formed during the de-watering of the overlying Utica Shale) (3) fracture-related dolomite (formed during deeper burial at approximately 80 degrees C based on geochemical results)

8) Budai and Wilson (1986) – They identified various MVT accessory minerals including pyrite, calcite, anhydrite, barite, celestite, sphalerite, and fluorite in

association with saddle dolomite cements. They proposed a hydrothermal model with Paleozoic and Precambrian basement rock as sources of iron, sulfur, and other trace metals.

9) Hurley and Cumella (1987) – They proposed a model based on carbon, oxygen, and strontium isotopes fluid-inclusion geothermometry, brine geochemistry and regional hydrologic constraints. Dolomitizing fluids were Silurian-Devonian hypersaline sea water that moved down fracture zones to meet with hot limestone-dissolving fluids moving up from the basement. These fluids mixed in a pattern that is consistent with the distribution of dolomite reservoirs and lost-circulation zones.

SOURCE ROCK

Trenton Black River Sequence is the primary source

- Shaley layers have TOC's 20-25 wt%
- Burial history indicates maturity reached in the Carboniferous for the central basin area
- TAI (visual kerogen) and pyrolysis (Tmax) indicate thermally maturity for oil and gas
- Utica Shale (above Trenton – traditionally considered source) – TOC's too low

HYDROCARBONS

Paraffinic
41-43 degree API
0.0.02% Sulfur
0.974 cp Viscosity (at reservoir conditions)
GOR's – 400 – 600 scf/STB
Cloud Point – 70 degree F
Free gas cap at time of discovery

WATER CHARACTERISITCS

Connate water dense, CA-rich brine
North of Albion - 234,000 mg/L Total dissolved solids
South of Scipio – 196,000 mg/L Total dissolved solids
Formation water resistivity approximately 0.03 ohm-m at 104 degree F (BHT)

RECOVERY MECHANISMS

Original Recovery

- Solution-gas drive

Gas cap expansion
Gravity drainage
Limited water drive

Current Recovery
Stoney Point Field – Pressure is still high (approximately 1100 psig)
Albion-Scipio Field
Pressures down to 100-150 psig
Gravity drainage now main mechanism

Volumetric Calculations meaningless – unable to accurately estimate porosities

Material Balance Calculations suggest:
Scipio Field – 170 MMB OOIP
Albion Field – 120 MMB OOIP
Stoney Point Field – Not Available

Secondary Recovery
Pilot Waterflood of the Haskell Unit (near south end Scipio Field) – discouraging results
Marathon Oil – drilled a number of horizontal wells with considerable promise

EXPLORATION TECHNIQUES

Originally - Advice of psychic after dry hole exploring for Devonian gas

Early - “Trendology”
Linear Fracture Zone (northwest – southeast)
Top-of-Trenton synclinal sag (up to 60’) recognized in producing wells

1960’s - early 70’s – Gravity defined basement fault along Scipio Trend
Limited drilling success
Dolomite porosity mutes density contrast between regional limestone and reservoir Dolomite

1970’s - Magnetics used to detect basement discontinuities and faults
Albion-Scipio does not appear as an individual feature on magnetic maps

Recently – Micromagnetic surveys and resistivity profiles have been employed
Significance not yet proven
Reflection-seismic currently the primary method – Problems:
Variable till (overburden) thicknesses produce noise and statics problems
Secondary porosity (dominant reservoir component) not detected by P-waves
Reservoir dolomites (2-5% porosity) have similar acoustic impedance as regional limestones
Reservoir geometries hard to image
Reflection-seismic Trenton-Black River discoveries based on
Disruptions (sags) at Trenton event
Internal waveform changes
Disruption of lower events
Recognition of faults from offsetting events and/or diffractions

Soil gas geochemistry studies above Scipio field showed no correlation between soil gas and producing parts of the field (despite Stoney Point Field discovery)

LANDSAT – effective as a regional tool but interpretations of individual anomalies subjective

Stoney Point Field - Soil-gas geochemistry

DEVELOPMENT

- Albion-Scipio Trend
  - Initial Maximum Allowable 150 BOPD and/or 200MCFGPD
  - 7/1/60 - Maximum Allowable reduced to 125 BOPD and/or 165 MCFGPD
  - 7/1/61 - Maximum Allowable reduced to 100 BOPD and/or 150 MCFGPD
    - (applies only to wells drilled in center of NW qtr of SE qtr of 40 acre unit
  - Current – Oil allowable lifted, gas allowable 150 MCFGPD
  - Developed on 20 acre spacing
  - Decline rate 15% per year
- Stoney Point Trend
  - Maximum Allowable 150 BOPD and/or 175 MCFGPD
  - Drilling window maximum is 10 acres per 40-acre unit
  - Developed on 40 acre spacing
  - Decline rate 15% per year
- Subsurfacing mapping useful as development tool
  - % dolomite in Trenton-Black River sequence
  - Hydrocarbon shows in Trenton-Black River sequence
  - Isopach Traverse Limestone (Devonian) to top of Salina Group (Silurian)
    - showing thick of synclinal sag over productive part of field

Trenton – Black River Trend: Production Analysis

General Observations

1. Production data for the Trenton – Black River trend varies in quality and completeness. The State of Michigan did not require complete production data reporting until xxx. Digital data bases developed by the state beginning in 1981 generally do not include data before that date or data before and after that date may be cataloged in different groupings.

2. Production data are often grouped by lease hold and not necessarily by either individual well or by geological producing unit (e.g. – Albion Scipio 1 – 7 South Units). There is no means to separate the data and recalculate results based upon more geologically based, flow-unit parameters.

3. Initial potential data was never recorded for most wells in the trend. Only long-term and/or average data are available in most instances. Data is often duplicated as leasehold results and trend summaries. However, it is seldom clear as to exactly what data are included.

4. The State of Michigan imposes a 200 barrel-per-day maximum allowable on production which often distorts the true capabilities/performance of the affected wells.

5. During the beginning stages of field development, many operators produced the oil and flared the gas. Complete gas production data were only recorded during the later stages of field development as oil production declined and the gas cap was blown down to extend the economic life of the field.

6. Graphs of “Cumulative Oil and Cumulative Gas Production by Field” show an expected exponential decline in field size. “Gaps” in the curve are “filled” by “trend data” which give a distorted view as to the particular field sizes discovered. When these trends are omitted (difficult to accurately identify) a pattern emerges showing a few very large fields discovered (Albion-Scipio Trend), a large number of 1-5 well size fields discovered, and only a few intermediate field sizes discovered. Dr. Christopher Swezey of the U.S.G.S. interprets this to mean that there are still intermediate sized Trenton-Black River fields to be found. He calculates that as much as 723 million barrels of oil, 2,002 billion cubic feet of gas, and 112 million barrels of NGL’s may yet remain. The play is not resource limited as much as it is technology limited. It represents the greatest single remaining potential reserves for a particular reservoir in the State of Michigan.

7. Most fields have produced more oil than gas. However, there are 5 fields in the trend that have produced more gas than oil. These are: Albion-Pulaski-Scipio Trend, Albion-Scipio 3 South, Albion-Scipio 4 South, Albion-Scipio 5 South, and Northville.

8. Only Stoney Point field has produced more brine (bbls) then gas (BOE).

9. Cumulative Oil Production can be divided into approximately 5 main groups:
   - **a.) <u>>10,000,000 bbls</u>**
     Albion-Pulaski-Scipio Trend, Scipio-Fayette-Moscow, Stoney Point, Pulaski-Homer Twp, Albion Twp.
   - **b.) <u>500,000 – 6,000,000 bbls</u>**
     Adams Twp, Sheridan Twp, Lee Twp, Hanover, Albion-Scipio 6 South, Albion-Pulaski-Scipio Trend, Albion-Scipio 5 South, Northville, Dearfield, Albion-Scipio 3 South, Albion-Scipio 4 South
   - **c.) <u>5,000 – 50,000 bbls</u>**
     Albion-Scipio 2 South, Reading Section 25, Albion-Scipio 1 South, Northville?, Henrietta, Tekonsha, Lee Section 34 (Black River), Freedom, Reading, Medina, Springport, Green Oak
   - **d.) <u>500 – 5,000 bbls</u>**
     Rattle Run, Summerfield, Albion-Scipio 7 South, Huron, Hanover Section 13, Summerfield Section 07, Macon Creek, Summerfield Section 19, Blissfield, New Boston, Newburg, Cadmus, Olivet, Sumpter
   - **e.) <u>0 - 60 bbls</u>**
     Ridgeway Section 01, Winterfield

10. Cumulative Gas Production can be divided into approximately 5 groups:
    - **a.) <u>>100,000,000 MCF</u>**
      Albion-Pulaski-Scipio Trend
    - **b.) <u>6,000,000 – 100,000,000 MCF</u>**
      Scipio-Fayette-Moscow Trend, Pulaski-Homer Twp, Stoney Point, Albion Twp, Northville, Albion Scipio 4 South
    - **c.) <u>1,000,000 – 6,000,00 MCF</u>**
      Adams Twp, Albion Scipio 5 South, Albion-Pulaski-Scipio Trend, Albion Scipio 3 South, Reading Section 3 South, Reading Section 25, Albion Scipio 1 South, Albion Scipio 6 South, Sheridan Twp
    - **d.) <u>300,000 – 1,000,000 MCF</u>**
      Albion Scipio 2 South, Hanover, Lee Section 34 (Black River), Lee Twp
    - **e.) <u>50,000 – 300,000 MCF</u>**
      Cadmus, Winterfield, Green Oak, Blissfield

11. There is little correlation between "Years of Production" vs. "Cumulative Oil Production by Field" or "Year of Discovery." Longest producing fields (most years of production) range from discovery dates of 1935 (Deerfield), 1947 (New Boston), 1954 (Northville), 1961Springport, and 1967 (Green Oak). However, these fields do not reflect the greatest cumulative oil totals. Instead, accumulations from these fields are similar to those from fields having produced

for the fewest years (Reading Section 25 – disc 1999, Henrietta – disc 1979, Albion-Pulaski-Scipio Trend – disc 1981). Fields reflecting "Maximum Oil Accumulation" are associated with "Years of Production" intermediate in range (Scipio-Fayette-Moscow Trend – disc 1957, Albion Twp – disc 1959, Albion-Pulaski-Scipio Trend – disc 1960, Pulaski-Homer Twp – disc 1959, Stoney Point – disc 1984, Albio-Scipio6 South – disc 1982, Adams Twp – disc 1967, Sheridan Twp – disc 1967). The lack of correlation between "Years of Production," "Cumulative Oil Production by Year" and "Year of Discovery" leads one to speculate that fields of varying reservoir types and production capabilities, overprinted by the learning curve of discovery, have been mixed into a single data base. Approximately four groups can be identified within this data base:

(1) > 30 years of production; Deerfield, Northville, Springport, New Boston,

(2) 20 – 30 years of production; Green Oak, Freedom, Ridgeway Section 01, Summerfield, Albion-Scipio 1 South, Albion Scipio 3 South, Hanover, Scipio-Fayette-Moscow, Tekonsha, Albion Twp, Albion-Pulaski-Scipio Trend, Macon Creek, Medina, Pulaski-Homer Twp, Stoney Point,

(3) 10 – 20 years of production; Blissfield, Lee Section 34 (Black River), Albion Scipio 2 South, Albion Scipio 5 South, Cadmus, Albion Scipio 6 South, Northville, Albion Scipio 4 South, Adams Twp, Lee Twp, Olivet, Sheridan

(4) 0 – 10 years of production; Reading, Albion Scipio 7 South, Summerfield Section 19, Winterfield, Rattle Run, Reading Section 25, Summerfield Section 07, Huron, Henrietta, Newburg, Sumpter, Albion-Pulaski-Scipio Trend, Hanover.

12. There appear to be four distinct groups of "Field Size" in comparison to "Year Discovered."

(1) 1935 -1960; Deerfield, Sumpter, Huron, New Boston, Freedom, Northville, Ridgeway Section 01, Scipio-Fayette-Moscow Twp, Summerfield, Albion Twp, Hanover, Pulaski-Homer Twp, Tekonsha, Albion-Pulaski-Scipio Trend,

(2) 1960 – 1967; Macon Creek, Medina, Springport, Blissfield, Adams Twp, Green Oak, Lee Twp, Sheridan Twp,

(3) 1969 – 1984; Olivet,, Reading, Henrietta, Newburg, Albion Scipio 1 – 6 South, Northville (Gas Storage), Albion Scipio 7 South, Stoney Point,

(4) 1985 – 1999; Winterfield, Cadmus, Lee Section 34 (Black River), Rattle Run, Hanover Section 13, Summerfield Section 07, Summerfield Section 19, Reading Section 25. Each group displays a general trend of increasing field size through time. This "re-setting of the curve" may reflect discovery of differing field types followed by increasing knowledge of how to explore and develop these new types.

13. Nearly one-half of the Trenton – Black River fields produce only oil (Albion-Scipio 7 South, Deerfield, Freedom, Henrietta, Macon Creek, Medina, New Boston, Newburg, Northville, Olivet, Reading, Ridgeway Section 01, Springport, Summerfield, Summerfield Section 07, Summerfield Section 19, Tekonsha, Hanover Section 13, Huron, Rattle Run, Sumpter) .

14. The other half of the Trenton – Black River fields produce both oil and gas (Albion-Pulaski-Scipio Trend, Scipio-Fayette-Moscow, Pulaski-Homer Twp, Stoney Point, Albion Twp, Northville, Albion-Scipio 1-6 South, Adams Twp, Reading Section 28, Sheridan Twp, Hanover, Lee Section 34 (Black River), Lee Twp, Cadmus, Winterfield, Green Oak, Blissfield) .

15. Winterfield is the only field in the trend to produce only gas. This is primarily a Dundee Formation field producing both oil and gas from that interval. Only one well in the field penetrates the deeper Trenton – Black River Formations producing gas from those intervals.

Current Activity

Data from the first 4 years of the Albion – Scipio field which are contained in the Albion – Scipio Field Folio Series is currently being entered into a computer data base. These data are lease based and reported upon a monthly schedule. It is thought that these data more accurately reflect initial production conditions and are more consistently reported. These data will be analyzed when data entry is complete.

1. Fields from each category defined above will be correlated to the newly developed index covering data quantity, quality and availability for each field. Fields in each category ranking high in data coverage will be selected for detailed study.

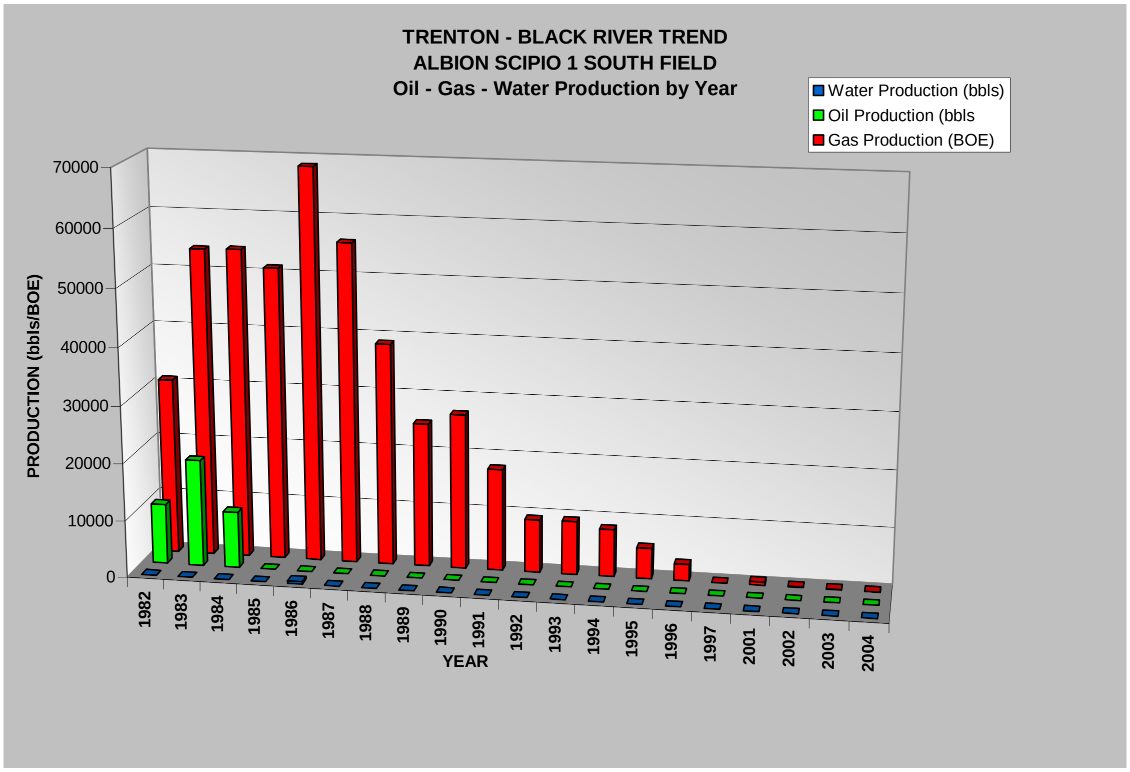
TRENTON - BLACK RIVER TREND
ALBION SCIPIO 1 SOUTH FIELD
Oil - Gas - Water Production by Year
Water Production (bbls)
Oil Production (bbls
Gas Production (BOE)
PRODUCTION (bbls/BOE)
70000
60000
50000
40000
30000
20000
10000
0
1982
1983
1984
1985
1986
1987
1988
1989
1990
1991
1992
1993
1994
1995
1996
1997
2001
2002
2003
2004
YEAR

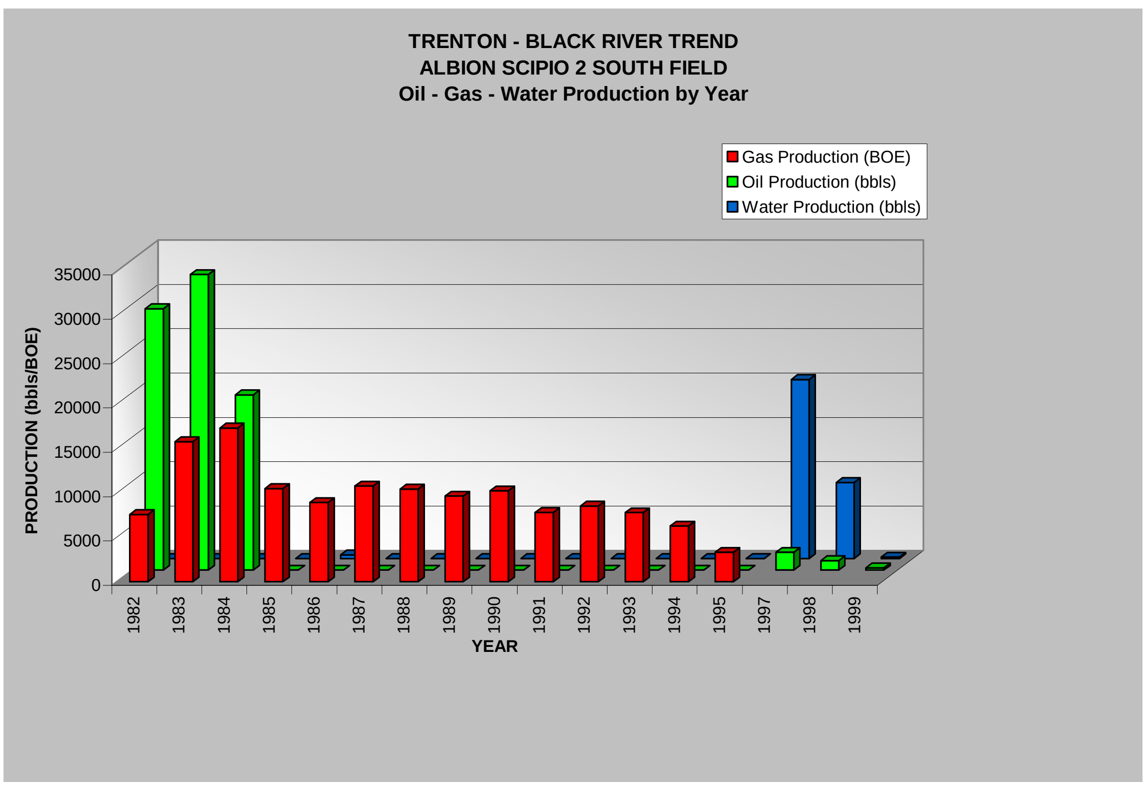
TRENTON - BLACK RIVER TREND
ALBION SCIPIO 2 SOUTH FIELD
Oil - Gas - Water Production by Year
Gas Production (BOE)
Oil Production (bbls)
Water Production (bbls)
PRODUCTION (bbls/BOE)
35000
30000
25000
20000
15000
10000
5000
0
1982
1983
1984
1985
1986
1987
1988
1989
1990
1991
1992
1993
1994
1995
1997
1998
1999
YEAR

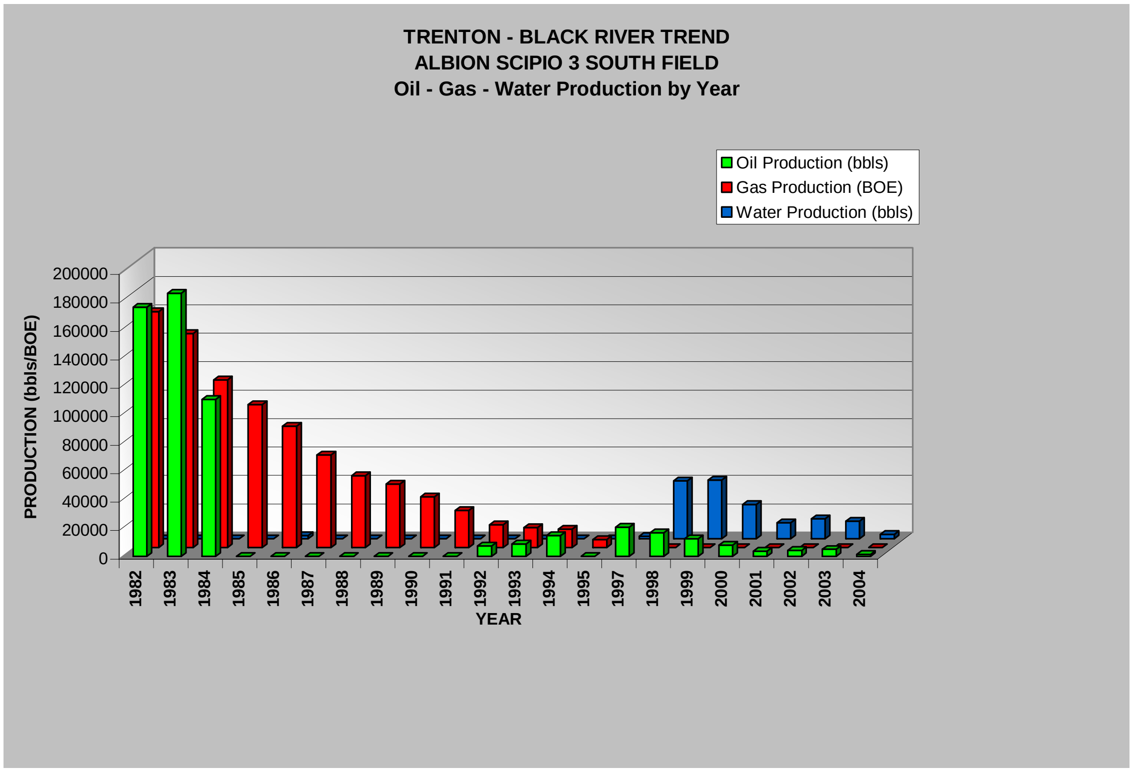
TRENTON - BLACK RIVER TREND
ALBION SCIPIO 3 SOUTH FIELD
Oil - Gas - Water Production by Year
Oil Production (bbls)
Gas Production (BOE)
Water Production (bbls)
PRODUCTION (bbls/BOE)
200000
180000
160000
140000
120000
100000
80000
60000
40000
20000
0
1982
1983
1984
1985
1986
1987
1988
1989
1990
1991
1992
1993
1994
1995
1997
1998
1999
2000
2001
2002
2003
2004
YEAR

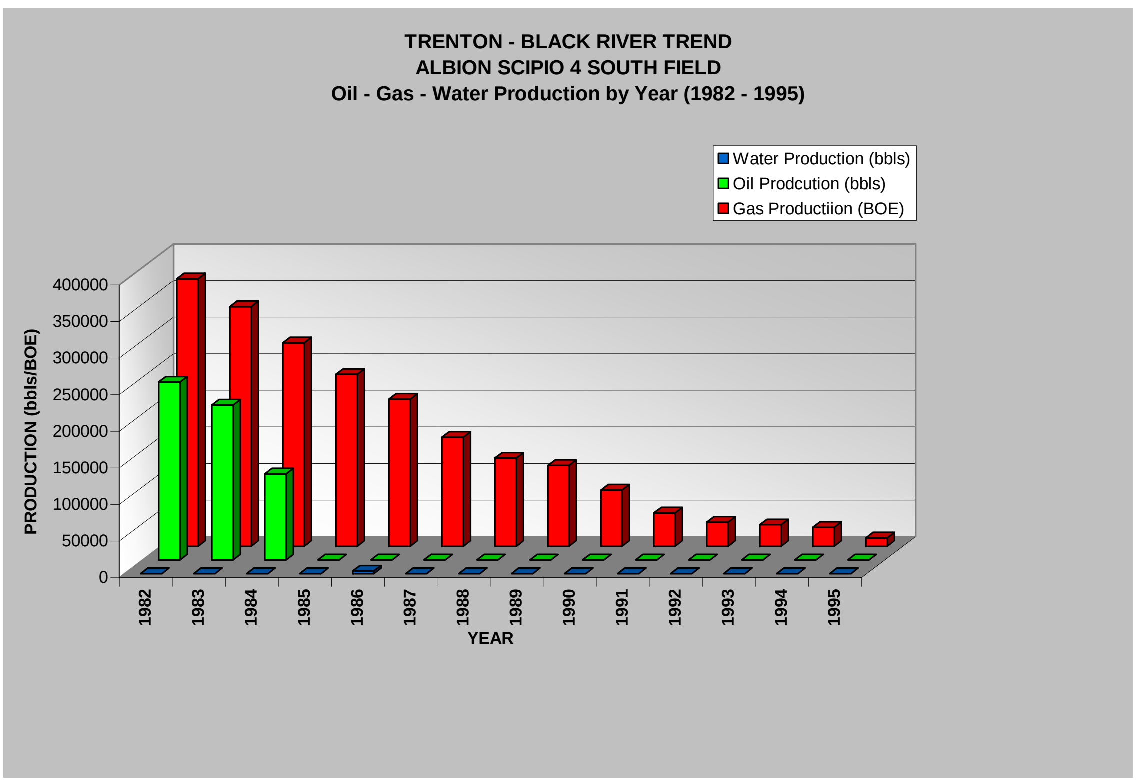
TRENTON - BLACK RIVER TREND
ALBION SCIPIO 4 SOUTH FIELD
Oil - Gas - Water Production by Year (1982 - 1995)
Water Production (bbls)
Oil Prodcution (bbls)
Gas Productiion (BOE)
PRODUCTION (bbls/BOE)
400000
350000
300000
250000
200000
150000
100000
50000
0
1982
1983
1984
1985
1986
1987
1988
1989
1990
1991
1992
1993
1994
1995
YEAR

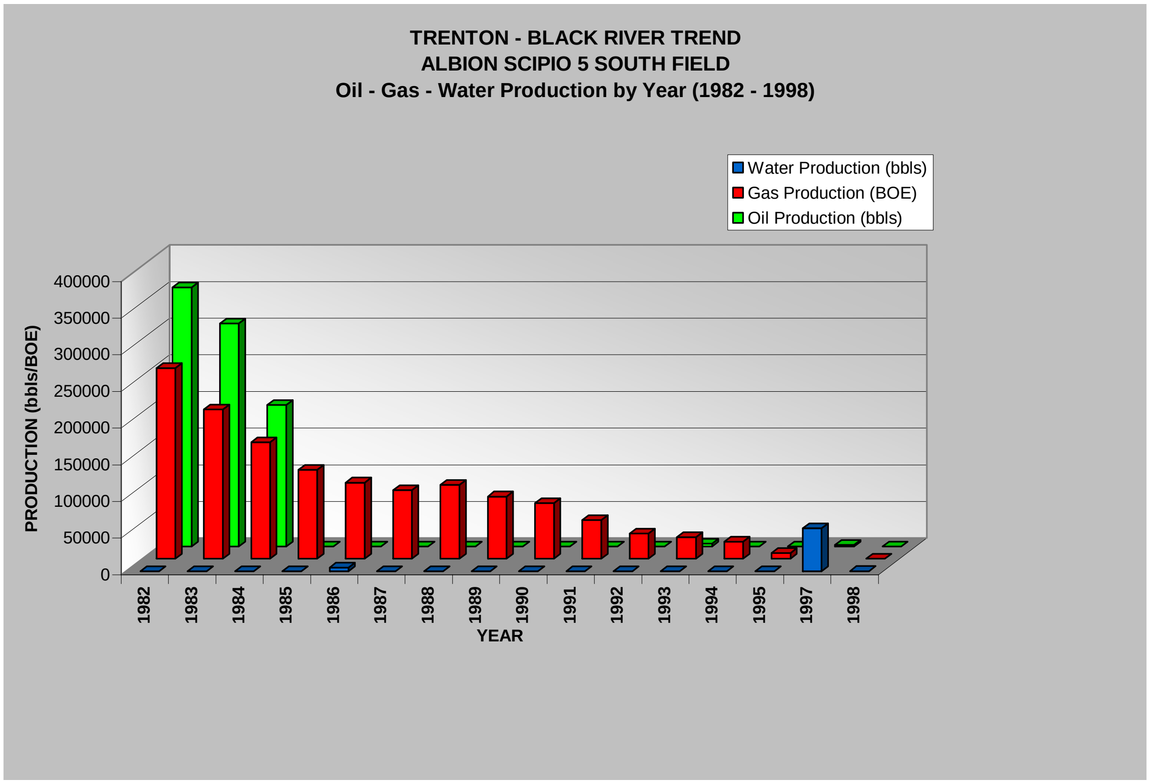
TRENTON - BLACK RIVER TREND
ALBION SCIPIO 5 SOUTH FIELD
Oil - Gas - Water Production by Year (1982 - 1998)
Water Production (bbls)
Gas Production (BOE)
Oil Production (bbls)
PRODUCTION (bbls/BOE)
400000
350000
300000
250000
200000
150000
100000
50000
0
1982
1983
1984
1985
1986
1987
1988
1989
1990
1991
1992
1993
1994
1995
1997
1998
YEAR

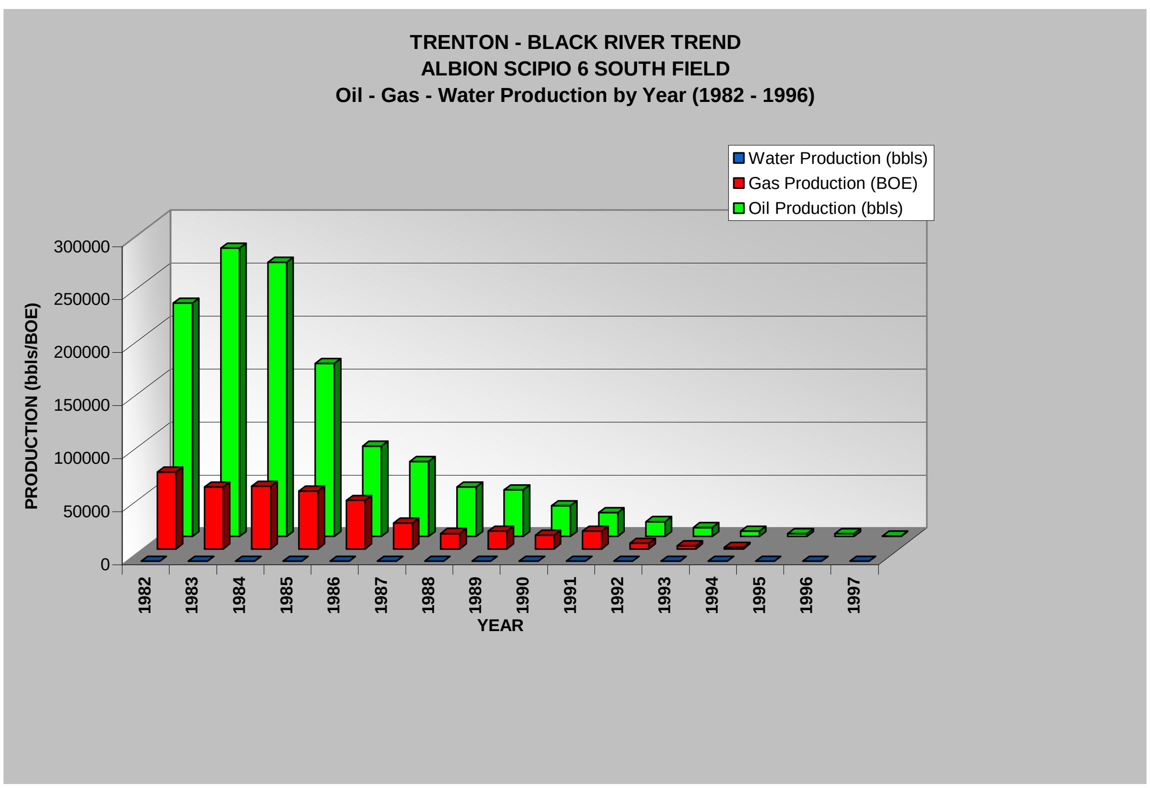
TRENTON - BLACK RIVER TREND
ALBION SCIPIO 6 SOUTH FIELD
Oil - Gas - Water Production by Year (1982 - 1996)
Water Production (bbls)
Gas Production (BOE)
Oil Production (bbls)
PRODUCTION (bbls/BOE)
300000
250000
200000
150000
100000
50000
0
1982
1983
1984
1985
1986
1987
1988
1989
1990
1991
1992
1993
1994
1995
1996
1997
YEAR

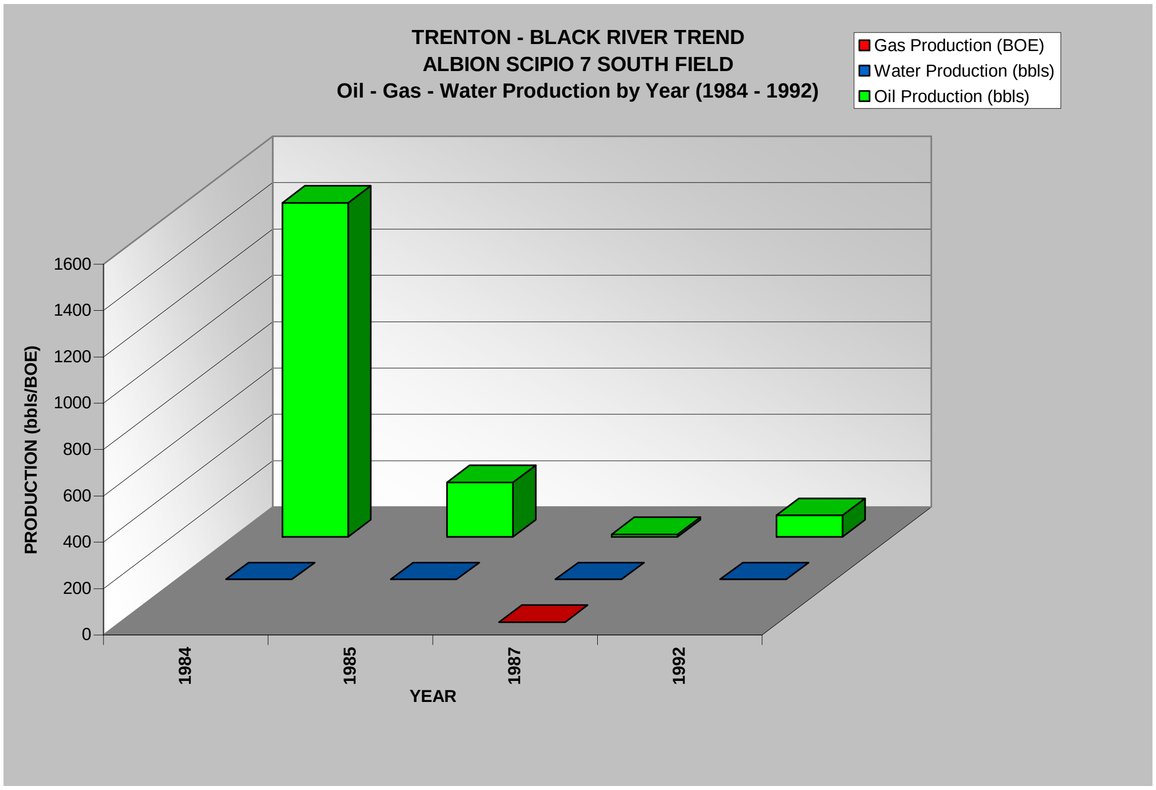
TRENTON - BLACK RIVER TREND
ALBION SCIPIO 7 SOUTH FIELD
Oil - Gas - Water Production by Year (1984 - 1992)
Gas Production (BOE)
Water Production (bbls)
Oil Production (bbls)
PRODUCTION (bbls/BOE)
1600
1400
1200
1000
800
600
400
200
0
1984
1985
1987
1992
YEAR

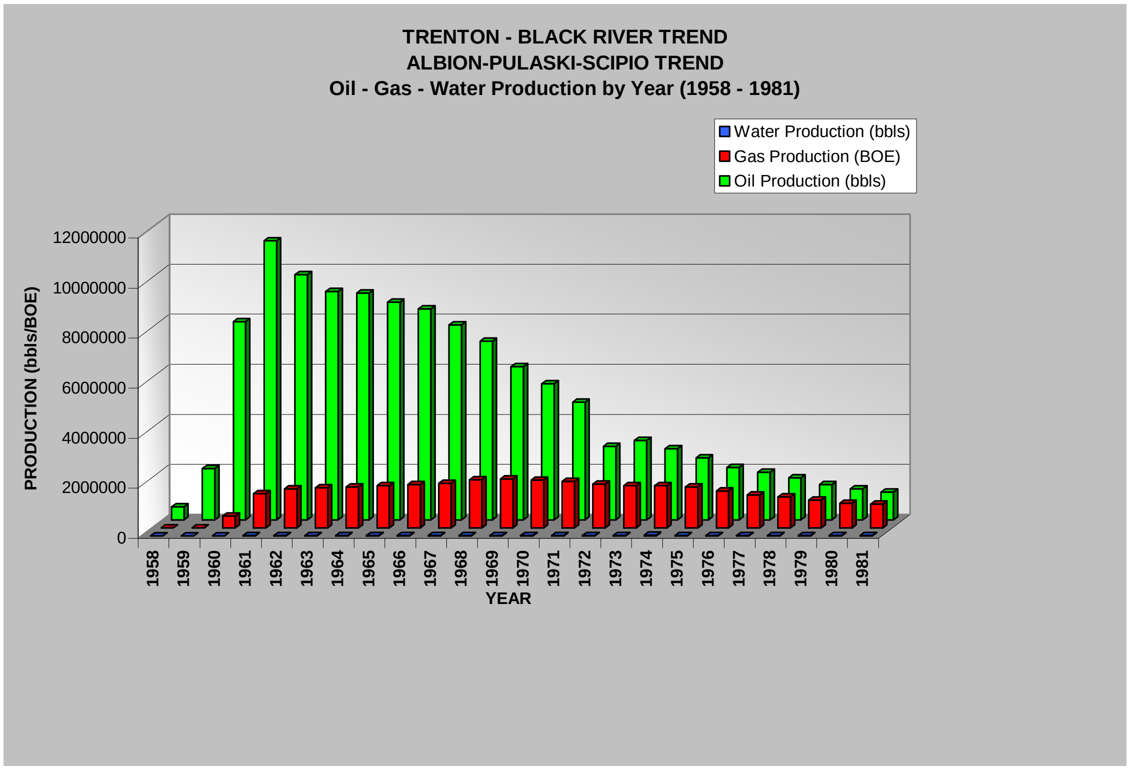
TRENTON - BLACK RIVER TREND
ALBION-PULASKI-SCIPIO TREND
Oil - Gas - Water Production by Year (1958 - 1981)
Water Production (bbls)
Gas Production (BOE)
Oil Production (bbls)
PRODUCTION (bbls/BOE)
12000000
10000000
8000000
6000000
4000000
2000000
0
1958
1959
1960
1961
1962
1963
1964
1965
1966
1967
1968
1969
1970
1971
1972
1973
1974
1975
1976
1977
1978
1979
1980
1981
YEAR

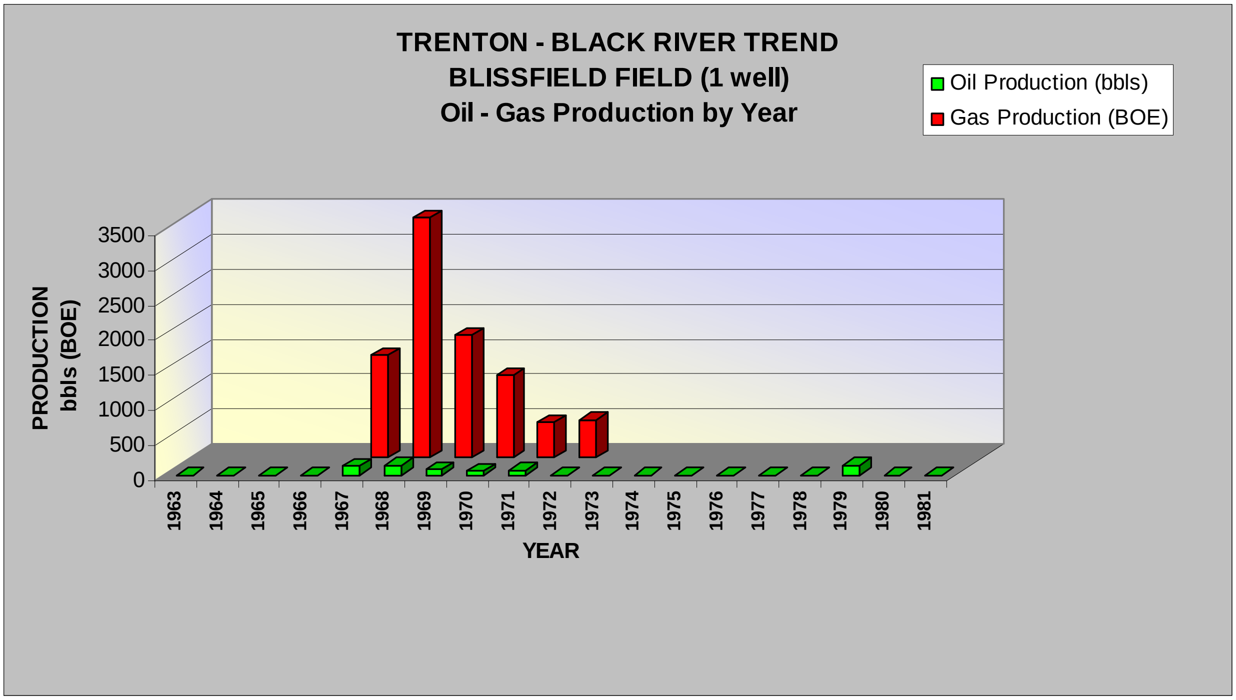

TRENTON - BLACK RIVER TREND
BLISSFIELD FIELD (1 well)
Oil - Gas Production by Year
Oil Production (bbls)
Gas Production (BOE)
PRODUCTION
bbls (BOE)
3500
3000
2500
2000
1500
1000
500
0
1963
1964
1965
1966
1967
1968
1969
1970
1971
1972
1973
1974
1975
1976
1977
1978
1979
1980
1981
YEAR

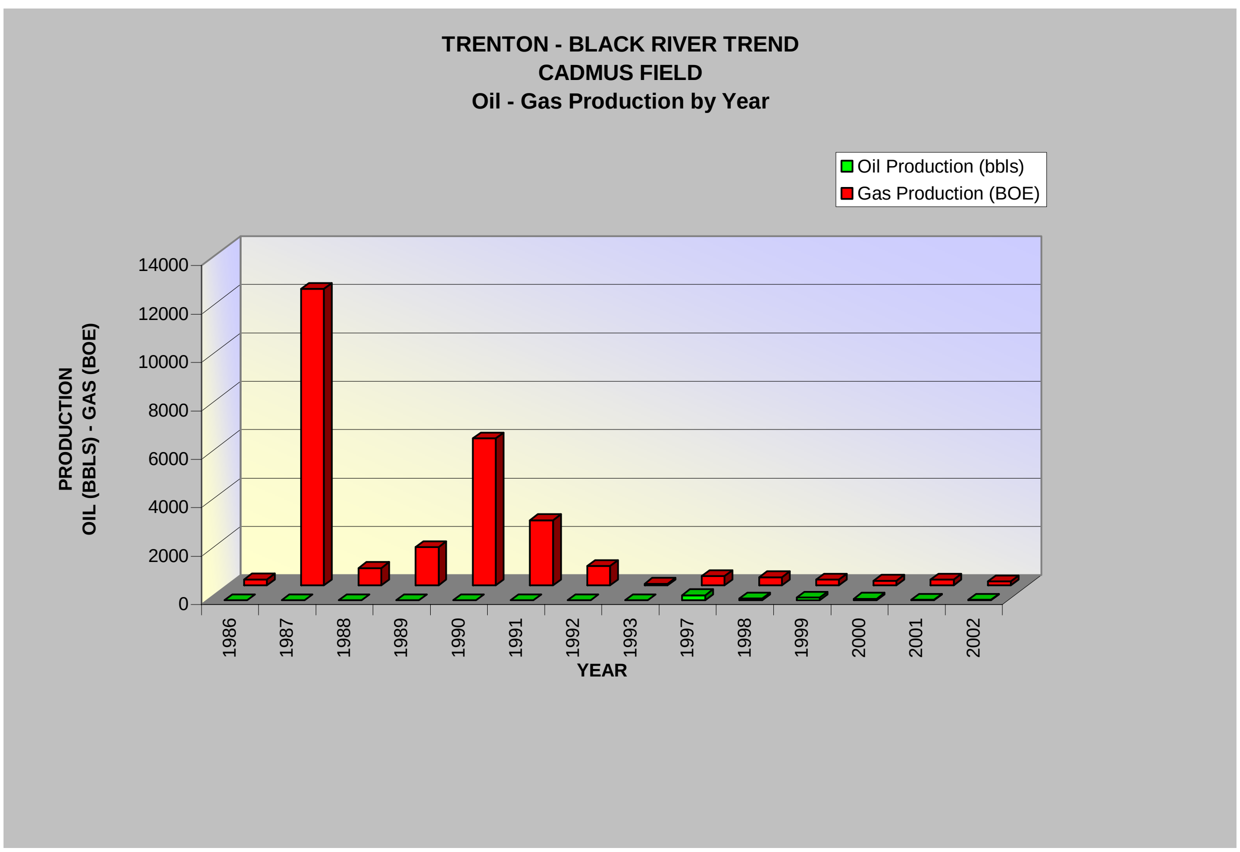

TRENTON - BLACK RIVER TREND
CADMUS FIELD
Oil - Gas Production by Year
Oil Production (bbls)
Gas Production (BOE)
PRODUCTION
OIL (BBLS) - GAS (BOE)
14000
12000
10000
8000
6000
4000
2000
0
1986
1987
1988
1989
1990
1991
1992
1993
1997
1998
1999
2000
2001
2002
YEAR

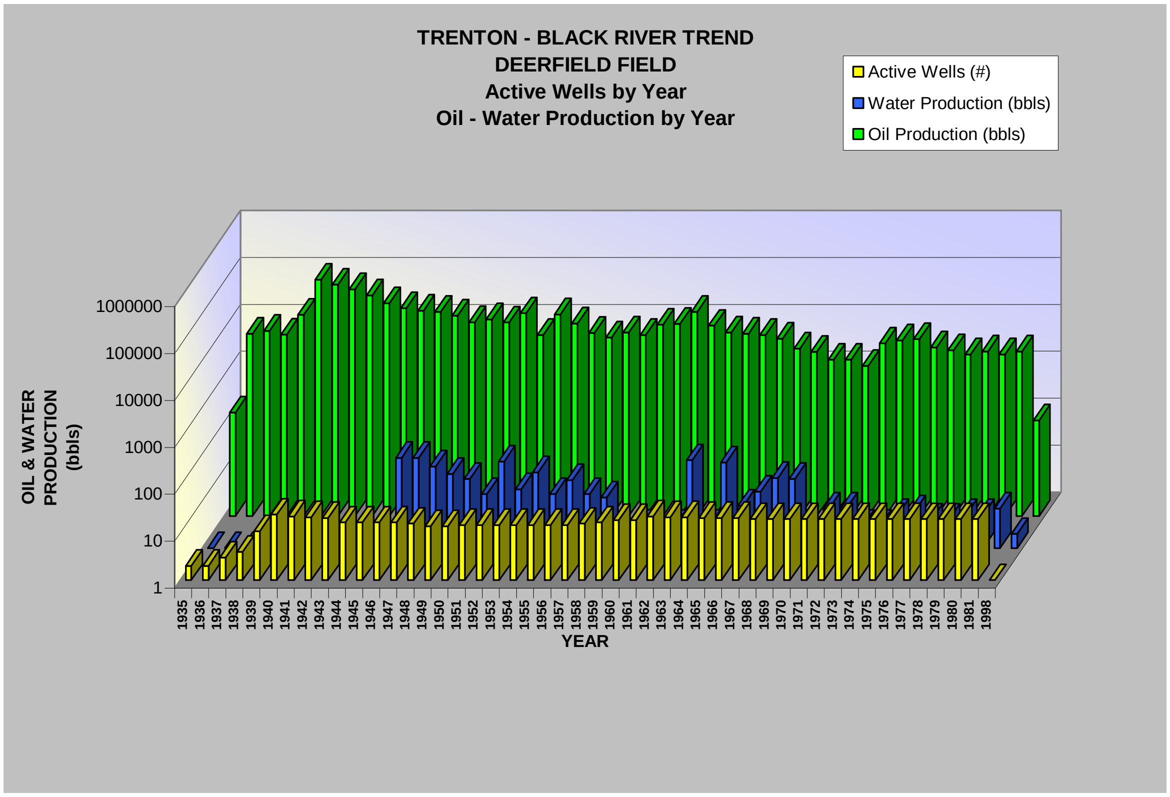
TRENTON - BLACK RIVER TREND
DEERFIELD FIELD
Active Wells by Year
Oil - Water Production by Year
Active Wells (#)
Water Production (bbls)
Oil Production (bbls)
OIL & WATER PRODUCTION (bbls)
1000000
100000
10000
1000
100
10
1
1935 1936 1937 1938 1939 1940 1941 1942 1943 1944 1945 1946 1947 1948 1949 1950 1951 1952 1953 1954 1955 1956 1957 1958 1959 1960 1961 1962 1963 1964 1965 1966 1967 1968 1969 1970 1971 1972 1973 1974 1975 1976 1977 1978 1979 1980 1981 1998
YEAR

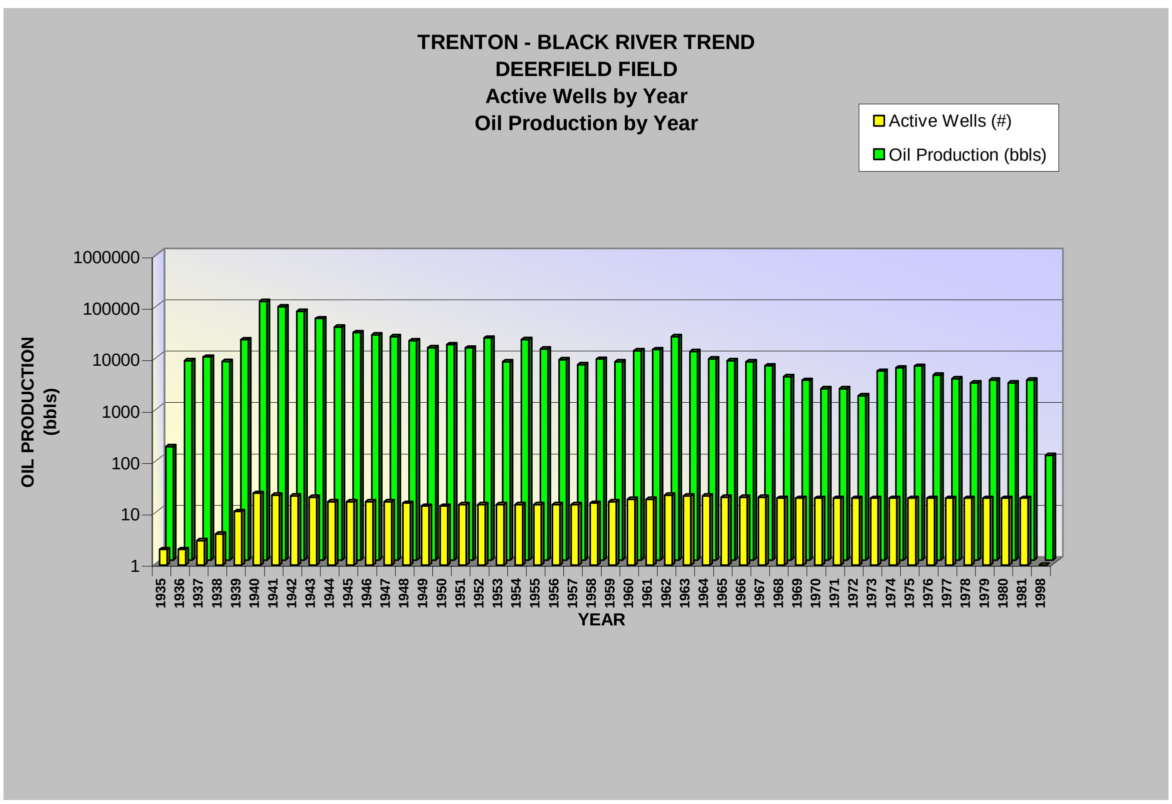
TRENTON - BLACK RIVER TREND
DEERFIELD FIELD
Active Wells by Year
Oil Production by Year
Active Wells (#)
Oil Production (bbls)
OIL PRODUCTION (bbls)
1000000
100000
10000
1000
100
10
1
1935 1936 1937 1938 1939 1940 1941 1942 1943 1944 1945 1946 1947 1948 1949 1950 1951 1952 1953 1954 1955 1956 1957 1958 1959 1960 1961 1962 1963 1964 1965 1966 1967 1968 1969 1970 1971 1972 1973 1974 1975 1976 1977 1978 1979 1980 1981 1998
YEAR

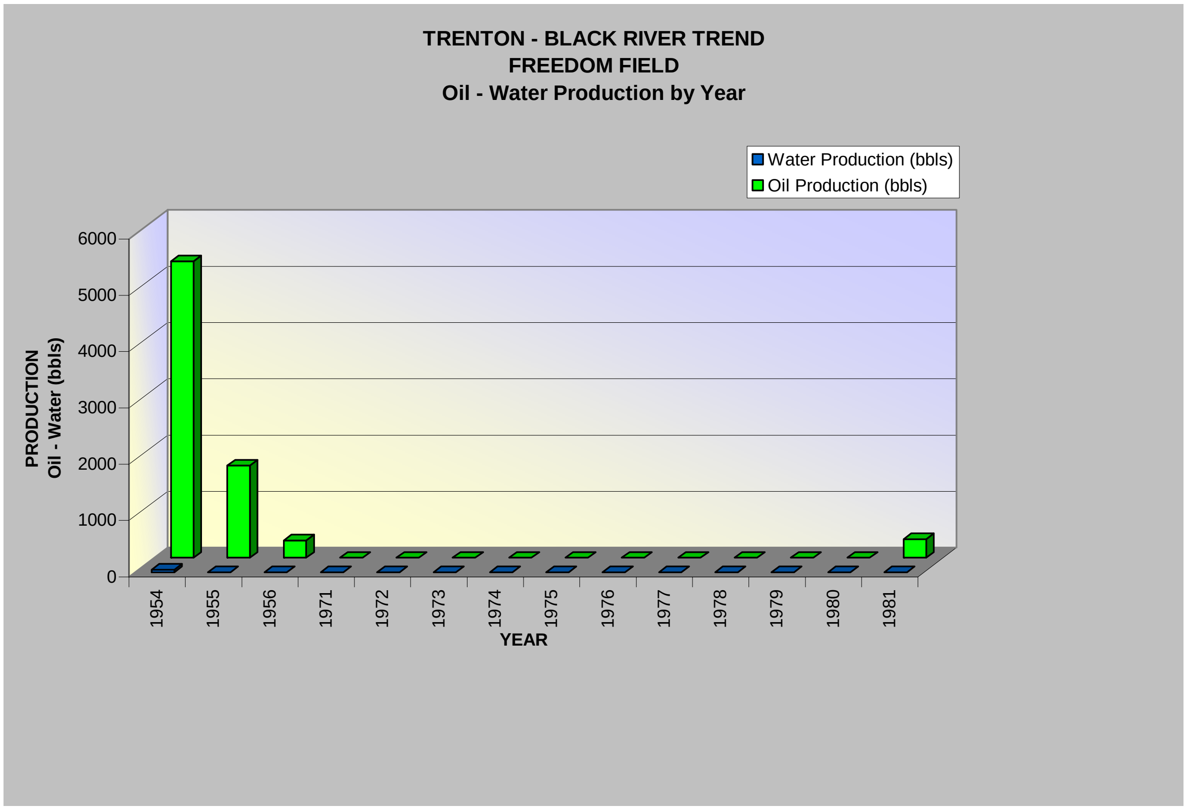
TRENTON - BLACK RIVER TREND
FREEDOM FIELD
Oil - Water Production by Year
Water Production (bbls)
Oil Production (bbls)
PRODUCTION
Oil - Water (bbls)
0
1000
2000
3000
4000
5000
6000
1954
1955
1956
1971
1972
1973
1974
1975
1976
1977
1978
1979
1980
1981
YEAR

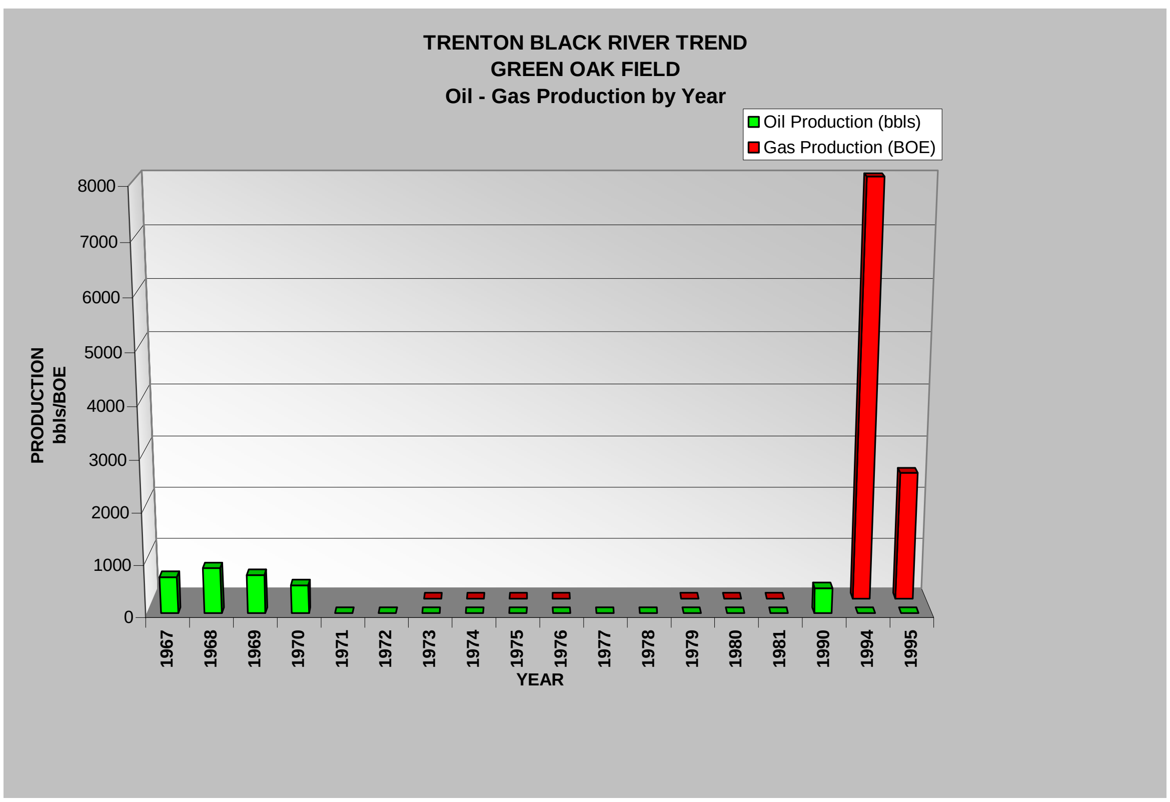
TRENTON BLACK RIVER TREND
GREEN OAK FIELD
Oil - Gas Production by Year
Oil Production (bbls)
Gas Production (BOE)
PRODUCTION
bbls/BOE
0
1000
2000
3000
4000
5000
6000
7000
8000
1967
1968
1969
1970
1971
1972
1973
1974
1975
1976
1977
1978
1979
1980
1981
1990
1994
1995
YEAR

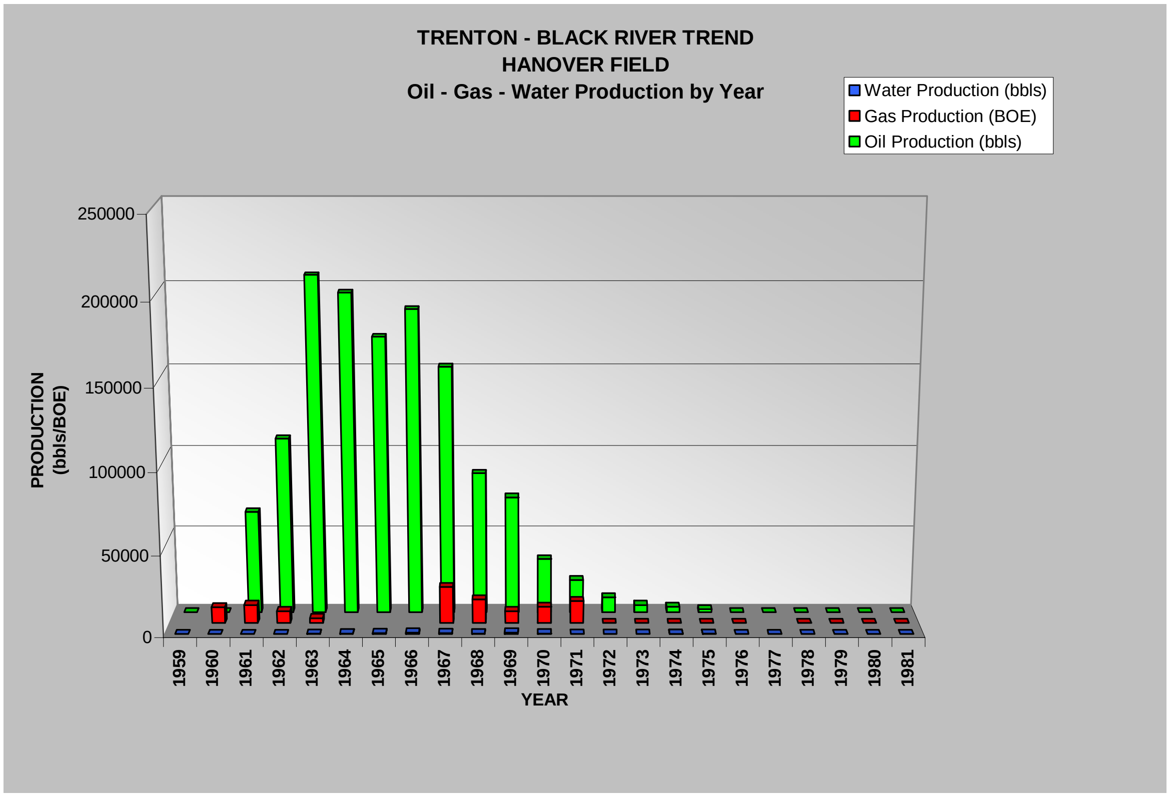
TRENTON - BLACK RIVER TREND
HANOVER FIELD
Oil - Gas - Water Production by Year
Water Production (bbls)
Gas Production (BOE)
Oil Production (bbls)
PRODUCTION
(bbls/BOE)
250000
200000
150000
100000
50000
0
1959
1960
1961
1962
1963
1964
1965
1966
1967
1968
1969
1970
1971
1972
1973
1974
1975
1976
1977
1978
1979
1980
1981
YEAR

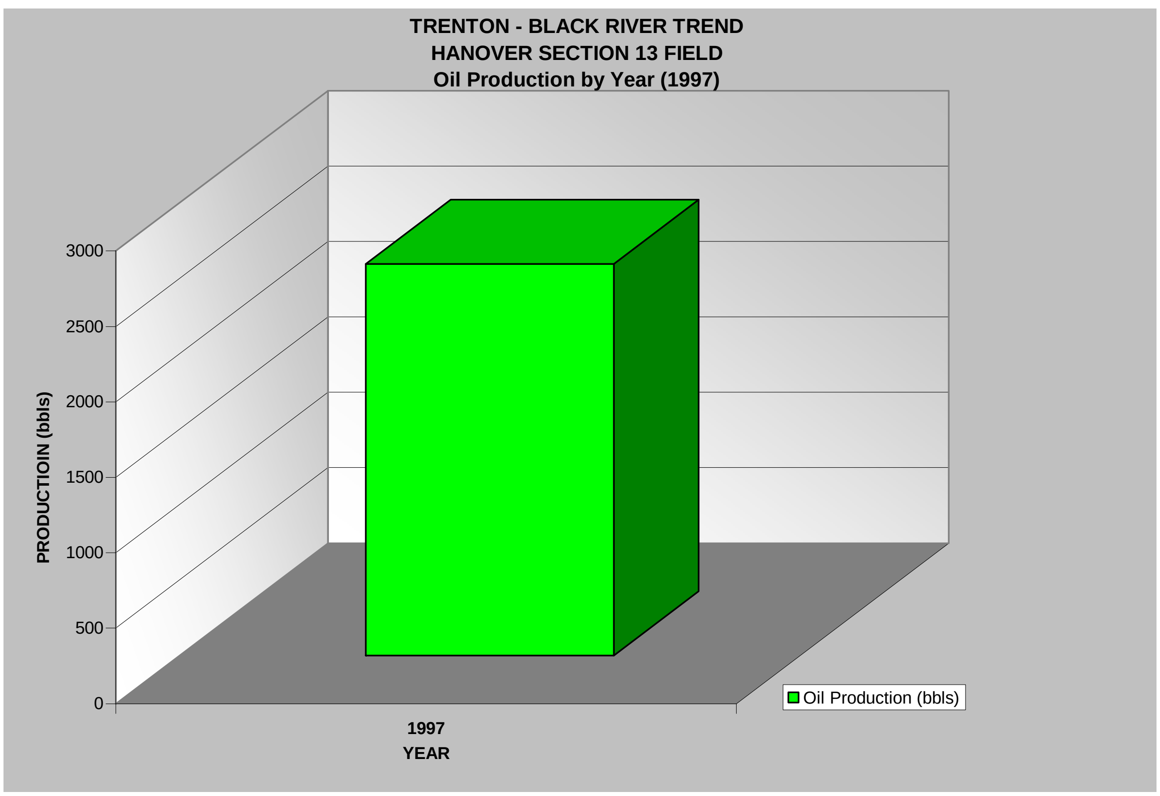
TRENTON - BLACK RIVER TREND
HANOVER SECTION 13 FIELD
Oil Production by Year (1997)
PRODUCTIOIN (bbls)
3000
2500
2000
1500
1000
500
0
1997
YEAR
Oil Production (bbls)

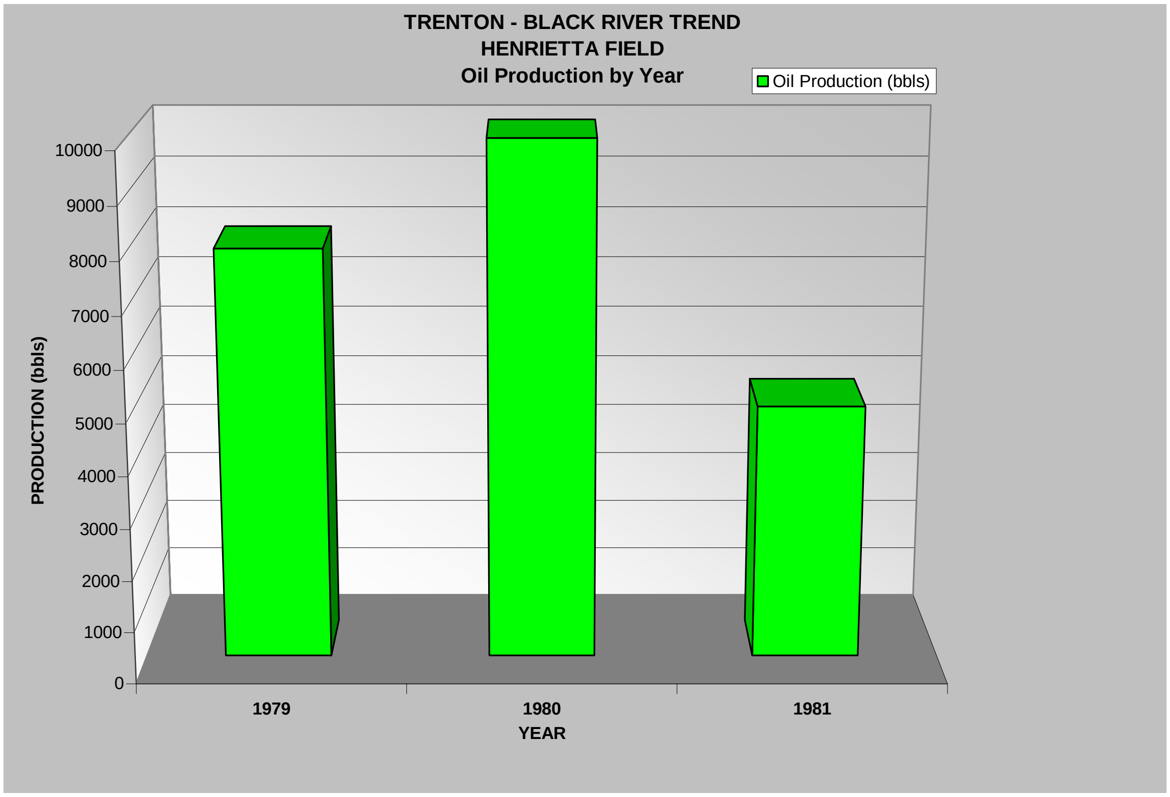
TRENTON - BLACK RIVER TREND
HENRIETTA FIELD
Oil Production by Year
Oil Production (bbls)
PRODUCTION (bbls)
10000
9000
8000
7000
6000
5000
4000
3000
2000
1000
0
1979
1980
1981
YEAR

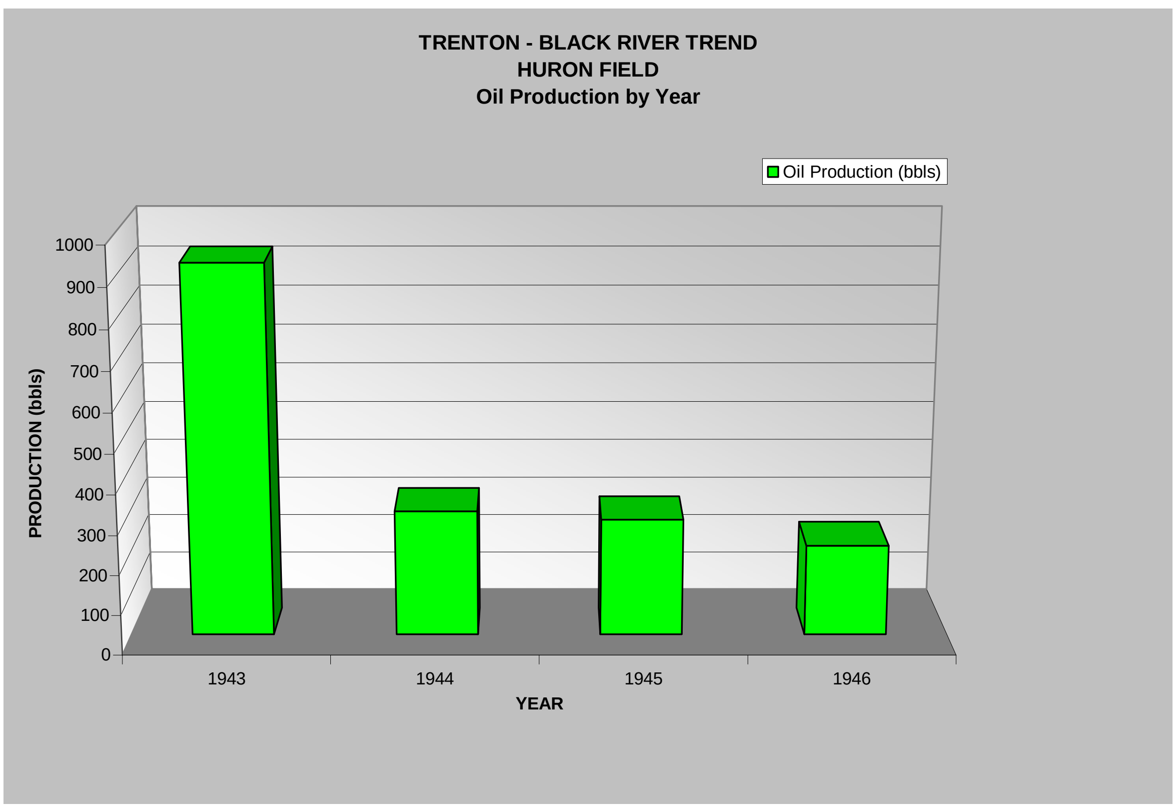
TRENTON - BLACK RIVER TREND
HURON FIELD
Oil Production by Year
Oil Production (bbls)
PRODUCTION (bbls)
1000
900
800
700
600
500
400
300
200
100
0
1943
1944
1945
1946
YEAR

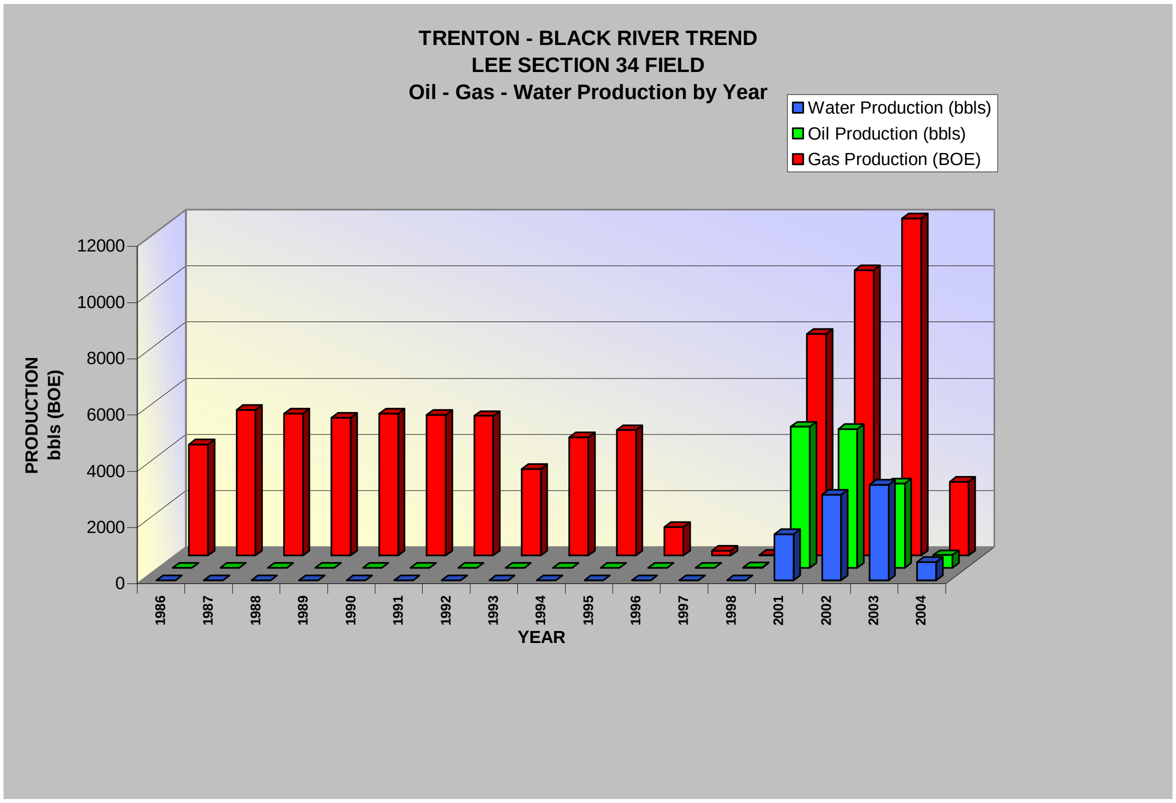
TRENTON - BLACK RIVER TREND
LEE SECTION 34 FIELD
Oil - Gas - Water Production by Year
Water Production (bbls)
Oil Production (bbls)
Gas Production (BOE)
PRODUCTION
bbls (BOE)
0
2000
4000
6000
8000
10000
12000
1986
1987
1988
1989
1990
1991
1992
1993
1994
1995
1996
1997
1998
2001
2002
2003
2004
YEAR

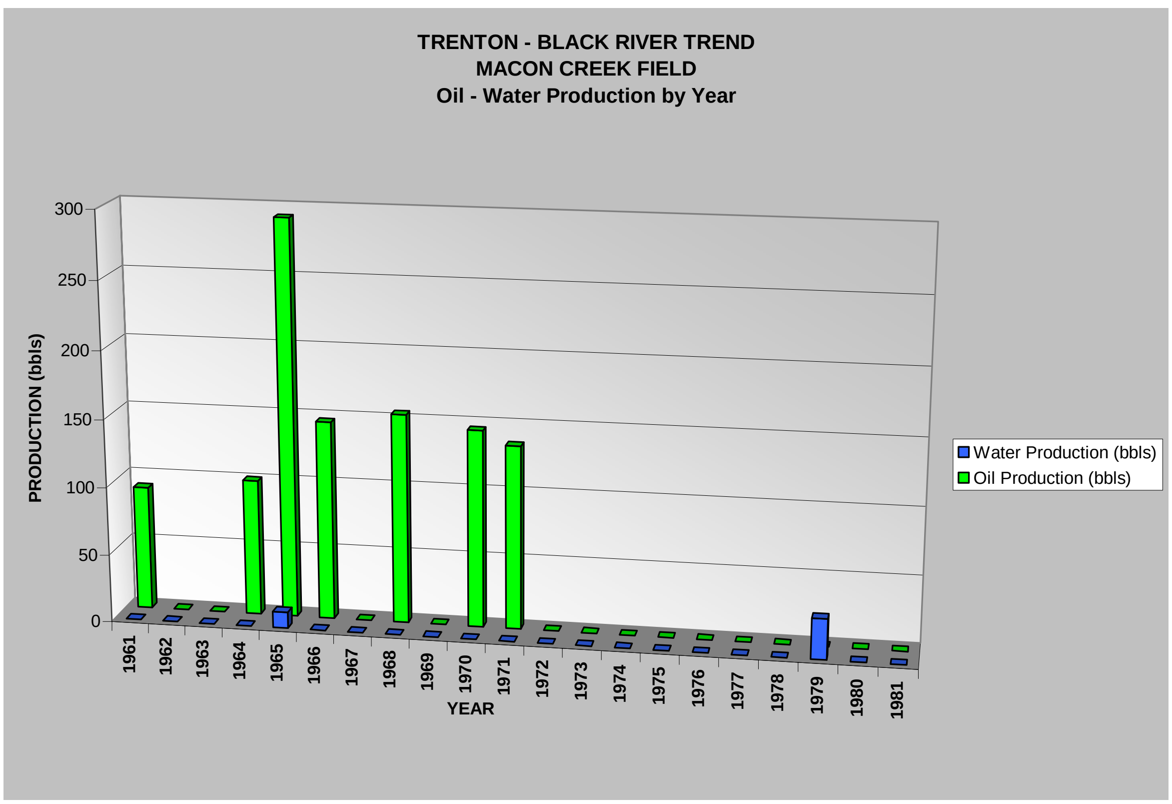
TRENTON - BLACK RIVER TREND
MACON CREEK FIELD
Oil - Water Production by Year
PRODUCTION (bbls)
0
50
100
150
200
250
300
1961
1962
1963
1964
1965
1966
1967
1968
1969
1970
1971
1972
1973
1974
1975
1976
1977
1978
1979
1980
1981
YEAR
Water Production (bbls)
Oil Production (bbls)

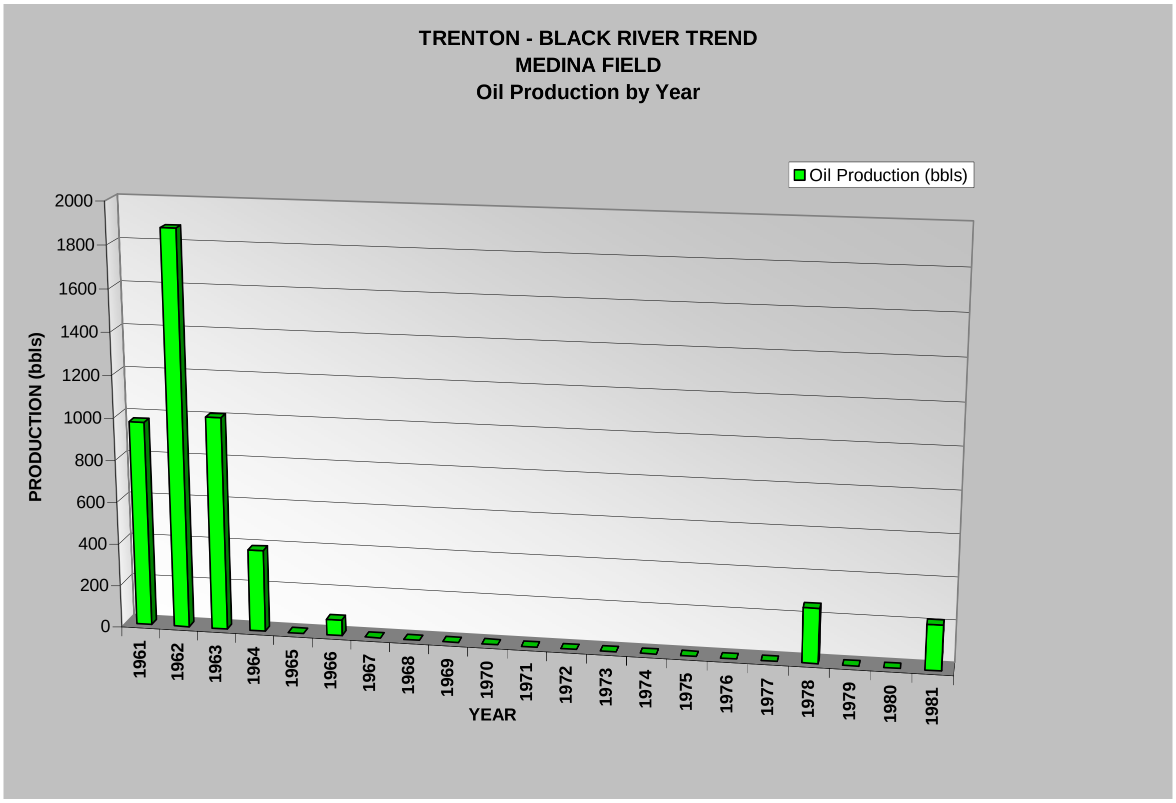
TRENTON - BLACK RIVER TREND
MEDINA FIELD
Oil Production by Year
Oil Production (bbls)
PRODUCTION (bbls)
2000
1800
1600
1400
1200
1000
800
600
400
200
0
1961
1962
1963
1964
1965
1966
1967
1968
1969
1970
1971
1972
1973
1974
1975
1976
1977
1978
1979
1980
1981
YEAR

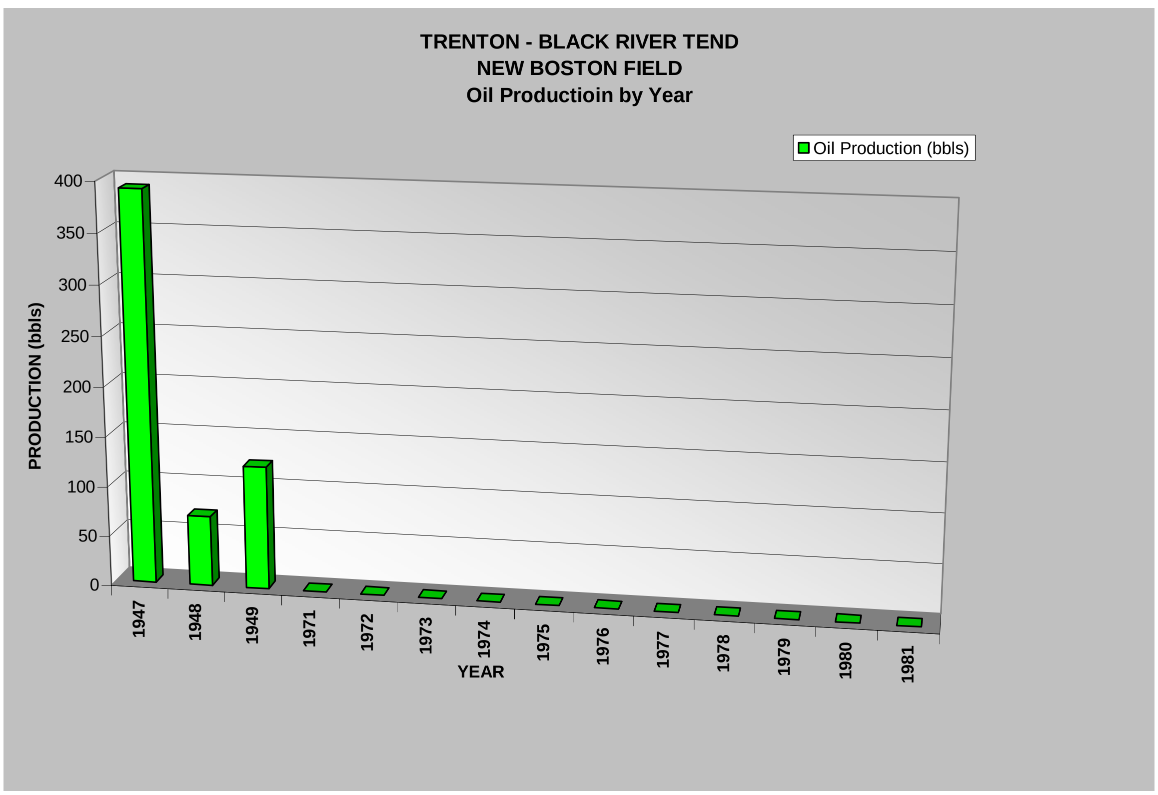
TRENTON - BLACK RIVER TEND
NEW BOSTON FIELD
Oil Productioin by Year
Oil Production (bbls)
PRODUCTION (bbls)
400
350
300
250
200
150
100
50
0
1947
1948
1949
1971
1972
1973
1974
1975
1976
1977
1978
1979
1980
1981
YEAR

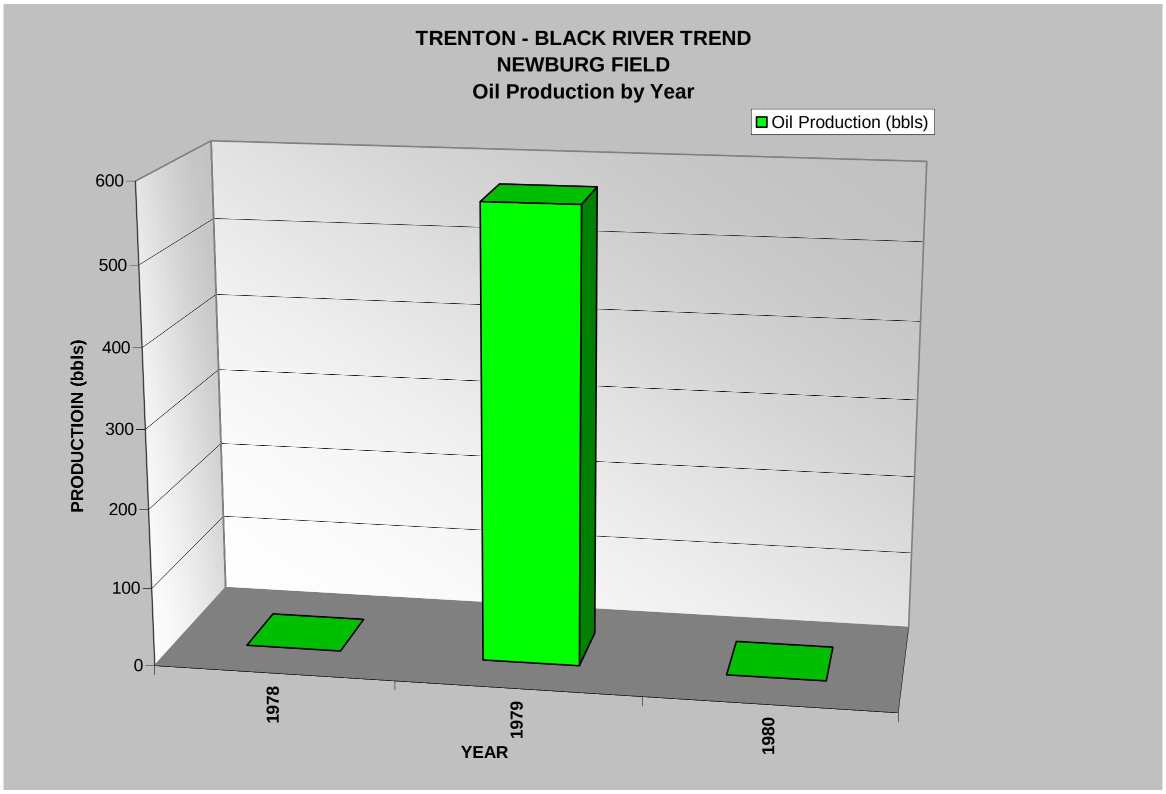
TRENTON - BLACK RIVER TREND
NEWBURG FIELD
Oil Production by Year
Oil Production (bbls)
PRODUCTIOIN (bbls)
0
100
200
300
400
500
600
1978
1979
1980
YEAR

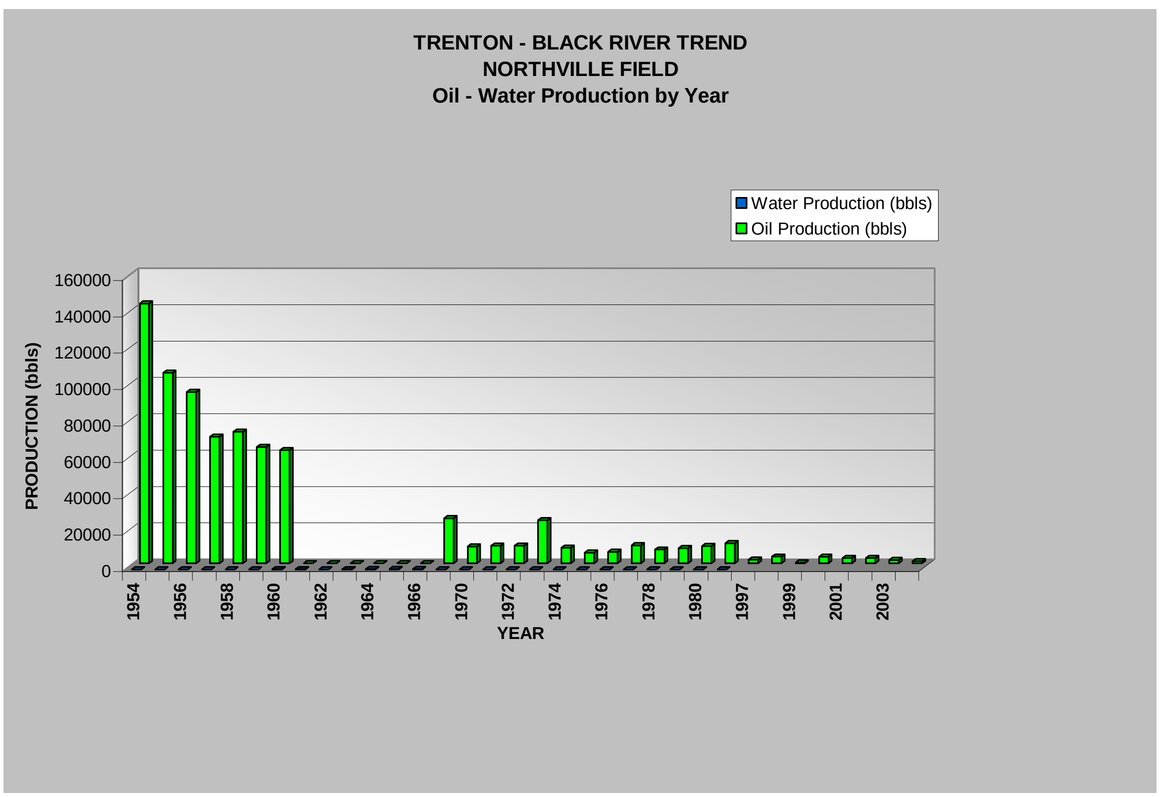
TRENTON - BLACK RIVER TREND
NORTHVILLE FIELD
Oil - Water Production by Year
Water Production (bbls)
Oil Production (bbls)
PRODUCTION (bbls)
0
20000
40000
60000
80000
100000
120000
140000
160000
1954
1956
1958
1960
1962
1964
1966
1970
1972
1974
1976
1978
1980
1997
1999
2001
2003
YEAR

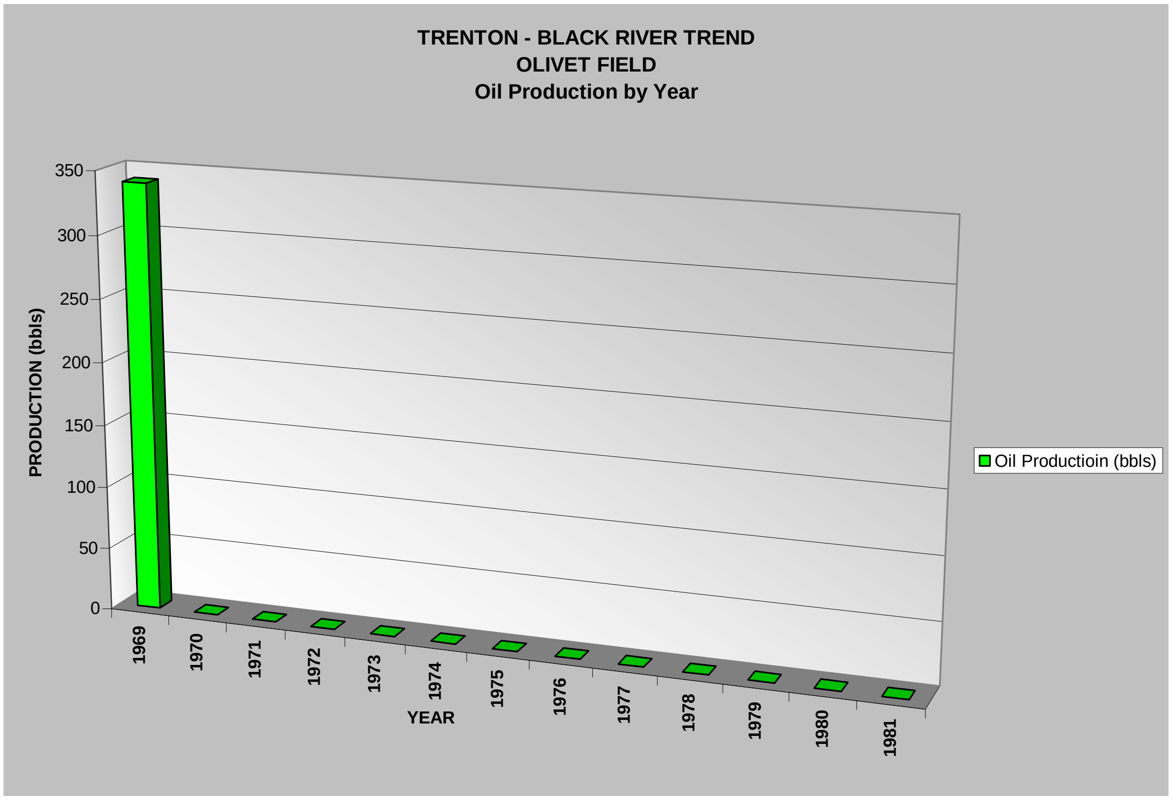
TRENTON - BLACK RIVER TREND
OLIVET FIELD
Oil Production by Year
PRODUCTION (bbls)
350
300
250
200
150
100
50
0
1969
1970
1971
1972
1973
1974
1975
1976
1977
1978
1979
1980
1981
YEAR
Oil Productioin (bbls)

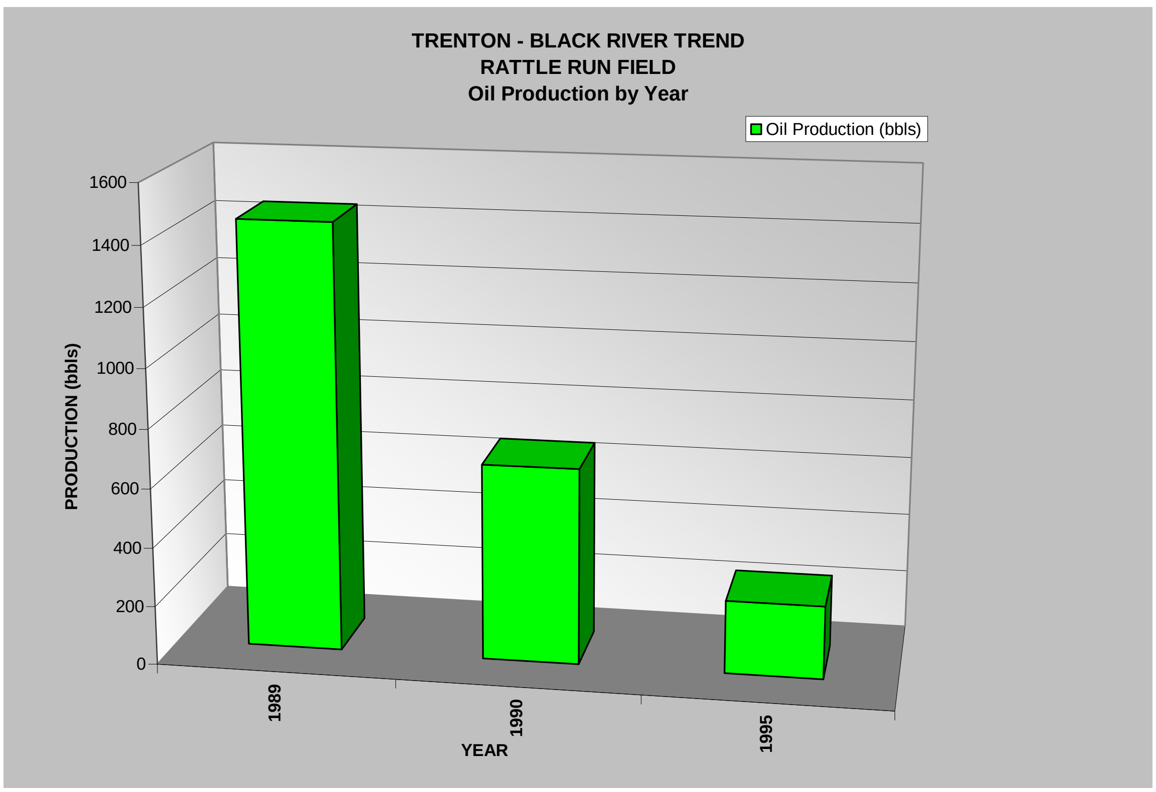
TRENTON - BLACK RIVER TREND
RATTLE RUN FIELD
Oil Production by Year
Oil Production (bbls)
PRODUCTION (bbls)
1600
1400
1200
1000
800
600
400
200
0
1989
1990
1995
YEAR

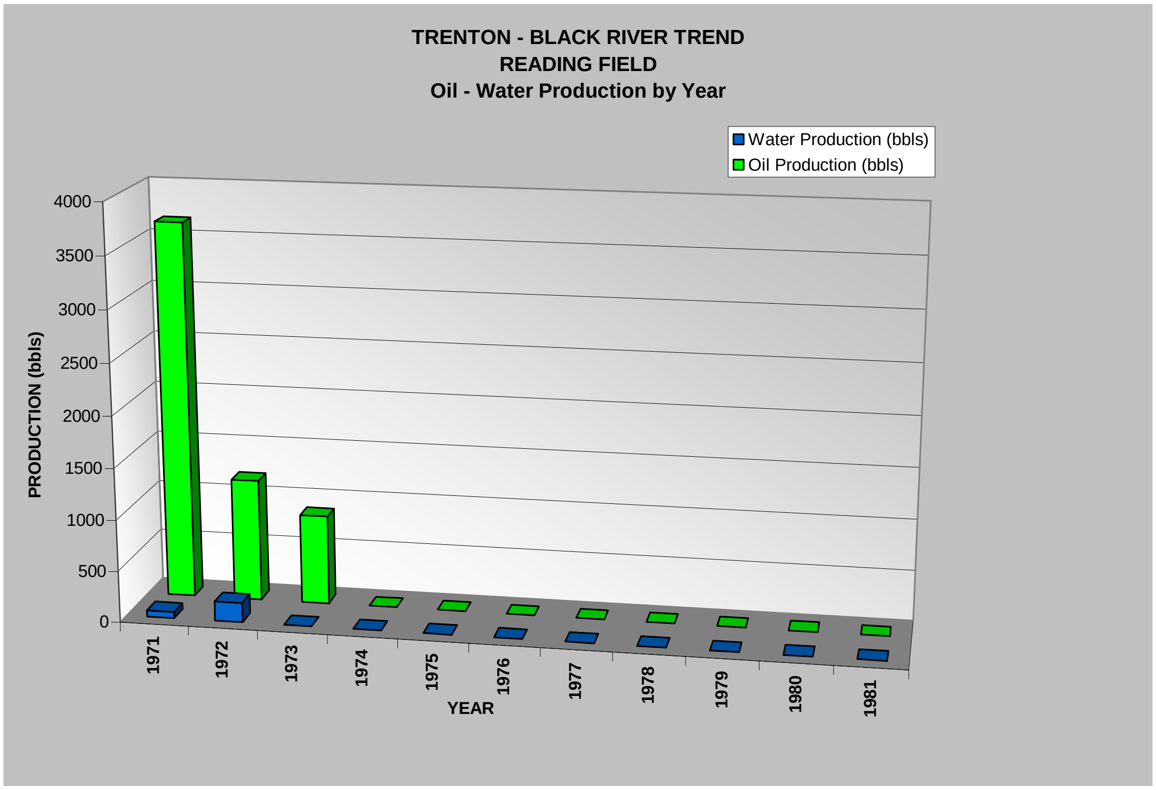
TRENTON - BLACK RIVER TREND
READING FIELD
Oil - Water Production by Year
Water Production (bbls)
Oil Production (bbls)
PRODUCTION (bbls)
4000
3500
3000
2500
2000
1500
1000
500
0
1971
1972
1973
1974
1975
1976
1977
1978
1979
1980
1981
YEAR

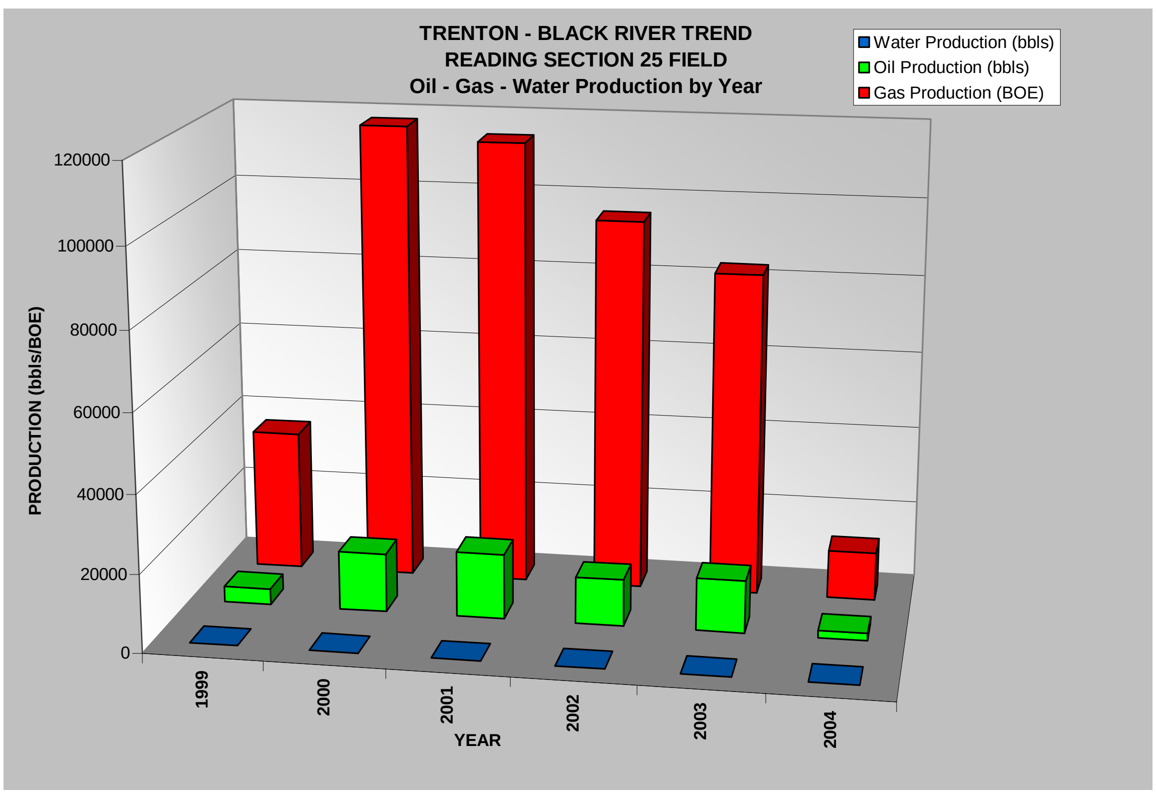
TRENTON - BLACK RIVER TREND
READING SECTION 25 FIELD
Oil - Gas - Water Production by Year
Water Production (bbls)
Oil Production (bbls)
Gas Production (BOE)
PRODUCTION (bbls/BOE)
120000
100000
80000
60000
40000
20000
0
1999
2000
2001
2002
2003
2004
YEAR

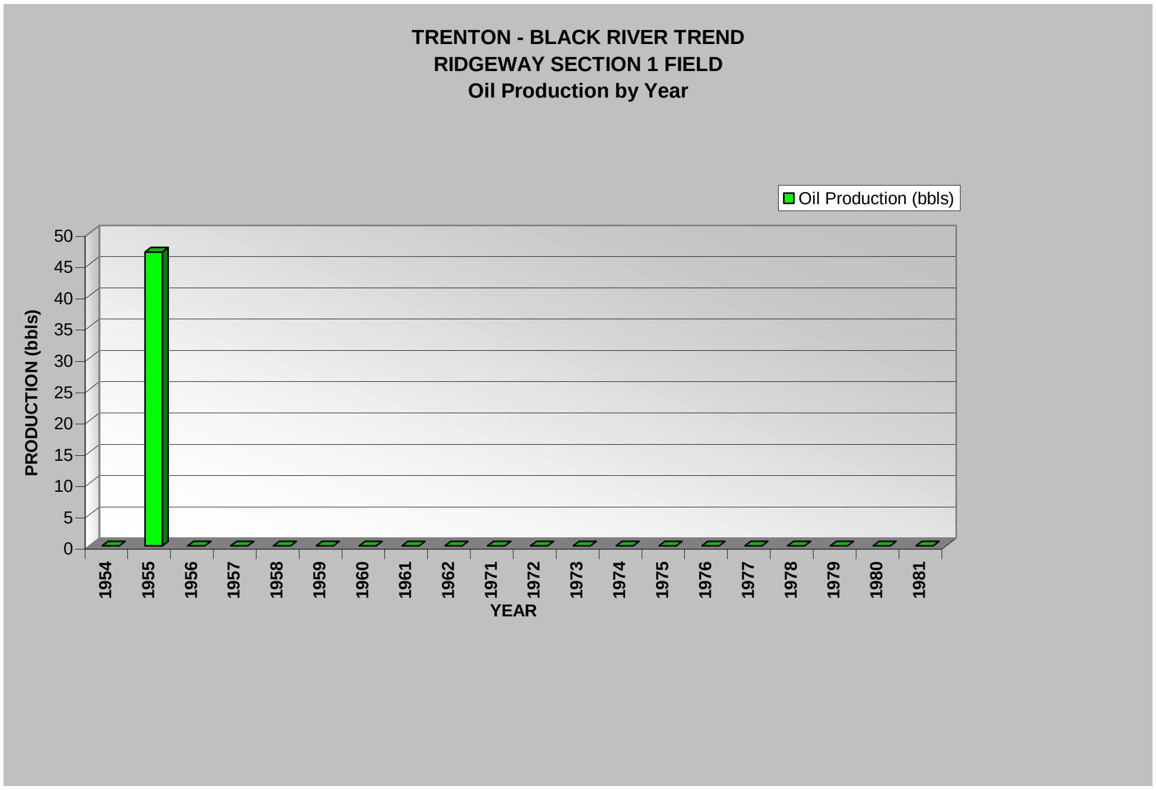
TRENTON - BLACK RIVER TREND
RIDGEWAY SECTION 1 FIELD
Oil Production by Year
Oil Production (bbls)
PRODUCTION (bbls)
0
5
10
15
20
25
30
35
40
45
50
1954
1955
1956
1957
1958
1959
1960
1961
1962
1971
1972
1973
1974
1975
1976
1977
1978
1979
1980
1981
YEAR

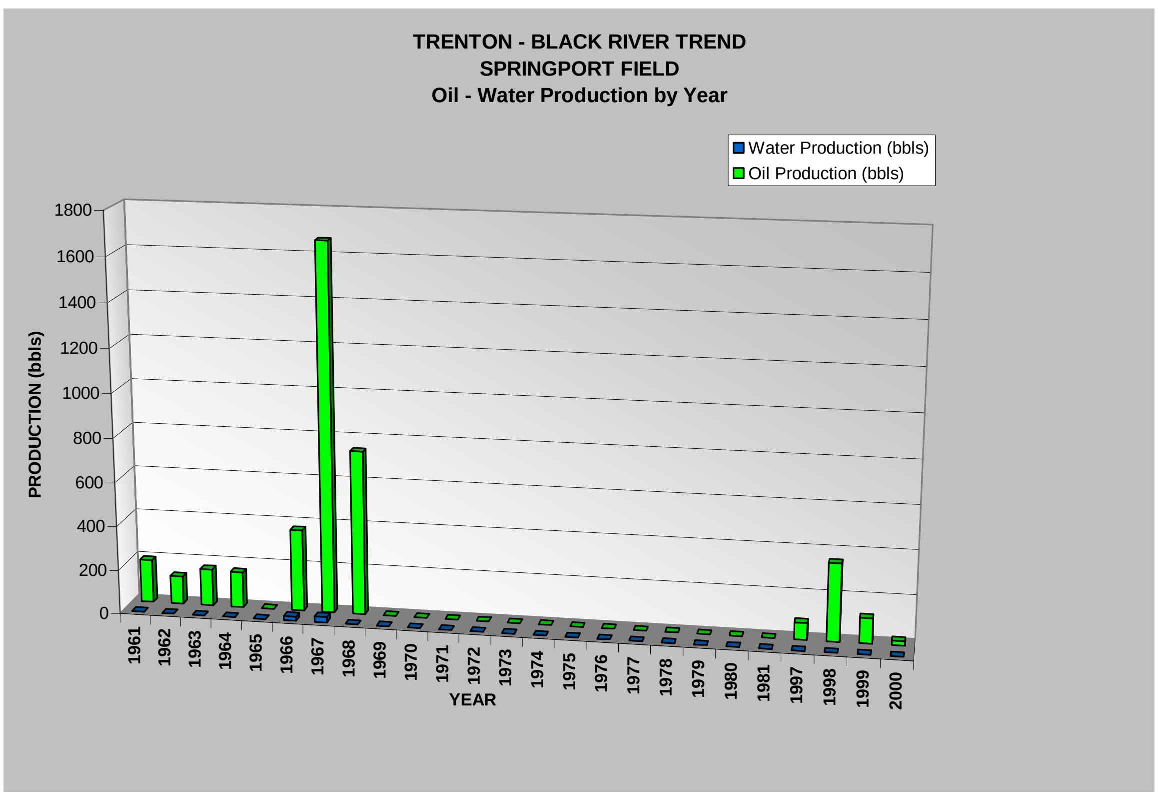
TRENTON - BLACK RIVER TREND
SPRINGPORT FIELD
Oil - Water Production by Year
Water Production (bbls)
Oil Production (bbls)
PRODUCTION (bbls)
0
200
400
600
800
1000
1200
1400
1600
1800
1961
1962
1963
1964
1965
1966
1967
1968
1969
1970
1971
1972
1973
1974
1975
1976
1977
1978
1979
1980
1981
1997
1998
1999
2000
YEAR

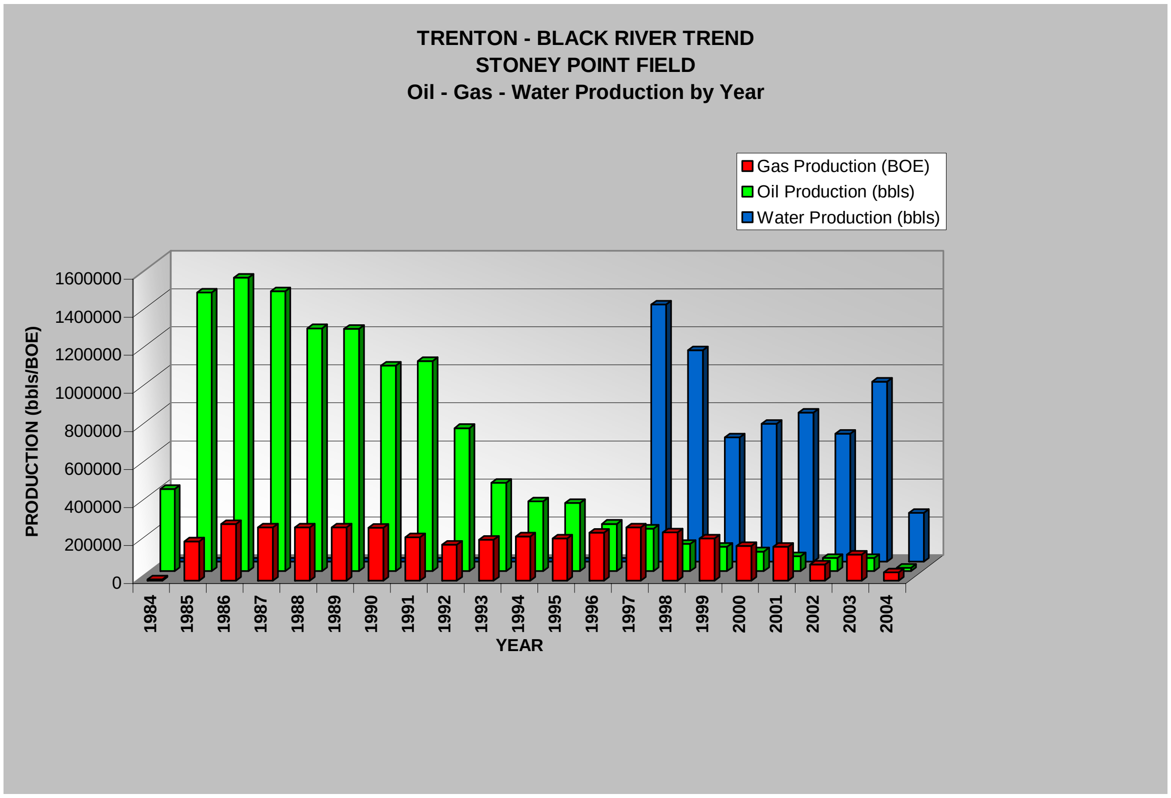
TRENTON - BLACK RIVER TREND
STONEY POINT FIELD
Oil - Gas - Water Production by Year
Gas Production (BOE)
Oil Production (bbls)
Water Production (bbls)
PRODUCTION (bbls/BOE)
1600000
1400000
1200000
1000000
800000
600000
400000
200000
0
1984
1985
1986
1987
1988
1989
1990
1991
1992
1993
1994
1995
1996
1997
1998
1999
2000
2001
2002
2003
2004
YEAR

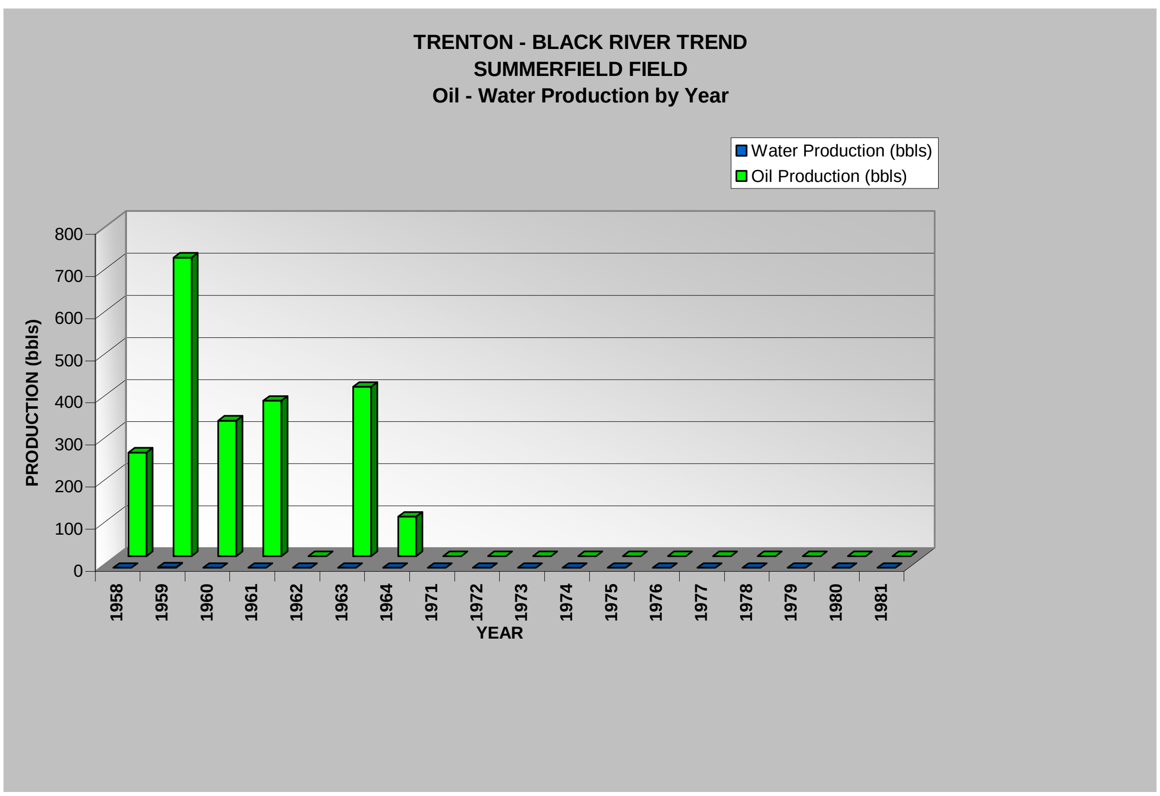
TRENTON - BLACK RIVER TREND
SUMMERFIELD FIELD
Oil - Water Production by Year
Water Production (bbls)
Oil Production (bbls)
PRODUCTION (bbls)
800
700
600
500
400
300
200
100
0
1958
1959
1960
1961
1962
1963
1964
1971
1972
1973
1974
1975
1976
1977
1978
1979
1980
1981
YEAR

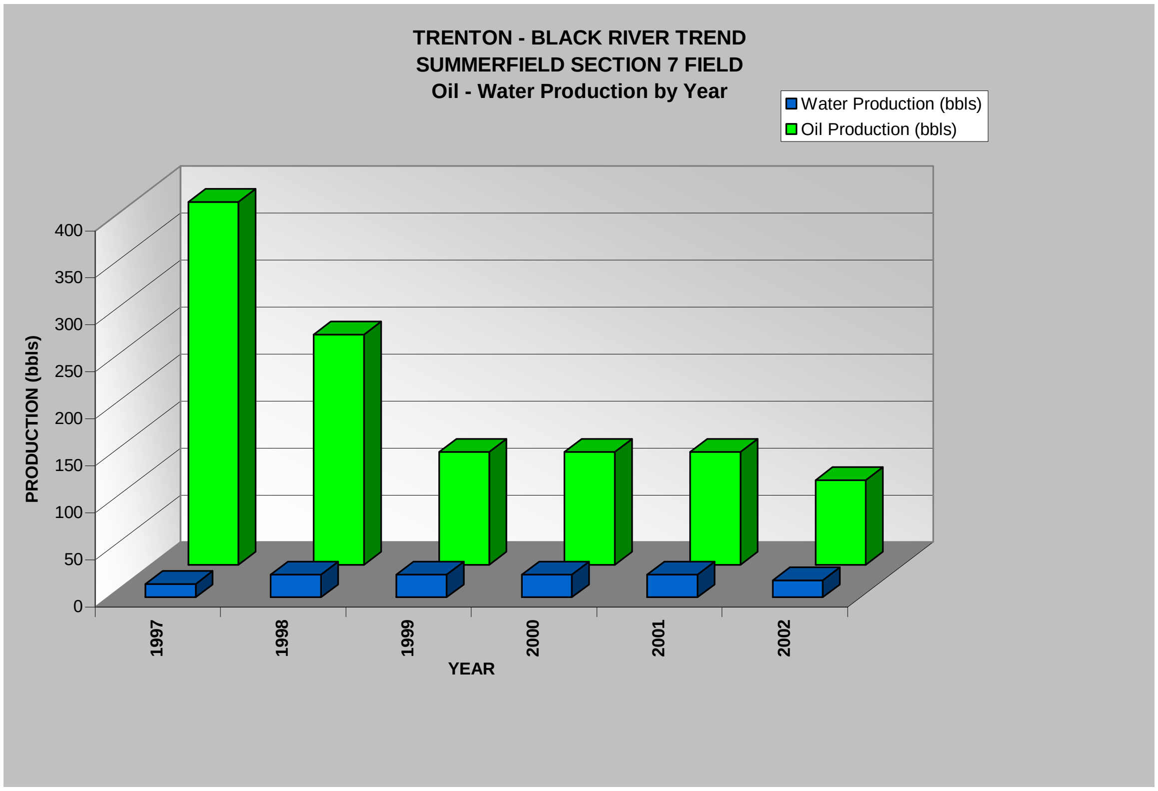
TRENTON - BLACK RIVER TREND
SUMMERFIELD SECTION 7 FIELD
Oil - Water Production by Year
Water Production (bbls)
Oil Production (bbls)
PRODUCTION (bbls)
0
50
100
150
200
250
300
350
400
1997
1998
1999
2000
2001
2002
YEAR

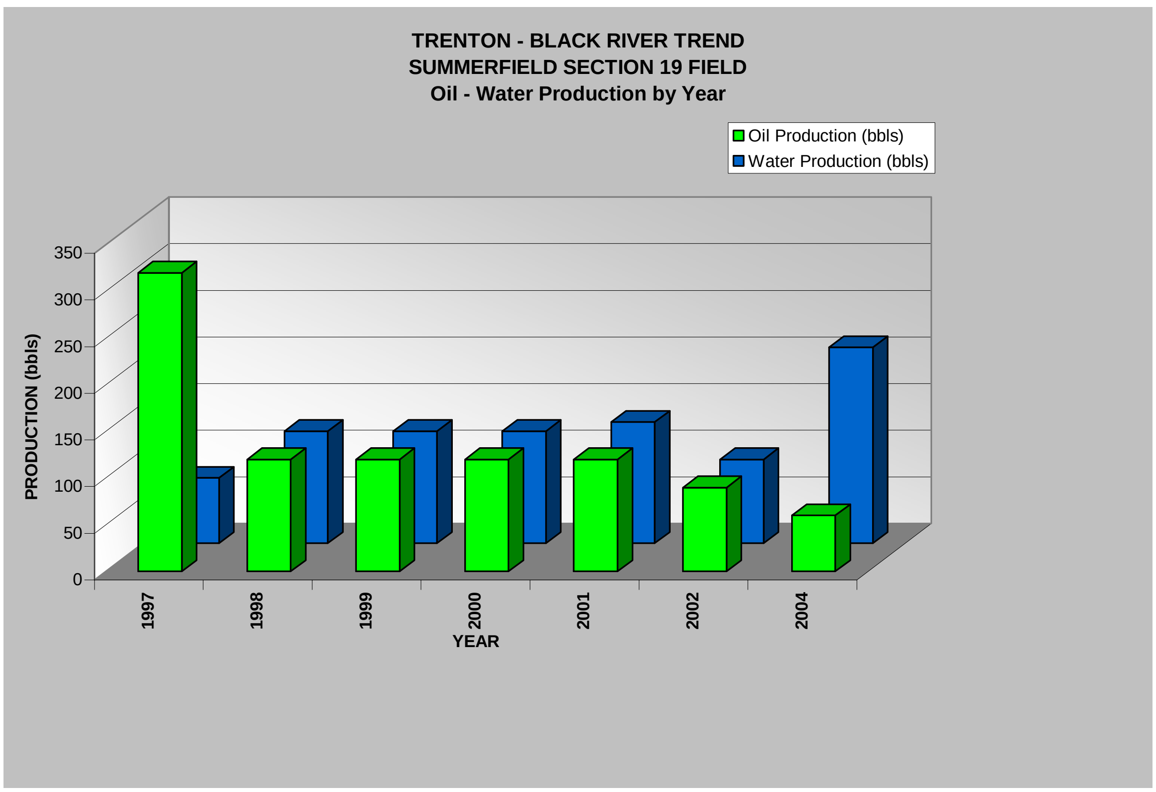
TRENTON - BLACK RIVER TREND
SUMMERFIELD SECTION 19 FIELD
Oil - Water Production by Year
Oil Production (bbls)
Water Production (bbls)
PRODUCTION (bbls)
0
50
100
150
200
250
300
350
1997
1998
1999
2000
2001
2002
2004
YEAR

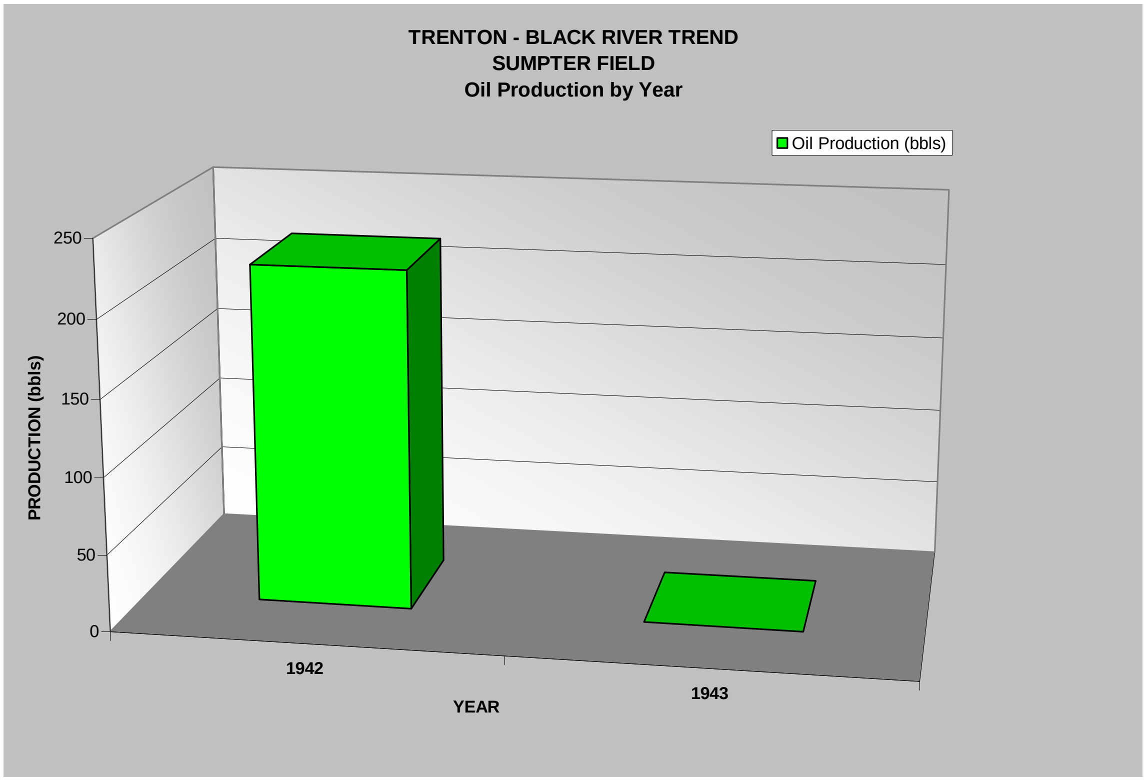

TRENTON - BLACK RIVER TREND
SUMPTER FIELD
Oil Production by Year
Oil Production (bbls)
PRODUCTION (bbls)
250
200
150
100
50
0
1942
1943
YEAR

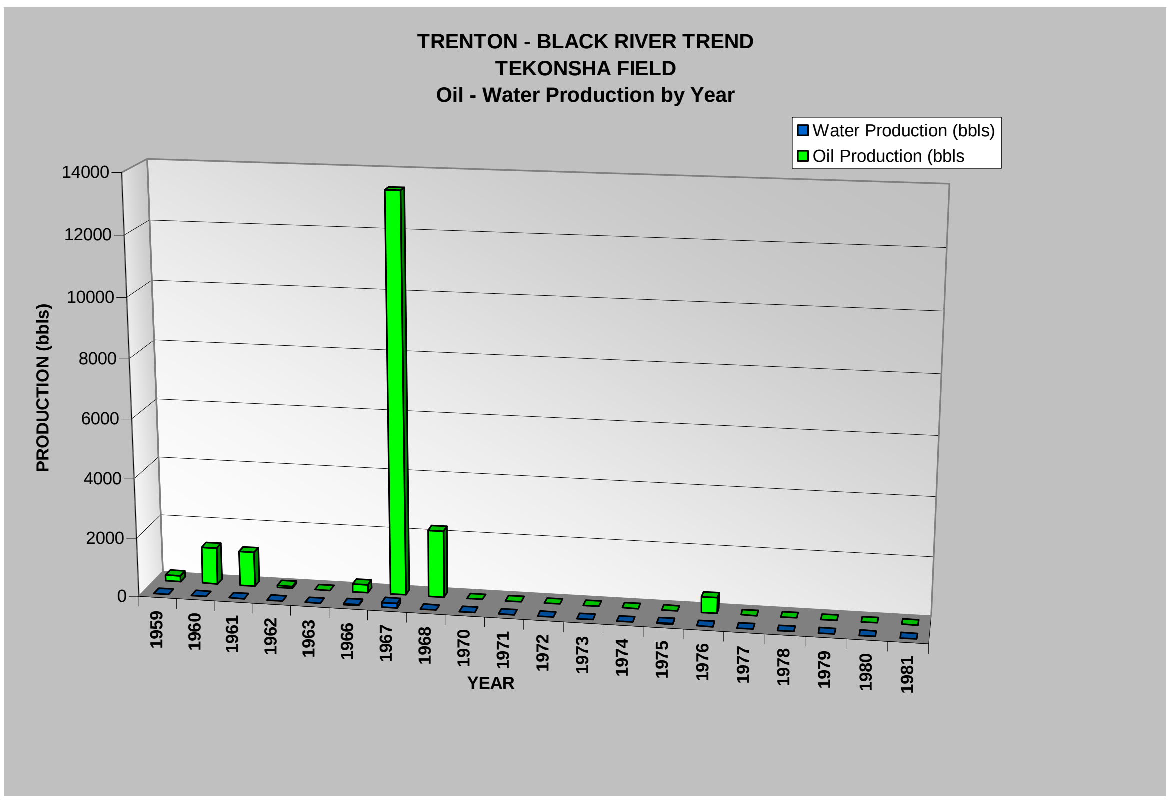

TRENTON - BLACK RIVER TREND
TEKONSHA FIELD
Oil - Water Production by Year
Water Production (bbls)
Oil Production (bbls
PRODUCTION (bbls)
14000
12000
10000
8000
6000
4000
2000
0
1959
1960
1961
1962
1963
1966
1967
1968
1970
1971
1972
1973
1974
1975
1976
1977
1978
1979
1980
1981
YEAR

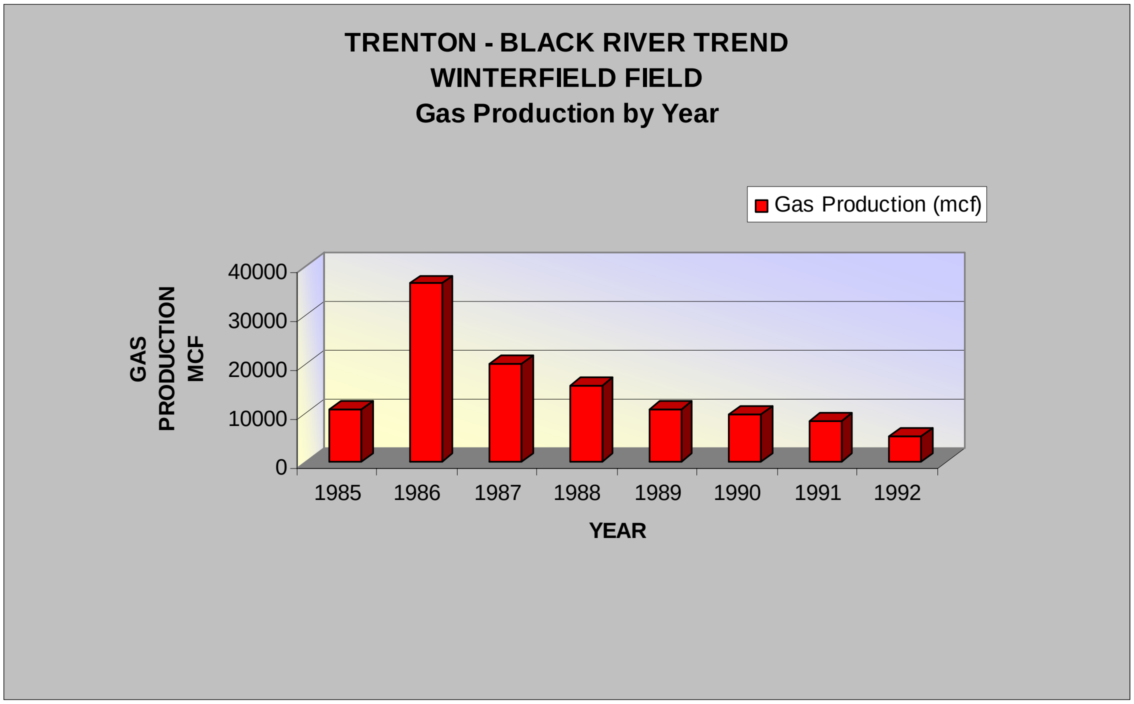

TRENTON - BLACK RIVER TREND
WINTERFIELD FIELD
Gas Production by Year
Gas Production (mcf)
GAS PRODUCTION MCF
40000
30000
20000
10000
0
1985
1986
1987
1988
1989
1990
1991
1992
YEAR

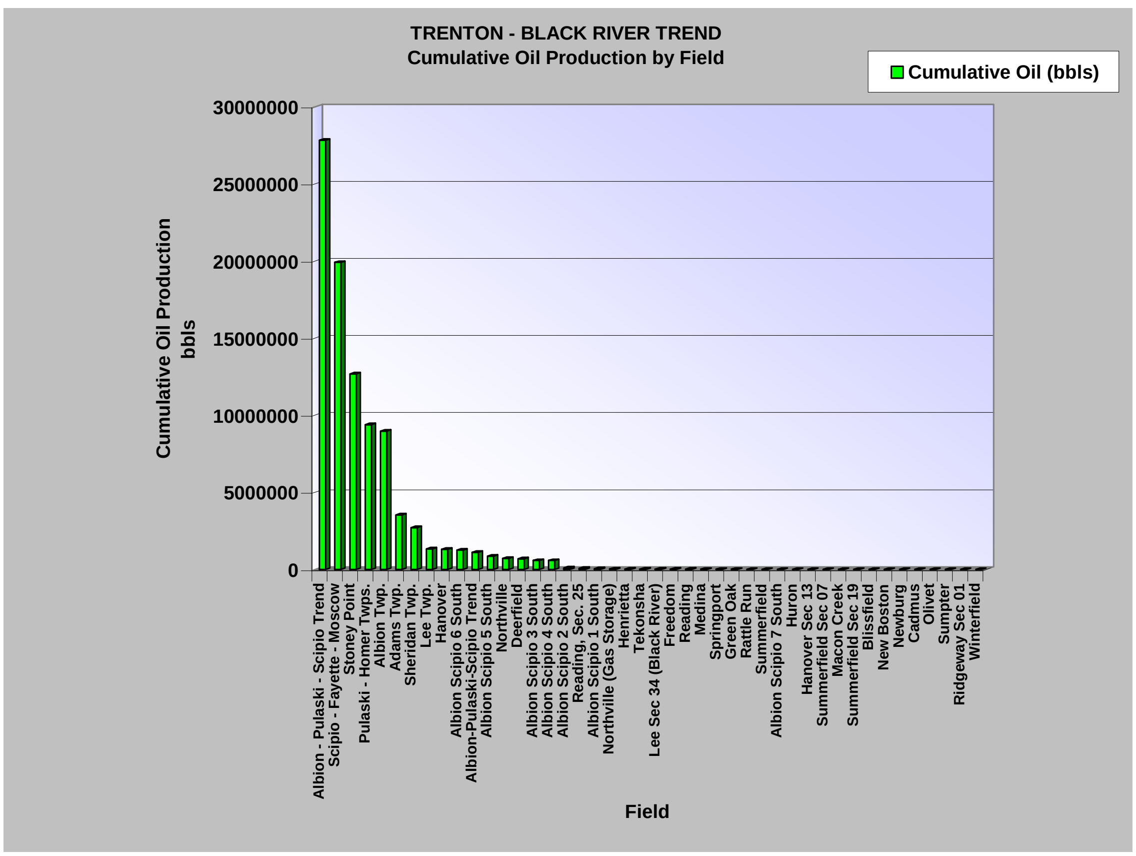

TRENTON - BLACK RIVER TREND
Cumulative Oil Production by Field
Cumulative Oil (bbls)
Cumulative Oil Production bbls
30000000
25000000
20000000
15000000
10000000
5000000
0
Albion - Pulaski - Scipio Trend
Scipio - Fayette - Moscow
Stoney Point
Pulaski - Homer Twps.
Albion Twp.
Adams Twp.
Sheridan Twp.
Lee Twp.
Hanover
Albion Scipio 6 South
Albion-Pulaski-Scipio Trend
Albion Scipio 5 South
Northville
Deerfield
Albion Scipio 3 South
Albion Scipio 4 South
Albion Scipio 2 South
Reading, Sec. 25
Albion Scipio 1 South
Northville (Gas Storage)
Henrietta
Tekonsha
Lee Sec 34 (Black River)
Freedom
Reading
Medina
Springport
Green Oak
Rattle Run
Summerfield
Albion Scipio 7 South
Huron
Hanover Sec 13
Summerfield Sec 07
Macon Creek
Summerfield Sec 19
Blissfield
New Boston
Newburg
Cadmus
Olivet
Sumpter
Ridgeway Sec 01
Winterfield
Field

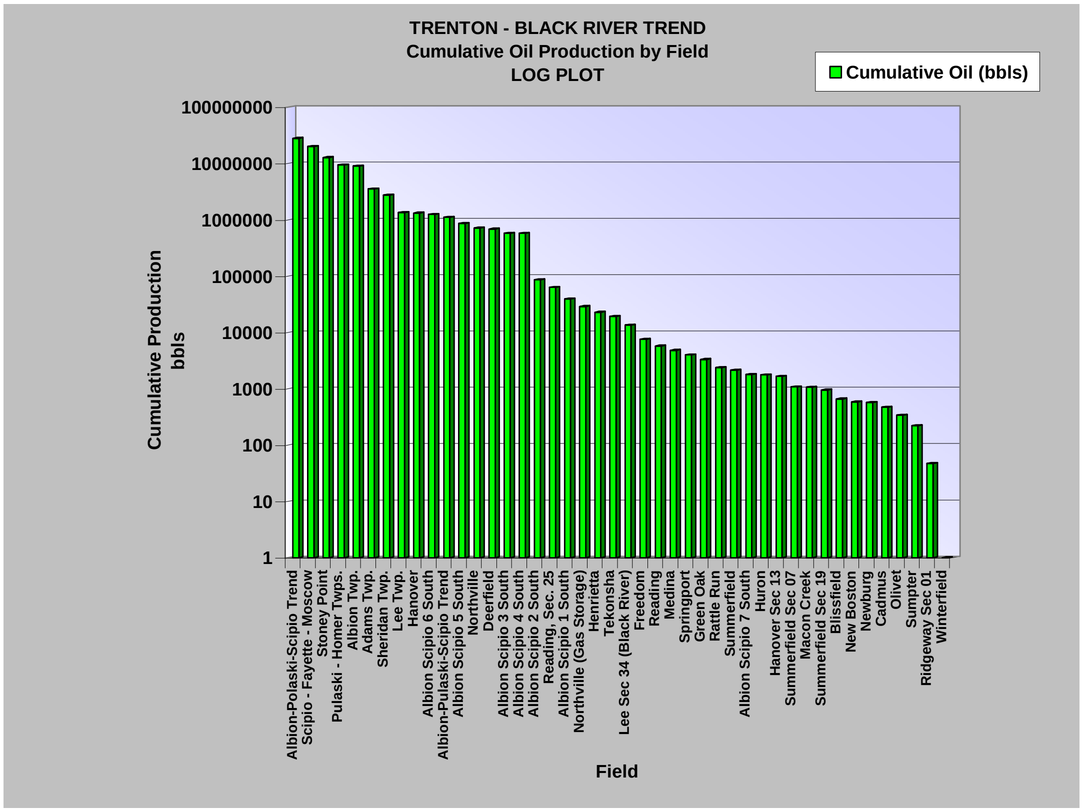
TRENTON - BLACK RIVER TREND
Cumulative Oil Production by Field
LOG PLOT
Cumulative Oil (bbls)
Cumulative Production
bbls
100000000
10000000
1000000
100000
10000
1000
100
10
1
Albion-Polaski-Scipio Trend
Scipio - Fayette - Moscow
Stoney Point
Pulaski - Homer Twps.
Albion Twp.
Adams Twp.
Sheridan Twp.
Lee Twp.
Hanover
Albion Scipio 6 South
Albion-Pulaski-Scipio Trend
Albion Scipio 5 South
Northville
Deerfield
Albion Scipio 3 South
Albion Scipio 4 South
Albion Scipio 2 South
Reading, Sec. 25
Albion Scipio 1 South
Northville (Gas Storage)
Henrietta
Tekonsha
Lee Sec 34 (Black River)
Freedom
Reading
Medina
Springport
Green Oak
Rattle Run
Summerfield
Albion Scipio 7 South
Huron
Hanover Sec 13
Summerfield Sec 07
Macon Creek
Summerfield Sec 19
Blissfield
New Boston
Newburg
Cadmus
Olivet
Sumpter
Ridgeway Sec 01
Winterfield
Field

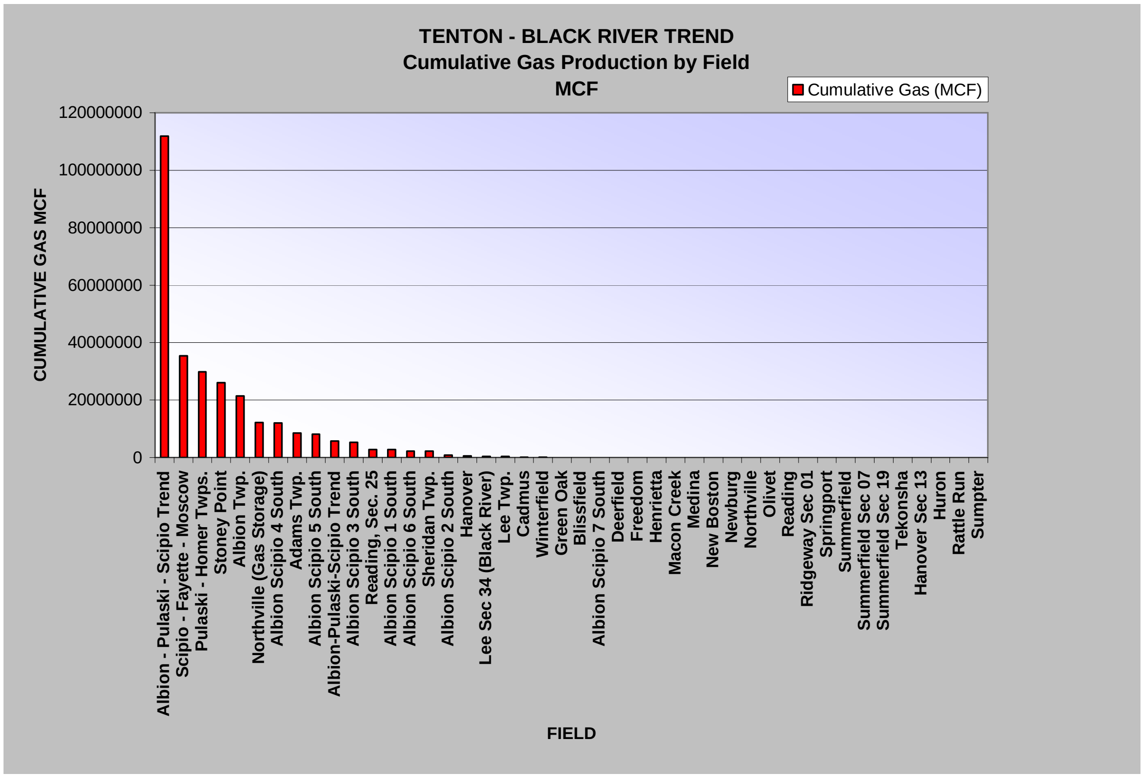
TENTON - BLACK RIVER TREND
Cumulative Gas Production by Field
MCF
Cumulative Gas (MCF)
CUMULATIVE GAS MCF
120000000
100000000
80000000
60000000
40000000
20000000
0
Albion - Pulaski - Scipio Trend
Scipio - Fayette - Moscow
Pulaski - Homer Twps.
Stoney Point
Albion Twp.
Northville (Gas Storage)
Albion Scipio 4 South
Adams Twp.
Albion Scipio 5 South
Albion-Pulaski-Scipio Trend
Albion Scipio 3 South
Reading, Sec. 25
Albion Scipio 1 South
Albion Scipio 6 South
Sheridan Twp.
Albion Scipio 2 South
Hanover
Lee Sec 34 (Black River)
Lee Twp.
Cadmus
Winterfield
Green Oak
Blissfield
Albion Scipio 7 South
Deerfield
Freedom
Henrietta
Macon Creek
Medina
New Boston
Newburg
Northville
Olivet
Reading
Ridgeway Sec 01
Springport
Summerfield
Summerfield Sec 07
Summerfield Sec 19
Tekonsha
Hanover Sec 13
Huron
Rattle Run
Sumpter
FIELD

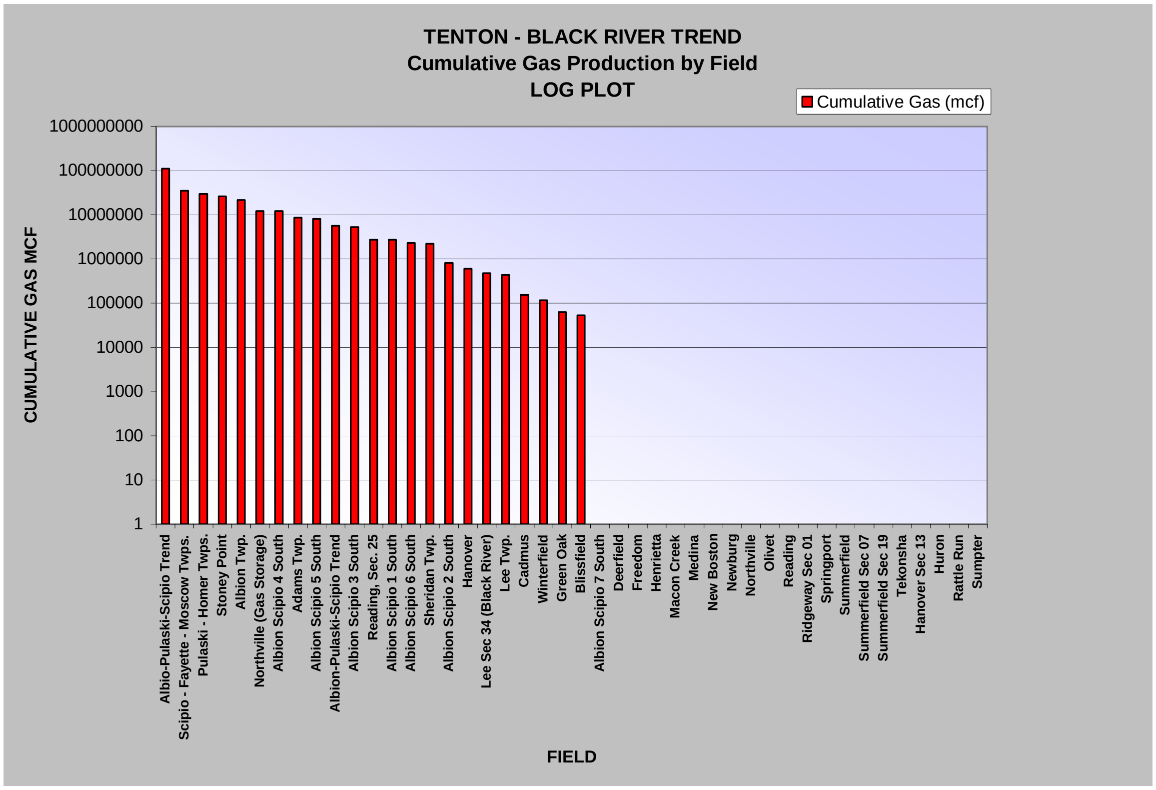

TENTON - BLACK RIVER TREND
Cumulative Gas Production by Field
LOG PLOT
Cumulative Gas (mcf)
CUMULATIVE GAS MCF
FIELD

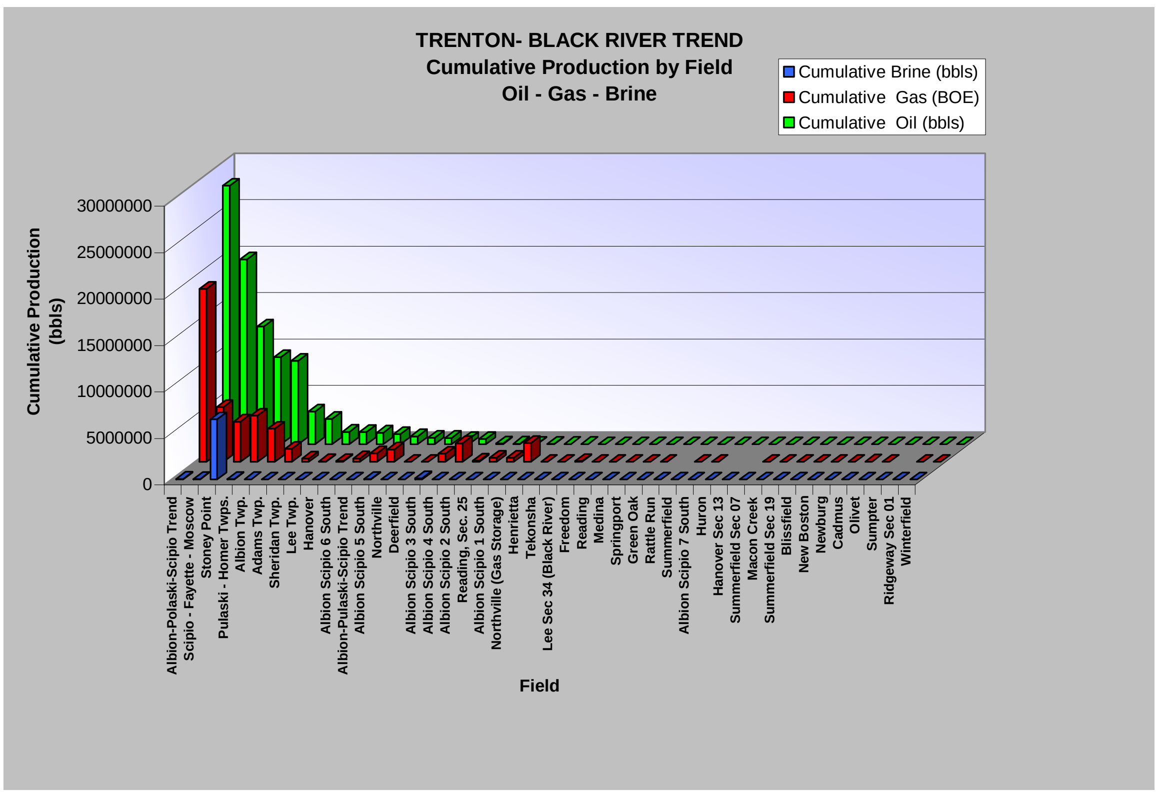

TRENTON- BLACK RIVER TREND
Cumulative Production by Field
Oil - Gas - Brine
Cumulative Brine (bbls)
Cumulative Gas (BOE)
Cumulative Oil (bbls)
Cumulative Production (bbls)
Field

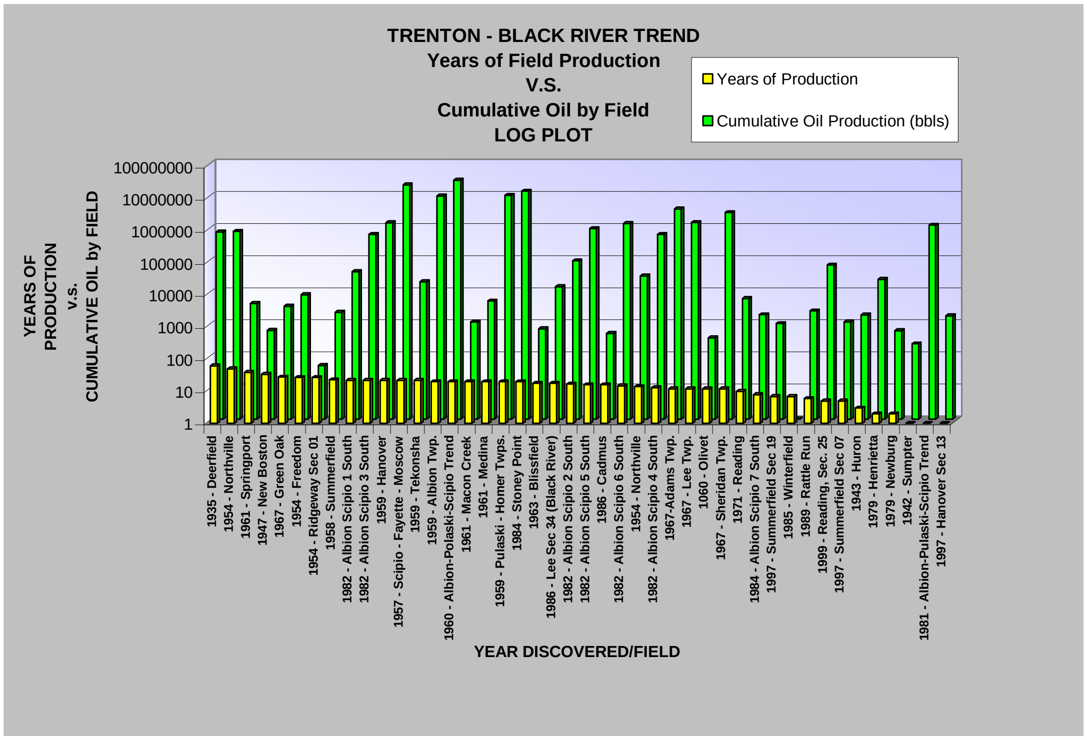

TRENTON - BLACK RIVER TREND
Years of Field Production
V.S.
Cumulative Oil by Field
LOG PLOT
Years of Production
Cumulative Oil Production (bbls)
YEARS OF PRODUCTION v.s. CUMULATIVE OIL by FIELD
YEAR DISCOVERED/FIELD

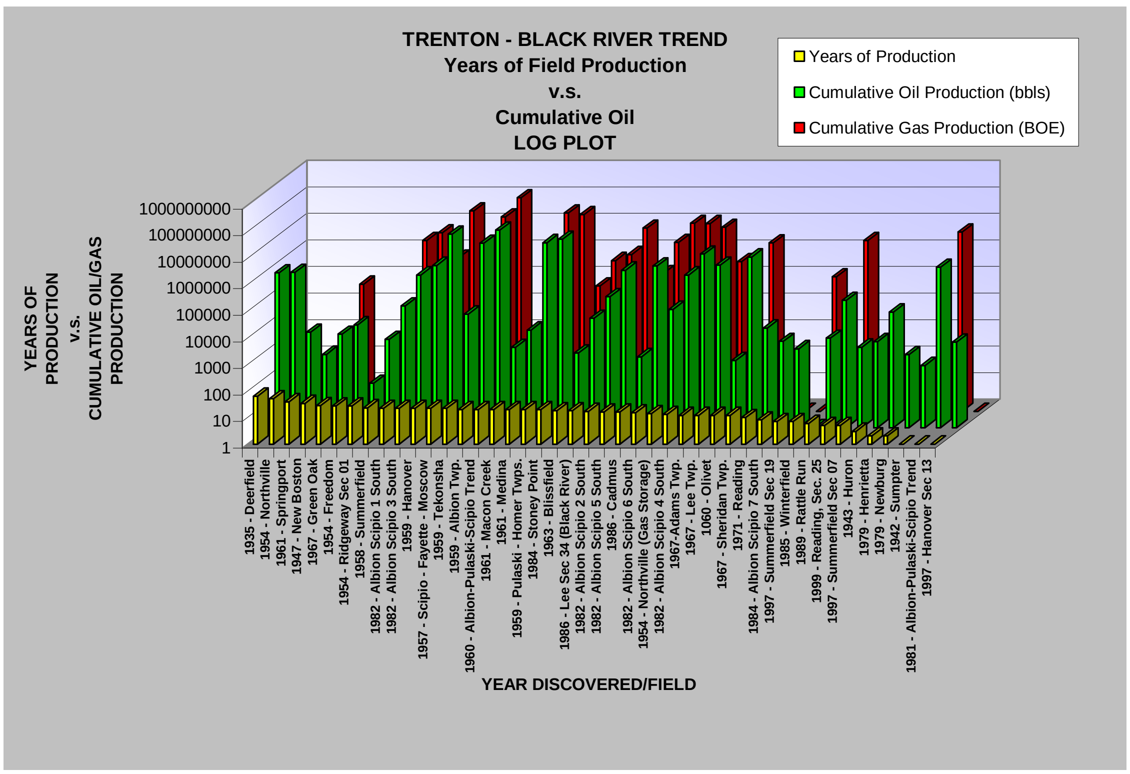

TRENTON - BLACK RIVER TREND
Years of Field Production
v.s.
Cumulative Oil
LOG PLOT
Years of Production
Cumulative Oil Production (bbls)
Cumulative Gas Production (BOE)
YEARS OF PRODUCTION v.s. CUMULATIVE OIL/GAS PRODUCTION
YEAR DISCOVERED/FIELD

Silurian Niagaran Trend
Production Analysis Graphs

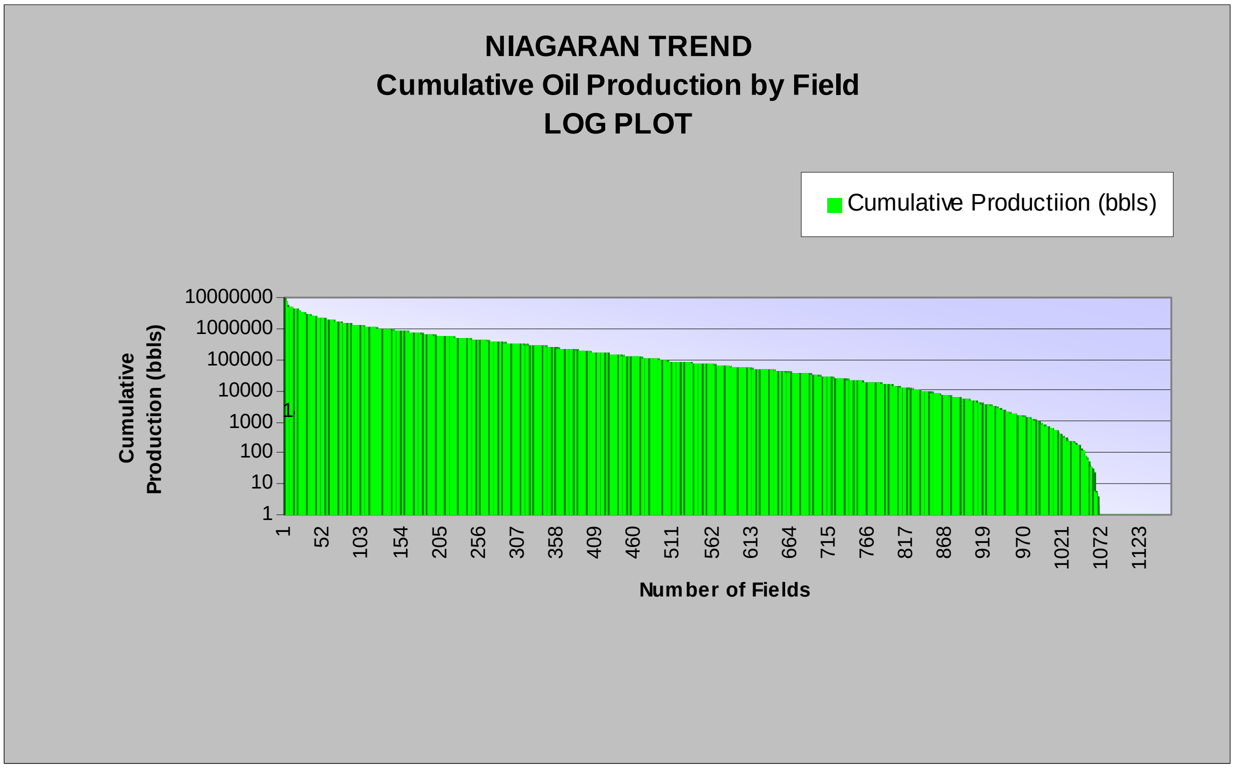

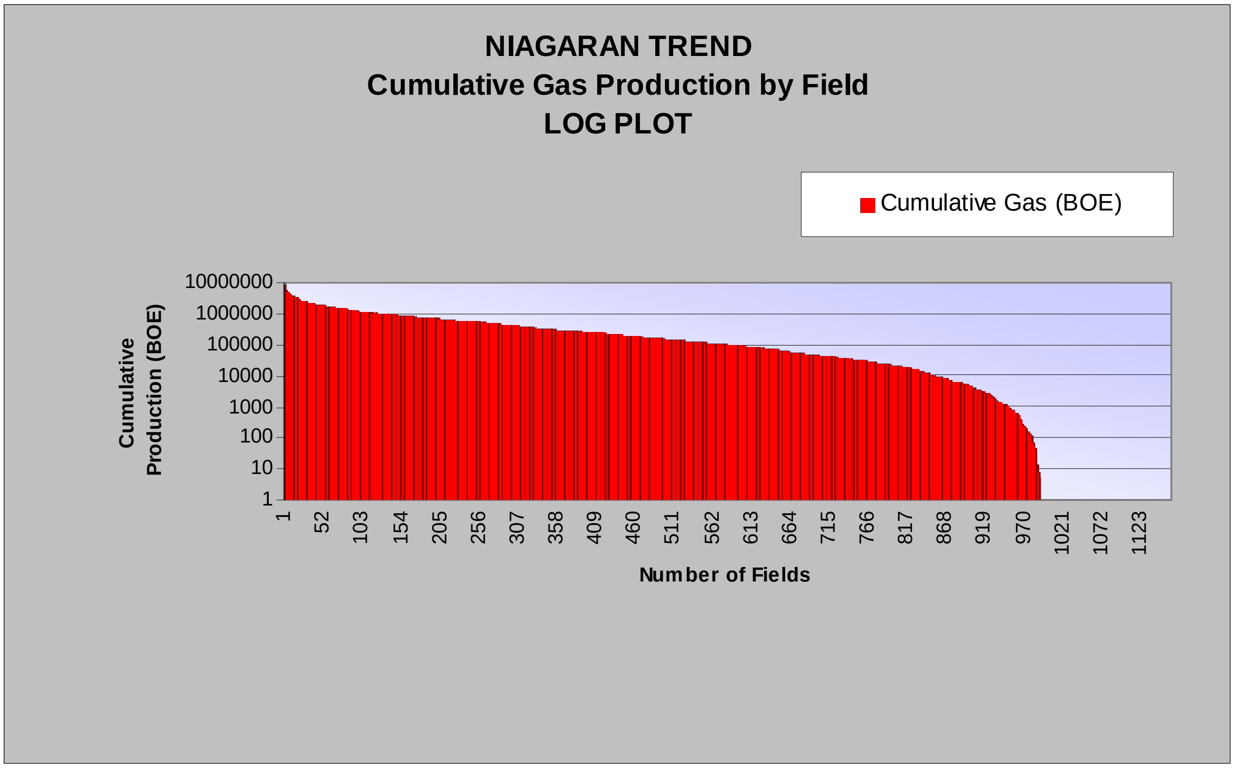
NIAGARAN TREND
Cumulative Gas Production by Field
LOG PLOT
Cumulative Gas (BOE)
Cumulative Production (BOE)
10000000
1000000
100000
10000
1000
100
10
1
1
52
103
154
205
256
307
358
409
460
511
562
613
664
715
766
817
868
919
970
1021
1072
1123
Number of Fields

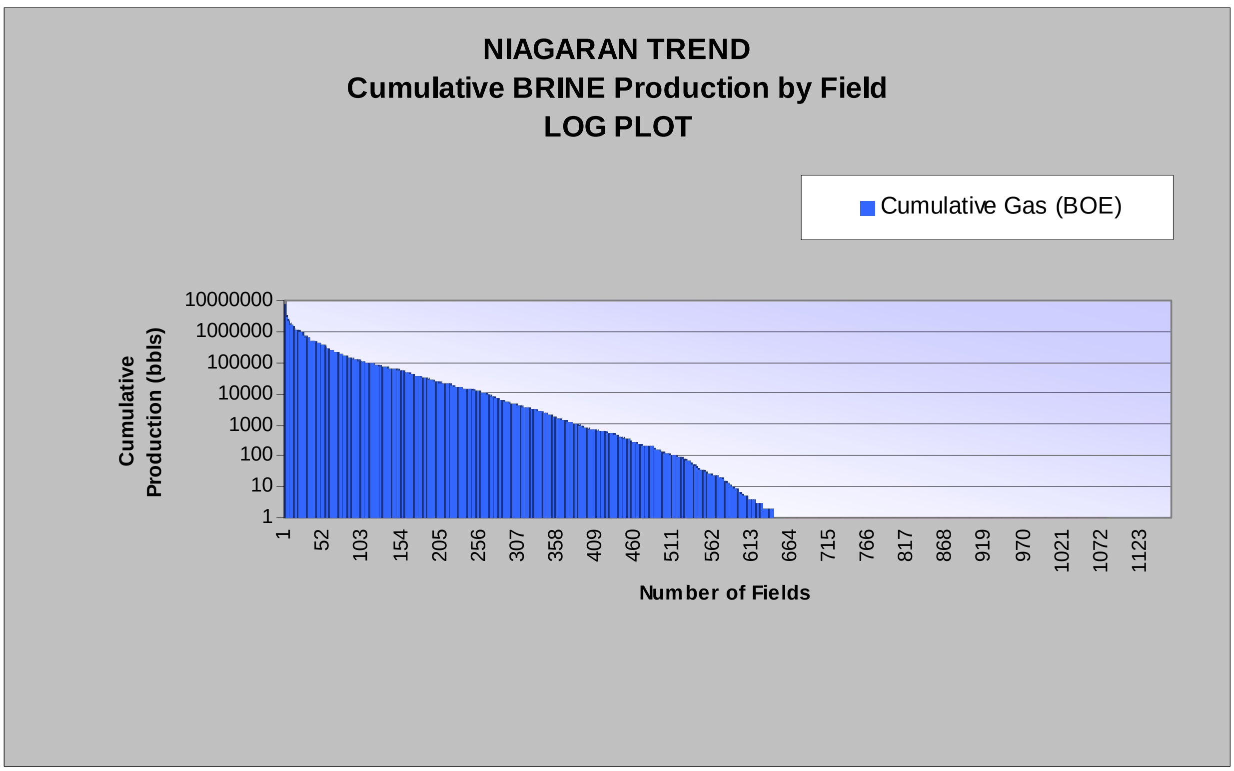
NIAGARAN TREND
Cumulative BRINE Production by Field
LOG PLOT
Cumulative Gas (BOE)
Cumulative Production (bbls)
10000000
1000000
100000
10000
1000
100
10
1
1
52
103
154
205
256
307
358
409
460
511
562
613
664
715
766
817
868
919
970
1021
1072
1123
Number of Fields

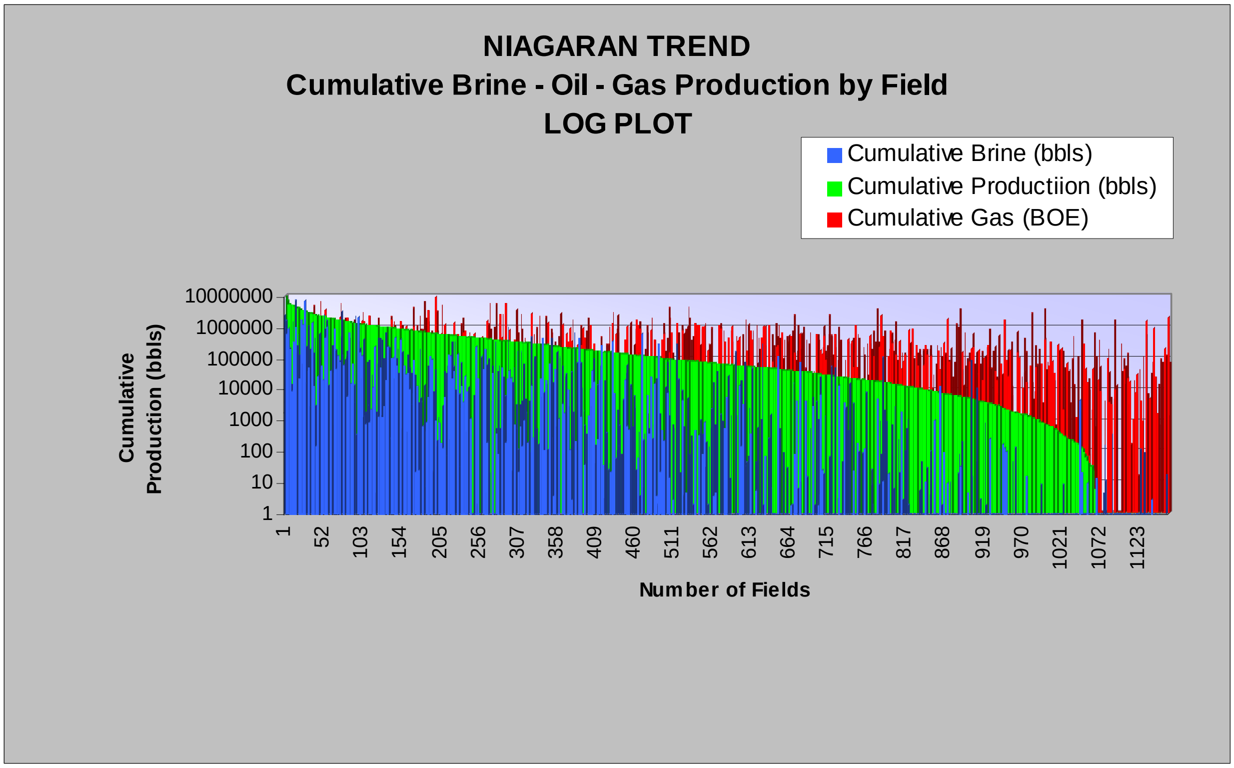
NIAGARAN TREND
Cumulative Brine - Oil - Gas Production by Field
LOG PLOT
Cumulative Brine (bbls)
Cumulative Productiion (bbls)
Cumulative Gas (BOE)
Cumulative Production (bbls)
10000000
1000000
100000
10000
1000
100
10
1
1
52
103
154
205
256
307
358
409
460
511
562
613
664
715
766
817
868
919
970
1021
1072
1123
Number of Fields

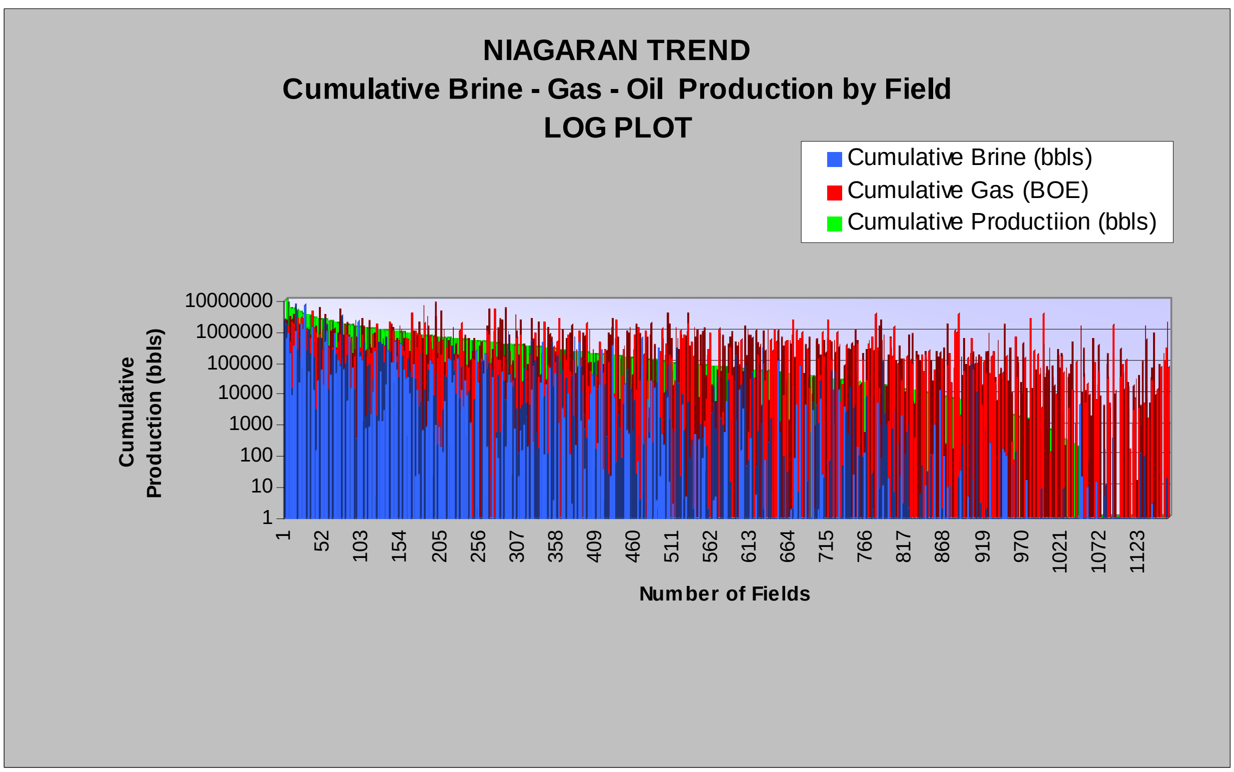
NIAGARAN TREND
Cumulative Brine - Gas - Oil Production by Field
LOG PLOT
Cumulative Brine (bbls)
Cumulative Gas (BOE)
Cumulative Productiion (bbls)
Cumulative Production (bbls)
10000000
1000000
100000
10000
1000
100
10
1
1
52
103
154
205
256
307
358
409
460
511
562
613
664
715
766
817
868
919
970
1021
1072
1123
Number of Fields

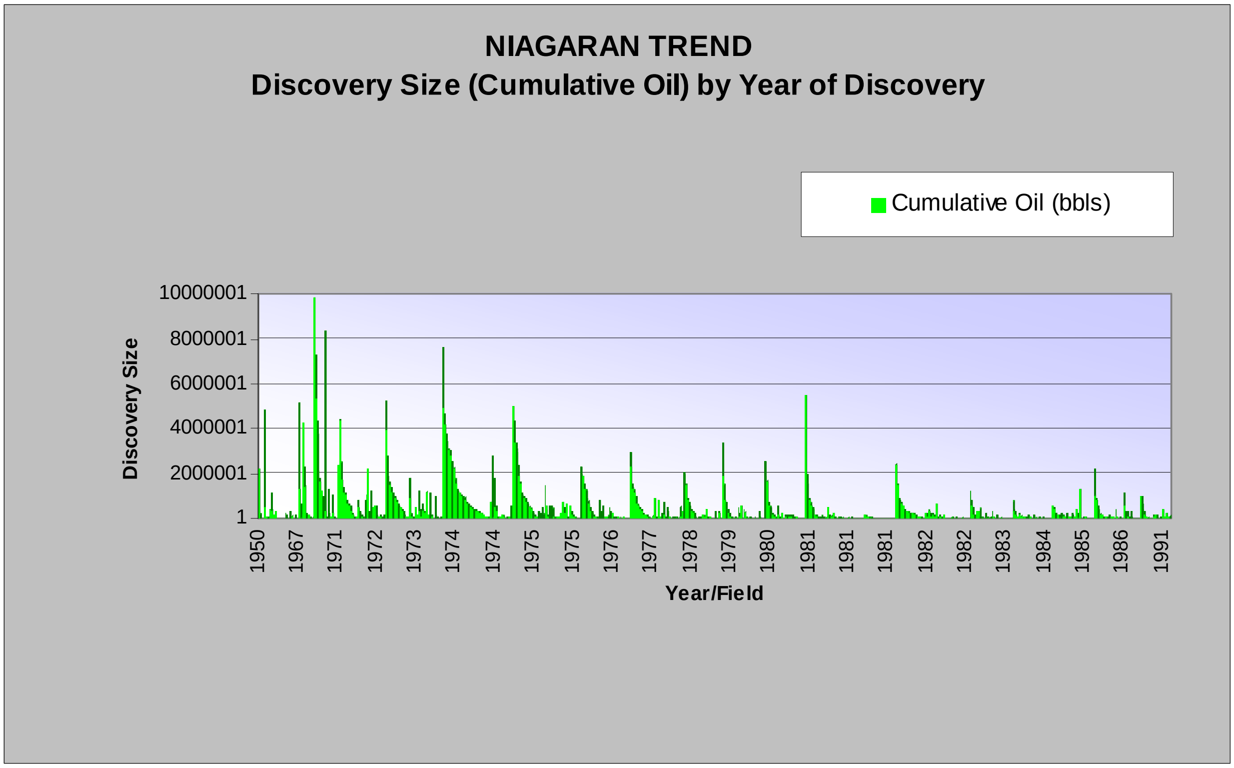
NIAGARAN TREND
Discovery Size (Cumulative Oil) by Year of Discovery
Cumulative Oil (bbls)
Discovery Size
10000001
8000001
6000001
4000001
2000001
1
1950
1967
1971
1972
1973
1974
1974
1975
1975
1976
1977
1978
1979
1980
1981
1981
1981
1982
1982
1983
1984
1985
1986
1991
Year/Field

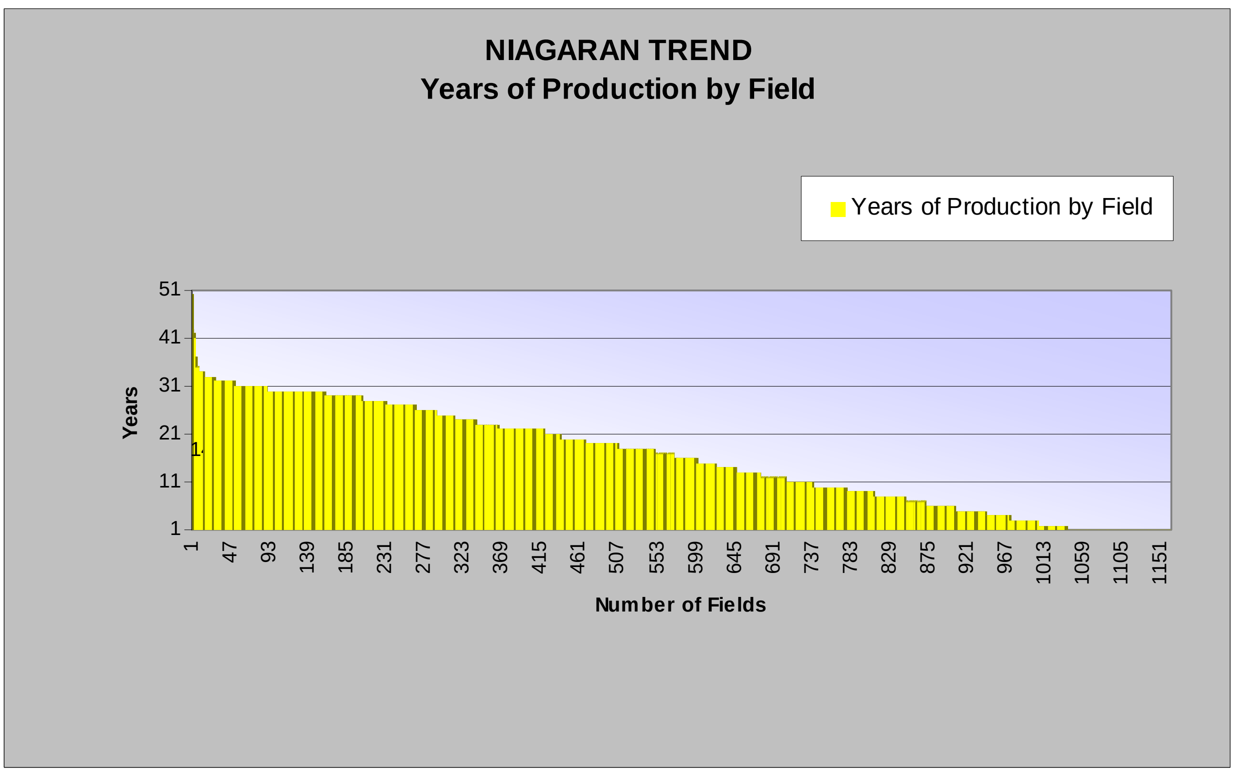
NIAGARAN TREND
Years of Production by Field
Years of Production by Field
Years
51
41
31
21
11
1
1
47
93
139
185
231
277
323
369
415
461
507
553
599
645
691
737
783
829
875
921
967
1013
1059
1105
1151
Number of Fields

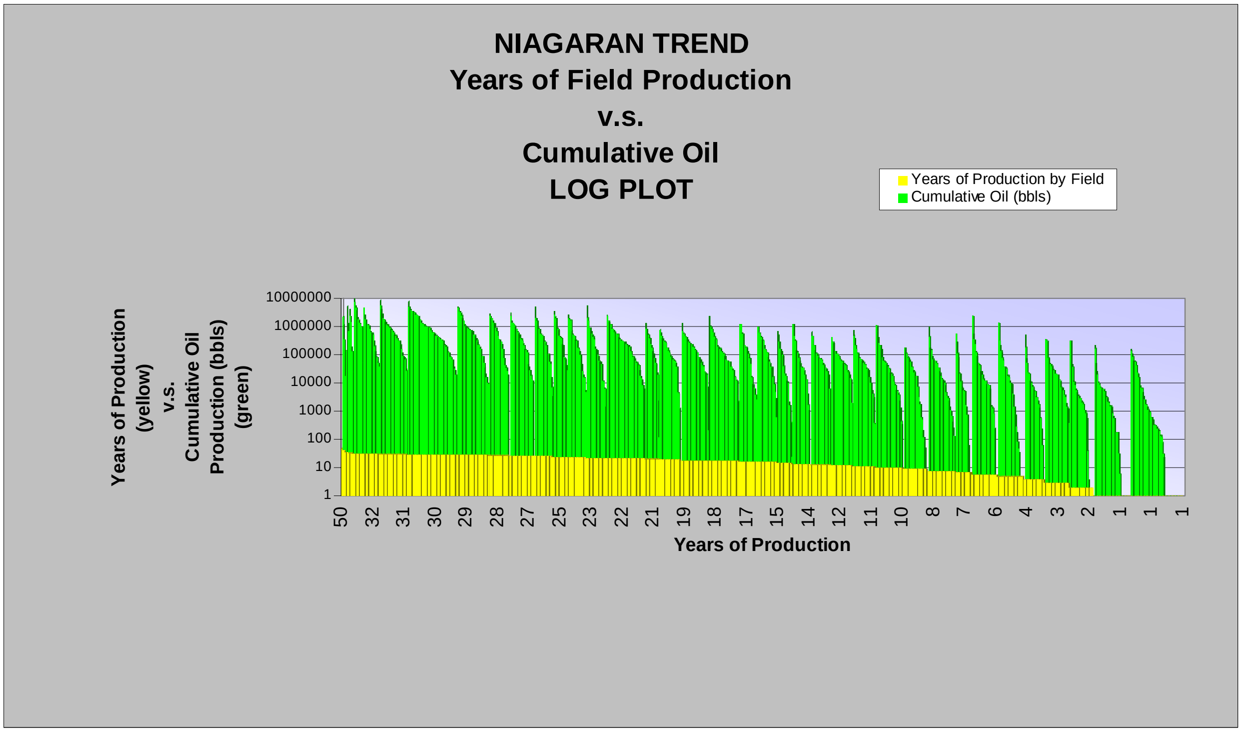

NIAGARAN TREND
Years of Field Production
v.s.
Cumulative Oil
LOG PLOT
Years of Production by Field
Cumulative Oil (bbls)
Years of Production (yellow) v.s. Cumulative Oil Production (bbls) (green)
10000000
1000000
100000
10000
1000
100
10
1
50
32
31
30
29
28
27
25
23
22
21
19
18
17
15
14
12
11
10
8
7
6
4
3
2
1
1
1
Years of Production

Devonian Dundee Trend
Production Analysis Graphs

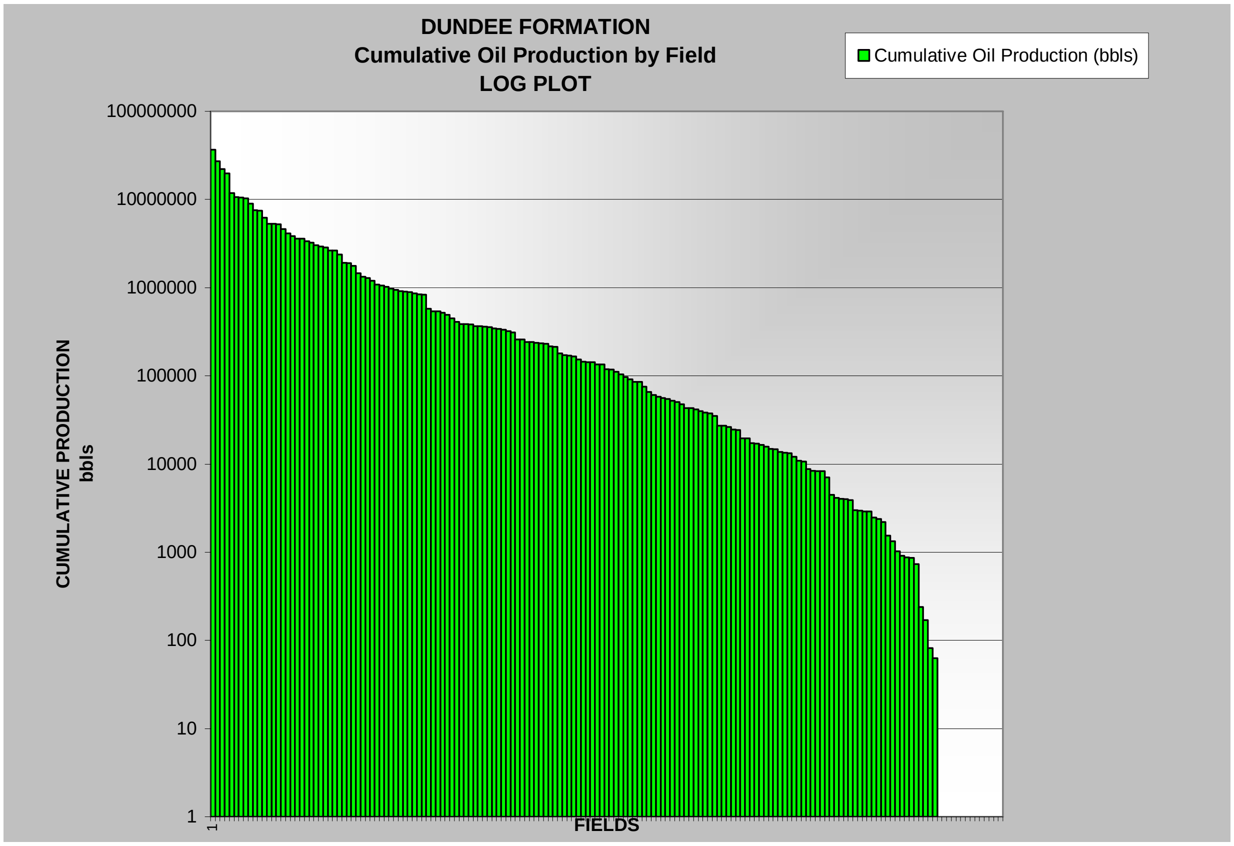

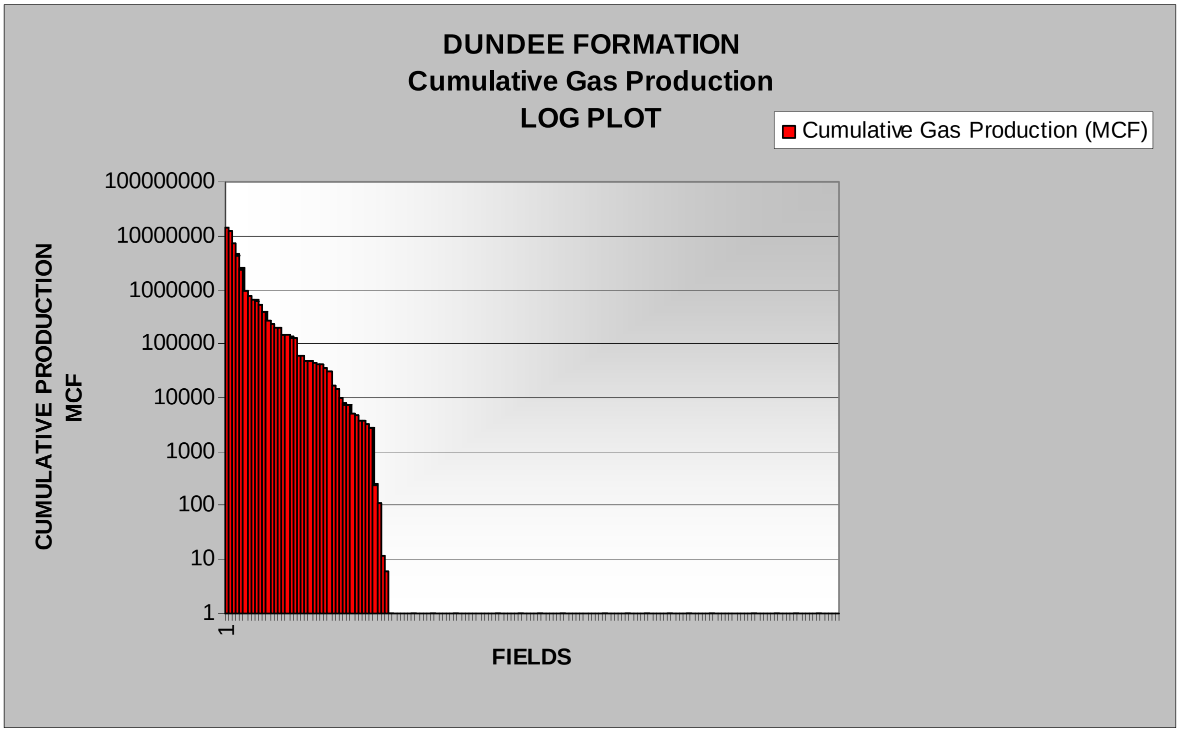
DUNDEE FORMATION
Cumulative Gas Production
LOG PLOT
Cumulative Gas Production (MCF)
100000000
10000000
1000000
100000
10000
1000
100
10
1
CUMULATIVE PRODUCTION
MCF
1
FIELDS

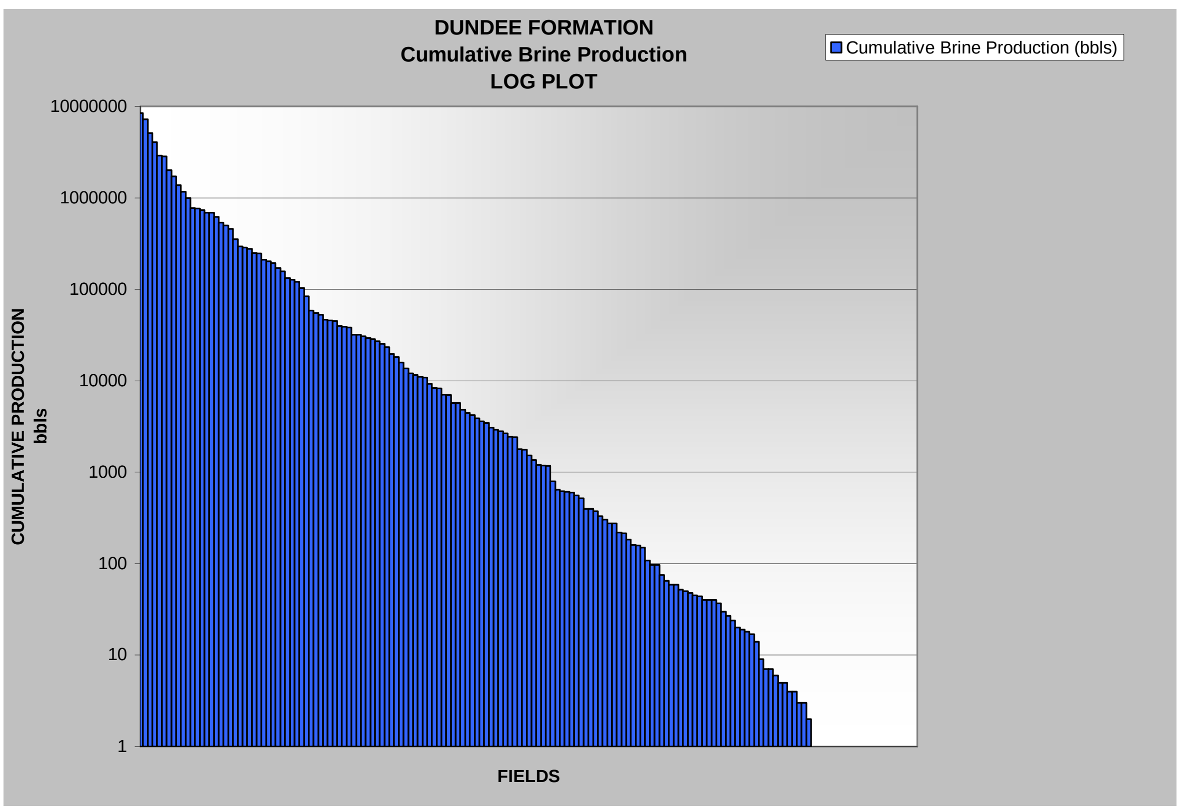
DUNDEE FORMATION
Cumulative Brine Production
LOG PLOT
Cumulative Brine Production (bbls)
10000000
1000000
100000
10000
1000
100
10
1
CUMULATIVE PRODUCTION
bbls
FIELDS

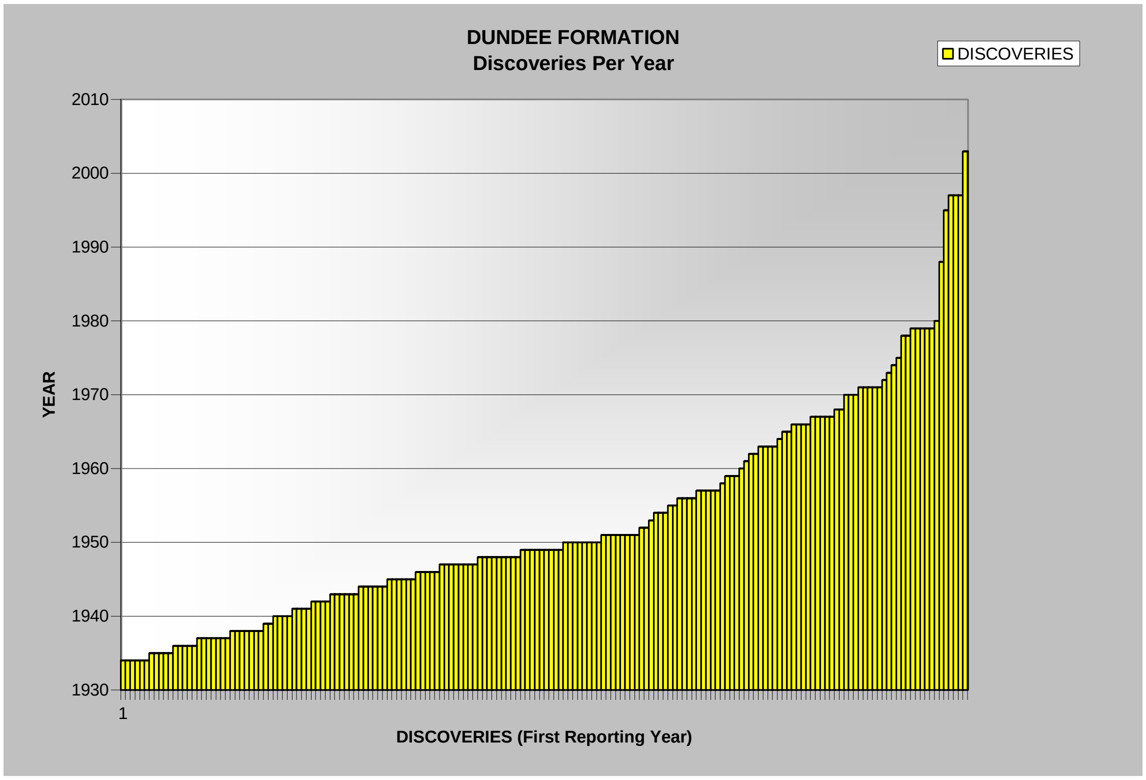
DUNDEE FORMATION
Discoveries Per Year
DISCOVERIES
2010
2000
1990
1980
1970
1960
1950
1940
1930
YEAR
1
DISCOVERIES (First Reporting Year)

Appendix 2

WMU Project Staff activity at Eastern Section AAPG Annual Meeting in Buffalo, NY October 8-11, 2006

Session Chair - Oral Technical Session: New Approaches to Carbonate Reservoirs of Eastern America, Michael Grammer
Session Chair - Oral Technical Session: Geological Carbon Sequestration in the Eastern U.S., William Harrison,

Papers presented:

- New Insight into the Reservoir Architecture of Silurian (Niagaran) Pinnacle Reefs in the Michigan Basin - G. Michael Grammer, W.B. Harrison, III, D.A. Barnes, and R. Gillespie, Western Michigan University, A.E. Sandomierski, Exxon Mobil Production Company
- Albion/Scipio Field, Michigan: What does a detailed look at cores tell us about the reservoir? - Robb Gillespie, David A. Barnes, G. Michael Grammer, and William Harrison, III, Western Michigan University
- Potential for Geological Carbon Sequestration in the Michigan Basin - William B. Harrison III, David A. Barnes, G. Michael Grammer, and Amanda Wahr, Western Michigan University
- Combining CO2 sequestration with EOR activities – a synergistic approach for the future: An example from the Michigan Basin - G. Michael Grammer, David A. Barnes, William B. Harrison III, Western Michigan University and Robert G. Mannes, CORE Energy
- Geological Carbon Sequestration Potential in Devonian Saline Aquifers of the Michigan Basin, USA - David A. Barnes, Amanda Wahr, William Harrison, III, G. Michael Grammer, Western Michigan University and Neeraj Gupta, Battelle Memorial Institute

Posters Presented:

- Hydrothermal Dolomite: Occurrence and Mechanisms, Michigan Basin, USA David A. Barnes, G. Michael Grammer, William Harrison, III, and Robb Gillespie, Western Michigan University

- Subsurface Stratigraphy of the Devonian Dundee Formation, Michigan Basin, USA – A Log Based Approach - Joshua P. Kirschner, and David A. Barnes, Western Michigan University

Posters Presented:

- Four Student Job Quest posters presented by Jessica Crisp, Josh Kirshner, Amy Noack and Amanda Wahr

Appendix 2a – abstract presented at Annual AAPG Meeting in March 2006

Hydrothermal Dolomite Reservoirs (HTDR) in a Mature Petroleum Province, Michigan Basin, USA

David A. Barnes, Department of Geosciences and Michigan Basin Core Research Laboratory, Western Michigan University, 1903 W. Michigan Ave, Kalamazoo, MI 49009, phone: (269) 387-8633, barnes@wmich.edu, **G. Michael Grammer**, Department of Geosciences, Western Michigan University, Kalamazoo, MI 49008, **William Harrison, III**, Western Michigan University, Kalamazoo, MI 49008, and **Robb Gillespie**, Michigan Basin Core Research Laboratory, Department of Geosciences, Western Michigan University, Kalamazoo, MI 49008.

Carbonate reservoirs with a strong overprint of fracture related hydrothermal dolomite (HTDR) have unique spatial distribution, internal geometry, and hydrocarbon production characteristics. Recognition of HTDR in mature but under-studied basins has important commercial implication. Improved reservoir characterization and enhanced recovery operations and support for untested exploration concepts can result from identification of HTDR. One of the first well-documented examples of HTDR in a giant oil field is the Trenton/Black River (T/BR), Albion-Scipio field in the Michigan basin, USA. Wrench faulting and Riedel shear related features, including dilational fractures, and primary facies controlled fluid flow conduits are considered fundamental to the origin of HTDR relative to regional limestone in Albion-Scipio.

Sedimentologic and petrologic analysis of several producing formations in core including T/BR, Ordovician St. Peter Sandstone (aka “PdC”), and Devonian Dundee Formation throughout the Michigan basin indicates a pervasive overprint of hydrothermal dolomite. Hydrothermal mineralization is also observed in units in the basin as young as Mississippian/Pennsylvanian age. Structural mapping and log analysis in the T/BR and Dundee suggest close spatial relationship among gross dolomite distribution and interpreted, wrench fault-related NW-SE and NE-SW structural trends. Hydrothermal origin of much dolomite in several stratigraphic intervals, from Ordovician through Mississippian/Pennsylvanian age and persistent association of this dolomite in reservoirs coincident with wrench fault-related features is strong evidence in support of HTDR in multiple producing intervals in the Michigan basin. Recognition of HTDR in these and other reservoir formations should result in revitalized and improved exploration/exploitation activity and increased production in Michigan and other mature petroleum provinces.

Appendix 2b – abstract presented at Annual AAPG in March 2006

Evaluating Controls on the Formation and Reservoir Architecture of Niagaran Pinnacle Reefs (Silurian) in the Michigan Basin: A Sequence Stratigraphic Approach

SANDOMIERSKI, A.E., GRAMMER,G.M. and HARRISON, W.B., III,
Western Michigan University, Kalamazoo, MI

Silurian-aged (Niagaran) pinnacle reefs have been productive in the Michigan Basin for 60+ years, but extensive lateral and vertical heterogeneity limits primary production to as little as 25%. Enhanced recovery efforts are generally focused on water and CO2 floods, or horizontal drilling, but the connectivity of the reefs laterally and vertically is poorly understood and unpredictable, leading to marginal success in many reefs. Niagaran pinnacle reef growth has previously been described as continuous growth during a single relative sea level rise. In this model, the characteristic shoaling upward sequence varies from a microbial mound facies at the base, with a stromatoporoid-dominated reef core capped by algal laminites and anhydrites that form a regional seal for many of the reefs in the Basin.

Detailed core analysis within a sequence stratigraphic framework, however, indicates that the overall shoaling sequence is made up of higher frequency depositional cycles, each bounded by exposure or flooding surfaces. These tens of meters to meter scale cycles support an episodic reef growth model controlled by multiple fluctuations in relative sea level, and provides a means to predict reservoir quality since porosity and permeability is often related to primary facies in these reefs. Because many cycles contain reservoir facies bounded by low permeability units, the result is often significant vertical compartmentalization. This core-based understanding of the episodic nature of pinnacle reef growth, as well as the vertical facies successions and resulting impact on reservoir heterogeneity, should lead to enhanced predictability of reservoir architecture from wireline log signatures alone.

Albion/Scipio Field, Michigan: What does a detailed look at cores tell us about the reservoir?

Gillespie, R. (robb.gillespie@wmich.edu 269-387-8633), Barnes, D. A., Grammer, G.M., and Harrison, W.B., Michigan Geological Repository for Research and Education, Western Michigan University, Kalamazoo, MI

Michigan's only giant oil field, the Albion/Scipio Field, has produced over 125 million barrels of oil and is used as an analog for much of the Trenton-Black River exploration in Eastern North America. Current reservoir models, based on published literature suggest extensive fracturing and brecciation followed by pervasive hydrothermal dolomitization created the field's reservoir architecture. The general impression of this reservoir is one of facies-independent and fabric-destructive processes, especially dolomitization that created the reservoir quality.

Detailed examination of numerous cores from the field and a few outside the field, do show some intervals of extensive fracturing and brecciation along with hydrothermal (saddle) dolomite cement. Many other cores show only limited fracturing and rare saddle dolomite cement. Some of the cores, in the heart of the field, show almost no fracturing although much of the cored interval is dolomitized. Several well cores show interbedded dolomite and limestone with primary facies fabrics and textures very well preserved in both lithologies. Depositional environments can easily be interpreted from most of the core material. These cores show a diverse set of shallow shelf and peritidal facies stacked in multiple cycles through the Black River and Trenton intervals.

It appears from this core study that fracturing and brecciation is very laterally restricted to the proximity of major faults within the field. Wells a short distance from these faults may show little or no fracturing. Dolomitization does, however, extend well beyond the fractured zone. Primary sediment texture and porosity may have provided sufficient fluid pathway to transmit the dolomitizing fluids substantial distance from the major faults.

Appendix 2d – abstract presented at Eastern Section AAPG in Oct. 2006

Subsurface Stratigraphy of the Devonian Dundee Formation, Michigan Basin, USA – A Log Based Approach

JOSHUA P. KIRSCHNER (joshua.p.kirschner@wmich.edu) and David A. Barnes
Western Michigan University, Geosciences and MGRRE, Kalamazoo, MI, 49008

A distinct hard ground surface separates two disparate facies tracts in numerous, Middle Devonian, Dundee Formation cores in the Michigan basin subsurface. This sharp stratigraphic contact can be distinguished by scour and/or dissolution of a partially lithified surface, which is commonly bored and/or eroded, and overlain by rip up clasts. This contact is thought to represent both a subaerial or subaqueous exposure surface and a subsequent period of slow sediment accumulation. Supratidal to shallow marine, shoal-water carbonate facies occur below this hard ground surface, basin wide. A lithologically homogeneous, fossiliferous mudstone-wackestone facies overlies the hard ground surface in core and is indicative of transgression to more distal, open marine conditions.

Careful analysis of hundreds of wireline logs throughout the basin reveals a ubiquitous gamma ray marker (grm) that coincides with this hard ground/marine flooding surface in core. Although present across much of the basin, the grm does not always occur apparently due to local variability of carbonate lithofacies, especially in more open marine Dundee successions in the eastern basin. A corresponding decrease in porosity, inferred from lithodensity logs, commonly coincides with the grm and is typically present even when the grm is not.

Formal lithostratigraphy does not subdivide the Dundee Formation in the Michigan basin subsurface. This investigation supports the idea that the Rogers City Limestone formation recognized in outcrop is a laterally extensive unit, which can be differentiated from the underlying Dundee (aka "Reed City equivalent") Formation throughout the Michigan basin subsurface. Log-based, member scale, stratigraphic subdivision of the Dundee Formation is important in understanding the primary depositional history and the distribution of highly productive secondary dolomite reservoirs in the upper Rogers City Member.

Appendix 2e – abstract presented at Eastern Section AAPG in Oct. 2006

New Insight into the Reservoir Architecture of Silurian (Niagaran) Pinnacle Reefs in the Michigan Basin

Grammer, G.Michael[1], Sandomierski, A.E.[2], Harrison, W.B., III[1], Barnes, D.A. and Gillespie, R.[1]
[1]Michigan Geological Repository for Research and Education, Western Michigan University, Kalamazoo, MI 49008
[2]ExxonMobil Production Company, Houston, TX 77002

Silurian-aged (Niagaran) pinnacle reefs have been productive in the Michigan Basin for over 60 years, but extensive lateral and vertical heterogeneity in the reservoirs may limit primary production to as little as 25%. Enhanced recovery efforts have generally been focused upon horizontal or directional drilling and waterfloods, but the internal reservoir architecture is often poorly understood which leads to marginal economic success in many reefs. Recent detailed facies analysis from core suggests that vertical compartmentalization in some pinnacle reefs is the result of complex facies variability, and that the vertical distribution of these facies can be constrained, and therefore predicted, within a sequence stratigraphic framework.

The sequence stratigraphic framework of the Miller Fox 1-11 reef, Oceana Co., MI, is characterized by a tripartite hierarchy of sequences, high frequency sequences, and cycles. Large-scale sequences (90-120 ft) correspond reasonably well to the commonly accepted "pinnacle reef model" in the Basin which describes an overall shoaling from mud mound to coral-stromatoporoid framework reef, to a restricted marine algal/stromatolitic unit which is ultimately capped with supratidal algal mats and evaporites. Smaller scale high frequency sequences (35-50 ft) and cycles (3-10 ft), however, consisting of shoaling upward packages bounded by low permeability facies, result in the potential for vertical permeability baffles or barriers within the overall "pinnacle reef" complex. Because there is a distinct correlation between various facies types and porosity/permeability values within these higher resolution packages, enhanced understanding of how these facies are distributed should result in more effective primary and enhanced production efforts.